

ROLE OF TOLL-LIKE RECEPTOR 4 IN OXIDANT-INDUCED INFLAMMATORY
PHENOTYPES

A DISSERTATION IN

Pharmacology

and

Cell Biology and Biochemistry

Presented to the Faculty of the University
of Missouri-Kansas City in partial fulfillment of
the requirements for the degree

DOCTOR OF PHILOSOPHY

by

YAN ZHANG

B.S., Sichuan University, 2006
M.S., Pharmacology, Peking Union Medical College, 2009

Kansas City, Missouri

2017

ROLE OF TOLL-LIKE RECEPTOR 4 IN OXIDANT-INDUCED
INFLAMMATORY PHENOTYPES

Yan Zhang, Candidate for the Doctor of Philosophy Degree

University of Missouri-Kansas City, 2017

ABSTRACT

A common mechanism by which redox stress may activate inflammatory responses to potentially initiate, propagate and maintain many diseases states has not been characterized. Accumulating evidence suggests that pattern recognition receptors of the innate immune system such as the toll-like receptors (TLRs) are involved. In the present study, we tested the *central hypothesis* that TLR4 is the link between reactive oxygen/nitrogen species (RONS), oxidative stress and inflammatory phenotypes that mediate diverse disease processes.

We first characterized the mediatory role of TLR4 in exogenous oxidant-induced nuclear factor- κ B (NF- κ B) activation in macrophage RAW-Blue cells with stable transfection of NF- κ B reporter gene SEAP. Our results show that inhibition of TLR4 significantly attenuated oxidant-induced NF- κ B activation, which caused an imbalance in TNF- α and IL-10 production.

We used primary peritoneal macrophage (pM) derived from TLR4-wildtype (TLR4-WT) and TLR4-knockout (TLR4-KO) mice to investigate the role of TLR4. Our data show that TLR4 is necessary for RONS-mediated disturbances in redox homeostasis and the production of TNF- α . Our results affirm that exogenous RONS can initiate the production of resolvin D1 by concurrently increasing the expression of its biosynthetic enzymes and its receptor through TLR4 stimulation. Our data show that

exogenous RONS-induced TLR4 stimulation plays a critical role in activating both proinflammatory and pro-resolving pathways.

Finally, we examined if primed TLR4 would influence the magnitude of responses to exogenous oxidants in pM. Our results indicate that treatment with oxidants alone had a limited effect on prostaglandin E₂ (PGE₂) synthesis. In contrast, pM sensitized by prior treatment with LPS-EK followed by oxidant stimulation exhibited increased expression of COX-2 and an enhanced PGE₂ production only in pM derived from TLR4-WT mice. Thus, we showed a critical role for primed TLR4 in oxidant-induced pro-inflammatory processes.

For the first time, we present evidence to support a central mechanism(s) for the intersection between exogenous and endogenous RONS in enhancing inflammatory phenotypes that may initiate, propagate, and maintain multiple disease states.

APPROVAL PAGE

The faculties listed below, appointed by the Dean of School of Graduate Studies have examined the dissertation titled “Role of Toll-Like Receptor 4 in Oxidant-induced Inflammatory Phenotypes in Macrophages” presented by Yan Zhang, candidate for the Doctor of Philosophy degree, and certify that in their opinion it is worthy of acceptance.

Supervisory Committee

Orisa J. Igwe, Ph.D., Committee Chair

Division of Pharmacology and Toxicology

Xiao-qiang (Sean) Yu, Ph. D.

Division of Molecular Biology and Biochemistry

Jianping Wang, Ph.D.

Division of Pharmacology and Toxicology

Charles S. Barnes, Ph.D.

Department of Pathology and Laboratory Medicine, Children’s Mercy Hospitals and Clinics

Mingui Fu, Ph.D.

Basic Medical Science

Contents

ABSTRACT.....	iii
ILLUSTRATIONS	xiii
ABBREVIATIONS	xviii
ACKNOWLEDGEMENTS.....	xxiv
Chapter.....	1
1. INTRODUCTION	1
Reactive Oxygen and Nitrogen Species (RONS)	1
Chemistry of RONS.....	1
Generation of RONS.....	5
Cellular Antioxidant Systems	17
Oxidative Stress	21
Inflammation.....	23
Oxidative Stress: An Important Mediator of Inflammation.....	24
Toll-like receptor (TLR) Activation: A Crucial Initiator of Inflammation.....	25
NF- κ B: A Critical Transcription Factor for Inflammatory Response.....	32
Key Pro-inflammatory Mediators Following NF- κ B Activation.....	33
Resolution of Inflammation	40
Macrophages: A Central Cellular Player in Inflammation	45
Rationale for this Dissertation Work	47
2. MATERIALS AND METHODS FOR RAW-BLUE CELLS.....	49

Generation of Oxidants	49
Synthesis/ Preparation of Potassium Peroxychromate (PPC)	49
SIN-1 (3-morpholinosydnonimine N-ethylcarbamide)	50
Cell Culture	50
Oxidant Treatments	52
Live Cell Counting	54
Quanti-Blue Secreted Embryonic Alkaline Phosphatase (SEAP) Reporter Assay ..	54
3-4,5-dimethylthiazol-2-yl)-2, 5-diphenyltetrazolium Bromide (MTT) Assay	54
Lactate Dehydrogenase (LDH) Cytotoxicity Assay	55
Quantification of Thiobarbituric Acid Reactive Substances (TBARS)	55
Quantification of 4-Hydroxynonenal (4-HNE)	56
Measurement of Intracellular ROS (iROS) Production by Fluorescent Imaging	
Microscopy and Flow Cytometry	56
Total Antioxidant Capacity (TAOC) Assay	57
RNA Extraction and Reverse Transcription	58
Quantitative Polymerase Chain Reaction (qPCR)	58
Preparation of Whole-cell Extract	58
Immunoblot Assay	59
Fractionation of Nuclear and Cytoplasmic Extracts from Cells	60
TransAM [®] Assay	60
Quantification of TNF- α and IL-10 Levels	61

Immunoprecipitation (IP).....	61
Statistical Analysis.....	62
3. ROLE OF TLR4 IN OXIDANT-INDUCED INFLAMMATORY RESPONSE THROUGH NF- κ B ACTIVATION IN RAW-BLUE CELLS.....	63
Confirmation of the Experimental System	63
Confirmation of the Release/Generation of ROS and RNS by Oxidants	63
Confirmation TLR4 Expression in RAW-Blue Cells	67
Determination of Optimal Concentrations of Oxidants to Which Cells were Exposed.....	69
Effects of Oxidants on Cellular Redox Homeostasis.....	73
Oxidants Increased iRONS Concentration in RAW-Blue Cells.....	73
Oxidants Decreased Cellular TAOC in RAW-Blue Cells	73
Role of TLR4 in Oxidant-induced NF- κ B Activation	77
Oxidants Stimulated NF- κ B Activation.....	77
Specificity of TLR4 in Oxidant-stimulated NF- κ B Activation	79
Role of TLR4 in Oxidant-increased NF- κ B p65 DNA Binding Activities	81
Oxidants Stimulated NF- κ B Nuclear Translocation.....	83
Mechanisms by which Oxidants Stimulate NF- κ B Activation.....	86
Oxidants Stimulated Degradation of I κ B α	86
Oxidants Stimulated Enhanced Phosphorylation of I κ B α at the Tyr42 Residue.....	86
Role of TLR4 in Oxidant-induced Production of Inflammatory Cytokines	90

Discussion	92
4. MATERIAL AND METHODS FOR PRIMARY PERITONEAL MACROPHAGES	106
Oxidants	106
Animals (Mice) used	106
Genomic DNA Extraction from Mouse Tail to Confirm Genotypes.....	106
PCR and Running DNA Gel	107
Isolation and Characterization of Thioglycollate (TGC)-elicited Peritoneal Macrophages (pM).....	107
Determination of the Purity of Primary pM.....	108
Using Immunocytochemistry	108
Using Flow Cytometry.....	109
Oxidant Treatments.....	109
3-4,5-dimethylthiazol-2-yl)-2, 5-diphenyltetrazolium Bromide (MTT) Assay	110
Lactate Dehydrogenase (LDH) Cytotoxicity Assay	110
Measurement of Intracellular ROS (iROS) by Fluorescent Imaging Microscopy and Flow Cytometry	110
Total Antioxidant Capacity (TAOC) Assay	110
RNA Extraction and Reverse Transcription	111
Quantitative Polymerase Chain Reaction (qPCR)	111
Preparation of Whole-cell Extract	111

Immunoblot Analysis.....	111
Quantification of TNF- α	111
Quantification of PGE ₂ Levels.....	111
Quantification of RvD1 Levels.....	111
Statistical Analysis.....	111
5. ROLE OF TLR4 IN OXIDANT-INDUCED INFLAMMATORY RESPONSES IN PRIMARY PERITONEAL MACROPHAGES	112
Confirmation of the Experimental System	112
Confirmation of Mouse Genotypes.....	112
Empirically Determined Concentrations for Oxidants Used in Primary pM.....	119
Role of TLR4 in Oxidant-induced Dysregulation in Redox Homeostasis	123
Role of TLR4 in Oxidant-induced iROS Production.....	123
Role of TLR4 in Oxidant-mediated Changes in Cellular TAOC	126
Effects of Oxidants on Gene Expression and Production of TNF- α	131
Effects of Oxidants on Prostaglandin E ₂ Production and Cyclooxygenase Protein Expression.....	140
Effects of Oxidants on the Production of Resolvin D1 a Pro-resolution Lipid Mediator and its Receptor Expression	149
Discussion.....	155
6. MATERIAL and METHODS FOR SENSITIZATION OF PRIMARY PERITONEAL MACROPHAGES.....	174

Oxidants	174
Preparation of Potassium Peroxychromate (PPC)	174
Sensitization and Treatment of pM.....	174
RNA Extraction and Reverse Transcription	174
Quantitative-Reverse Transcription & Polymerase Chain Reaction (RT-qPCR)..	174
Quantification of PGE ₂	174
Statistical Analysis.....	175
7. TLR4 PRIMING SENSITIZES PRIMARY PERITONEAL MACROPHAGES TO OXIDANT-MEDIATED PGE ₂ PRODUCTION	176
Role of TLR4 Priming in Mediating Oxidants-induced PGE ₂ Production.....	177
Role of TLR4 Priming in Mediating Oxidants-induced Phospholipase A ₂ (PLA ₂)	179
Gene Expression	179
Role of TLR4 Priming in Mediating Oxidants-induced Cyclooxygenase (COX) Gene Expression	181
Role of TLR4 Priming in Mediating Oxidants-induced mPGES Gene Expression	182
Role of TLR4 Priming in Mediating Oxidant-induced Protein Expression	183
Discussion.....	188
General Conclusions	195
Future Studies	196

APPENDIX.....	197
Solutions	197
Cell Culture.....	197
3% Thioglycollate (TGC) Preparation.....	197
Tail Lysis buffer Preparation	198
Tris-EDTA buffer Preparation.....	198
Immunocytochemistry (ICC) Solutions.....	199
Flow cytometry Solutions	199
RNA Extraction Solution.....	199
Immunoblotting Solutions	200
Primers	202
Antibodies	204
Commercial Kits	206
REFERENCE LIST	207
VITA.....	237

ILLUSTRATIONS

Figures	page
1. Reactive oxygen/nitrogen species (RONS)..	3
2. Different exogenous sources of free radicals including reactive oxygen/nitrogen species (RONS).....	6
3. Endogenous sources of reactive oxygen/nitrogen species (RONS).....	11
4. Oxidative protein folding in endoplasmic reciculum (ER).....	16
5. Antioxidants.....	20
6. Structure of TLRs and signaling pathways of TLR4.....	31
7. PGE ₂ Biosynthetic pathway.....	38
8. Biosynthesis of Resolvin D1.....	43
9. Oxidants used in the study.....	51
10. Lipid peroxidation.....	64
11. Confirmation of the generation of ROS and RNS by oxidants by lipid peroxidation and protein tyrosine nitration.....	66
12. Expression of TLR4 mRNA and protein in RAW-Blue cells.....	68
13. Effects of oxidants on RAW-Blue cell viabilities and SEAP release.....	70
14. Effects of oxidants on RAW-Blue cell viability and SEAP release..	72
15. Effects of oxidants on levels of intracellular ROS (iROS) and total antioxidant capacity (TAOC) following stimulation of RAW-Blue cells..	75
16. Time course of oxidant-mediated iROS levels in RAW-Blue cells.	76
17. Pretreatment with anti-oxidant reagent EUK-134 reduced oxidants induced SEAP release in RAW-Blue cells.....	78

18. Pretreatment with anti-TLR4 pAb or CLI-095 reduced oxidants or LPS-EK induced SEAP release in RAW-Blue cells.....	80
19. Pretreatment with CLI-095 reduced oxidant-mediated increase in DNA binding of NF- κ B p65 in RAW-Blue cells.....	82
20. The role of TLR4 in PPC-stimulated p65 nuclear translocation.....	84
21. The role of of TLR4 in PPC-stimulated p65 nuclear translocation..	85
22. Role of TLR4 in oxidants mediated I κ B α degradation and phophsorylation in RAW-Blue cells.....	89
23. Role of TLR4 in oxidants induced TNF α and IL-10 production.....	91
24. Confirmation of mouse genotypes.....	113
25. Characterization of thioglycollate-elicited peritoneal exudate cells (PECs) isolated from TLR4-WT and TLR4-KO mice..	115
26. Characterization of peritoneal macrophages (pM) isolated from TLR4-WT and TLR4-KO mice.....	118
27. Determination of appropriate concentrations of oxidants for long-term exposure in primary peritoneal macrophages (pM).....	120
28. Determination of appropriate concentrations of oxidants for short-term exposure in primary peritoneal macrophages (pM).....	122
29. Role of TLR4 in oxidant-mediated iROS levels.....	124
30. Role of TLR4 oxidant-mediated iROS levels.....	125
31. Role of TLR4 in oxidant-mediated cellular total antioxidant capacity (TAOC) at 2 h.....	128
32. Role of of TLR4 in oxidant-mediated cellular total antioxidant capacity (TAOC) at 16 h.....	130

33. Role of Role of TLR4 in oxidant-mediated production of TNF α and IL-10 in peritoneal macrophages (pM).....	133
34. Effects of oxidants on TNF- α production and gene expression upon long-term exposure with low concentration of oxidants or LPS-EK.	136
35. Effects of oxidants on IL-1 β gene expression upon long-term exposure with oxidants or LPS-EK.	138
36. Effects of oxidants on iNOS protein expression upon long-term exposure oxidants or LPS-EK.....	139
37. Effects of of oxidants on prostaglandin E ₂ (PGE ₂) production upon short-term treatment paradigm..	142
38. Effects of oxidants on cyclooxygenase (COX) protein expression upon short-term treatment paradigm..	144
39. Effects of oxidants on prostaglandin E ₂ (PGE ₂) production up on long-term treatment paradigm..	146
40. Effects of oxidants on cyclooxygenase (COX) protein expression up on long-term treatment paradigm..	148
41. Effects of PPC on resolvin D1 (RvD1) production and its receptor FPR2 expression.. ..	151
42. Effects of of PPC on the expression 12-lipoxygenase (LOX) and 5-LOX.....	154
43. Proposed working model.	173
44. Role of TLR-4 on oxidant-induced prostaglandin E ₂ production in sensitized pM.. ..	178
45. Role of TLR-4 on oxidant-induced gene expression in sensitized pM.....	180

46. Role of TLR-4 on oxidant-induced protein expression in sensitized pM derived from TLR4-WT.....	185
47. Role of TLR-4 on oxidant-induced prostaglandin E ₂ production in sensitized pM derived from TLR4-KO mice..	187

TABLES

Table	page
1. Source of endogenous antioxidant.....	18
2. Toll-like receptors (TLRs) and their pathogen-associated molecular patterns (PAMPs) ligands.....	28
3: Treatment paradigm.....	53

ABBREVIATIONS

AA	Arachidonic acid
Ab	Antibody
AQP	Aquaporin
BSA	Bovine serum albumin
CD-14	Cluster of differentiation 14
CF	Cytoplasmic fraction
cGMP	Cyclic guanosine monophosphate
CLR	C-type lectin receptor
CNS	Central nerve system
Cys	Cysteine
COX	Cyclooxygenase
cPLA ₂	Cytosolic phospholipase A ₂
cPGES	Cytoplasmic prostaglandin E synthase
DD	Death domain
DHA	Docosahexaenoic acid
DMAPs	Damage associated molecular patterns
DPBS	Dulbecco's phosphate-buffered saline
ds RNA	Double-stranded RNA

EMR	Electromagnetic radiation
eNP	Engineered Nanoparticle
eNOS	Endothelial NOS
EPA	Eicosapentaenoic acid
ER	Endoplasmic Reticulum
ETC	Electron transport chain
FADH	Flavin adenine dinucleotide
GM-CSF	Granulocyte-macrophage colony-stimulating factor
GPCR	G-protein-coupled receptor
GSH	Glutathione
HMGB1	High mobility group box 1
HNE	Hydroxynonenal
HSP	Heat shock protein
IBD	Inflammatory bowel diseases
I κ B	Inhibitory nuclear κ B
IKK	I κ B kinase
IL	Interleukin
iNOS	Inducible NOS
IP	Immunoprecipitation

iPLA ₂	Ca ²⁺ -independent PLA ₂
IRAK	IL-1 associated kinase
iROS	Intracellular ROS
iTAOC	intracellular total antioxidant capacity
LDH	Lactate dehydrogenase
LOX	Lipoxygenase
LPS	Lipopolysaccharide
LRR	Leucine-rich repeats
MAPK	Mitogen-activated protein kinase
MCP1	Monocyte chemoattractant protein 1
MD-2	Myeloid differential protein-2
MDA	Malondialdehyde
MEKK	MAPK kinase kinase
Met	Methionine
MIP	Macrophage inflammatory protein
MS	Multiple Sclerosis
MsrA	Methionine sulphoxide reductase
mPGES	Microsomal prostaglandin E synthase
mRNA	Messenger RNA

mtROS	mitochondrial ROS
MyD88	Myeloid differentiating primary response gene 88
NADH	Nicotine adenine dinucleotide (reduced)
NF	Nuclear fraction
NF- κ B	Nuclear Factor- κ B
NLPs	NOD-like receptors
NLRP3	NLR pyrin domain containing 3
NO	Nitric Oxide
NOD	Nucleotide binding and oligomerization domain
NOS	NO synthase
nNOS	Neuronal NOS
NP	Nanoparticles
PAMPs	Pathogen-associated molecular patterns
PDI	Protein Disulfide Isomerase
PGE2	Prostaglandin E2
PI3K	Phosphoinositide 3 kinase
PLA ₂	Phospholipase A ₂
pM	Peritoneal macrophages
PN	Peroxynitrite

PPAR- γ	Peroxisome proliferator-activated receptor- γ
RA	Rheumatoid arthritis
RIG	Retinoic acid-inducible gene
RLP	RIG-like receptor
RNS	Reactive nitrogen species
RONS	Reactive oxygen species/nitrogen species
ROS	Reactive oxygen species
PPC	Potassium peroxychromate
PRR	Pattern recognize receptor
Rvs	Resolvins
SEAP	Secreted embryonic alkaline phosphatase
SOD	Superoxide dismutase
sPLA ₂ -V	Secretory group V phospholipase A ₂
SPM	Specialized pro-resolving mediators
ssRNA	Single stranded RNA
STAT3	Single transducer and activator of transcription 3
TAB	TAK binding protein
TACE	TNF- α -converting enzymes
TAK	Transforming growth factor β activated kinase

TAOC	Total antioxidant capacity
TBA	Thiobarbituric acid
TBARS	Thiobarbituric acid reactive substance
TIR	Toll/interleukin-1 receptor
TIRAP	TIR adaptor protein
TLR	Toll like receptor
TNF	Tumor Necrosis Factor
TNFR	TNF receptor
TRAF	Tumor necrosis factor receptor associated factor
TRAM	TIRF-related adaptor molecule
TRIF	TIR-domain-containing adaptor-inducing interferon- β
TrX	Thioredoxin
TrxR	Thioredoxin reductase
Tyr	Tyrosine
UBC13	Ubiquitin-conjugating enzyme 13
UEV1A	Ubiquitin-conjugating enzyme E2 variant 1
UV	Ultraviolet

ACKNOWLEDGEMENTS

I would like to thank all those people who helped me during my graduate studies in the interdisciplinary (IPh.D.) program. First, I would like to extend many thanks to my advisor Dr. Orisa J. Igwe for recruiting me from China, and his expertise, continuous support and excellent guidance through the dissertation work. My Ph.D. project would not have been possible without his expert guidance. I would also like to express my appreciation to my dissertation committee members: Dr. Jianping Wang from Division of Pharmacology and Toxicology, School of Pharmacy, Dr. Xiao-qiang (Sean) Yu from Division of Molecular Biology and Biochemistry, School of Biological Sciences, Dr. Charles S. Barnes from Department of Pathology and Laboratory Medicine, Children's Mercy Hospital and Clinical and Dr. Mingui Fu from Basic Medicine Sciences, School of Medicine for their expert advice and help regarding my project.

I would like to thank all my fellow graduate students from the School of Pharmacy, especially my lab mates, for their support, encouragement, and friendship. In addition, my thanks also go to all faculty and staff of School of Pharmacy for their encouragement and support.

I would also like to appreciate the financial support received from the School of Pharmacy as a teaching assistant. I also appreciate the financial support from the

UMKC School of Pharmacy Foundation and UMKC Women's Council, as well as a constant assistance given by School of Graduate Studies.

CHAPTER 1

INTRODUCTION

Reactive Oxygen and Nitrogen Species (RONS)

This chapter presents a foundational general overview of reactive oxygen and nitrogen species (RONS), their structures, sources (both extracellular & intracellular), and their functional relevance in biological systems. The section lays the frame work for appreciating the rationale for subsequent experiments, and for understanding the role of RONS in Toll-like receptor activation.

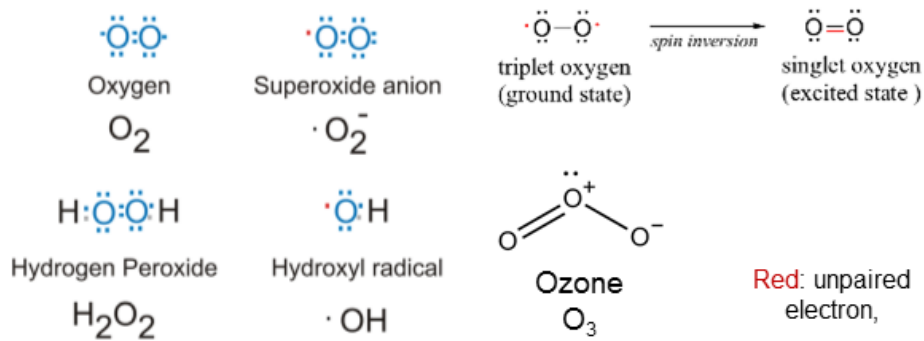
Chemistry of RONS

Free radicals are defined as atoms or group of atoms that have one or more unpaired electrons in their outer orbital. They can be positively charged, negatively charged or neutral (no charge). The prominent feature of free radicals is that they are highly chemically reactive because of the unpaired electron. There are many types of free radicals, but those of most concern in biological systems are derived from oxygen or nitrogen, thus their nomenclature of reactive oxygen species/nitrogen species (RONS). In fact, RONS encompass a family of molecules of distinct chemical entities, which are of critical importance in determining their chemical reactivity and biological responses.

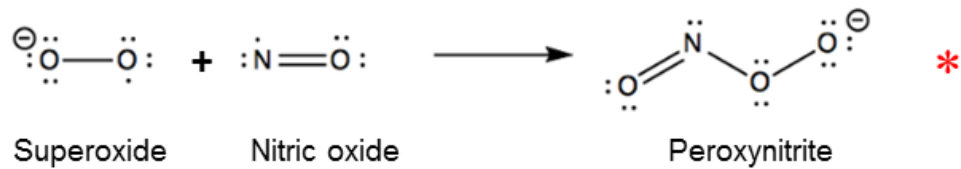
Reactive oxygen species (ROS) are the most important class of radical species generated in living system because oxygen is essential in aerobic life; and ROS are especially susceptible to additional radical formation. Here we highlight the most biologically relevant ROS, which include superoxide anion radical ($O_2^{\bullet-}$), hydroxyl radical ($\bullet OH$), hydrogen peroxide (H_2O_2), oxygen singlet (1O_2), and ozone (O_3).

Biologically relevant reactive nitrogen species (RNS) include nitric oxide (NO) and peroxyxynitrite (PN) radical (ONOO^\cdot). The structure of relevant ROS and RNS are shown in **Fig. 1**.

A. (i) ROS



(ii) RNS



B.

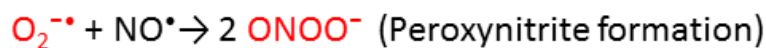
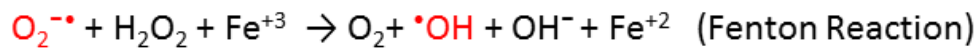
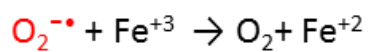
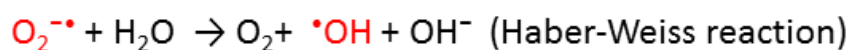
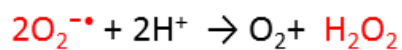
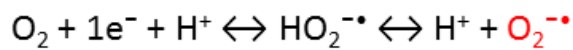


Figure 1. Reactive oxygen/nitrogen species (RONS). (A) Chemical structure of important RONS. *****: Hogg et al., 1992 (B) Generation of reactive oxygen species and peroxynitriate from superoxide via different reactions.

Superoxide Anion

Superoxide anion ($O_2^{\bullet-}$) is a reduced form of molecular oxygen (O_2) formed by accepting one electron with a half-life of 10^{-3} s. It is considered the 'primary' ROS and can generate secondary ROS by interacting with other molecules **Fig. 1 B** (Robb et al., 1999; Murakami et al., 2000; Buonocore et al., 2010). It undergoes spontaneous dismutation to H_2O_2 and O_2 under physiological conditions or catalyzed by superoxide dismutase (SOD). The passage of $O_2^{\bullet-}$ across biological membranes is highly restricted because of its negative charge. However, a voltage-gated anion channel present in the mitochondria mediates trans-membrane passage of $O_2^{\bullet-}$ from mitochondria to cytosol (Han et al., 2003).

Hydroxyl Radical ($\bullet OH$)

It is the neutral form of the hydroxide ion with a very short *in vivo* half-life of about 10^{-9} s. It is the most potent oxidizing species and is able to attack most cellular components. Due to its extreme reactivity, hydroxyl radical reacts with the first molecule it encounters and is eliminated at its site of formation/generation.

Hydrogen Peroxide (H_2O_2)

H_2O_2 is lipid soluble and highly diffusible, crossing plasma membrane through aquaporin (AQP) channels, such as AQP3 and AQP8 allowing H_2O_2 to enter cells that are in contact with one another (Miller et al., 2010). It is the least reactive molecule among ROS, with weak oxidizing and reducing properties.

Singlet Oxygen (1O_2)

As the excited state of oxygen, it can be generated by an input of energy that rearranges the electron. It is non-radical with mild reactivity. In singlet forms of oxygen,

the spin reaction is removed and oxidizing ability is greatly increased. Therefore, $^1\text{O}_2$ can directly oxidize proteins, DNA and lipids.

Ozone (O_3)

Ozone is an oxygen molecule consisting of three oxygen atoms (O_3) instead of the usual oxygen with two atoms (O_2) making ozone a very unstable and highly reactive molecule.

Nitric Oxide (NO)

NO is a gaseous free radical with greater stability, and readily diffusible through the plasma membranes.

PN (ONOO^-)

PN is formed in a rapid reaction between $\text{O}_2\bullet^-$ and NO (Hogg et al., 1992). It is a lipid soluble and potent oxidizing agent that causes direct protein nitration, DNA fragmentation and lipid oxidation.

Generation of RONS

Exogenous Sources of Free Radicals Generation

RONS can be generated from exposure to exogenous substances, such as exposure to nanoparticles (e.g. TiO_2 and SiO_2 nanoparticles), X-rays, ozone, cigarette smoke, air pollutants, and industrial chemicals, which humans are constantly exposed to (see **Fig.2**).

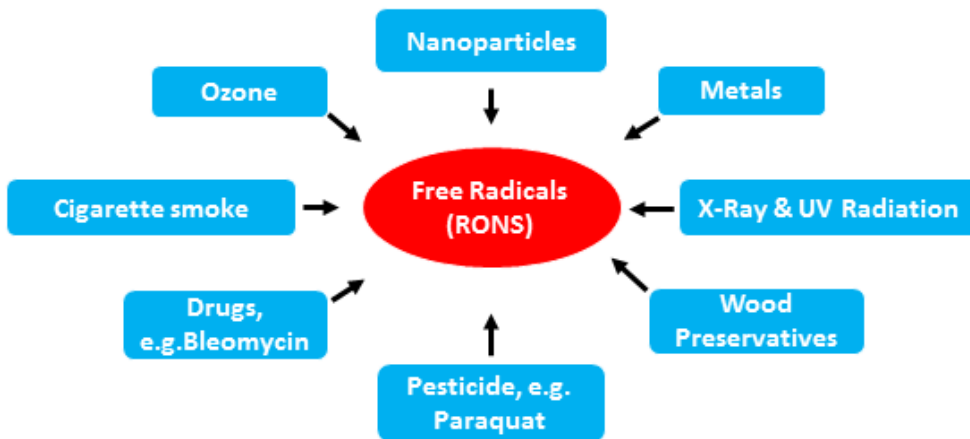


Figure 2. Different exogenous sources of free radicals including reactive oxygen/nitrogen species (RONS). Revised from (Lucas and Maes, 2013).

Nanoparticles

Nanoparticles (Berghaus et al.) are particles with at least one dimension smaller than 1 μ m and potentially as small as atomic and molecular length scales (Nel et al., 2006). NP can have amorphous or crystalline form with naturally and occurring engineered types. Natural NP include volcanic ash, soot from forest fires, or are produced as incidental byproducts of combustion processes (e.g., welding, diesel engines). Engineered NP (eNP) are now being manufactured and used in sporting goods, tires, stain-resistant clothing, sunscreens, cosmetics and electronics due to their novel physicochemical, thermal, and electrical properties. Increasingly, NP will be utilized in medical practice for purposes of diagnosis, imaging, and drug delivery (Nel et al., 2006). On the other hand, novel properties of eNP raise concerns about their consequent deleterious effects on biological systems. Accumulating clinical and experimental studies suggest that inhaled or instilled nanomaterials can induce pulmonary inflammation, oxidative stress, and distant organ involvement.

Generation of RONS is one of the most frequently reported mechanisms of NP-associated toxicities. The key factors involved in NP-induced production of RONS include (i) presence of oxidant functional groups on the reactive surface of NP, (ii) active redox cycling on the surface of NP in transition metal-based NP and (iii) interaction between particle and cells (Manke et al., 2013).

Free radicals can be generated from the surfaces of NP when oxidants and free radicals are bound to the particle surface as functional groups (Fubini and Hubbard, 2003). Interestingly, as the size of a particle decreases, its surface area increases allowing a greater proportion of reactive groups to be displayed on the surface. These

reactive groups in turn interact with O_2 leading to the formation of $O_2\bullet^-$ and another subsequent ROS.

Apart from surface-dependent properties, metals on the surface of NP, including iron (Fe), copper (Cu), and chromium (Cr), are capable of catalytically generating ROS through Fenton and Haber-Weiss reactions (see **Fig. 1 B**) (Voinov et al., 2011). In addition, NP can induce endogenous production of ROS following their interactions with biological systems. First, activation of immune cells can occur following cellular internalization of NP by activated immune cells (e.g., macrophages and neutrophils), which results in ROS production. Second, once NP gain access into cells, they can stimulate ROS production via impaired electron transport chain (ETC), activation of the NADPH oxidase enzyme system, and depolarization of mitochondrial membrane (Manke et al., 2013).

Cigarette Smoke

Epidemiological studies reveal that smoking is one of the most important environmental causes of human mortality and morbidity. RONS and stable free radicals are critical players in cigarette smoke-induced oxidative damage and carcinogenesis (Valavanidis et al., 2009). Thousands of RONS are produced upon burning or heating of tobacco leaves and these cannot be completely removed by cigarette butt filters (Huang et al., 2005). The products of combustion can be divided into gaseous and particulate components. RONS, such as H_2O_2 in the gaseous phase are often short-lived, affecting primarily the upper airways. RONS in the particulate phase are often long-lived and can generate secondary free radicals, e.g., semiquinone radicals, carbon-centered radicals (Pryor, 1992). Furthermore, cigarette smoke has synergistic effects

with environmental respirable particles (asbestos fibers, coal dust, etc.), ambient particulate matter and diesel exhaust particles with respect to OH• production (Valavanidis et al., 2009).

Ionizing Radiation

Generally, ionizing radiation can be divided into two types: particulate and electromagnetic radiations. Particulate radiation induces direct molecular disruption of electrons, protons, neutrons, atoms and particles, which can disrupt atoms and molecules in the cell, generating free radicals and ions (Vallyathan and Shi, 1997). Electromagnetic radiation (EMR), such as x-ray and ultraviolet (UV) light, can cause indirect heat-induced energy absorption that results in generation of free radicals in the tissue (Jurkiewicz and Buettner, 1994; Cheng and Caffrey, 1996; Jung et al., 2008; Lucas and Maes, 2013).

Other sources of EMR, which human beings are frequently exposed, include wireless communication, power transmissions broadcast, and medical equipment. In recent years there has been increasing public concern on potential health risks from exposure to electromagnetic fields (Hardell and Sage, 2008).

Ozone

Usually ozone is present in the higher layers of the atmosphere to protect the earth from sun's UV radiation. Ozone is produced from several photochemical reactions and from the combustion of automobile fuels. NO emission from automobiles is oxidized to nitrogen dioxide which in turn can be photochemically oxidized to ozone (Vallyathan and Shi, 1997). The mechanism of ozone-induced damage to cells is caused by the generation of free radicals. Various RONS and free radical can be produced from

ozone through different reactions. Ozone can be converted to H₂O₂ and other free radicals by chemicals, chlorofluorocarbons, nitrogen dioxide, combustion engines, and several industrial processes (Vallyathan and Shi, 1997). At an alkaline pH, ozone reacts with water and other biological molecules to produce $\cdot\text{OH}$ and $\text{O}_2\cdot^-$, respectively. Ozone can interact with aerosol particles to generate long-lived RONS (Hiscott et al.) with chemical lifetime of more than 100 s (Lucas and Maes, 2013).

Other extracellular sources

RONS can be generated from pesticides, drugs, wood preservation chemicals, and toluene as well (Vallyathan and Shi, 1997; Lucas and Maes, 2013).

Endogenous Sources of RONS

RONS are continuously generated, transformed and consumed in all living organisms. The subcellular location where a particular RONS is generated is a key consideration for its chemistry and biological effects. Here we highlight four major subcellular regions for RONS generation under physiological conditions (**Fig. 3**).

Mitochondria and Electron Transfer

Among the various organelles within most mammalian cells, the mitochondria are thought to be the largest contributor to intracellular oxidant production. Approximately 90% of cellular RONS, in particular superoxide anion, can be traced back to the mitochondria. Generation of mitochondrial RONS (mtRONS) mainly takes place during the process of oxidative phosphorylation at the electron transport chain (ETC), which is located on the inner mitochondrial membrane.

The ETC consists of four large protein complexes: NADH-Q oxidoreductase, Q-cytochrome c oxidoreductase, cytochrome c oxidase and succinate-Q reductase,

which are also known as complexes I, II, II and IV, respectively. All generate RONS. Electrons at complex I and complex II pass through the ETC and ultimately reduce oxygen molecule to water at complex IV.

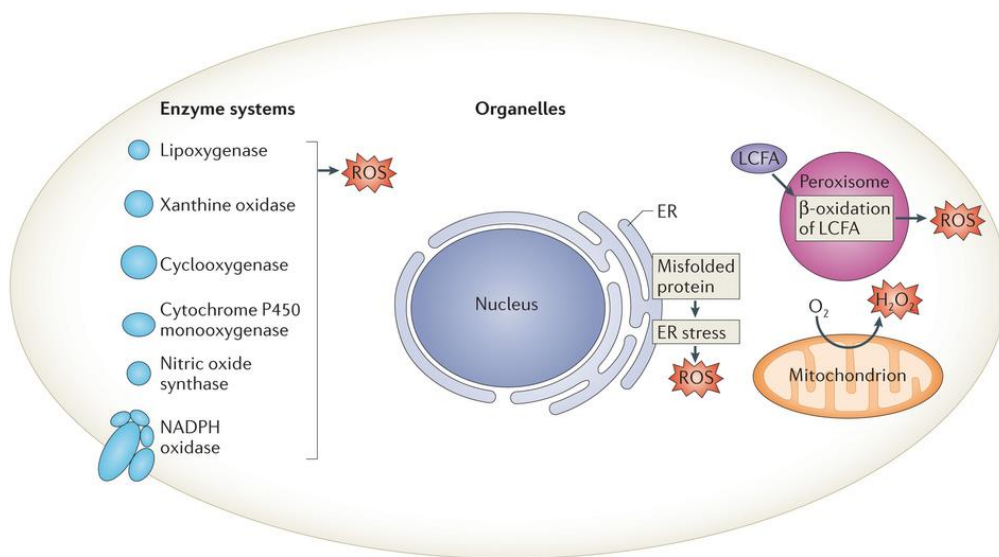


Figure 3. Endogenous sources of reactive oxygen/nitrogen species (RONS). Various organelles within the cell can generate RONS with a potential additive or synergistic interactions with exogenous RONS. Revised from (Holmstrom and Finkel, 2014)

However, either by accident or by design, the process of electron transport is imperfect. Leakage of electrons at complex I and III leads to partial reduction of oxygen O_2 to generate superoxide anion, which is subsequently converted to H_2O_2 . Approximately 0.2 to 2.0% of the O_2 consumed by mitochondria generates superoxide (Li et al., 2013). This fact has been identified for 50 years (Jensen, 1966), but the precise magnitude of ROS generation has not been fully understood. Studies of isolated mitochondria have revealed that the two distinct molecular sites of superoxide production are complex I and complex III (Balaban et al., 2005).

Realistically, mitochondrial leakage of ROS is an unavoidable consequence of aerobic respiration. It is believed that cells have evolved exquisite mechanisms to harness mitochondrial RONS in a controlled manner for physiological benefits (Dickinson and Chang, 2011).

Cell Membrane and NADPH Oxidases

Other key sources of physiological RONS are the NOX family of NADPH oxidases (NOXs) and their dual oxidase relatives (Duox). NOX family is comprised of seven (7) members with various tissue distributions and activation mechanisms (Panday et al., 2015). NOXs are transmembrane proteins that transport electrons from cytosolic NADPH to molecular oxygen to purposely produce superoxide ($O_2^{\bullet-}$). Typically, NOX is comprised of six different subunits that interact to form an active enzyme complex responsible for superoxide anion production.

NOXs were originally described in the context of their functional relevance in neutrophils. After activation by various inflammatory mediators, neutrophils produce a large amount of ROS as part of their essential role in host defense.

However, the expression of NOX in various tissue provides evidence that the intentional generation of ROS, rather than being a unique characteristic of phagocytes, is a general feature of many and perhaps all cell types (Lambeth, 2004). Excessive ROS produced from NOX contributes to various diseases. The NOX-mediated generation of superoxide has been clinically associated with atherosclerosis (a chronic inflammatory disease characterized by lipid retention and atherosclerotic lesions) (Ma et al., 2011). In addition, increased level of superoxide via the activation of NOX exacerbates pulmonary inflammation and contributes to the chronicity of cigarette-related lung diseases (Talbot et al., 2011).

Cytosol and Nitric Oxide Synthases

Nitric oxide (NO) is identified as an important free radical in biology and pathology. NO is generated by enzymatic oxidation of L-arginine by NO synthase (NOS). There are three isoforms of NOS: inducible NOS (iNOS), endothelial NOS (eNOS), and neuronal NOS (nNOS). Generally, eNOS and nNOS are constitutively expressed in endothelial cells, and central and peripheral neurons, respectively. The expression of constitutive NOS can be activated as result of calmodulin (CaM) binding following a rise in intracellular Ca^{2+} (MacMicking et al., 1997). Vascular NO dilates all types of blood vessels by stimulating soluble guanylyl cyclase and increasing cyclic guanosine monophosphate (cGMP) in smooth muscle cells.

In contrast, activation of iNOS is calcium-independent. The expression of iNOS can be transcriptionally regulated by pro-inflammatory cytokines [such as tumor necrosis factor- α (TNF- α), Interleukin (IL)-6] and /or microorganism resulting in abundant NO production (Patel et al., 2007b). NO produced by activated macrophages

via iNOS is implicated in various human autoimmune and chronically inflammatory diseases. For example, in active demyelinating lesions of multiple sclerosis (MS) patients, macrophages were found to stain for iNOS protein and nitrotyrosine suggesting nitrosative stress. The NO oxidative product nitrite was found to be increased 6 to 35-fold in the synovial fluid of RA patients compared with osteoarthritis (Kroncke et al., 1998).

Moreover, nitric oxide and superoxide interact with each other to generate PN (OONO). The sites of PN formation are assumed to be spatially associated with the generation of superoxide, such as plasma membrane NOX, or the mitochondrial respiratory complexes. This is because although NO is a relatively stable and highly diffusible free radical, superoxide is much short-lived and has restricted diffusion (Szabo et al., 2007).

Endoplasmic Reticulum and Oxidative Protein Folding

Proteins need to acquire specific three-dimensional structure for function. Protein folding is the most error-prone step in gene expression. In eukaryotic cells, the endoplasmic reticulum (ER) is a membrane-bound organelle and specialized for the folding and post-translational maturation of almost all membrane proteins and most secreted proteins (Cao and Kaufman, 2014).

Oxidative protein folding of eukaryotic cells is mediated by ER protein disulfide isomerase (PDI) and glycoprotein endoplasmic reticulum oxidoreductin-1 (Ero1). PDI is a multifunctional oxidoreductase and chaperone that catalyzes the formation, isomerization, and reduction of disulfide bonds in the ER. As **Fig. 4** shows, cysteine residues of PDI accept two electrons from the cysteine residues in polypeptide

substrates, resulting in the reduction of PDI and oxidation of the substrate. Then PDI transfers the electrons to the acceptor Ero1 to start another cycle of disulfide bond formation. After accepting electrons from PDI, Ero1 transfers the electrons to molecular oxygen leading to H₂O₂ production for each disulfide bond formation (Dickinson and Chang, 2011). The highly oxidized environment in the ER, which is established by GSH/GSSG, is essential for oxidative protein folding.

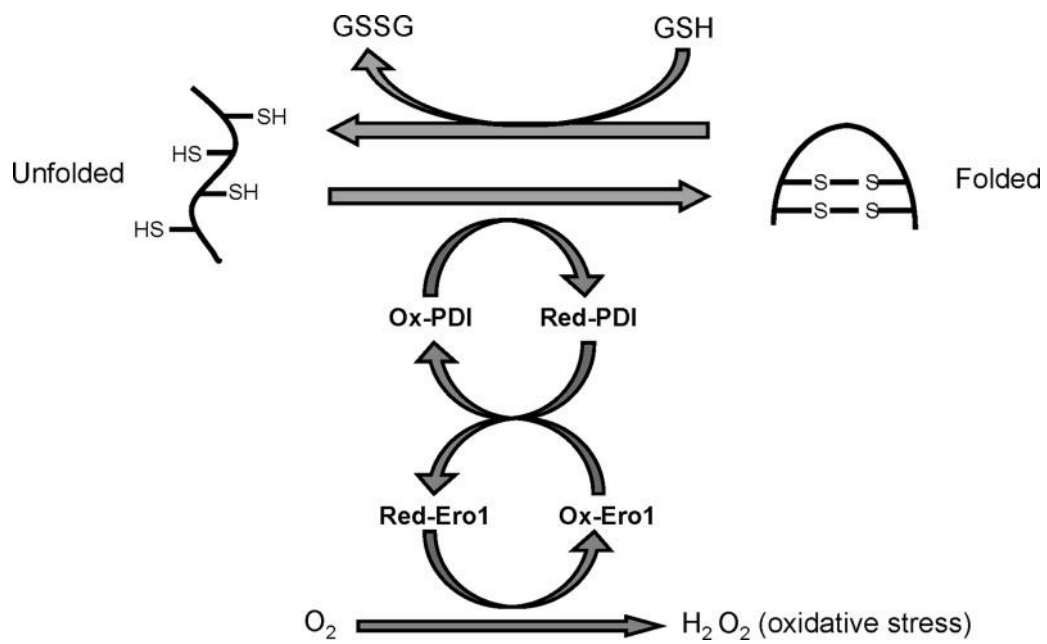


Figure 4. Oxidative protein folding in endoplasmic reticulum (ER). Oxidative protein folding in eukaryotic cells occurs in the ER, which is mediated by ER protein protein disulfide isomerase (PDI) and endoplasmic reticulum oxidoreductin-1 (ERO1). ROS are generated as a byproduct of oxidative protein folding. Scheme is revised from (Cao and Kaufman, 2014)

Accumulation of unfolded and misfolded protein in the ER lumen is known as ER stress. In many ER stress-related *in vitro* and *in vivo* models, ER stress and oxidative stress accentuate each other in a positive feed-forward loop (Cao and Kaufman, 2014). ER stress and oxidative stress are coupled in many inflammatory-related diseases including inflammatory bowel diseases (IBD), chronic obstructive pulmonary diseases, chronic kidney diseases, alcoholic liver diseases, and rheumatoid arthritis (Cao and Kaufman, 2014).

Other endogenous sources of ROS include xanthine oxidase, lipoxygenase, cyclooxygenases, and cytochrome P450s (Nathan and Cunningham-Bussel, 2013). In addition, superoxide anion ($O_2^{\bullet-}$) and/or H_2O_2 can be converted to hydroxyl radical (OH^{\bullet}) by free copper or iron ions, which are released from heme groups or metal storage proteins.

Cellular Antioxidant Systems

Evolutionarily, cells possess antioxidant systems to counteract RONS and reduce their damage. The ability of cells to counteract ROS is of critical importance in determining the biological consequences of ROS production. The total antioxidant system can be divided into non-enzymatic and enzymatic systems (**Table 1**).

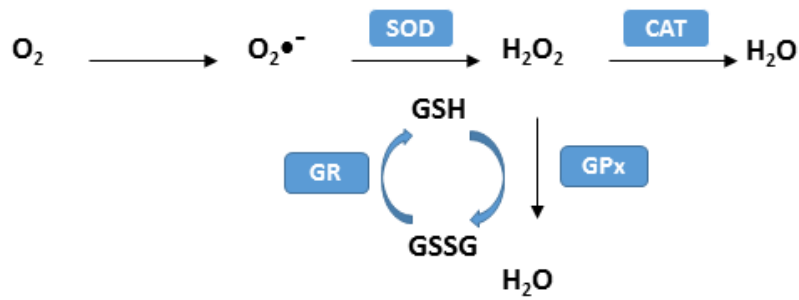
Table 1. Source of endogenous antioxidant. Revised from Nathan and Cunningham-Bussel, 2013

Box 1 Sources of endogenous antioxidants
Enzymatic systems
<ul style="list-style-type: none">• Superoxide dismutase• Catalases• Glutathione peroxidases• Glutathione reductase• Thioredoxins• Thioredoxin reductase• Methionine sulphoxide reductases• Peroxiredoxins
Non-enzymatic systems
<ul style="list-style-type: none">• Ascorbate• Pyruvate• Transferrin• β-Carotene

The major enzymatic antioxidant system includes superoxide dismutases (SOD), catalase, and glutathione (GSH) redox cycle. Superoxide generated by mitochondria is quickly dismutated to H_2O_2 by either manganese (Mn) or copper/zinc (Cu/Zn)-dependent SOD, which are located in the matrix and intermembrane space, respectively. When H_2O_2 reaches high concentration, it is then degraded into water and oxygen by catalase (CAT) (**Fig.5 A**). Catabolism of ROS is especially important in mitochondria because the enzymes that drive ATP production are rich in thiol residues that can be irreversibly oxidized.

The glutathione cycle consists of glutathione peroxidase (GPx) and glutathione reductase. Reduced GSH reduces hydrogen peroxide (H_2O_2) into water, forming oxidized glutathione (GSSG) in the process. GSSG in turn is converted back to GSH by glutathione reductase (**Fig.5 A**). A balance between GSH and GSSG maintains the redox homeostasis within cell. The cytosol is a reducing environment with a GSH/GSSG ratio ranging from 30:1 to 100:1.

A.



B.

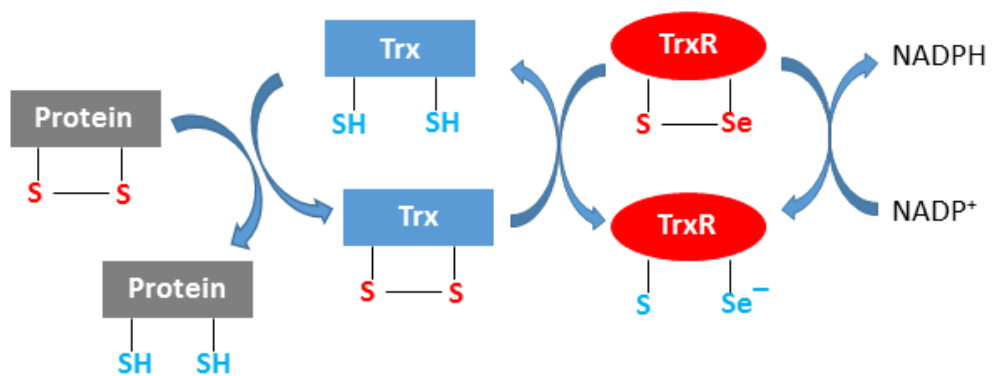


Figure 5. Antioxidants. (A) Antioxidant effects of superoxide dismutase (SOD), catalase and glutathione cycle. (B) Antioxidant effects of thioredoxins (Trx) and thioredoxin reductase (TrxR) cycle. Revised from (Karlenius and Tonissen, 2010)

More physiologically important ROS-regulating enzymes are now well recognized. The thioredoxins (Trx) system is composed of Trx, thioredoxin reductase (TrxR) and NADPH. It catalyzes disulfide bond reduction in many proteins maintaining a reducing intracellular redox state (**Fig. 5 B**) (Holmgren and Lu, 2010). Methionine (Met) is easily oxidized into methionine sulfoxide (Met O). Peptide methionine sulphoxide reductase (Msr A) can reduce Met O back to Met to maintain the reduced state of amino acids (Weissbach et al., 2002). PN reductase, known as peroxiredoxin, catalytically detoxifies PN to nitrite rapidly enough to forestall the oxidation of bystander molecules such as DNA (Bryk et al., 2000).

In addition, many small molecules including ascorbate, pyruvate, β -carotene and transferrin, react with ROS non-enzymatically. They can be recycled or replenished to maintain their ROS-buffering capacity.

Oxidative Stress

Conventionally, *oxidative stress* results when cellular production of RONS exceeds the cellular ability to catabolize them. However, the term “stress” is considered as imprecise because of the broad restricted range of ROS signaling running from adaptive to maladaptive. Under physiological conditions, ROS production is restricted to appropriate subcellular locations, time duration, levels and even molecular species to maintain reduction-oxidation (redox) homeostasis through antioxidants. Therefore, RONS generation at an inappropriate place or time, for too long, at too high a level or of inappropriate form can cause macromolecular damage resulting in irreversibly impaired cellular function or pathological gain of function (Nathan and Cunningham-Bussel, 2013). RONS were previously thought to be purely toxic, and merely the by-

products of cellular metabolism. Accumulating evidence now suggests that RONS are critical for healthy cell function and serve as important signaling molecules (Sena and Chandel, 2012). For example, under normal physiological conditions, RONS derived from mitochondria play an invaluable role in vascular homeostasis (Li et al., 2013).

Inflammation

Inflammation is a complex, highly regulated sequences of events that can be initiated by a variety of stimuli, such as pathogens, noxious mechanical, and chemical agents, and autoimmune responses. The subsequent cascade of events is characterized by the signs and symptoms of redness, swelling, heat, and pain. Inflammatory responses usually occur in vascularized connective tissue, including plasma, circulating cells, blood vessels, and cellular and extracellular components. This corresponds with increased microvascular caliber, enhanced vascular permeability, recruitment of immune cells, and release of inflammatory mediators (Fujiwara and Kobayashi, 2005).

The process of inflammation can be divided into two stages: short-term (acute) and long-term (chronic) inflammation. Localized short-term inflammation is a part of the host's normal protective response to tissue injury and infection by invading microbial pathogens(Ricciotti and FitzGerald, 2011). Although the short-term inflammation is protective to the host, if kept unchecked, it can result in a long-term, chronic and systemic inflammatory disorders (Ricciotti and FitzGerald, 2011). Indeed, some of the most common and difficult to treat diseases are linked to excessive, uncontrollable or chronic inflammation, including cardiovascular diseases, rheumatoid arthritis, asthma, diabetes, and inflammatory bowel diseases (IBD), as well as neurological disorders (Ricciotti and FitzGerald, 2011).

The ultimate goal of inflammatory response to protect the host and get rid of invading organism or to repair cellular injury. However, exaggerated or unregulated prolonged inflammatory process can induce tissue damage resulting in many chronic diseases. At the site of inflammation, activated cells release enzymes (neutral proteases,

collagenase, phosphatase, etc.), reactive species, chemical mediators (eicosanoids, cytokines, chemokines, nitric oxide, etc.) and thereby induce tissue damage and oxidative stress (Biswas, 2016).

Oxidative Stress: An Important Mediator of Inflammation

Oxidative (or oxidant) stress and inflammation are interdependent. They are linked in many chronic diseases, such as cancer, diabetes, aging, hypertension and cardiovascular diseases, and neurodegenerative diseases (Biswas, 2016). Oxidative stress can induce inflammation through activation of multiple pathways. First, RONS can induce inflammatory pathways by activation of transcription factor nuclear factor- κ B (NF- κ B) (Takada et al., 2003). PN profoundly influences inflammatory responses by oxidation and nitration of cytosolic and nuclear receptor (such as peroxisome proliferator-activated receptor (PPAR)- γ) and activation of transcription factors (such as NF- κ B) (Szabo et al., 2007).

Second, ROS can activate inflammatory responses through inflammasome activation. A recent study has revealed that mitochondria-derived ROS can activate the cytosolic nucleotide binding and oligomerization domain (NOD)-like receptor (NLR) family, NLRP3-containing inflammasome (Zhou et al., 2011) leading to the maturation and secretion of proinflammatory cytokines, such as interleukin (IL)-1 β , IL-18. More recent studies have identified that mitochondria-derived ROS can promote the production of pro-inflammatory cytokines in TNF receptor-1 (TNFR-1)-associated periodic syndrome, which is an autoinflammatory disorder associated with enhanced innate immune responsiveness (Bulua et al., 2011).

Furthermore, the ROS-induced DNA base modification has also been shown to induce inflammation. 7,8-Dihydro-8-oxoguanine (8-oxo G) is the most frequent oxidized product of DNA and RNA. Repairing of 8-oxo G by the DNA base excision repair pathway (OGG1) can induce the activation of mitogen-activated protein kinase (MAPK), phosphoinositide 3 kinase (PI3K), and NF- κ B, resulting in pro-inflammatory gene expression (Aguilera-Aguirre et al., 2014). Furthermore, oxidized cysteine (Cys) and its disulfide (CyS-S) of the extracellular redox control system can trigger monocyte adhesion, activate NF- κ B, and increase the expression of the pro-inflammatory cytokine IL-1 β (Iyer et al., 2009).

On the other hand, during inflammation, mast cells and leukocytes are recruited to the sites of damage, leading to a 'respiratory burst' and subsequent enhanced release and accumulation of RONS. Then inflammatory cells, such as macrophages release cytokines, chemokines, or prostaglandins which further recruit inflammatory cells to the sites of damage exaggerating oxidative stress. Therefore, oxidative stress and inflammation are tightly related pathophysiological events that are coupled to one another (Reuter et al., 2010).

Toll-like receptor (TLR) Activation: A Crucial Initiator of Inflammation

Toll like Receptor (TLRs)

As a crucial component of the innate immune reaction, germline-encoded pattern recognition receptors (PRR) are responsible for sensing the presence of microorganism (Takeuchi and Akira, 2010). TLRs, the prototype PRR, are the mammalian homologues of Toll protein present in *Drosophila*, which plays an essential role in development (Anderson et al., 1985) and immunity (Lemaitre et al., 1996). TLRs

also play a role in the activation of innate as well as adaptive immune response in mammals. To date, the ten (10) TLRs have been identified in humans and twelve (12) in mice. TLR12 and TLR13 are not expressed in humans (Takeuchi and Akira, 2010).

As PRR, TLRs are organized to recognize invading microbial pathogens through interaction with pathogen associated molecular patterns (PAMPs), which are conserved and possess unique structures in microbes. The TLR expressional location, ligands of PAMPs and ligands' sources are listed in **Table 2**. As **Table 2** shows, TLR3, TLR7, TLR8 and TLR9, which recognize DNA or RNA, reside in endosomal vesicles inside of cell. However, TLRs, which recognize protein and lipid, such as TLR1, TLR2, TLR4, and TLR5, TLR6 and TLR10, are expressed on the cell surfaces. Ten TLRs have recognized ligands, and collectively these receptors detect all known infectious agents.

However, TLRs are not organized to just distinguish self from non-self, but instead to recognize threats dangerous to the host, such as substances released in injury or in tissue damage designated damage associated molecular patterns (DAMPs), which suggests a role beyond that of simple pathogen recognition. As the host-derived (endogenous) non-microbial pro-inflammatory molecules, DAMPs are intracellularly sequestered and remain unrecognized by the immune system under normal physiological conditions. However, under conditions of cellular stress or tissue injury, DAMPs are either actively secreted by immune cells or passively released from dying cells or the damaged extracellular matrix as “alarmins” (Land, 2015). The typical DAMPs include high mobility group box 1 (HMGB1), uric acid, heat shock proteins (HSPs), as well as hyaluronan, and heparan sulphate, which are components of the extracellular matrix. There is mounting evidence that TLRs, in particular TLR2 and

TLR4, sense endogenous DAMPs to mediate “sterile inflammation” in the absence of invading pathogens (Paul-Clark et al., 2009; Kawai and Akira, 2010).

Table 2. Toll-like receptors (TLRs) and their pathogen-associated molecular patterns (PAMPs) ligands. Modified from (Takeuchi and Akira, 2010)

TLRs	Localization	Ligand	Sources of the ligand
TLR1	Plasma membrane	Triacyl lipoprotein	Bacteria, mycoplasma
TLR2	Plasma membrane	Lipoprotein	Bacteria (gram-positive), viruses, parasites, self
TLR3	Endolysosome	dsRNA	Virus
TLR4	Plasma membrane	LPS	Bacteria (gram-negative), viruses, self
TLR5	Plasma membrane	Flagellin	Bacteria
TLR6	Plasma membrane	Diacyl lipoprotein	Bacteria, viruses
TLR7 (human TLR8)	Endolysosome	ssRNA	Virus, bacteria, self
TLR9	Endolysosome	CpG-DNA	Virus, bacteria, protozoa
TLR10	Endolysosome	Unknown	Unknown
TLR11	Plasma membrane	Profilin-like molecule	Protozoa

TLRs are expressed in a wide variety of immune as well as non-immune cells such as hepatocytes, vascular smooth muscle cells and neurons (Gill et al., 2010). However, immune cells, such as macrophages, microglia, oligodendrocytes, astrocytes, dendritic cells (Groeger et al.) or neutrophils express an almost complete panel of the different TLRs while other cells only express a restricted repertoire (Ospelt and Gay, 2010). Naturally, the expression of TLRs tends to lie at sites of high host-pathogen interactions such as intestinal or airway epithelial cells. However, in line with the above mentioned hypothesis that TLRs are activated in response to danger signals, functional TLR expression has also been found in cell types which do not fulfill such barrier function. Thus functional TLR expressed in different cells of the central nervous system (CNS), kidney, and synovial fibroblasts appears to be involved in non-infectious pathological events such as ischemic or traumatic injury or autoimmunity (Ospelt and Gay, 2010).

TLR4-mediated NF- κ B Hyper Inflammatory Signaling Pathway

TLR4, being the first member of the TLR family to be discovered, is one of the best characterized PRR. It recognizes a broad variety of substances from viruses, fungus and mycoplasma associated with the classical ligand, lipopolysaccharide (LPS), a part of cell wall of gram-negative bacteria. In this study, we are particularly interested in TLR4 for following reasons: (1) TLR4 can recognize DAMPs such as HMGB1 to play a role in “sterile” inflammation (Zhang et al., 2015); (2) unlike other TLRs, TLR4 responds to a wide range of non-canonical ligands, including nickel (Schmidt et al., 2010), cobalt (Raghavan et al., 2012), fibrinogen (Smiley et al., 2001) and many environmental factors (such as ozone, atmospheric particulate matter, long-lived reactive oxygen intermediates, and nanoparticles etc.) (Lucas and Maes, 2013).

Like other TLRs, TLR4 is a single-pass type I glycoproteins. TLRs and IL-1Rs share a conserved region of ~200 amino acids in their cytoplasmic domain, known as Toll/interleukin-1 (IL-1) receptor (TIR) domain.

As **Fig.6 A** shows, within the TIR domain, there are three conserved boxes, which are crucial for signal transduction. The extracellular domain of TLR4 contains 19-25 tandem copies of the leucine-rich repeats (LRRs) (Akira and Takeda, 2004). Extracellular LRR domains are crucial for ligand recognition.

The best understood mechanism of TLR4 activation comes from the studies with LPS (Lu et al., 2008). Several proteins are involved in LPS-stimulated TLR4 activation. First, LPS-binding protein (LPS-BP) transfers LPS to cluster of differentiation 14 (CD14). CD14, in turn, facilitates the transfer of LPS to the TLR4/myeloid differential protein-2 (MD-2) complex. MD-2 is physically associated with TLR4.

Upon ligand binding, TLR4 undergoes dimerization and initiate intracellular cascades via recruitment of TIR domain containing adaptor proteins including myeloid differentiating primary response gene 88 (MyD88), TIR adaptor protein (TIRAP), TIR-domain-containing adapter-inducing interferon- β (TRIF), and TRIF-related adaptor molecule (TRAM) (Gill et al., 2010). Generally, TLR4 signaling is largely divided into two pathways: MyD88-dependent and TRIF-dependent which is known as MyD88-independent pathway. Both of these pathways commonly activate the canonical NF- κ B pathway resulting in induction of inflammatory cytokines. In this study, we have focused on the MyD88-dependent pathway.

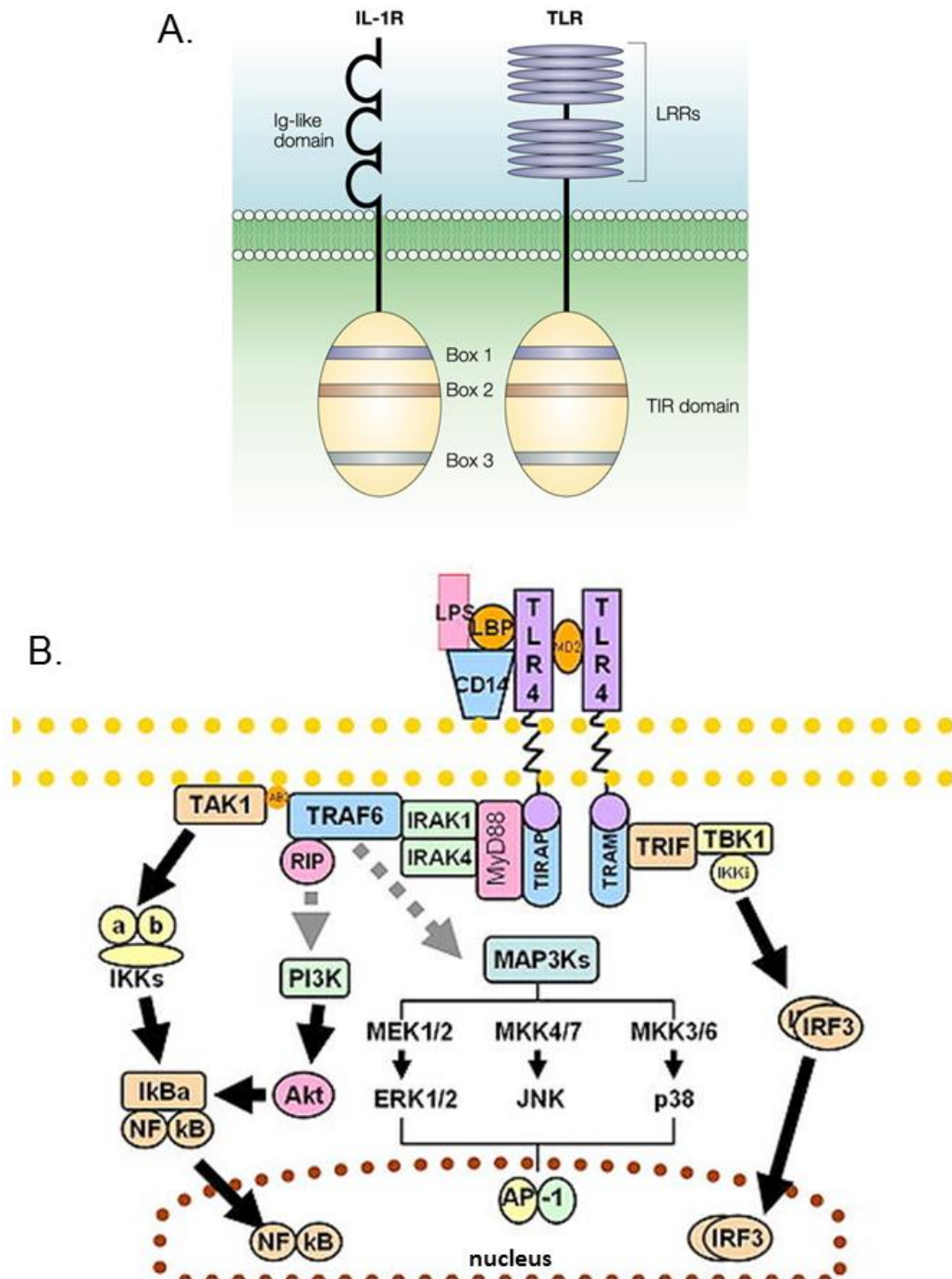


Figure 6. Structure of TLRs and signaling pathways of TLR4. (A) Structure of TLRs. See (Akira and Takeda, 2004). (B) TLR4/NF-κB signaling pathway <https://www.wikipedia.org/>. Abbreviations: LBP: LPS binding protein, CD14: cluster of differentiation 14, MD-2: Myeloid differentiation protein 2, TLR: toll-like receptor, MyD88: myeloid differentiating primary response gene 88, IRAK: IL-1 receptor-associated kinase, TRAF: tumor-necrosis-factor receptor associated factor 6, TAK: transforming growth factor β activated kinase, TAB: TAK1-binding protein, UBC13: ubiquitin-conjugating enzyme 13, UEV1A: ubiquitin-conjugating enzyme E2 variant 1, NF-κB: nuclear factor κB, IKK: inhibitor of NF-κB (IκB)-kinase

In the MyD88-dependent pathway (**Fig.6 B**), TLR4 dimerization triggers the association of MyD88, which in turn recruits IL-1 receptor-associated kinase (IRAK) 4 through interaction with the death domain (DD), thereby allowing the association of IRAK1. IRAK4 then phosphorylates and activates IRAK1, which stimulate recruitment of tumor-necrosis-factor receptor associated factor 6 (TRAF6) to the receptor complex. Phosphorylated IRAK1 and TRAF 6 then dissociate from the receptor and form a complex with transforming growth factor β activated kinase (TAK1), TAK1-binding protein (Merolla et al.) TAB 1 and TAB2 at the plasma membrane (Merolla et al.). After degradation of IRAK1 at the plasma membrane, the remaining complex (containing TRAF6, TAK1, TAB1 and TAB2) translocates to the cytosol, where it associates with two ubiquitin ligases ubiquitin-conjugating enzyme 13 (UBC13) and ubiquitin-conjugating enzyme E2 variant 1 (UEV1A). This leads to degradation of TRAF6 and activation of TAK1.

TAK1, in turn, phosphorylates both the inhibitor of nuclear factor- κ B (I κ B)-kinase (IKK) complex and MAPK. In the present study, we focused on the TLR4/NF- κ B signaling pathway. The IKK complex consisting of IKK α , IKK β and IKK γ then induces the phosphorylation of I κ B, which leads to its ubiquitination and subsequent degradation, thereby allowing NF- κ B to translocate to the nucleus and induce the expression of inflammatory cytokines (Akira and Takeda, 2004).

NF- κ B: A Critical Transcription Factor for Inflammatory Response

NF- κ B was the first well-documented example of a transcription factor whose binding to DNA is induced by a post-translational mechanism (Smale, 2011). Since NF- κ B is an inducible rather than cell type-specific transcription factor that responds

to pro-inflammatory cytokines and microbial products, NF- κ B is thought of as the key regulator of inflammation (Ben-Neriah and Karin, 2011).

Indeed, NF- κ B binding sites have been found in the promoter regions of about 500 genes encoding of most cytokines and chemokines, which are implicated in inflammation related responses (Smale, 2011). NF- κ B activation has been shown to be essential for their induction in response to immune and inflammatory challenges (Ben-Neriah and Karin, 2011). Furthermore, activated NF- κ B has been found in many chronic inflammatory conditions, including rheumatoid arthritis (RA) (Tak and Firestein, 2001), cancer (Ben-Neriah and Karin, 2011), IBD (Zhang and Li, 2014), and neurodegenerative disorders (Shih et al., 2015). Correspondingly, mouse models of these diseases respond positively to inhibition of NF- κ B, which has raised enthusiasm about NF- κ B and IKK as therapeutic targets in chronic inflammation and autoimmunity (Ben-Neriah and Karin, 2011).

Indeed, the roles of NF- κ B in inflammation are very complex. In addition to its pro-inflammatory function in the onset of short-term inflammation, NF- κ B may also exert a direct anti-inflammatory effect through induction of the expression of anti-inflammatory genes.

Key Pro-inflammatory Mediators Following NF- κ B Activation

NF- κ B activation induces the expression of genes encoding inflammatory mediators. These mediators bind to their receptors expressed on immune cells to promote inflammation by increasing the permeability of the vascular endothelium to plasma. This increases the propensity of neutrophils to bind to the microvascular endothelial surface and move out of the vascular system to cause the release of

antimicrobial peptides and ROS (Tak and Firestein, 2001). In the foregoing experiments, we have highlighted **TNF- α** (as a representative pro-inflammatory cytokine), **IL-10** (as a representative anti-inflammatory cytokine) prostaglandin E₂ (**PGE₂**) (as a representative pro-inflammatory lipid mediators) and **resolving D1** (7S, 8R, 17S-trihydroxy-4Z, 9E, 11E, 13Z, 15E, 19Z-docosaenoic acid, RvD1) (as a representative anti-inflammatory lipid mediator).

TNF- α

TNF- α is a master of inflammation and a key player in the cytokine network. It is rapidly released after trauma, infection, or exposure to bacterial-derived LPS and has been shown to be one the most abundant early mediators in inflamed tissue (Parameswaran and Patial, 2010). Messenger RNA (mRNA) for TNF- α is widely expressed. The regulation of its gene expression in myelomonocytic cells is complex and stimulus-dependent. However, the binding site for NF- κ B has been identified in the proximal promoter region of the TNF- α gene (Liu et al., 2000). Thus, NF- κ B is a key regulator for TNF- α gene expression and production. Newly synthesized pro-TNF- α (26-kDa) is expressed on the plasma membrane, and is then cleaved through the action of TNF- α -converting enzymes (TACE) to release a mature soluble 17-kDa soluble TNF- α (Black et al., 1997). Cells of the myelomonocytic lineage including macrophages, astroglia, microglia, Kupffer cells, and alveolar macrophages are the primary synthesizers of TNF- α .

TNF- α acts through two transmembrane receptors: TNF receptor 1 (TNFR1), known as p55 or p60, and TNF receptor 2 (TNFR2), known as p75 or p80. Activation of TNFR1 seems to be primarily responsible for pro-inflammatory and shock-

producing properties TNF- α (Parameswaran and Patial, 2010). Mice with TNFR1 deficiency are resistant to LPS-induced mortality and hepatic injury (Josephs et al., 2000). In addition, stimulation of TNFR1 triggers intracellular signaling cascades and results in activation of receptor interacting protein-1 (RIP1)/ MAP kinase kinase kinase 3(MEKK3)/TAK1-mediated activation of the NF- κ B pathway, which forms a positive feedback loop (Parameswaran and Patial, 2010).

The role of TNF- α in inflammatory diseases, for example RA, mainly comes from studies in rodent models. Notably, mice with genetic overexpression of TNF- α spontaneously develop RA-like lesions in the joints with progressive inflammation, cellular proliferation and bone destruction (Palladino et al., 2003). In addition, mice overexpressing the TNFR alone developed significant inflammation of liver, pancreas, and kidney (Douni and Kollias, 1998).

TNF- α has the capability to induce the expression of other pro-inflammatory cytokines such as IL-1 and several chemokines (Parameswaran and Patial, 2010). Furthermore, TNF- α is also able to increase the production of lipid signal transduction mediators such as prostaglandins (PGs). Therefore, some uncertainty exists over the direct role of TNF- α in the inflammatory condition. In rodent model of RA, for instance, aberrant TNF- α expression in the synovium contributed to disease progression. Meanwhile, arthritic changes in response to TNF- α signaling inhibition were partially mediated by other pro-inflammatory cytokines, most notably IL-1 (Palladino et al., 2003).

Therefore, TNF- α is proposed as a central player in inflammation and is suggested to play a critical role in the development of many chronic inflammatory

diseases (Fujiwara and Kobayashi, 2005). Development of antagonists to block the action of TNF- α has revolutionized the treatment of RA and other inflammatory diseases.

IL-10

IL-10 is a pleiotropic cytokine produced by many cells types including monocytes/macrophages, which play a critical role in inflammatory processes. The IL-10 gene is transcribed to some degree constitutively and subject to regulation by posttranscriptional RNA degradation mechanisms (Moore et al., 2001). IL-10 functions through interacting with IL-10 receptor (IL-10R) which is composed of at least two subunits IL-10R1 and IL-10R2. IL-10R1 functions as a ligand-binding subunit with high-affinity while the principal function of IL-10R2 is an accessory subunit for signaling.

IL-10 potently inhibits production of IL-1 α , IL-1 β , IL-6, IL-10 itself, IL-12, IL-18, granulocyte-macrophage colony-stimulating factor (GM-CSF), and TNF- α by activated macrophages. The inhibitory effects of IL-10 on IL-1 and TNF- α production are crucial to its anti-inflammatory activities, because these cytokines often have synergistic activities on inflammatory pathways and processes (Moore et al., 2001). IL-10 also inhibits production of chemokines including monocyte chemoattractant protein (MCP) 1, MCP-5, IL-8, macrophage inflammatory protein (MIP)-2 by activated monocytes, and PGE₂ through down-regulation of cyclooxygenase-2 (COX-2) expression (Niino et al., 1995).

PGE₂

PGE₂ is not stored but synthesized *de novo* from membrane-released arachidonic acid (AA) when cells are activated by stimuli such as mechanical trauma, cytokines, and growth factors. As **Fig. 7** shows, *PGE₂* synthesis is initiated by a family member of phospholipase A (PLA), a family of enzymes that catalyze the hydrolysis of membrane phospholipids at the sn-2 position, liberating A (a 20-carbon unsaturated fatty acid). Both cytosolic PLA₂ (cPLA₂) and secretory group V PLA₂ (sPLA₂-V) are shown to be involved in regulating AA mobilization response of macrophages exposed to TLR4 activation (Ruiperez et al., 2009).

Membrane-released AA is rapidly oxidized into the unstable metabolite, PGG₂, which is subsequently presented to PGH₂ by COX. There are two major isoforms: COX-1 and COX-2. COX-1, expressed constitutively in most cells, is the dominant source of prostanoids that subserves housekeeping functions. Whereas COX-2, induced by inflammatory stimuli, hormones, and growth factors, is the more important source of prostanoid formation in inflammation (Ricciotti and FitzGerald, 2011).

Membrane phospholipids

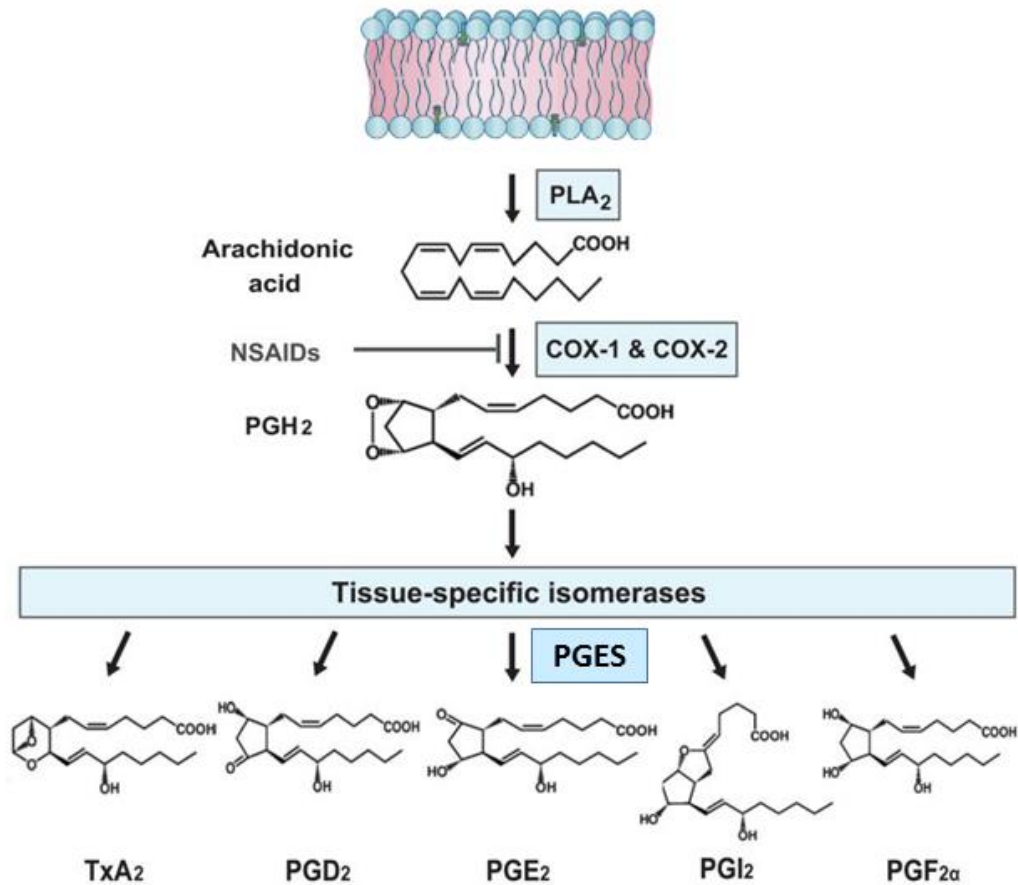


Figure 7. PGE₂ Biosynthetic pathway. PLA₂ = cytosolic phospholipase A₂; COX = cyclooxygenases; NSAIDS = nonsteroidal anti-inflammatory drugs; PGH₂ = prostaglandin H₂; PGES = prostaglandin E synthase, PGD₂ = prostaglandin D₂; PGE₂ = prostaglandin E₂; PGI₂ = prostaglandin I₂; PGF_{2α} = prostaglandin F_{2α}; TxA₂ = Thromboxane A₂. Revised from (Chizzolini and Brembilla, 2009)

Once synthesized, PGH₂ is rapidly catalyzed to PGE₂ by a family of prostaglandin E synthase (PGES) comprised of microsomal PGES-1 (mPGES-1, mPGES-2 and cytoplasmic PGES (cPGES)). mPGES-1 has been shown to respond to inflammatory stimuli and frequently induced concomitantly with COX-2 after stimulation by LPS, TNF- α , and IL-1 β (Samuelsson et al., 2007). NF- κ B serves as a transcriptional regulator of COX2 (Plummer et al., 1999). In contrast, mPGES-2 and cPGES, constitutively expressed in a wide spectrum of tissues, are generally not sensitive to inflammatory stimuli and are equally expressed in both the normal and pathological samples.

PGE₂ then exerts its action locally through binding to one or more of its four cognate receptors, termed EP1-EP4, which are all G-protein-coupled receptors (GPCRs). Under physiological conditions, PGE₂ is an important mediator of many biological functions such as regulation of immune responses, blood pressure, gastrointestinal integrity, and fertility (Ricciotti and FitzGerald, 2011).

In the onset of the inflammatory response, PGE₂ acts as a vasodilator to facilitate tissue influx of neutrophil of immune cells from the blood stream resulting in swelling and edema at the site of infection or tissue injury (Nakanishi and Rosenberg, 2013). Furthermore, PGE₂ can stimulate sensory nerves to increase pain response and can act on neurons in the preoptic area to promote pyrogenic effects (Nakanishi and Rosenberg, 2013). In addition, recent studies underscore that PGE₂ exacerbates inflammation by promoting the activation of T_H 17 cells, a subset of CD4⁺ helper T cells. PGE₂-mediated production of IL-17 has been shown to exacerbate the

development of multiple inflammatory diseases, such as IBD and collagen-induced arthritis in mice (Sheibanie et al., 2007a; Sheibanie et al., 2007b).

However, it should be realized that PGE₂ also elicits powerful immunosuppressive properties that contribute to the resolution phase of short-term inflammation, thereby facilitating tissue regeneration and the return to homeostasis (Nakanishi and Rosenberg, 2013). These multifaceted properties of PGE₂ are both cell type and context specific.

Resolution of Inflammation

Inflammation has two phases: short-term and chronic. Physiologically, the protective short-term inflammation should cease and be resolved once the triggering insults are eliminated, the infection is cleared, or the damaged tissue is repaired. Not only pro-inflammatory mediators are produced during the inflammatory response, but also anti-inflammatory and pro-resolving mediators are generated. Termination of the inflammatory response and transition to homeostasis, once thought to be a passive process, has now been shown to be an active and highly regulated process known as the resolution of inflammation (Serhan et al., 2008; Medzhitov, 2010).

Resolution of inflammation is accompanied by an active switch in lipid mediators (Ji et al., 2011). Initially, prostaglandins such as PGE₂ are generated to activate and amplify the cardinal signs of inflammation. Next, PGE₂ in turn actively switches on the transcription of enzymes required for the generation of mediators with both anti-inflammatory and pro-resolution activities which are referred to as specialized pro-resolving mediators (SPM). SPM include lipoxins and resolvins, which are derived

from endogenous AA and omega-3 poly-unsaturated fatty acid, respectively (Serhan and Savill, 2005).

Resolvins represent a new family of pro-resolution mediators that are organically identified in exudates formed in the resolution phase of short-term inflammation in both rodents and humans (Serhan et al., 2002). Resolvins are biosynthesized from omega-3 fatty acids docosahexaenoic acid (DHA) and eicosapentaenoic acid (EPA), thereby are categorized as either D-series or E-series, respectively. DHA and EPA can either be endogenously released from membrane phospholipids by PLA₂ activity or obtained exogenously from diet (Leigh et al., 2014).

The D-series are comprised of four bioactive compounds, resolvin D1-D4. In this study, we have focused on resolvin D1 (RvD1) because of the following reasons: (i) it was first identified in resolving inflammatory exudates from short-term self-limited murine peritonitis (Serhan et al., 2002); (ii) it may act as an early inflammation resolving lipid product to facilitate transition from proinflammation to resolution (Fredman et al., 2014); (iii) it has been shown to protect against oxidative stress-induced inflammation (Spite et al., 2009); (iv) the commercial ELISA kit for the other resolvins was not available.

RvD1 biosynthesis involves the enzymatic steps as depicted in **Fig. 8**: (i) DHA can be either obtained from diet or released from membrane phospholipids by the hydrolytic action of Ca²⁺-independent PLA₂ (iPLA₂) (Sun et al., 2010), (ii) DHA is then oxygenated via 12/15-lipoxygenase (LOX) and converted into 17S-hydroxy-DHA, (iii) 17S-hydroxy-DHA is oxygenated via 5-LOX into 7S-hydroperoxy-17S-hydroxy-DHA, followed by enzymatic epoxidation into 7S, 8-epoxy-17S-hydroxy-DHA and

furthermore converted into RvD1. RvD1 biosynthesis has been previously studied in mammalian whole blood, retina, brain and salivary gland (Hong et al., 2003; Leigh et al., 2014). However, RvD1 biosynthesis has not been previously described in macrophages either in resting state or under oxidative stress.

Notably, RvD1, at very low concentration (pico to nano-molar range), exhibits potent anti-inflammatory action. It promotes pro-resolution of inflammation by dysregulating pro-inflammatory cytokines production, inhibiting aberrant neutrophil recruitment by stimulating apoptosis of neutrophils. RvD1 also markedly decreases LPS-induced pro-inflammatory cytokines (TNF- α , IL-6 and IL-1 β) gene expression but increases the expression of anti-inflammatory cytokine (IL-10) gene expression (Wang et al., 2014; Rey et al., 2016). In mice, administration of RvD1 *in vivo* blocks LPS-induced recruitment of neutrophils and activation of macrophages resulting in resolution and amelioration of short-term injury in kidney and lung (Duffield et al., 2006; Wang et al., 2014). RvD1 exert its action through interacting with its receptors. Two specific human G protein coupled receptors (GPCR), FPR2/ALX and G protein coupled receptor (GPR)32, are known to specifically and directly interact with RvD1 to exert its effects (Krishnamoorthy et al., 2010).

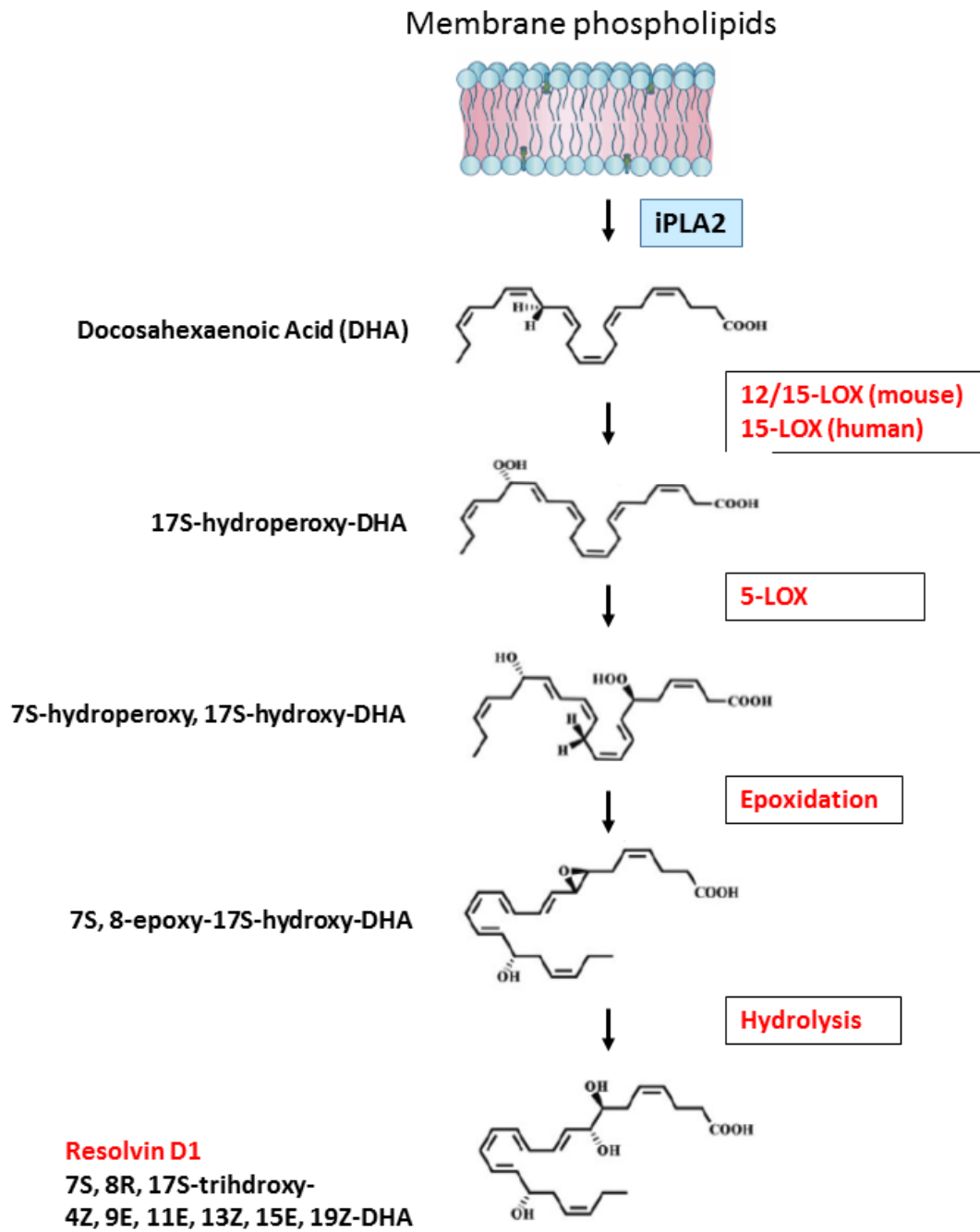


Figure 8. Biosynthesis of Resolvin D1. iPLA₂ = Ca²⁺-independent PLA₂; LOX = lipoxygenase. Revised from (Leigh et al., 2014)

More interestingly, RvD1 is implicated in protecting against oxidative stress. Pretreatment with RvD1 decreased LPS-induced levels of the lipid peroxidation product malondialdehyde (MDA) (Wang et al., 2014). Glutathionyl-HNE (GS-HNE) promotes cellular oxidative stress by stimulating the production of superoxide, and COX and LOX-derived pro-inflammatory eicosanoids including PGE₂, leukotriene B₄ and cysteinyl leukotrienes (Spite et al., 2009). Administration of RvD1 protected against GS-HNE-initiated inflammation by inhibition of leukocyte infiltration (Spite et al., 2009). RvD1 rescued macrophages from oxidative stress-induced apoptosis during efferocytosis (the process by which apoptotic or necrotic cells are removed by phagocytic cells) through inactivation of NOX2 and up-regulation of anti-apoptotic protein expression (Lee and Surh, 2013).

Accumulating evidence suggests that resolution of inflammation is a distinct process separate from the anti-inflammatory process for control of inflammation (Ji et al., 2011). This is because in addition to serving as agonists to stop and lower neutrophil infiltration into inflamed tissues, pro-resolution mediators promote uptake and clearance of apoptotic cells as well as microbes by macrophages in inflamed sites, and stimulate antimicrobial activities of mucosal epithelia cells (Ji et al., 2011).

It is believed that a failure to resolve short-term inflammation leads to uncontrolled chronic inflammation. This has been linked to some of the most common and difficult to treat diseases including: cardiovascular diseases, rheumatoid arthritis, asthma, diabetes, IBD, and neurological disorders (Ricciotti and FitzGerald, 2011; Serhan and Petasis, 2011). Therefore, early promotion of the resolution of inflammation is considered as a new and novel therapeutic frontier (Fullerton and Gilroy, 2016).

Macrophages: A Central Cellular Player in Inflammation

Macrophage and microglia cells are two critical cellular components of the innate immune system in peripheral and central nervous systems, respectively. In this study, we focused our efforts on macrophages. Macrophages, generated in bone marrow and differentiated from circulating monocytes, form the first line of defense against invading pathogens or tissue damage. They are structurally heterogeneous and widely distributed throughout the body. This remarkable plasticity allows macrophages to efficiently respond to environmental signals and change their phenotype (Mosser and Edwards, 2008).

Macrophages are crucial component in inflammation, tissue homeostasis, coordination of adaptive immune responses, and repair (Parameswaran and Patial, 2010). As the first line of defense, macrophages are one the major contributors to short-term inflammation induced by microbial infection or tissue damage (Takeuchi and Akira, 2010). In inflammation, macrophages have three major functions: antigen presentation, phagocytosis, and immunomodulation through production of various cytokines and growth factors. Macrophages play a critical role in the initiation, maintenance, and resolution of inflammation (Fujiwara and Kobayashi, 2005).

In the resting stage, macrophages produce only low levels of pro-inflammatory mediators. Upon exposure to pro-inflammatory cytokines, interferons, PAMPs or DAMPs, macrophages acquire a pro-inflammatory, or “classically activated” phenotype, which is known as the M1 phenotype (Koh and DiPietro, 2011). Following activation, pro-inflammatory macrophages themselves produce a large number of

mediators and cytokines including interleukin (IL)-1, IL-6, IL-12, tumor necrosis factor (TNF) α , and inducible nitric oxide synthases (iNOS). These participate in the regulation of inflammatory responses (Koh and DiPietro, 2011). Activated macrophages also produce chemokines that stimulate leukocytes movement and migration from the blood to tissue.

In addition to “classically activated” macrophages, *in vitro* studies suggests that macrophage are capable of transitioning from a pro-inflammatory to an “alternatively activated”, or “reparative, phenotype”, which is known as the M2 phenotype induced by IL-4 (Stein et al., 1992). The M2 phenotype is characterized in part by expression of anti-inflammatory mediators, such as IL-10, decoy IL-1 receptor type II, and by the production of growth factors such as transforming growth factor (TGF)- β 1, and vascular endothelia growth factor (VEGF). The alternatively activated macrophages are assumed to be requisite for the switch from inflammation to proliferation.

Notably, uncontrolled inflammatory cytokine production by “classically activated” macrophages are key mediators of the immunopathology that occurs during several autoimmune diseases including rheumatoid arthritis, and IBD (Zhang and Mosser, 2008).

Rationale for this Dissertation Work

A common mechanism(s) by which redox stress may activate the inflammatory response to potentially initiate, propagate and maintain many human diseases has not been previously demonstrated. However, accumulating evidence suggests that pattern recognition receptor (PRR) of innate immune system such as TLRs may be involved in mediating this all-encompassing response (Gill et al., 2010).

Among the TLR family members, TLR4 is of particular interest. Various environmental factors, including ozone, atmosphere particulate matter, long-lived reactive oxygen intermediate, ionizing radiation, cigarette smoke extracts, and oxidants can activate the TLR4 pathway through increased production of RONS and inflammatory mediators (Paul-Clark et al., 2009; Lucas and Maes, 2013). TLR4 is structurally different from other TLRs because it is the only member of the PRR family with MD-2 and CD14 as co-receptors. Furthermore, a systematic review of the TLR literature shows that TLR4 is involved in many chronic disorders. TLR4 polymorphisms are associated with susceptibility for childhood chronic obstructive pulmonary diseases (COPD) and IBD (Kerkhof et al., 2010; Cheng et al., 2015). In addition, TLR4 single nucleotide polymorphisms is associated with increased risk for colorectal cancer (Downes and Crack, 2010). Furthermore, obese mice with type 2 diabetes following hyperglycemia showed a 5.6-fold increased expression of TLR4 as compared with normal lean mice (Ladefoged et al., 2013). Thus, TLR4 can be regarded as a potential therapeutic target for a host of inflammatory diseases (Hennessy et al., 2010), leading us to focus our study on this PRR subtype.

The response elicited by TLR4 activation is a classic inflammatory phenotype through the activation of NF- κ B and subsequent production of a battery of pro-inflammatory mediators. The purpose of inflammatory responses to infection is to protect the host, and eradicate invading pathogens. Release of pro-inflammatory cytokines following DAMPs mediated-TLR4 activation may be more harmful and cause tissue damage. Therefore, long-term TLR4 activation by exogenous insults may result in abnormal production of pro-inflammatory mediators that may initiate, propagate and maintain pathological inflammation.

Our previous studies using HEK-293 cells stably transfected with mouse TLR4 had demonstrated that TLR4 is involved in exogenous oxidant- mediated NF- κ B stimulation (Karki and Igwe, 2013; Karki et al., 2014). In the foregoing set of studies, we further determined the mediatory role of TLR4 in oxidant-induced NF- κ B activation in macrophages, a more biologically relevant cell model because TLR4 is primarily expressed in immune cells including macrophages.

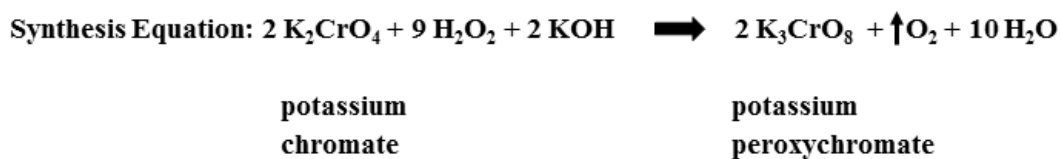
Therefore, we tested the *central hypothesis* that TLR4 is the link between RONS, oxidative stress and inflammatory phenotypes that mediate diverse disease processes. In addition, we investigated the biosynthetic machinery of resolvin D-1 (RvD1) production through lipoxygenase (LOX) & its FPR2 receptor expression in macrophages under normal and oxidative stress conditions. We believe that a better understanding of the resolution of inflammatory pathways in macrophages will be critical in conceptualizing and developing new therapies for oxidative stress-induced inflammation.

2. MATERIALS AND METHODS FOR RAW-BLUE CELLS

Generation of Oxidants

Synthesis/ Preparation of Potassium Peroxychromate (PPC)

PPC, used in the study as a source of ROS, is not available commercially, but was synthesized from 30% aqueous hydrogen peroxide (H_2O_2 , Sigma-Aldrich, St Louis, MO) and potassium chromate (K_2CrO_4 , Sigma-Aldrich, St Louis, MO) in the laboratory according to a published protocol (Miesel et al., 1995). Briefly, into an Erlenmeyer flask we placed 4.0 g of potassium chromate and a solution of 4.0 g KOH in 50 ml H_2O_2 . The mixture was cooled down with stirring until it formed a thick slurry without freezing. For continuous cooling, we used a salted ice bath. To the thick slurry, we slowly added 25 ml of 30 % H_2O_2 with constant stirring. The color of the slurry changed from yellow to a dark brown, with evolving bubbles. The cooling was continued with occasional stirring for 2 -3 hrs. At the end of the reaction, the crystals of potassium peroxychromate (PPC) were filtered, washed twice with distilled H_2O and dried overnight at 37 °C. The yield was always > 80%. The product was characterized by elemental and infrared analyses with a purity of $\geq 98\%$.



PPC has been used as a source of ROS to examine their effects on biochemical and biological functions (Edwards and Quinn, 1982). PPC decomposes readily in aqueous systems to release several oxygen-centered free radicals including H_2O_2 ,

hydroxyl radical ($\bullet\text{OH}$), singlet oxygen ($^1\text{O}_2$) and possibly superoxide anion ($\text{O}_2\bullet^-$) according to the following reaction (shown in **Fig. 9 A**). The peroxychromate anion, CrO_8^{3-} , consists of a central chromium atom in the oxidation state of +5 surrounded by four peroxy anions (O_2^{2-}) in a dodecahedral arrangement.

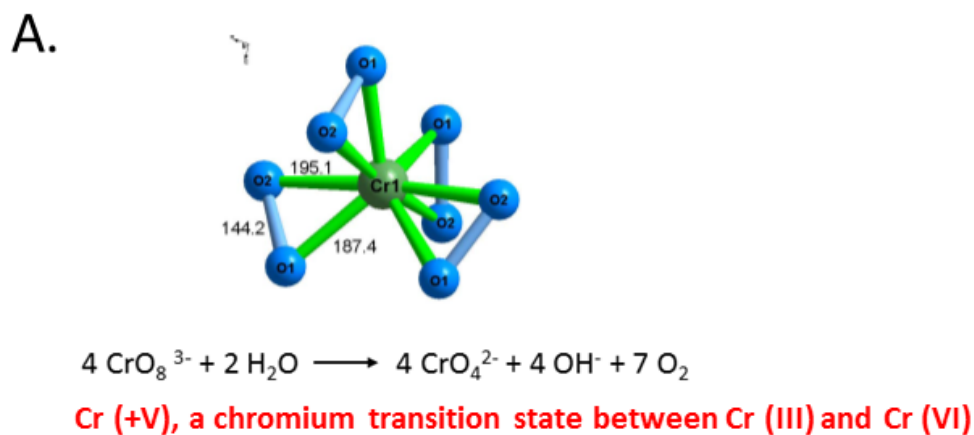
SIN-1 (3-morpholinopyridone N-ethylcarbamide)

We also used SIN-1 (3-morpholinopyridone N-ethylcarbamide) (AdipoGen, San Diego, CA), as a peroxynitrite (PN) donor. Under physiological condition, SIN-1 releases superoxide and nitric oxide, which interact at close proximity to form PN with rate constant k of $3.7 \times 10^{-7} \text{ M}^{-1}\text{S}^{-1}$ (Trackey et al., 2001) (**Fig. 9 B**). PN, a powerful oxidizing agent, rapidly causes nitration of proteins at tyrosine or tryptophan residues. Therefore, tyrosine nitration of proteins can be used as a biomarker for the presence of PN (Galinares and Matata, 2002).

Cell Culture

RAW-Blue cells, purchased from InvivoGen (San Diego, CA), are derived from the murine macrophage-like RAW 246.7 cell line. It has been suggested that RAW264.7 cells most closely mimic bone marrow-derived macrophages in terms of cell surface receptors and response to TLR4 and TLR3 ligand (Berghaus et al., 2010). However, RAW-Blue cells are chromosomally integrated with secretable embryonic alkaline phosphatase (SEAP) reporter construct inducible by NF- κ B and AP-1 activation. Cells were grown in a 37°C, 100% humidified incubator in Dulbecco's modified Eagle's medium (DMEM) (4.5 g of glucose/L) without pyruvate, but supplemented with 2 mM L-glutamine, FBS [10 % (v/v)], 50 units/ml penicillin and 50 $\mu\text{g/ml}$ streptomycin. RAW-Blue cells were maintained in growth medium

supplemented with a selective antibiotic reagent 50 µg/ml Zeocin. We assessed the levels of SEAP released into the culture medium to quantify the extent of NF-κB transcriptional activity.



B.

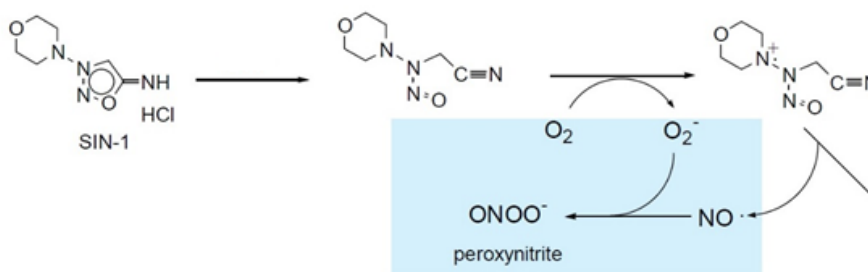


Figure 9. Oxidants used in the study. (A) Crystalline lattice structure of PPC and reactions during its decomposition. Cr (+V), the active valency state, which is a transition state between Cr (III) and Cr (+VI). (B) The structure of SIN-1 chloride and peroxynitrite release during its decomposition at physiological pH. Obtained from <http://www.dojindo.com/store/p/250-SIN-1.html>.

Oxidant Treatments

Exposure duration is one of the key kinetic parameters for biological responses resulting from oxidants. We used short-time and long-term treatment paradigms with oxidants *in vitro* according to established protocols (Jakab et al., 1995). For example, exposure of human alveolar macrophages to ozone (0.1-1 ppm) for 2 h caused a concentration-dependent increase in the release of inflammation modulator PGE₂ (Becker et al., 1991). However, release of thromboxane B₂ (TxB₂), PGE₂ and leukotriene C₄ (LTC₄) was detected after long-term exposure to ozone at a concentration of 0.5 ppm in human bronchial epithelial cell line BEAS-S6 (McKinnon et al., 1993).

To provide a relatively complete understanding of the effects of oxidants, we used two treatment paradigms: long-term & low concentration of oxidants and short-term & high concentration of oxidants (**Table 3**). For long-term and low concentration treatment, cells were incubated in a medium containing varying concentrations of oxidants (0.1 - 2.5 μ M for PPC; and 10 - 500 μ M for SIN-1) or LPS-EK (InvivoGen, San Diego, CA) for 16 h. However, for short-term and high concentration treatment, cells were stimulated with oxidants at varying concentrations ranges of (100 - 500 μ M for PPC; and 1000 - 5000 μ M for SIN-1) for 2 h, following which media containing the oxidants or LPS-EK were removed. Cells were then rinsed once with fresh media followed by further incubation for 16 h in fresh media in the absence of oxidants or LPS-EK.

Table 3: Treatment paradigm

Treatment Time	Oxidants	Concentrations
16 h continuous treatment	PPC	0.1 - 2.5 μ M
16 h continuous treatment	SIN-1	10 - 500 μ M
2 h initial treatment with oxidant, rinse once with fresh media followed by 16 h further in the absence of oxidant	PPC	100 - 500 μ M
2 h initial treatment with oxidant, rinse once with fresh media followed by 16 h further in the absence of oxidant	SIN-1	1000 - 5000 μ M

Cells were preincubated for 30 min with EUK-134, a catalase (CAT) / superoxide dismutase (SOD) [CAT/SOD] inhibitor (Cayman Chemical, Ann Arbor, MI), or for 3 h with low endotoxin azide-free (LEAF) affinity purified rat IgG2a, κ -isotype anti-mouse TLR4/MD-2 complex polyclonal antibody (pAb) (BioLegend, San Diego, CA) or for 3 h with CLI-095 (InvivoGen, San Diego, CA) before incubation with either oxidants or LSP-EK. EUK-134, a synthetic serum-stable scavenger for oxidant species (Lawler et al., 2014), was used to clarify the role of oxidants. Anti-TLR4/MD-2 pAb, a neutralizing Ab for TLR4, was used as well to block the interaction with its ligands. CLI-095, a specific TLR4 signaling inhibitor that binds to TIR domain

of TLR4 (Matsunaga et al., 2011), was used to block signal transduction following TLR4 activation.

Live Cell Counting

To determine live cell numbers, we plated cells (5×10^5 /well) in 6-well plates and grew to 70% confluence overnight. Cells were scrapped and counted either after 2 h stimulation or 16 h incubation using the Countess Automated Cell counter (Life Technologies, CA). Live and dead cells were identified using 0.2% Trypan Blue dye based on the fact that live cells will exclude the dye while dead cells will take up the dye into their cytoplasm.

Quanti-Blue Secreted Embryonic Alkaline Phosphatase (SEAP) Reporter Assay

Quanti-Blue assay was used to quantify SEAP levels in cell supernatant, which is a measure of NF- κ B activation. Cells (3×10^6) were plated in 96-well plates and grown to 70% confluence overnight. Aliquots of cell culture medium (5 μ l) were removed and transferred to new 96-well plates containing 195 μ l of prewarmed Quanti-Blue detection reagent (Catalog No. rep-qb1, InvivoGen, San Diego, CA) per well as per the manufacturer's instructions. Color was allowed to develop for 30 min, and absorbance was read spectrophotometrically at 650 nm using a Bio-Tek microplate reader.

3,4,5-dimethylthiazol-2-yl)-2, 5-diphenyltetrazolium Bromide (MTT) Assay

At the end of treatment with oxidants or inhibitors, 50 μ l 5 mg/ml MTT (Life technologies, CA, USA) in PBS was added to each well followed by incubation at 37 °C for 3 h. At the end of incubation, medium containing MTT was carefully removed, followed by addition of 500 μ l DMSO to each well. Aliquots (200 μ l) from each

treatment were transferred to a 96-well plate for reading at 570 nm as reference using the Powerwave X spectrophotometer (Biotek, Winooski, VT, USA). Percentage of proliferation was calculated by the ratio of absorbance at 570 nm between control and treated cells.

Lactate Dehydrogenase (LDH) Cytotoxicity Assay

Lactate dehydrogenase (LDH) cytotoxicity assay was conducted to provide a rationale for the oxidant concentrations used in all subsequent studies. LDH levels in culture supernatant were quantified using the PierceTM LDH Cytotoxicity Assay Kit (Catalog No. 88953, ThermoFisher Scientific) according to the manufacturer's instructions. LDH catalyzes the formation of red colored formazan and its absorbance is read at 490 nm. The amount of formazan produced is proportional to the activity of LDH. The content of LDH released into culture medium was determined from standard curves. LDH levels upon cell lysis were used as total LDH activity.

$\% \text{ Cytotoxicity} = (\text{LDH levels}_{\text{oxidant-treated}} - \text{LDH levels}_{\text{control}}) / \text{Total LDH levels} \times 100\%$.

Quantification of Thiobarbituric Acid Reactive Substances (TBARS)

To confirm ROS release from PPC decomposition, we quantified the levels of malondialdehyde (MDA) as TBARS in cell culture supernatant after PPC exposure, which is indicative of treatment-induced lipid peroxidation.

The levels of MDA in the cell culture medium were quantified by a TBARS Assay Kit (Catalog No. KGE013, R&D System, Minneapolis, MN) according to the manufacturer's instructions. Briefly, culture medium was centrifuged to remove debris, and then clarified with 0.3 N trichloroacetic acid (TCA) to precipitate proteins present. The precipitated interfering protein and other substances were removed by

centrifugation at 12,000 × g for 4 min. In the presence of heat and acid, free MDA in the sample reacts with thiobarbituric acid (TBA) to produce MDA-TBA adduct, which was quantified spectrophotometrically in a Bio-Tek microplate reader at 532 nm. The content of MDA in cell lysate was determined from thiobarbituric acid reactive substance (TBARS) standard curves.

Quantification of 4-Hydroxynonenal (4-HNE)

The levels of 4-HNE adduct in the cell culture medium was quantified by a Oxiselect™ HNE Adduct Competitive ELISA Kit (Catalog No. STA-838, Cell Biolabs, San Diego, CA) according to the manufacturer's instruction. Briefly, an HNE conjugate was coated on an ELISA plate overnight at 4 °C. After two washes, culture supernatant or HNE-bovine serum albumin (BSA) standards were added to the HNE conjugate preabsorbed on the ELISA plate. After 10 min incubation, anti-HNE antibody was added, followed by an HRP-conjugated secondary antibody. The content of HNE protein adducts in cell lysate was determined from HNE-BSA standard curves.

Measurement of Intracellular ROS (iROS) Production by Fluorescent Imaging

Microscopy and Flow Cytometry

CellROX® Deep Red reagent was used to detect cellular oxidative stress. Cells were incubated with oxidants or LPS-EK for 2 hr. The iROS production was determined using the CellROX deep red reagent by fluorescent imaging microscopy and flow cytometry as previously described (Zhang et al., 2015). Images were acquired using a fluorescence microscope (Axiovert 200M; Zeiss) at excitation and emission wavelengths of ~644/655 nm for CellROX and 405/410-550 nm for NucBlue®.

Fluorescent density was quantitatively analyzed by Image J software (Version 1.44, <http://imagej.nih.gov/ij/>).

The flow cytometric data acquisition and analysis were conducted on FACSCanto II flow cytometer (BD Biosciences, San Jose, CA, USA). Electronic gating was used to exclude doublets and subcellular debris with forward scatter threshold set at 500. The fluorescence intensity corresponding to iROS was determined using Allophycosyanin (APC) filter at excitation and emission wavelengths of 645/660 nm (which corresponds to the excitation/emission λ of CellROX[®] Deep Red reagent). Unstained cells were used as negative controls for iROS. For each parameter investigated, at least 10^4 events (cells) were analyzed per sample. The fluorescence intensities as logarithmically amplified data were compared between different treatments.

Total Antioxidant Capacity (TAOC) Assay

After simulation with oxidants or LPS-EK, cells were lysed for analysis of intracellular total antioxidant capacity (iTAOC) using an Antioxidant Assay Kit (Item No. 709001, Cayman Chemical, Ann Arbor, MI) as per manufacturer's instructions. The assay relies on the ability of antioxidants in the sample to inhibit the formation of oxidized ABTS^{®+•} 2,2-Azino-di- (3-ethylbenzthiazoline) sulphonate by metmyoglobin. The amount of ABTS^{®+•} produced was monitored by reading the absorbance at 405 nm using a Bio-Teck microplate reader (Burlington, VT, USA). The capacity of the antioxidants in cell lysate was calculated from Trolox (a water-soluble vitamin E analogue) standard curves.

RNA Extraction and Reverse Transcription

RAW-Blue cells were collected in TRI Reagent (Catalog No. RT 111, Molecular Research Center Inc, Cincinnati). Total RNA was extracted from cells using Tri Reagent according to the manufacturer's instruction. Total RNA was quantified in a Nanodrop spectrophotometer (ThermoFisher Scientific, Waltham MA). An aliquot of RNA sample (2 μ l) with a ratio of A260/280 nm absorbance of 1.8 to 2.0 was reverse transcribed in a 20 μ l reaction volume using a High-Capacity cDNA Reverse Transcription Kit (Catalog No. 4368814, ThermoFisher Scientific, Waltham MA)

Quantitative Polymerase Chain Reaction (qPCR)

Quantitative-polymerase chain reaction (RT-qPCR) was performed using Step-One™ Real-Time PCR System (Applied Biosystem, Foster City, CA) via standard fluorescent methodology and thermal cycling conditions following the manufacture's recommendations, including validation of each gene amplification tested by identification of single peaks in melting curves. The qPCR reaction mixture contained 1 μ l cDNA, 10 μ l of the Real-time Bullseyes EvaGreen qPCR Mastermix-ROX (Catalog No. BEQPCR-R, MIDSCI, Valley Park, MO), 0.4 μ l of primer pairs (10 μ M) and 8.6 μ l H₂O in a complete reaction volume of 20 μ l. C_T values were normalized to β -Actin or GAPDH as a reference gene. Gene expression was determined as up/down regulation of the gene of interest compared to the control.

Preparation of Whole-cell Extract

Cells cultured in 6-well plates were washed with ice-cold PBS and lysed in whole cell extraction lysis buffer PE LB™ for Mammalian Cells (Catalog No. 786-180,

G-Biosciences, St. Louis, MO) supplemented with appropriate protease inhibitors ProteaseArrest™ (Catalog No. 786-108, G-Biosciences, St. Louis, MO). Cell lysates were centrifuged at $12,000 \times g$ at 4°C for 20 min to remove cell debris. Protein assay was performed using BCA Protein Assay kit (Catalog No. 23225, Thermo Scientific, Waltham, MA) according to the manufacturer's instructions. Protein samples were diluted at 1:20 with the extraction buffer, and 5 μ l of the dilution was added into a 96-well plate, and incubated with 200 μ l working solution for 30 min at 37°C. Total protein was quantified by absorbance reading at 562 nm.

Immunoblot Assay

Aliquots of whole cell extracts containing 20-30 μ g of total protein were mixed with 5 X SDS loading buffer in a total volume of 20 μ l and denatured at 100 °C for 10 min. Equal amount (30 μ g) of denatured total protein along with 5 μ l of PageRuler™ Prestained Protein ladder (Catalog No.26616, Fisher Scientific, Pittsburg, PA) was loaded per lane, fractionated on a 4-12% Bis-Tris electrophoresis gel (Catalog No. NP0336BOX, Fisher Scientific, Pittsburg, PA), and transferred onto PVDF membranes. After blocking with 5% non-fat milk in TBST (Tris-buffered saline, 0.1% Tween 20), the membranes were probed overnight at 4 °C with primary antibody (Ab). After three washes in TBS-T, the membranes were incubated for 2 h with secondary Ab. Finally, the membranes were developed using SuperSignal West Femto Chemiluminescent Substrate kit (Catalog No. PI34095, Thermo Scientific, Waltham, MA), and signals were visualized with the Fujifilm LAS-400 imaging system (Fujifilm, Stamford, CT).

To determine the expression of more than one protein on the same membrane, Restore Western Blot Stripping Buffer (Catalog No. 46430, ThermoSicentific,

Waltham, MA, USA) was used for reblotting. Fifteen (15) ml of stripping buffer was added to the membrane, and incubated for 15 min with shaking at room temperature. After removal of the stripping buffer, the membrane was washed 3 times for 5 min each in 0.5 % TBS Tween-20, followed by blocking, and incubation with primary Ab and secondary Ab. The effectiveness of initial stripping was tested before blocking.

Fractionation of Nuclear and Cytoplasmic Extracts from Cells

Nuclear fraction (NF) and cytoplasmic fraction (CF) were prepared using Nuclear Extract Kit (Catalog No. 40410, Active Motif, Carlsbad, CA) as per manufacturer's instructions.

Briefly, cells were first collected in ice-cold PBS supplemented with phosphatase inhibitors. Cells were then resuspended in hypotonic buffer to swell the cell membrane and make them fragile. Addition of a detergent caused leakage of the cytoplasmic proteins into the supernatant. The CF was collected by centrifugation at $14,000 \times g$ for 10 min at 4°C . The nuclei were lysed and the nuclear proteins solubilized with detergent-free lysis buffer supplemented with protease inhibitor cocktail (provided in the kit). NF was used to determine NF- κ B p65 DNA binding activity using TransAM[®] NF- κ B p65 Kit (Catalog No. 40096, Active Motif, Carlsbad, CA). NF and CF were subjected to immunoblot assay as well.

TransAM[®] Assay

Nuclear extract was prepared for analysis of NF- κ B p65 DNA binding activities using TransAM[®] NF- κ B p65 Kit as per manufacturer's instructions. Briefly, 10 ng nuclear extract was added into a 96-well plate and incubated for 1 h at room temperature with mild shaking. On the 96-well plate was immobilized an

oligonucleotide containing the NF- κ B consensus sequence (5'-GGGACTTTCC-3'). After 3 \times washes, the primary antibodies were added, followed by incubation for 1 h at room temperature. Then, HRP-conjugated secondary antibody was added to provide a sensitive colorimetric readout that was quantified by reading absorbance spectrophotometrically at 450 nm.

Quantification of TNF- α and IL-10 Levels

Culture supernatant was collected and centrifuged to remove cell debris. The contents of TNF- α and IL-10 released into the medium were quantified by using LEGEND MAX Mouse TNF- α ELISA Kit (Catalog No.430907, BioLegend, San Diego, CA) and LEGEND MAX Mouse IL-10 ELISA Kit (Catalog No. 431417, BioLegend, San Diego, CA), respectively. The assays were performed according to the manufacturer's instructions.

Immunoprecipitation (IP)

The supernatant of whole-cell extract was precleared by adding rabbit IgG together with Protein A/G PLUS-Agarose for 30 min at 4°C followed by centrifugation at 1,000 \times g for 5 min at 4°C. Lysate containing 500 μ g of total protein in extraction buffer was incubated with 2.5 μ g/ml I κ B α (c-terminal) pAb together with Protein A/G PLUS-Agarose for overnight at 4°C. Beads with the immunoprecipitates were collected by centrifugation, washed 4 \times in lysis buffer, resuspended in 1 \times loading buffer, and then heated at 100 °C for 10 min, and subjected to immunoblot assay probed with anti p-I κ B α (Tyr 42) Ab.

Statistical Analysis

The IBM Statistical Package for the Social Sciences (SPSS) version 22 was used to perform data analysis in all experiments. Data are presented as the mean \pm SEM from at least 3 to 6 independent experiments carried out in duplicates or triplicates, where applicable, and analyzed by 1-or 2-way analysis of variance (ANOVA) followed by Tukey's post hoc tests with $p \leq 0.05$ considered as significant.

3. ROLE OF TLR4 IN OXIDANT-INDUCED INFLAMMATORY RESPONSE THROUGH NF- κ B ACTIVATION IN RAW-BLUE CELLS

Confirmation of the Experimental System

Confirmation of the Release/Generation of ROS and RNS by Oxidants

The peroxychromate anion, CrO_8^{3-} with chromium in the +5 valency state, decomposes readily in aqueous systems to release several ROS such as hydrogen peroxide, hydroxyl radical, singlet oxygen, and possibly superoxide (Edwards and Quinn, 1982). Unsaturated lipids of biological membranes are susceptible to these ROS resulting in potential lipid peroxidation. Exposure of plasma membranes to ROS leads to lipid peroxidation in which MDA and 4-HNE are generated as the end products as shown in **Fig. 10**. We determined levels of MDA and 4-HNE as a measure of PPC- or SIN-1-mediated lipid peroxidation end products.

EUK-134, a synthetic serum-stable scavenger for oxidative species, was used to provide evidence for the role of prooxidants. Cells were preincubated with EUK-134 (4 μM) for 30 min before stimulation with oxidants for 2 h. Culture supernatant at the end of 2 h stimulation was collected to quantify lipid peroxides. MDA was quantified as TBARS according to the manufacturer's instructions in the Parameter TBARS assay kit (see method part of Chapter 2, page 60).

To confirm ROS release following PPC decomposition, the level of MDA in cell culture supernatant following PPC exposure, indicative of treatment-induced lipid peroxidation product, was quantified as TBARS. Treatment with PPC significantly increased TBARS concentration in a dose-dependent manner (**Fig. 11 A**). Increased

TBARS levels were reduced by pretreatment with anti-oxidant reagent EUK-134 (4 μ M) (Fig. 11A).

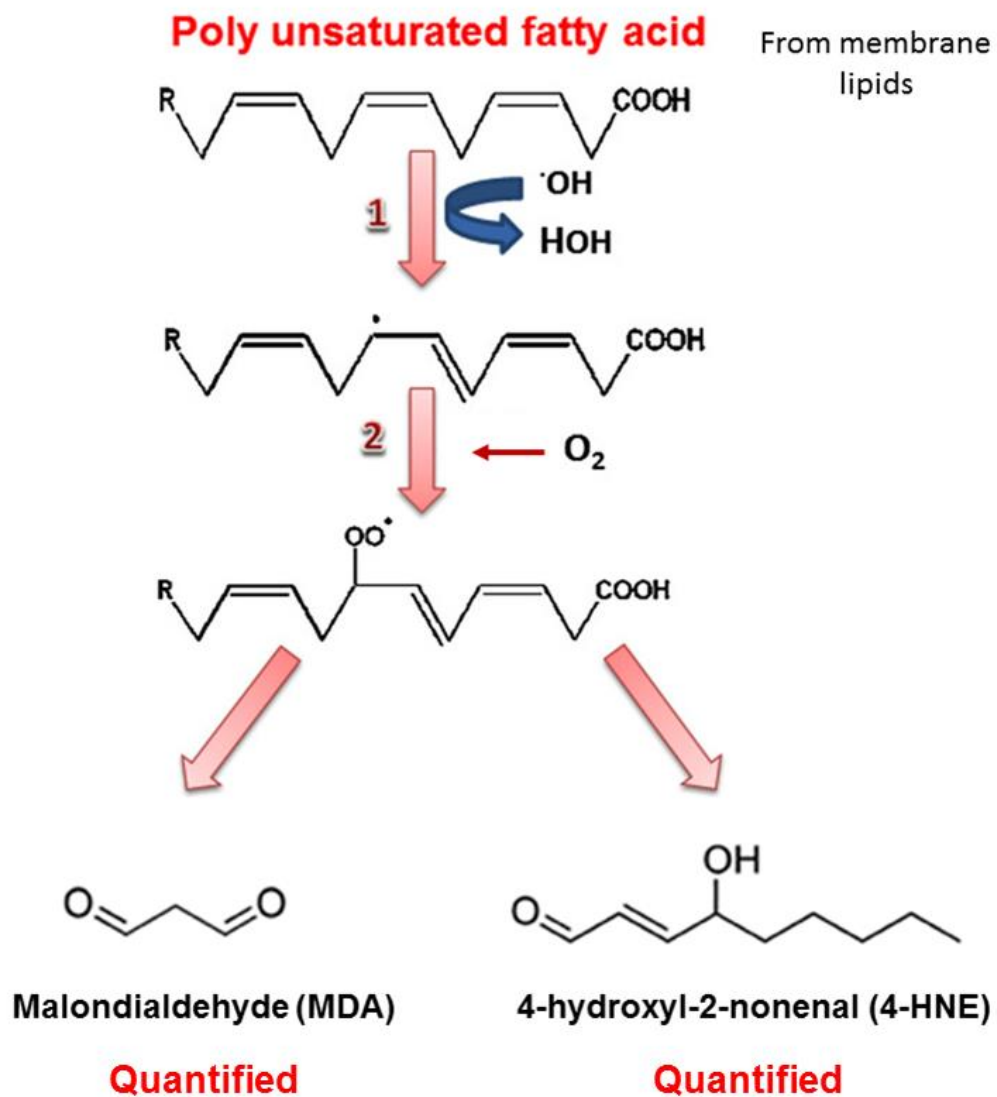


Figure 10. Lipid peroxidation. Lipid peroxides malondialdehyd (MDA) and 4-hydroxynonenal (4-HNE) production following lipid peroxidation by ROS. Revised from (Shah et al., 2014)

SIN-1 releases superoxide and nitric oxide *in situ*, which interact with each other resulting in the generation of PN, which cause protein nitration at tyrosine or tryptophan residues (Trackey et al., 2001; Karki et al., 2014). To confirm generation of PN from SIN-1 (**Fig. 9 B**), the extent of protein tyrosine nitration was measured by Western blot following SIN-1 treatment. Treatment with SIN-1 produced a single band of nitrated protein confirming its effectiveness in generating nitrated proteins (**Fig. 11 B**). Potassium PN, which generate PN directly, was used as comparative positive control. Nitrated bovine serum albumin was used as positive marker of nitrated proteins.

In addition, we confirmed the production of PN from SIN-1, we quantified the levels of levels of 4-HNE, another major end product of lipid peroxidase (**Fig. 10**), in cell culture supernatant after treatment with SIN-1 for 2 h. We found that 5 mM SIN-1 significantly increased the concentration of 4-HNE in the cell supernatant, which was also reduced by pre-incubation with EUK-134 (4 μ M) (**Fig. 11 C**). The reduced lipid peroxidation could be due to the scavenging of ROS by EUK-134.

We measured 4-HNE instead of MDA following stimulation with SIN-1 because of interference of SIN-1 in the TBARS assay (**Fig. 11 D**). TBARS concentrations in the medium containing SIN-1 alone, were increased to the same extent as those of cell culture supernatant following SIN-1 treatment. This suggested that increase in TBARS could be due to by SIN-1 itself or its breakdown product(s) in the TBARS assay.

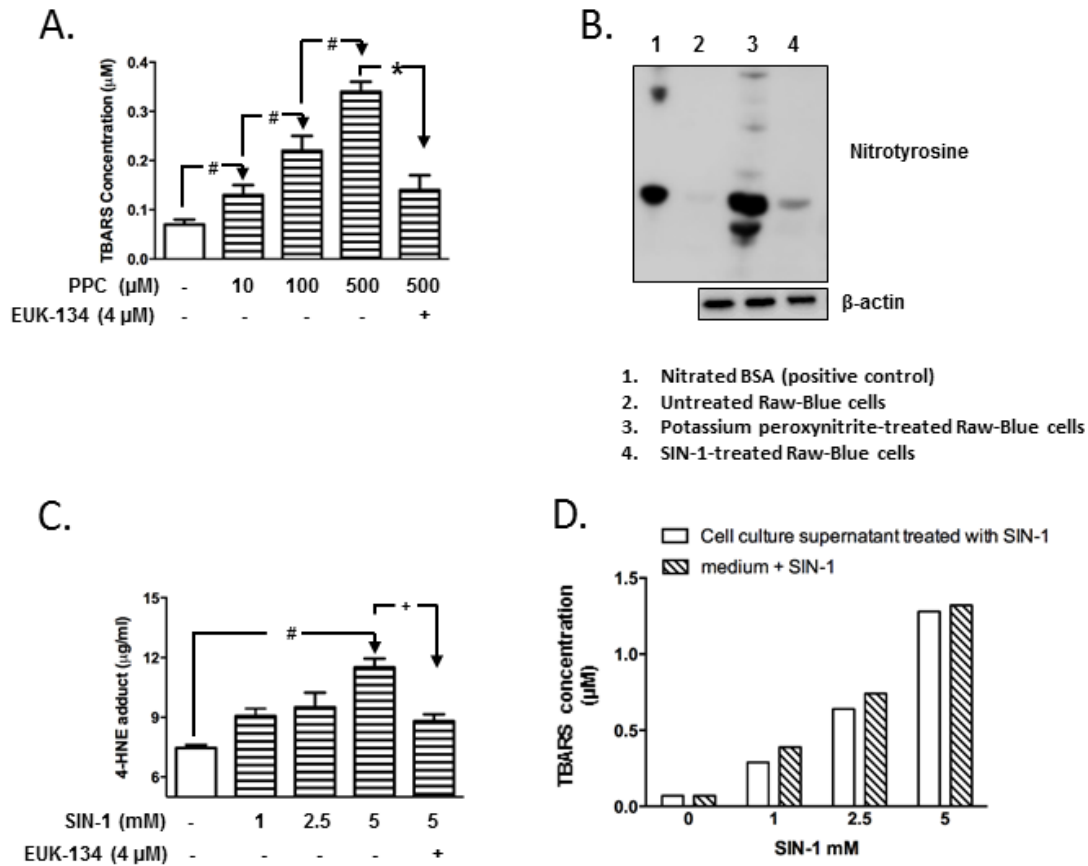


Figure 11. Confirmation of the generation of ROS and RNS by oxidants, by lipid peroxidation and protein tyrosine nitration. **(A)** Cells were preincubated with antioxidant EUK-134 ($4 \mu\text{M}$) for 30 min, followed by stimulation with PPC at various concentrations for 2 h. Cell culture supernatant was used to quantify the end product of MDA TBARS as for treatment with PPC. The data represent 3 independent experiments carried out in duplicates. # $p \leq 0.01$, * ≤ 0.01 . **(B)** Representative immunoblots of nitrated protein. Cells were treated with equimolar concentration (1 mM) of either PN or SIN-1 for 2 h and cell lysates were subjected to immunoblot using anti-nitrotyrosine polyclonal antibody. Nitrated BSA (Cell Biolabs Inc) was used as positive marker for protein nitration. **(C)** Cells were preincubated with EUK-134 ($4 \mu\text{M}$) for 30 min, followed by stimulation with SIN-1 at various concentrations for 2 h. Cell culture supernatant was used to quantify end product of 4-HNE as for treatment with PPC according to the manufacturer's instructions. The data represent 3 independent experiments carried out in duplicates. + $p \leq 0.05$, # $p \leq 0.01$. **(D)** The presence of SIN-1 in the culture medium caused unacceptable interference in the TBARS assay.

Confirmation TLR4 Expression in RAW-Blue Cells

TLR4 is predominantly expressed in immune cells, such as macrophages, monocytes and microglia. RAW-Blue cells are derived from murine macrophage-like cell line RAW 264.7, which expresses TLR4 complex and responds to TLR4 agonist stimulation (Wang et al., 2015). To determine the role of TLR4 in exogenous oxidant-induced NF- κ B activation, we confirmed the expression of TLR4 in Raw-Blue cells at both the mRNA and protein levels using RT-PCR and Western blot, respectively. Expression of TLRs mRNA, including TLR4 mRNA was determined in RAW-Blue cells by InVivoGen (**Fig. 12A**), which showed that TLR4 is the most abundant TLR expressed in this cell line. Our data unequivocally confirmed that RAW-Blue cells express both TLR4 mRNA (**Fig. 12 B**) and protein. (**Fig. 12 C**).

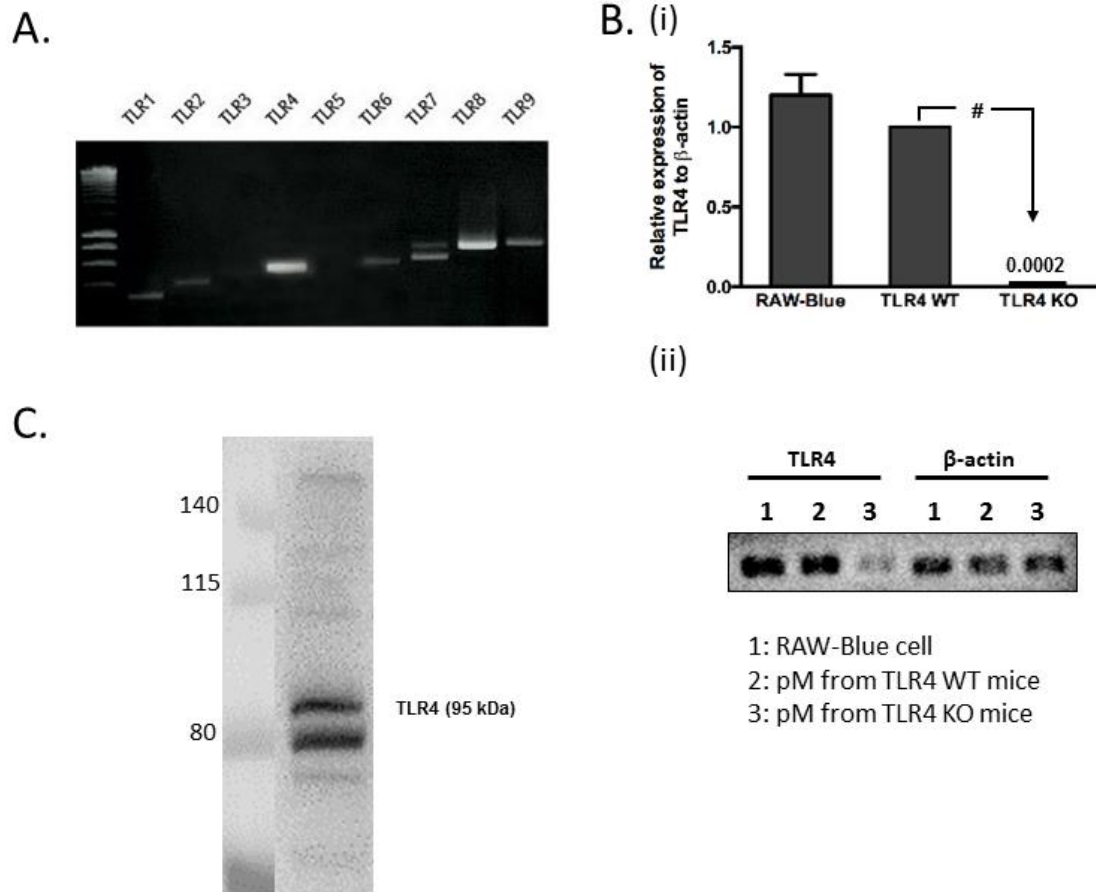


Figure 12. Expression of TLR4 mRNA and protein in RAW-Blue cells. **(A)** Comparative expression levels of TLR4 mRNA in RAW-Blue cells from the datasheet of RAW-Blue cells purchased from InvivoGen. **(B) (i)** RT-quantitative PCR comparative confirmation of the expression of TLR4 mRNA in RAW-Blue cells and in peritoneal macrophages (pM) isolated from TLR4-WT and TLR4 homozygous knockout mice used as positive and negative controls, respectively. # $p = 0.0001$, $n = 3$. **(ii)** DNA gel electrophoresis of TLR4 RT-quantitative PCR product. **(C)** TLR4 protein expression. Lysates of the RAW-Blue cells were subjected to Western blot analysis.

Determination of Optimal Concentrations of Oxidants to Which Cells were Exposed

To obviate effects resulting from oxidant cytotoxicity, we used concentrations of oxidants at which cells viability is 85 to 90%. Viabilities of RAW-Blue cells were determined by LDH release assay and live cell number counting with Trypan blue staining.

We initially challenged Raw-Blue cells with varying concentrations of oxidants for 16 h and determined cell viability using MTT assay. We found that oxidant treatment caused cytotoxicity in a dose-dependent manner (**Fig. 13**). The maximal concentration at which cellular viability was above 90% for both PPC and SIN-1 were 1 μ M and 500 μ M (**Fig. 13 A and B**), respectively. However, we found that treatment with PPC (1 μ M) and SIN-1 (500 μ M) for 16 h did not increase the levels of SEAP released into the culture medium (**Fig. 13 C and D**) suggesting that long-term incubation with PPC or SIN-1 for 16 h at the concentrations indicated failed to stimulate NF- κ B activation any further.

On the basis of this empirical evidence, we chose the treatment method of short-term treatment with high-concentrations of oxidants (see **Table 3** in Chapter 2). Previous kinetic studies revealed that PPC (Edwards and Quinn, 1982) and SIN-1 (Thome et al., 2003) can completely generate their inherent free radicals within 2 h in an aqueous medium at pH 7.4. For this treatment paradigm with PPC or SIN-1 at high concentration, or LPS-EK (10 ng/ml) for 2 h following which cell culture medium was replaced with fresh medium in the absence of either oxidants or LPS-EK.

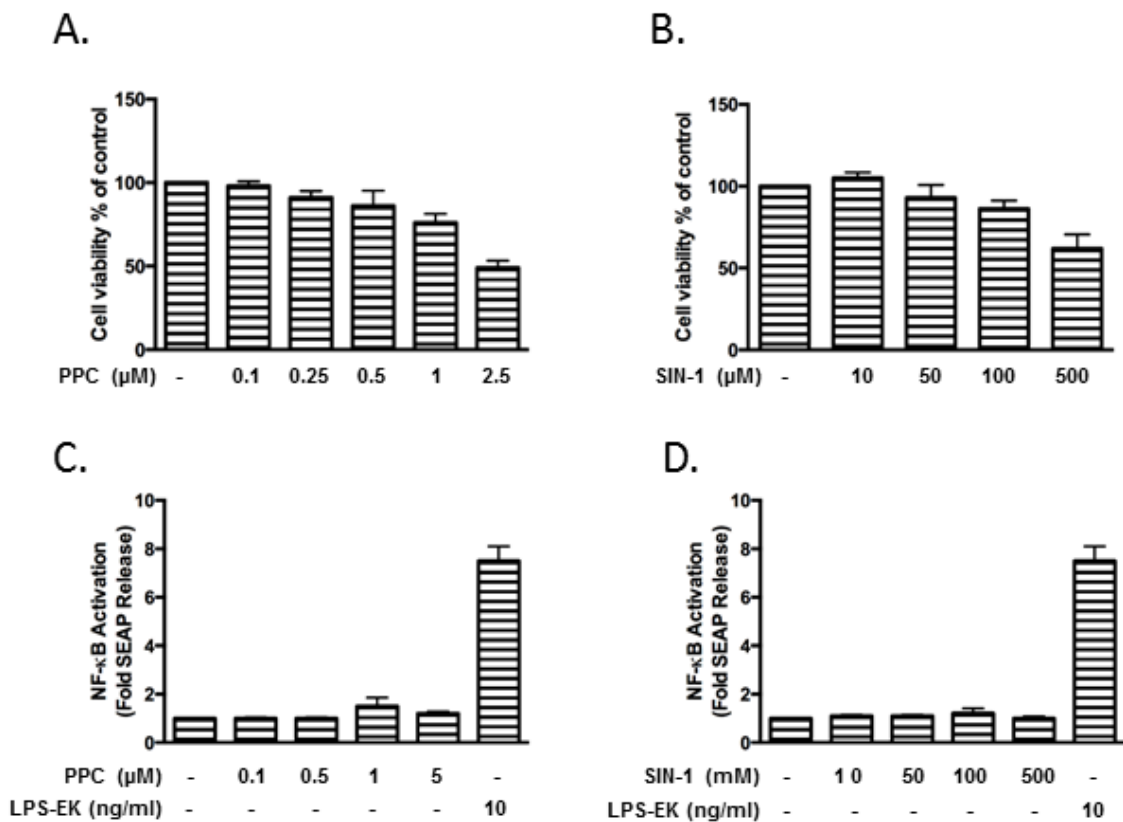


Figure 13. Effects of oxidants on RAW-Blue cell viabilities and SEAP release. Cells were exposed to PPC (A) or SIN-1 (B) at the indicated concentrations for 16 h followed by MTT assay. Cells were exposed to PPC (C), SIN-1 (D) or LPS-EK at the indicated concentrations for 16 h followed by quantification of LDH released into culture medium.

We found that PPC (500 μ M), SIN-1 (5 mM), or LPS-EK (10 ng/ml) did not significantly increase LDH release either at 2 h (**Fig. 14 A**) or 16 h (**Fig. 14 B**) in comparison with vehicle control. Then, we also confirmed the effects of oxidants on cell viabilities by live cell counting stained with trypan blue. Incubation of Blue cells for 2 h (**Fig. 14 C**) with PPC (100, 500 μ M), or SIN-1(1, 5 mM) did not affect the number of live cells compared with untreated cells. At 16 h incubation (**Fig. 14 D**), PPC (500 μ M) and SIN-1 (5 mM) significantly reduced cell numbers compared to untreated control cells, although the cell numbers were still higher than initial seeding number (5×10^5 cells/well). These results suggested that short-term and high-concentration exposure to PPC (100, 500 μ M) or SIN-1 (1, 5 mM) could inhibit cell grow but not cause significant cell death.

We further examined whether short-term and high-concentration treatment with oxidants could stimulate NF- κ B activation. Both PPC and SIN-1 induced SEAP release (an indicator of NF- κ B activation) in a dose-dependent manner in this treatment model. PPC (500 μ M) (**Fig. 14 E**) and SIN-1 (5 mM) (**Fig. 14 F**) treatment induced SEAP release by 3.2- and 2.7- fold over the same cells in the absence of either oxidants, respectively. To validate the experimental system, we incubated cells with LPS-EK, as a positive control of TLR4 activation, which produced a robust SEAP release.

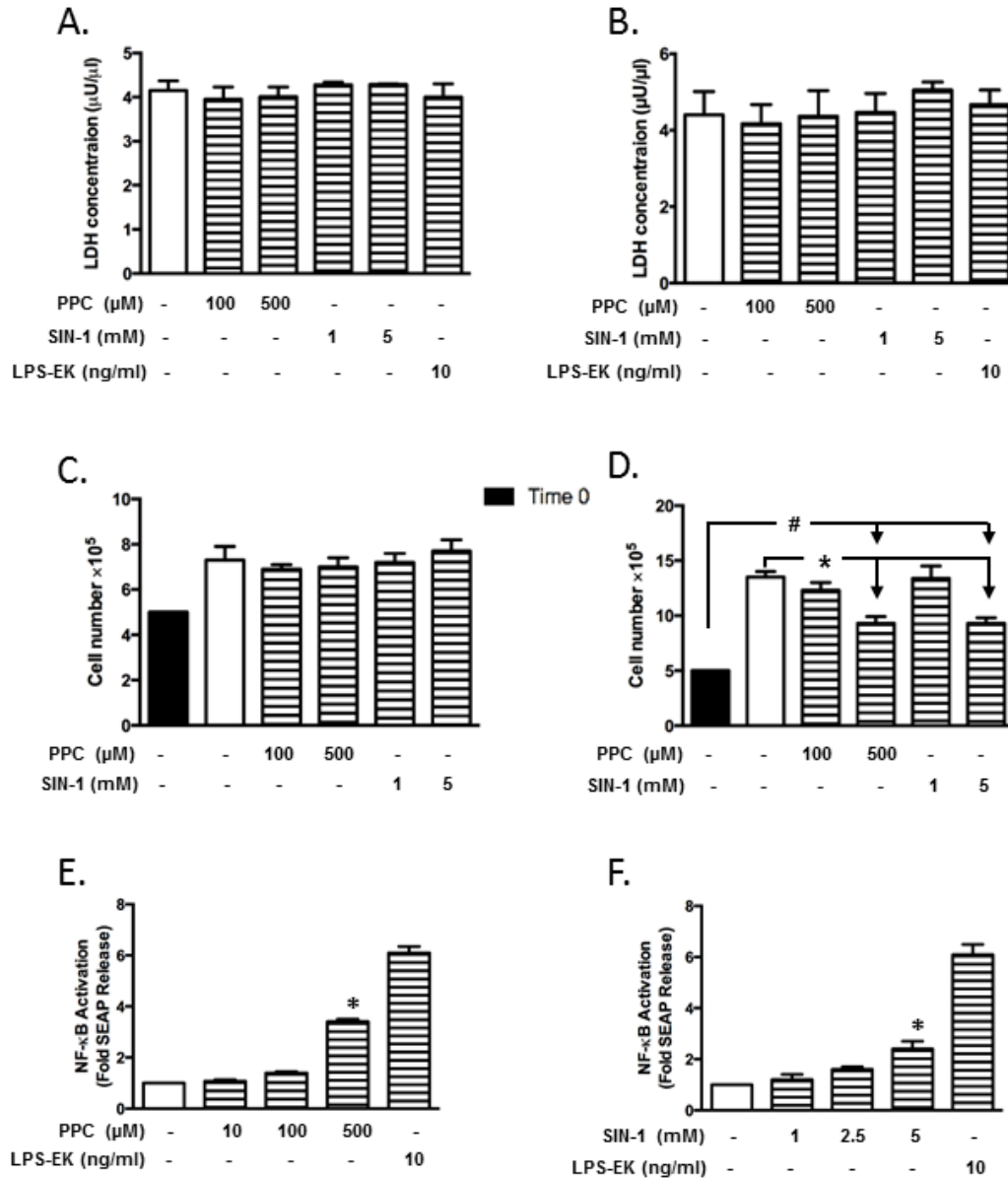


Figure 14. Effects of oxidants on RAW-Blue cell viability and SEAP release. Cells were exposed to oxidants or LPS-EK at the indicated concentrations for 2 h followed by incubation with fresh growth medium in the absence of oxidants or LPS-EK for next 16 h. LDH released into the culture medium quantified following 2 h (A) and 16 h incubation (B). Cell viabilities upon oxidant treatment were determined by live cell counting with trypan blue staining at 2 h (C) and 16 h (D). Black solid bars represent the initial cell seeding numbers while the blank bars represent cell numbers after 16 h treatment with vehicle control. The data represent 3 independent experiments. # $p \leq 0.01$ vs live cell number at time 0 h; * $p \leq 0.05$ vs untreated cells. The levels of SEAP released into culture medium was quantified at the end of 16 h incubation (E and F). (E) PPC induced SEAP release in a dose-dependent manner. The data represent 6 independent experiments carried out in triplicate. * $p \leq 0.005$ vs control. (F) SIN-1 stimulated SEAP release in a dose-dependent manner. The data represent 6 independent experiments carried out in triplicate. * $p \leq 0.005$ vs control.

Effects of Oxidants on Cellular Redox Homeostasis

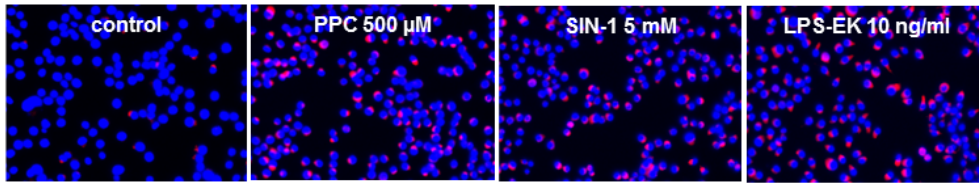
Oxidants Increased iROS Concentration in RAW-Blue Cells

Using fluorescent microscopy imaging with Image J analysis, we showed that 2 h treatment with PPC (500 μ M) or SIN-1 (5 mM) increased iROS levels by a mean of 4.2- and 3.6-fold over control cells under the same conditions (**Fig. 15 A and 15 B**). Enhanced iROS following treatment with PPC and SIN-1 was further confirmed by flow cytometry. Incubation of cells with PPC (500 μ M), or SIN-1 (5 mM) for 2 h increased iROS levels by a mean of 25%, and 30%, over control cells, respectively (**Fig. 15 C and D**). The positive control treatment with TLR4 agonist LPS-EK (10 ng/ml) also increased iROS levels, which would suggest that increased iROS levels by oxidants might be through TLR4 activation. We also measured iROS levels at 6, 12, and 24 h post PPC treatment and found that maximal levels of iROS increase occurred at 2 h (**Fig. 16**).

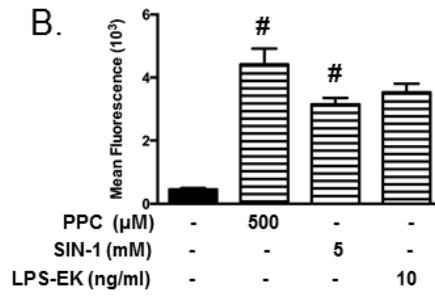
Oxidants Decreased Cellular TAOC in RAW-Blue Cells

The burden of iROS levels is largely counteracted by an intricate antioxidant defense system (Finkel and Holbrook, 2000). Following the determination that oxidants increased iROS levels, we examined the effects of PPC or SIN-1 on intracellular (iTAOC). Treatment of cells with PPC (500 μ M) or SIN-1 (5 mM) for 2 h decreased iTAOC by 12 % and 19 %, respectively, in comparison with control (Fig. 3.5E). LPS-EK (10 ng/ml) decreased iTAOC by 30% in comparison with control cells. These results affirmed that oxidants through TLR4 stimulation can cause an imbalance between iROS levels and TAOC, which could lead to disturbances in redox homeostasis inside cells.

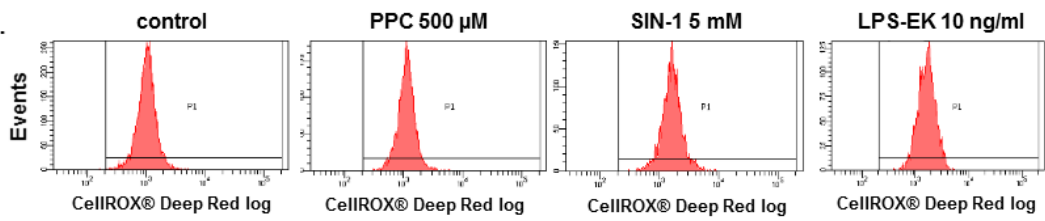
A.



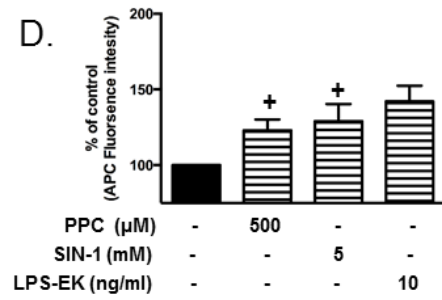
B.



C.



D.



E.

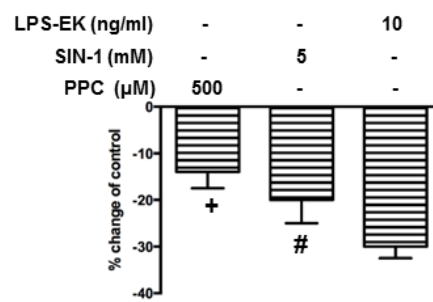


Figure 15. Effects of oxidants on levels of intracellular ROS (iROS) and total antioxidant capacity (TAOC) following stimulation of RAW-Blue cells. Cells were treated with oxidants or LPS-EK for 2 h followed by determination of iROS production and TAOC. **(A)** Cells were incubated with CellROX™ or together with NucBlue live cell stain followed by image acquisition using a fluorescence microscope. Merged representative pictures of fluorescent images showing **(B)** Semi-quantitative histograms of **(A)** generated with image J software. The data represent 4 independent experiments. # $p \leq 0.01$ vs control. **(C)** Fluorescence intensity following CellROX incubation was analyzed by flow cytometer with representative images of flow cytometry and **(D)** Quantitative histograms of fluorescence intensity. The data represent 3 independent experiments. + $p \leq 0.05$ vs control. **(E)** Cell lysates were subjected to total antioxidants capacity analysis according to the manufacturer's instructions. TAOC was quantified as mM Trolox equivalents (TE). The % Change over control was calculated as $(TE_{\text{treatment}} - TE_{\text{control}}) / TE_{\text{control}} \times 100\%$ to present the effects of oxidants or LPS-EK on TAOC over control cells. The data represent 3 independent experiments carried out in triplicate. # $p \leq 0.01$ vs control (0%), + $p \leq 0.05$ vs control (0%).

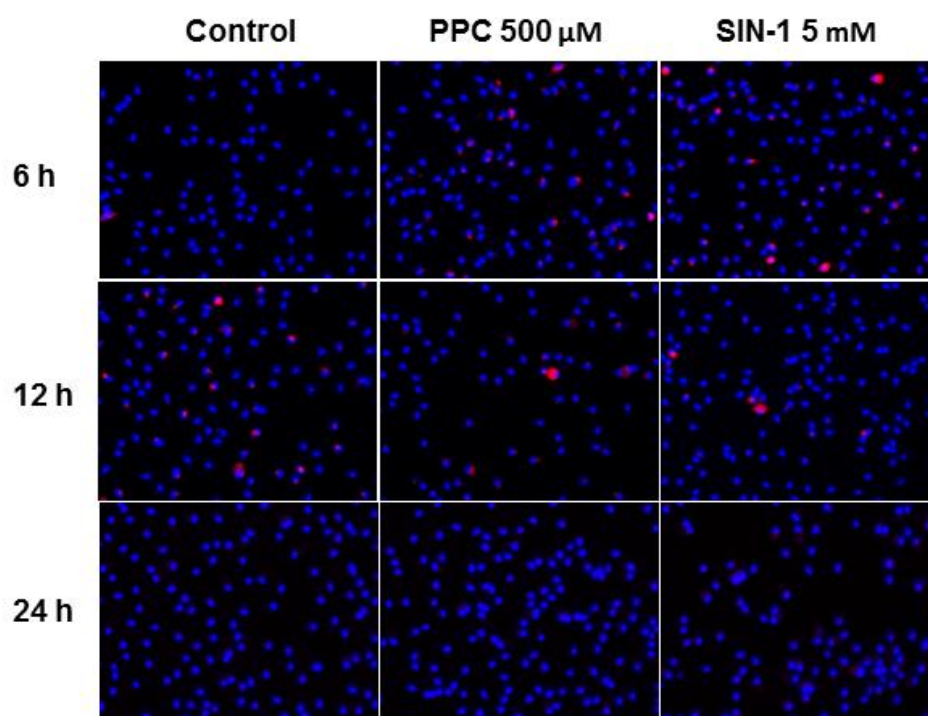


Figure 16. Time course of oxidant-mediated iROS levels in RAW-Blue cells.

Role of TLR4 in Oxidant-induced NF- κ B Activation

We had earlier demonstrated that TLR4 mediates exogenous oxidant-induced NF- κ B activation in an artificial cell system HEK-Blue mTLR4 cells (Karki and Igwe, 2013). In this study, we further confirmed the role of TLR4 in a more biologically relevant system, macrophages. RAW-Blue cells provide a reliable *in vitro* system to study NF- κ B activation, which can be quantified by measuring the levels of SEAP released into culture medium, as a reporter gene following NF- κ B activation.

Oxidants Stimulated NF- κ B Activation

We have shown that short-term and high concentration treatment with PPC or SIN-1 stimulated NF- κ B activation (**Fig. 14 E and F**). To further clarify the role of the oxidants in activating NF- κ B, we pretreated cells with EUK-134 (4 μ M) for 30 min prior to stimulation with oxidants. The lipid peroxidation results had shown that EUK-134 blocked oxidant-induced increase in iROS that caused decreased concentration of lipid peroxidation. Our results showed that pre-incubation with EUK-134 decreased PPC- or SIN-1-induced SEAP release by 53.1% and 44.4% compared with cells stimulated with PPC or SIN-1 alone, respectively (**Fig. 17**), which implies that oxidant-induced NF- κ B activation could result from released ROS that stimulated TLR4.

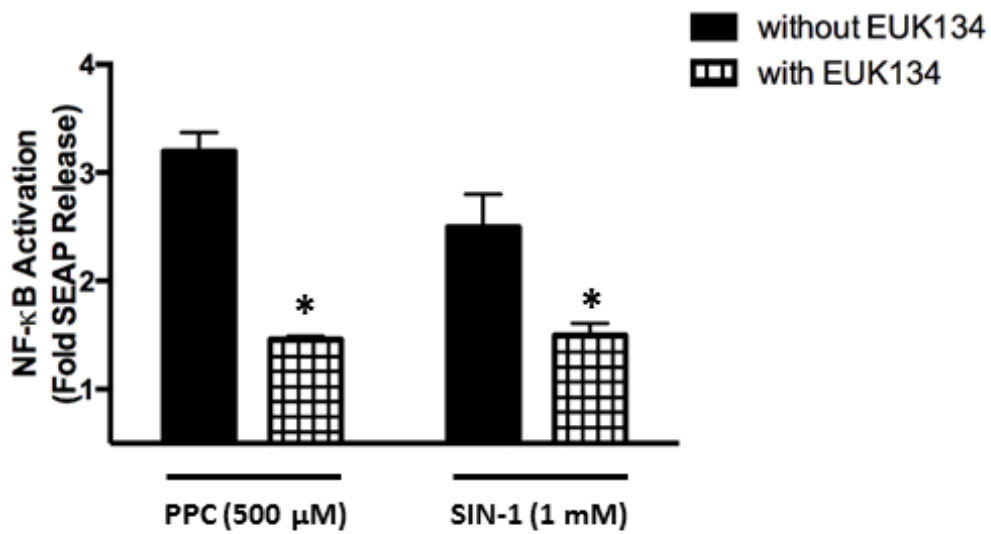


Figure 17. Pretreatment with anti-oxidant reagent EUK-134 reduced oxidants induced SEAP release in RAW-Blue cells. RAW-Blue cells were pretreated with anti-oxidant reagent EUK-134 (4 μM) for 30 min. Cells were then treated with oxidants or LPS-EK at the indicated concentrations for 2 h followed by incubation with fresh growth medium in the absence of oxidants or LSP-EK for the next 16 h. SEAP released in the culture medium at the end of 16 h incubation was determined using Quanti-Blue assay. The data represent 4 independent experiments carried out in triplicate. * $p \leq 0.005$ vs treatment with PPC or SIN-1 alone.

Specificity of TLR4 in Oxidant-stimulated NF- κ B Activation

To define the mediatory role of TLR4 in oxidant-stimulated NF- κ B activation, we used TLR4 neutralizing Ab and a specific TLR4 signaling inhibitor CLI-095. We chose an anti-mouse TLR4/MD-2 clone MT510 because it is reported to bind to an epitope of TLR4/MD-2 complex that blocks interaction with the native ligand of TLR4 (Laplante et al., 2011). TLR4 is the only TLR (though there is still ongoing debate regarding association of TLR2 with MD-2) that is confirmed to form an active heterodimer with MD-2 (Shimazu et al., 1999; Dziarski and Gupta, 2000).

CLI-095 has been shown to covalently bind to the Cys747 residue within TIR domain of TLR4 among the 10 human TLRs (Matsunaga et al., 2011), thus interfering with interactions between TLR4 and its adaptor molecule TIRAP and TRAM (Takashima et al., 2009). CLI-095 can selectively inhibit TLR4 signal transduction pathway (Ii et al., 2006; Takashima et al., 2009), and showed beneficial effects in a mouse endotoxin model (Sha et al., 2007).

RAW-Blue cells were incubated with anti-TLR4/MD-2 pAb or CLI-095 for 3 h prior to treatment with oxidants or LPS-EK. Pre-incubation of the cells with anti-TLR4 pAb inhibited PPC- or SIN-1-mediated SEAP release by 23.5% or 20.8%, respectively (**Fig. 18**). Similarly, pre-treatment with CLI-095 inhibited PPC- or SIN-1-mediated SEAP release by 61.8% or 37.5%, respectively (**Fig. 18**). Pre-incubation with anti-TLR4 pAb or CLI-095 reduced SEAP release induced by LSP-EK by 28.1% and 71.9%, respectively. These results clearly affirmed that TLR4 stimulation was involved in mediating oxidant-stimulated NF- κ B activation measured by quantification of the reporter gene SEAP expression in macrophages.

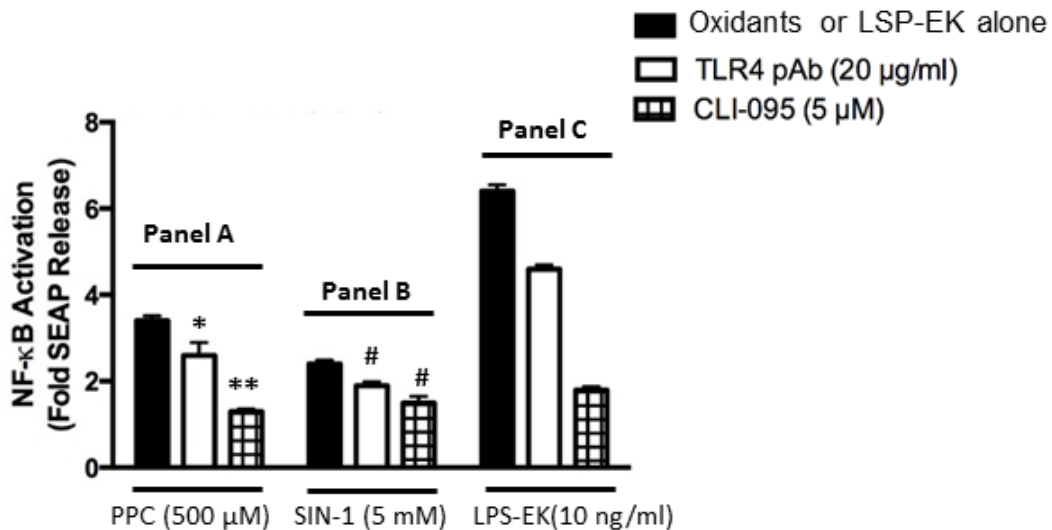


Figure 18. Pretreatment with anti-TLR4 pAb or CLI-095 reduced oxidants or LPS-EK induced SEAP release in RAW-Blue cells. Cells were preincubated with anti-TLR4/MD-2 pAb (20 μg/ml) or CLI-095 (5 μM) for 3 h before addition of oxidants or LPS-EK. Cells were exposed to oxidants or LPS-EK for 2 h followed by incubation with fresh growth medium in the absence of oxidants or LSP-EK for next 16 h. SEAP released in the culture medium at the end of 16 h incubation was determined using Quanti-Blue assay. The data represent 4 independent experiments carried out in triplicate. * $p \leq 0.05$, ** $p \leq 0.005$ vs treatment with PPC alone; # $p \leq 0.05$ vs SIN-1 treatment alone.

Role of TLR4 in Oxidant-increased NF- κ B p65 DNA Binding Activities

The most frequently activated form of NF- κ B in TLR4-dependent signaling is a heterodimer composed of p65 and p50 (Kawai and Akira, 2007). In the resting state, NF- κ B is retained in cytosol by direct interaction with I κ B proteins. Upon stimulation, phosphorylation of I κ B leads to its ubiquitination and subsequent degradation. Nuclear localization signal of NF- κ B heterodimer is unmasked, and NF- κ B translocates into nucleus and binds to the promoter region of target genes. To further confirm oxidants stimulated NF- κ B activation, DNA binding capacity of p65 in nuclear extract was quantified using the TransAM[®] assay. PPC (500 μ M) increased the DNA binding activity of p65 by 22.5%, 83.5% and 68.0%, at 15, 30 and 120 min, respectively, compared with untreated controls (at time = 0 min)(**Fig. 19**). Whereas, SIN-1 (1 mM) initially decreased DNA binding activity of p65 by 13% at 15 min, then increased it to 32% at 30 min, but this returned to the resting state levels at 120 min.

Additionally, we found that the increased transcriptional activities of p65 due to PPC were significantly decreased by 20%, 53%, and 34% in the presence of CLI-095 (**Fig. 19**). Similarly, pretreatment with CLI-095 decreased stimulated DNA binding activities of p65 caused by SIN-1 treatment at 30 min. LPS-EK, as a positive activator of TLR4, increased DNA binding activity by 124% at 30 min which also was blocked by pretreatment with CLI-095. These results confirmed that TLR4 activation is required in oxidant-mediated NF- κ B activation in macrophages.

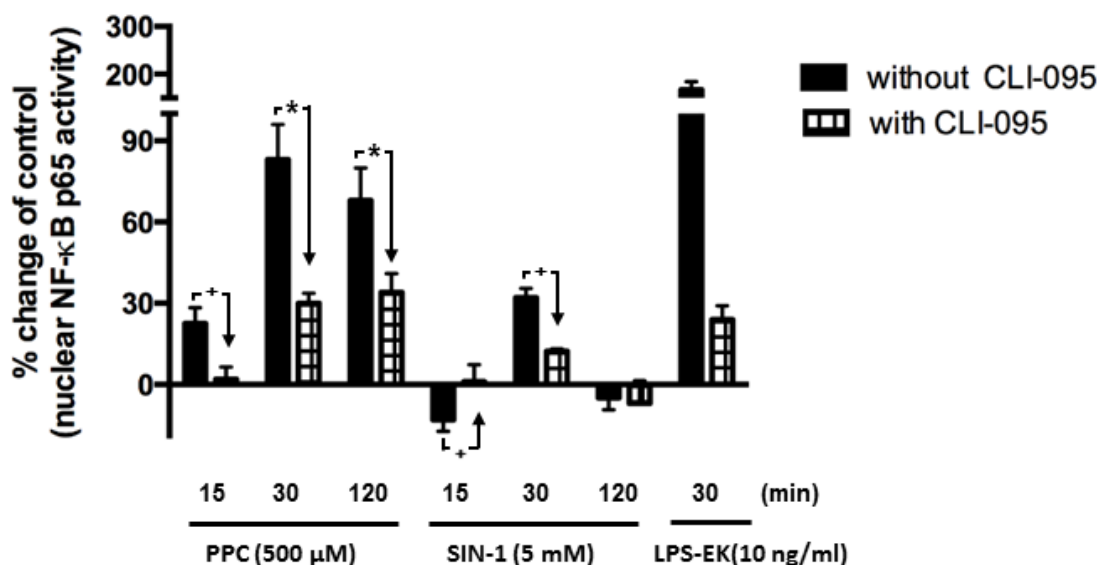


Figure 19. Pretreatment with CLI-095 reduced oxidant-mediated increase in DNA binding of NF- κ B p65 in RAW-Blue cells. Cells were preincubated with CLI-095 for 3 h followed by stimulation with either oxidants for 0, 15, 30 and 120 min, or LPS-EK for 30 min. Nuclear fraction (NF) was prepared. p65 DNA binding activity in NF was determined by TransAM[®] assay as per manufacturer's instruction, and the absorbance was read at 450 nm. % Change of control was calculated as $(OD_{\text{treatment}} - OD_{\text{control}}) / OD_{\text{control}} \times 100\%$ to present the effects of oxidants or LPS-EK on p65 DNA binding activity over control cells without treatment. The data represent 3 independent experiments carried out in duplicate. + $p \leq 0.05$, * $p \leq 0.001$.

Oxidants Stimulated NF- κ B Nuclear Translocation

To further confirm NF- κ B activation by oxidants, we determined the level of p65 nuclear translocation. Complete fractionation of CF and NF was confirmed by Western blot (**Fig. 20**). α -Tubulin, a marker for CF was undetectable in the NF, and lamin B, a marker for NF, was undetectable in the CF. β -Actin present in both NF and CF was used as housekeeping gene for semi-quantitative normalization because the expression of lamin B was affected by PPC (**Fig. 20**) and SIN-1 (**Fig. 21**) treatment.

In the resting state (at t = 0 min), p65 was mainly sequestered in the CF with a negligible amount located in NF (**Fig. 20 A**). PPC treatment increased the levels of p65 in NF in a time-dependent manner with maximal effect at 120 min and had no significant effect on levels of p65 in CF (**Fig. 20 A**). On the other hand, SIN-1 treatment maximally enhanced levels of p65 in NF at 30 min without affecting p65 levels in CF (**Fig. 21 A**). LPS-EK increased nuclear levels of p65 at 30 min, which was blocked by TLR4 signal inhibitor CLI-095 (Fig. 3.11B and **Fig. 21 B**). These results suggested that oxidants stimulated NF- κ B p65 translocation to nucleus, which was consistent with results of SEAP release (**Fig. 14 E and Fig.14 F**) and TransAM[®] assay (**Fig. 19**). The effects of CLI-095 on oxidant-stimulated p65 nuclear translocation were not detectable by Western blot.

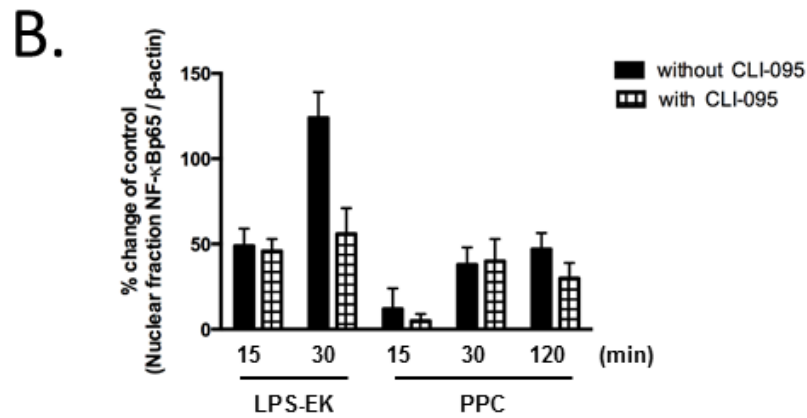
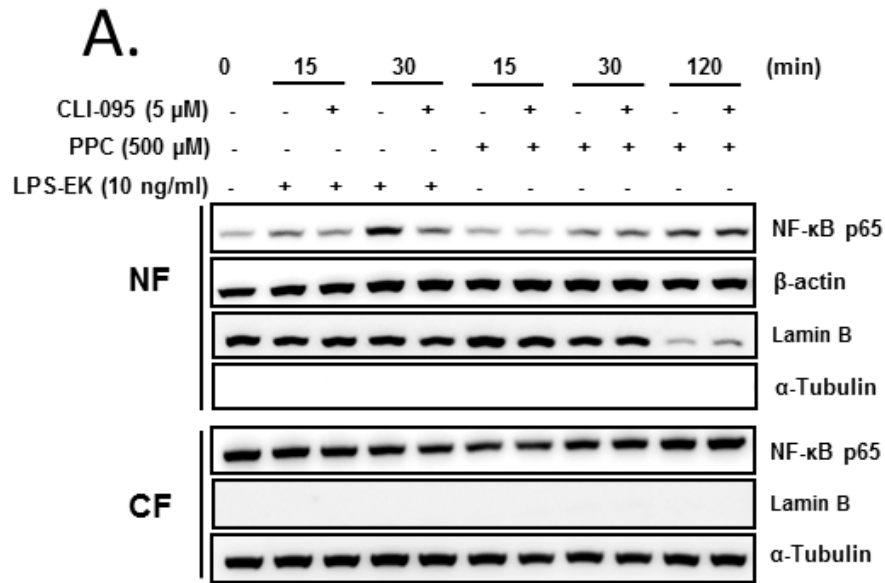


Figure 20. The role of TLR4 in PPC-stimulated p65 nuclear translocation. Cells were preincubated with CLI-095 for 3 h followed by stimulation with either PPC for 0, 15, 30 and 120 min. LPS-EK was used as a positive control of TLR4 activation. Nuclear fraction and cytoplasmic fraction were separated. The levels of NF- κ B p65 in NF and CF were analyzed by Western blot. Lamin B and α -Tubulin were used as markers for NF and CF, respectively. β -Actin in NF was used as housekeeping gene to semiquantify the amount of p65 in NF. **(B)** The histogram represents the OD ratios of p65 immunoblot signals in NF normalized to those of β -actin in NF from **(A)**.

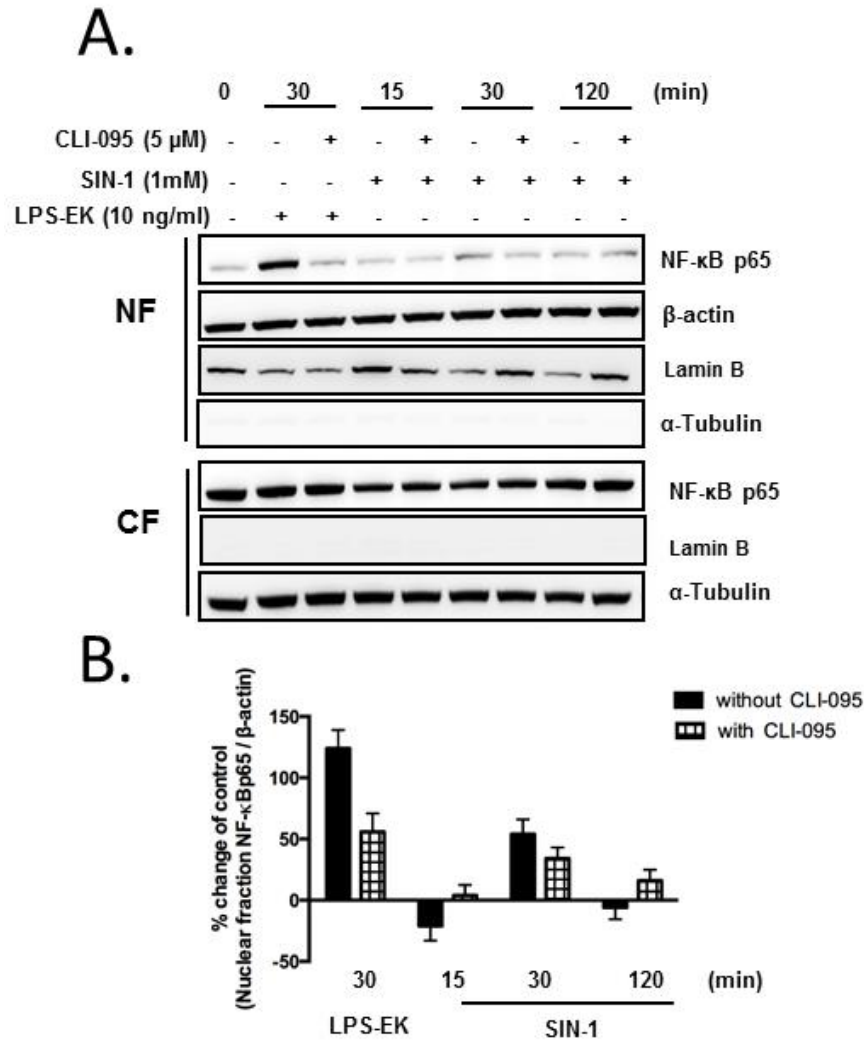


Figure 21. The role of TLR4 in PPC-stimulated p65 nuclear translocation. Cells were preincubated with CLI-095 for 3 h followed by stimulation with either SIN-1 for 0, 15, 30 and 120 min. LPS-EK was used as a positive control of TLR4 activation. Nuclear fraction and cytoplasmic fraction were separated. (A) The levels of NF- κ B p65 in NF and CF were analyzed by Western blot. Lamin B and α -Tubulin were used as marker for NF and CF, respectively. β -actin in NF was used as housekeeping gene to semiquantify the amount of p65 in NF. (B) The histograms represent the OD ratios of p65 immunoblot signals in NF normalized to those of β -actin in NF from (A).

Mechanisms by which Oxidants Stimulate NF- κ B Activation

Oxidants Stimulated Degradation of I κ B α

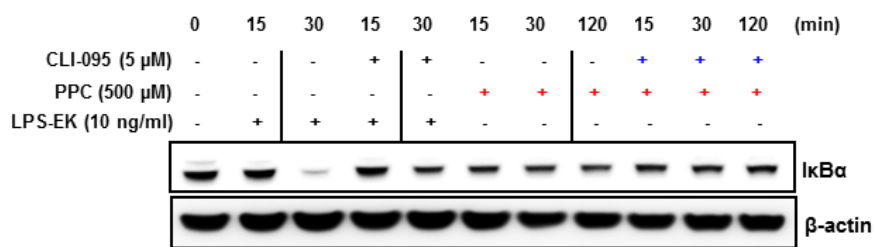
We have shown that oxidants stimulated NF- κ B activation, next we determined the mechanisms involved in this process. TLR4 native agonist LPS-EK mediates NF- κ B activation by inducing I κ B α degradation (Takada et al., 2003). We investigated whether oxidant-induced NF- κ B activation was mediated through the same mechanisms. The effects of oxidants on levels of I κ B α at different time points were determined by Western blot. PPC induced I κ B α degradation as early as 15 min, which lasted up to 120 min (**Fig. 22 A and 22 B**). To investigate the role of TLR4 in the process, we preincubated cells with the TLR4-specific signal inhibitor CLI-095 before stimulation with PPC. The results showed that PPC-mediated I κ B α degradation was blocked by pretreatment with CLI-095 suggesting TLR4 activation is necessary in the process (**Fig. 22 A and 22 B**). LPS-EK also induced robust I κ B α degradation at 30 min, which was inhibited by CLI-095 (**Fig. 22 A and 22 B**).

Oxidants Stimulated Enhanced Phosphorylation of I κ B α at the Tyr42 Residue

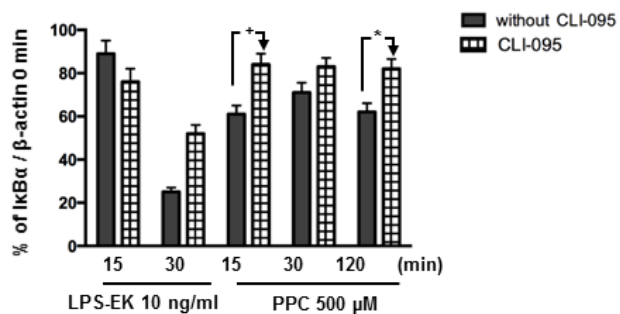
LPS-EK induces phosphorylation of serine (Ser) 32/36 residues in I κ B α leading to a rapid degradation of I κ B α by the proteasomes (Takada et al., 2003). We investigated whether PPC induced phosphorylation of I κ B α at the same residues. Consistent with previous studies, LPS-EK appeared to stimulate phosphorylation of I κ B α on Ser32/36 residues at 15, 30 and 120 min, whereas PPC had no effect on the Ser residues of I κ B α (**Fig. 22 C and 22 E**). Previously our laboratory (Karki et al., 2014) and others have shown that oxidants can activate NF- κ B through tyrosine 42 (Tyr 42) phosphorylation (Takada et al., 2003). We determined phosphorylated I κ B α (Tyr 42) by immunoprecipitation (IP) with anti- I κ B α Ab (c-terminal) followed by immunoblot

probed with anti-p-I κ B α (Tyr42) Ab. Cells following PPC treatment exhibited enhanced Tyr42 phosphorylation of I κ B α in a time-dependent manner (**Fig. 22 D and 22 F**). PPC stimulated Tyr42 phosphorylation at 30 min, which continued for up to 120 min. We confirmed the specificity of immunoprecipitation by stripping the membrane and probing it with anti-I κ B α Ab (c-terminal). One band was observed at similar sites on the membrane. Similar levels of β -Action demonstrated an equal amount of total protein was used for IP.

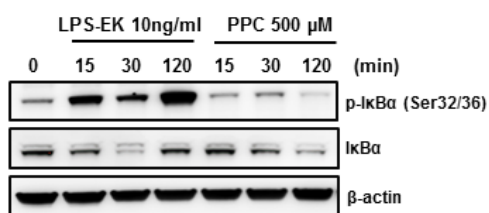
A.



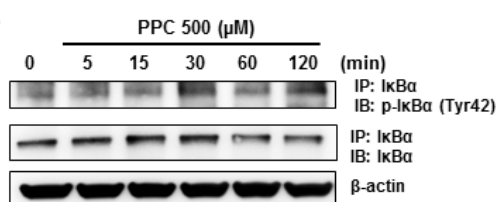
B.



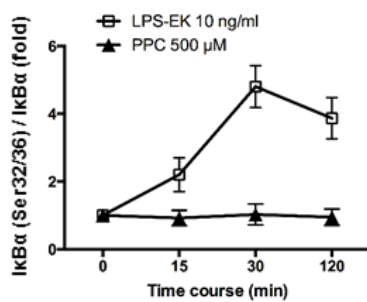
C.



D.



E.



F.

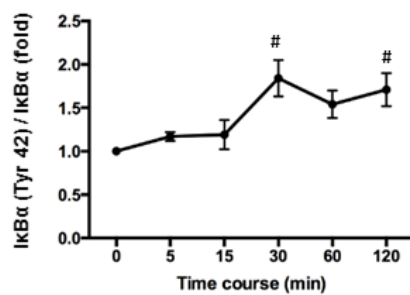


Figure 22. Role of TLR4 in oxidants mediated I κ B α degradation and phosphorylation in RAW-Blue cells. **(A)** Cells were preincubated with CLI-095 for 3 h followed by stimulation with either LPS-EK or PPC for 0, 15, 30 and 120 min. I κ B α degradation was determined by Western blot. % Change of OD ratios (I κ B α to β -actin) compared at t = 0 min was used to present the effects of oxidants on I κ B α expression. Representative immunoblot results are shown. **(B)** The graphs represent the OD ratio of p-I κ B α immunoblot signal from (A) after normalization to total β -actin. The data represent 3 independent experiments conducted in duplicate (+ p \leq 0.05, *p \leq 0.01). **(C)** and **(D)** Cells were stimulated with LPS-EK or PPC for the indicated time points. I κ B α phosphorylation at Ser32/36 was determined by Western blot **(C)**. I κ B α phosphorylation at Tyr42 was determined by immunoprecipitation (IP) followed by Western blot **(D)**. Total I κ B α was immunoprecipitated with anti-I κ B α antibody (c-terminal). Anti-p-I κ B α (Tyr 42) was used to probe the membrane. **(E and F)** The time-course representation of the OD ratio of p-I κ B α immunoblot signal from **(C)** and **(D)** after normalization to total I κ B α . Representative immunoblot results are shown here. #p \leq 0.05 vs time 0 min, n = 3.

Role of TLR4 in Oxidant-induced Production of Inflammatory Cytokines

We have demonstrated that oxidants can stimulate NF- κ B activation through TLR4 stimulation, we next investigated the biological significance of NF- κ B activation in macrophages. NF- κ B is the central transcriptional regulator of myriads of pro- and anti-inflammation mediators. A major outcome of NF- κ B activation in macrophages is the production of myriad of cytokines including TNF- α and chemokines (Murray and Wynn, 2011). The production of pro- & anti-inflammatory cytokines during inflammation orchestrates the inflammatory response (Lawrence and Gilroy, 2007). Effects of oxidants on the production of TNF- α (a representative pro-inflammatory cytokine) and IL-10 (a representative anti-inflammatory cytokine) in macrophages were investigated. Exposure of PPC to cells significantly induced TNF- α production, whereas SIN-1 treatment had no detectable effect (**Fig. 22 A**).

The role of TLR4 in oxidant-mediated TNF- α production was further confirmed using CLI-095 (**Fig. 22 A**). For the anti-inflammatory mediator IL-10, both oxidants and LPS-EK had no effect on its production (**Fig. 22 B**). The ratios of TNF- α and IL-10 following stimulation with oxidants and LPS-EK were calculated as a parameter to represent the balance between the potential biological effects. Both PPC and LPS-EK treatment increased the ratio of TNF- α to IL-10 whereas SIN-1 had no effect on it (**Fig. 22 C**).

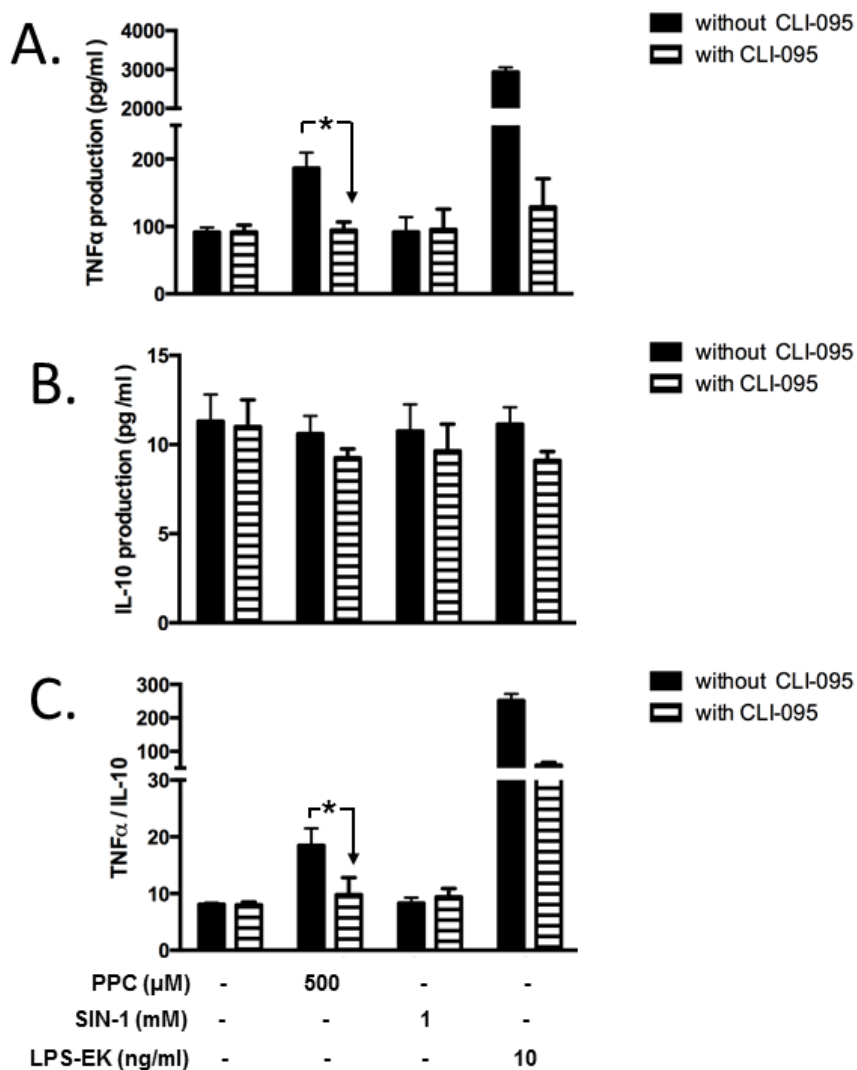


Figure 23. Role of TLR4 in oxidants induced TNF α and IL-10 production. Cells were exposed to oxidants or LPS-EK for 3 h followed by incubation with complete growth medium (oxidants and LSP-EK free) for next 16 h. CLI-095 (5 μ M) was added 3 h before oxidants or LPS-EK stimulation. TNF α (A) and IL-10 (B) levels in the conditioned medium were determined using their respective ELISA kits according to the manufacturer's instructions. The ratios of TNF α to IL-10 after treatment with oxidants or LPS-EK were calculated. The data represent 3 independent experiments carried out in duplicate with * $p \leq 0.01$

Discussion

In this chapter, we tested the hypothesis that TLR4 mediates exogenous oxidant-induced NF- κ B activation in macrophages. We used murine macrophage RAW-Blue cells, which are stably transfected with NF- κ B reporter gene SEAP. We confirmed the generation of reactive intermediates from ROS/RNS-producing agents (PPC or SIN-1), and the expression of TLR4 in RAW-Blue cells at both the mRNA and protein levels. We treated cells with oxidants followed by measurement of SEAP release, DNA binding activity and nuclear translocation of p65 as readouts of NF- κ B activation, and TNF- α and IL-10 production as inflammatory outcomes of NF- κ B activation. We used TLR4 neutralizing antibody and a specific TLR4 signal transduction inhibitor CLI-095 to more substantively characterize the role of TLR4 activation in the ROS/TLR4 signaling. A major finding of this study is that TLR4 is involved in oxidant-mediated NF- κ B activation in macrophages. The data supporting this conclusion includes the following findings: (i) anti-TLR4/MD-2 pAb and CLI-095 significantly attenuated oxidant-induced SEAP release; (ii) CLI-095 significantly inhibited oxidant-induced p65 DNA binding activity, I κ B α degradation and imbalance between TNF- α and IL-10 production. Our findings further characterized and confirmed the mediatory role of TLR4 in exogenous oxidant-mediated NF- κ B activation in macrophages. Thus, our data presents for the first time, critical mechanisms that may explain / support the intersection between exogenous and endogenous ROS in enhancing inflammatory phenotypes that may initiate, propagate and maintain multiple human disease states.

We used two oxidants (PPC and SIN-1) as exogenous ROS-generating system. For a long time, hydrogen peroxide (H₂O₂) has been widely used as an oxidant (Takada et al., 2003; Safaeian et al., 2015). But it cannot represent a true ROS because it carries

no charge and diffuses through lipid plasma membrane rapidly by unproven or unknown mechanisms. Furthermore, the high concentrations normally used are physiologically unrealistic. In contrast, most of RONS are charged such as superoxide and PN. Therefore, we used PPC, which readily decomposes to release several oxygen-centered free radicals *in situ* including hydroxyl radicals, singlet oxygen, hydrogen peroxide, and possibly superoxide (Hodgson and Fridovich, 1974; Baird et al., 1977). Among of them, singlet oxygen and hydroxyl radicals having been suggested as the primary lipid pro-oxidants (Baird et al., 1977; Edwards and Quinn, 1982). Quantitatively, one superoxide anion and one singlet oxygen are release during the course of the decomposition of CrO_8^{3-} to CrO_4^{3-} (Baird et al., 1977).

Thus, we first confirmed release of ROS from PPC decomposition by measuring the end products of lipid peroxidation, MDA (**Fig. 11 A**). Consistent with previous studies (Baird et al., 1977; Edwards and Quinn, 1982; Sharma and Ebadi, 2003), *in vitro* exposure of cells to PPC resulted in increase of the end production of lipid peroxidation MDA in culture medium, which was attenuated by an antioxidant EUK-134 (**Fig. 11A**). Our experimental system cannot exclude the biological effects of trace chromium in the Cr (+V) valency state, which may also produce hydroxyl radicals (Valko et al., 2005).

NO couples to superoxide anion at a diffusion-dependent rate to produce peroxynitrite (PN) (Hogg et al., 1992). The occurrence of this reaction has been suggested *in vivo*, in particular, in pathological conditions. For example, macrophages and neutrophils, recruited to a site of injury, can be activated to produce both superoxide and nitric oxide as part of the inflammatory response (Marletta et al., 1988). PN

decomposes rapidly in physiological buffers with a half-life of 1.9s at pH 7.4 (Hogg et al., 1992), which renders it difficult to use.

In contrast, SIN-1 (also known as a Syndonimine), which decomposes to generate equimolar amounts of NO and superoxide anion, is used to provide a long-term source of PN under physiological conditions (Hogg et al., 1992). PN spontaneously nitrates phenolic compounds including free and protein-bound Tyr residues resulting in specific formation of nitrotyrosine (Beckman et al., 1992). In the present study, we detected increased formation of cellular nitrotyrosine (nTyr) upon treatment with SIN-1 (**Fig. 11 B**), confirming formation of OONO^- , which has been reported *in vitro* in other cell culture system (Trackey et al., 2001). In the case of protein nitration, the effects of SIN-1 were less potent, which may be due to different kinetics in PN formation. PN released from potassium PN (PPN) directly and rapidly reacts with Try residues whereas PN produced from the NO and superoxide generated from SIN-1 reacts with Tyr more slowly (Szabo et al., 2007).

PN can decompose to nitrogen dioxide and hydroxyl radicals (Hogg et al., 1992), which induce membrane lipid peroxidation (Radi et al., 1991). In our experiments, we observed that *in vitro* exposure of cells to SIN-1 increased levels of lipid peroxide 4-HNE in the culture medium (**Fig. 11 C**). This confirmed that free radicals were generated during SIN-1 decomposition in the biological system. We determined the levels of 4-HNE instead of MDA upon treatment with SIN-1, because SIN-1 appear to interfere with TABRS assay (**Fig. 11 D**), which has not been previously reported. It is likely that the morpholinyl structure within SIN-1 may interfere with pyrimidine moiety within TBA.

With the capability to produce PN *in situ* for a long time, SIN-1 is used as a PN donor (Trackey et al., 2001; Seo et al., 2009). However, limitations of using SIN-1 should also be noted. First, PN formation rate is variable. The combination of NO with superoxide proceeds at 20 °C, with a rate constant of $3.7 \times 10^7 \text{ M}^{-1} \cdot \text{S}^{-1}$, which effectively competes with other reactions and the reaction depend on diffusion of NO and superoxide. Many experimental factors can have impact on this reaction. For example, temperature and medium components may impact the diffusion rate. The presence of electron acceptors in medium will favor SIN to primarily decompose NO instead of producing PN (Trackey et al., 2001). H₂O₂ can be formed from SIN-1 in the presence of HEPES buffer (Kirsch et al., 1998). Second, the exact amount of PN generated from SIN-1 is still not completely clear. Under physiological condition (37°C, pH 7.4), it appears that the rate formation of NO and superoxide from SIN-1 (1 mM) are 3.68 μM/min, and 7.02 μM/min, respectively. However, to our knowledge, no study has shown the exact amount of PN produced from SIN-1 decomposition. This is probably because there is no direct method to quantify PN (Trackey et al., 2001). Finally, the chemical component after SIN-1 decomposition is not pure, but a mixture of RONS. After NO release and superoxide, SIN-1 decomposes to the stable compound SIN-1c, which also showed biological effects such as modulation of chloride secretion in murine airway cells (Trackey et al., 2001). Furthermore, PN is substantially protonated to produce peroxynitrous acid, which in turn decomposes to produce hydroxyl radical and nitrogen dioxide (Hogg et al., 1992).

We first determined the concentrations of PPC and SIN-1 that will activate NF-κB in RAW-Blue cells as quantified by the level of SEAP release (**Fig. 13 C and 13 D**). Our initial use of low concentrations of PPC or SIN-1 resulted in undetectable levels

of SEAP release. However, we determined empirically that treatment with much high concentrations of the oxidants for 2 h only, followed by continued incubation with fresh medium in the absence of oxidants resulted in a robust SEAP release. In this treatment protocol, we confirmed that cell viabilities were above 90% (**Figs. 14 A - D**) and that NF- κ B activation occurred as quantified by SEAP release (**Figs. 14 E and 14 F**). This could be explained by the aqueous decomposition rate of PPC of 80 μ M/min (Hodgson and Fridovich, 1974). It is conceivable that at low concentration, decomposition of PPC was completed during the dilution phase and ROS released from PPC would have degraded *in situ* because of their very short half-life lives. For example, the half-life time of hydroxyl radical is 10^{-9} seconds. The dose-dependent cell toxicity caused by PPC at lower concentration could be due to Cr (+V) itself (Stohs et al., 2001). Higher concentrations of PPC required fewer steps of dilution and therefore the ROS released from PPC decomposition have much longer $t_{1/2}$ in solution, which would allow interaction with TLR4.

Cellular oxidative stress occurs when there is an imbalance between ROS generation *in situ* and the total antioxidant capacity of the cell. This may be caused by both increased free radical generation and /or decreased antioxidant defenses. Therefore, to determine cellular oxidant stress caused by oxidants, we used a combination of fluorescence microscopy (FM) and flow cytometry (FCM) to determine iROS production. In the present study, we found that cellular iROS was increased upon treatment with oxidants or LPS-EK (**Fig. 16 A and 15 B**), thus implicating ROS generated exogenously in TLR4 stimulation.

We determined levels of iROS by both FM and FCM. Interestingly, FM yielded a greater magnitude of iROS increase than those obtained by FCM for the same treatments (**Fig. 15 C and 15 D**), which was consistently observed in our previous study (Zhang et al., 2015). This could be due to potential loss of fluorescent positive cells, inherent in sample preparation prior to FCM. Alternatively, FM could encompass an approximation of ROS in both extra-and intra-cellular compartments whereas FCM represents fluorescence reading of intact cells only (Muratori et al., 2008).

Indeed, ROS quantification remains challenging. The present available methods to determine iROS are not direct and ROS and RNS can react with each other. In addition, using CellRox deep red reagent to detect cellular oxidative stress has a limitation, because it mainly identifies superoxide in live cells (Plaza Davila et al., 2015). Furthermore, distinguishing ROS from each other by specific assays is fraught with difficulties (Nathan and Cunningham-Bussel, 2013). Therefore, cellular oxidative stress caused by other ROS such as hydrogen peroxide cannot even be detected or quantified.

Moreover, to determine the subcellular location of ROS production is more relevant, but challenging as well. Because it is being recognized that ROS production at an inappropriate place or time, for too long at too high a level, or inappropriate forms, can cause disturbances in ROS homeostasis. Thus total levels of iROS cannot be used as the final or the only indicator of disturbances in ROS homeostasis. Our approaches only suggest what is possible with enhanced levels of iROS. However, new strategies will be needed for subcellular localization of iROS.

We quantified another marker of oxidative stress, iTAOC, which has been used to monitor oxidative status in cancer patients (Patel et al., 2007a) and passive smoking exposure in infants (Aycicek et al., 2005). Unlike CellRox reagent, which mainly measures one individual superoxide anion component, iTAOC reflects more comprehensive biological information of reduction-oxidation status inside cells. In the present study, we quantified iTAOC in cell lysate and found that oxidants as well as LPS-EK decreased iTAOC (**Fig. 15 E**), suggesting impaired iTAOC may fail to buffer ROS production caused by oxidants thereby resulting in cellular oxidative stress.

Cellular catabolism of ROS includes enzymatic antioxidants, e.g. SOD, GSH reductase, CAT and nonenzymatic antioxidative agents like ascorbic acid, pyruvate, α -ketoglutarate, and oxaloacetate (Nathan and Cunningham-Bussel, 2013). The mechanisms of decreased iTAOC requires additional experimentation to clarify its utility in monitoring in health and disease. It is conceivable that ROS produced following oxidants treatment exceeded and depleted cellular antioxidants. In the case of SIN-1, it could be due to tyrosine nitration of mitochondrial manganese (Mn) SOD which has been demonstrated to diminish the ability of cells to cope with oxidative stress (MacMillan-Crow et al., 1996).

The pathway by which oxidants induce cellular oxidative stress will need further clarification in future experiments. It is of critical importance to understand the role of increased iROS by exogenous oxidants, not only in their classical role of causing injury by disruption of cells membranes, DNA strand breaks, or enzyme inactivation, but also as precise signaling molecules (Gill et al., 2010). For example, they can physiologically regulate Tyr and Ser/Thr kinases and phosphatases. Furthermore, they

also contribute to the activation of transcription factors by several mechanisms (Nathan and Cunningham-Bussel, 2013).

We examined the effects of oxidants on NF- κ B activation by quantifying the expression of SEAP reporter gene. NF- κ B signaling is regarded as redox sensitive and ROS strongly affects its activation. The effects of ROS on NF- κ B is cell and stimulus dependent. For example, H₂O₂ stimulated NF- κ B activation in Raw 264.7 (Takada et al., 2003) but failed to do so in monocytic cells line and peripheral T cells (Brennan and O'Neill, 1995). In the present study, our data confirmed that exposure of cells to PPC for a short time but at higher concentration (500 μ M) stimulated NF- κ B activation in Raw-Blue macrophages (**Fig. 14 E**).

We used anti-oxidant EUK-134 to clarify the activation of TLR4 by oxidants. Inhibition of SEAP caused by EUK-134 (**Fig. 17**) suggests that it is RONS released from oxidants that stimulate TLR4 and activate NF- κ B. Since the EUK-134 is a synthetic cell permeable anti-oxidant (Lawler et al., 2014), it can diffuse through plasma membrane and reside within the cells. Hence, our results cannot exclude the possibilities that NF- κ B activation may also results from RONS localized within the cells. Using antioxidant which are not cell permeable might be necessary to clarify this question.

Presently, for the first time, we defined the role of TLR4 in oxidant-stimulated NF- κ B activation using TLR4 neutralizing Ab and CLI-095. Soluble MD-2 is specifically physically associated with the extracellular domain (ECD) of TLR4 on cell surface other than other TLRs (Takashima et al., 2009). MD-2 binds to the ECD of TLR4 during protein biosynthesis such that the heterodimer of TLR4/MD2 forms in

the absence of ligands (Gay et al., 2014). When the hydrophobic core of MD-2 binds lipid A, MD-2 exposes an interface that binds a second TLR4 ECD to promote the formation of a heterotetrameric TLR4/MD-2 signaling complex (Gay et al., 2014). Anti-mouse TLR4/MD-2 pAb (Clone MTS 510) has been shown to be able to bind to an epitope of the TLR4/MD-2 complex that is lost after LPS stimulation (Akashi et al., 2003). In addition, anti-TLR4/MD-2 pAb (Clone MTS 510) recognize distinct epitopes and doesn't cross block other receptors (Akashi et al., 2003). Our data clearly showed that preincubation with anti-TLR4/MD-2 pAb at the concentration we used partially attenuated oxidant-induced SEAP release (**Fig. 18**), suggesting that oxidant might be able to activate TLR4 expressed at least partially via a MD-2 dependent mechanisms. More experiments will be necessary to prove this notion.

Activation of intracellular signaling requires the interaction between TLR4 and adaptor molecules containing TIR domain such as TIRAP and TRAM. A single point mutation can abolish the response to TLR4 activation (Poltorak et al., 1998). Dimerization of TIR domains was sufficient to induce signaling (Daringer et al., 2015). Therefore, TIR domain is critical for signal transduction of TLR4. CLI-095 has been shown to covalently bind to the Cys747 residue within TIR domain of TLR4 among 10 human TLRs, thus interfering with TLR4 signal transduction (Li et al., 2006; Takashima et al., 2009), and showed beneficial effects in a mouse sepsis model (Sha et al., 2007). Our results clearly showed that pre-treatment with CLI-095 markedly inhibited oxidant-induced SEAP release (**Fig. 18**), further confirming that the TIR domain of TLR4 is required in oxidant-induced NF- κ B activation. Although TIR domain of TLR4 share a high homology with that of type I IL-1 receptor, type I IL-1 receptor is predominantly expressed on T cells and fibroblasts. By far, there are no reports on the

interaction between CLI-095 and IL-1 receptor. Furthermore, the mediatory role of TLR4 in oxidant-induced NF- κ B activation has been demonstrated in peritoneal macrophages derived from TLR4-KO mice in our previous paper (Zhang et al., 2015).

TLR4 neutralizing pAb showed less potent effects on oxidant or LPS-EK-mediated NF- κ B activation in comparison with CLI-095 (**Fig. 18**), which could be due to two reasons. First, at the concentrations we used, the interaction between cysteine (Cys) 747 within TIR domain of TLR4 and CLI-095 is through strong covalent binding which is normally irreversible. In contrast, the forces joining the antigen-antibody complex are not strong covalent bonds but weaker interactions such as ionic and hydrophobic bonds, which are generally reversible (Reverberi and Reverberi, 2007). Data of LPS-EK support this explanation. Under LPS-EK stimulation, pretreatment with neutralizing Ab caused about 31% inhibition while pretreatment with CLI-095 caused about 61% inhibition (**Fig. 18**). It is also conceivable that the concentration of pAb we used was too low. Theoretically, the higher inhibition will be observed when concentration of neutralizing Ab is increased.

Second, as a co-receptor, MD-2 is necessary in LPS-EK induced TLR4 dimerization and subsequent activation. However, a recent study has shown that unlike LPS, metal-induced TLR4 dimerization did not require MD-2 (Raghavan et al., 2012). About 20% inhibition observed with TLR4/MD-2 neutralizing pAb indicates that oxidant-induced TLR4 stimulation might be partially through a MD-2 mechanism. In contrast, the TIR domain is necessary for transducing signal upon oxidant-induced TLR4 activation. Therefore, inhibition of the TIR domain revealed more potent inhibitory effects on oxidant-mediated TLR4 activation.

We determined oxidant-induced activation of NF- κ B by measuring p65 DNA binding activities and nuclear translocation of p65 from cytosolic I κ B 50/65 complex. Consistent with our results in the SEAP release assay (**Fig. 14 E and 14 F**), our data clearly showed increased p65 DNA binding activity (**Fig. 19**) and nuclear translocation following treatments with oxidants (**Fig. 20 and 21**). However, we observed a discrepancy regarding the effects of CLI-095: its inhibitory effects on p65 DNA binding activity was not detected in p65 nuclear translocation by Western blot. Compared with semi-quantification of p65 in NF by western blot, use of TransAM[®] assay is a more accurate method to quantify transcriptional factor activation. First, it is a quantitative ELISA-based assay. Second, the primary antibody used in the TransAM[®] assay specifically recognizes the transcriptionally active form of p65 when it binds to DNA. Therefore, the assay quantifies the transcriptionally active form of p65 while Western blotting is a semi-quantitative measurement of total p65 in the NF.

We examined the mechanisms of NF- κ B activation in response to oxidants. Our results clearly suggest different post-TLR4 mechanisms for NF- κ B activation following LPS-EK exposure. First, levels of I κ B α reverted to the basal level after LPS-EK treatment for 120 min (**Fig. 22 C**) suggesting resynthesis of I κ B α (Takada et al., 2003). Newly synthesized I κ B α , which is one of the target genes of NF- κ B activation, can enter the nucleus, remove NF- κ B from DNA, and export the complex back to the cytosol, where it remains in an inactive state until stimulated again (Yates and Gorecki, 2006). In contrast, oxidant induced degradation of I κ B α occurred as early as 15 min and continued for up to 120min (**Fig. 22 A and 22 C**). These results are very intriguing because they imply that no detectable I κ B was newly synthesized and the absence of

negative feedback regulation loop would lead to constitutive NF- κ B activation for longer duration.

Second, PPC induced robust phosphorylation at Tyr 42 residue but not Ser 32/36 residue, which was shown following LPS-EK treatment (**Fig. 22 C and 22 D**). This suggests that oxidants can stimulate NF- κ B activation mainly by phosphorylation at Tyr 42 residue and subsequent degradation of I κ B α , which takes a much longer time. Our study are in agreement with mechanisms by which pervanadate or UV radiation activates NF- κ B, in which phosphorylation of I κ B α at Tyr 42 residue and its subsequent degradation was shown for NF- κ B activation (Li and Karin, 1998; Mukhopadhyay et al., 2000). Our data also provide further evidence for our previous hypothesis that phosphorylation of I κ B α at the Tyr 42 residue leads to delayed degradation of I κ B α , which would activate NF- κ B for a long time (Karki et al., 2014) resulting in an extended synthesis expression of inflammatory gene phenotypes. Differences in TLR4 signaling in response to DAMPs released under oxidative stress stimulations compared to PAMPs released by infective stress are beginning to emerge. For example, HMGB1 activates both IKK α and IKK β , but LPS stimulates activity of IKK β only in cultured neutrophils and macrophages (Park et al., 2004b).

Finally, our results clearly showed that oxidant-stimulation of the TLR4 signaling pathway significantly induced the production of TNF- α , a proinflammatory cytokine, but not IL-10, an anti-inflammatory cytokine, and increased the ratio between them (**Fig. 23**). TNF- α appears to generate a feed-forward mechanism to amplify the inflammatory response by regulating the expression of other pro-inflammatory cytokines including IL-1, IL-6, PDGF, and TGF- β and enhancing chemotaxis of

macrophages and neutrophils at the site of inflammation (Larrick and Wright, 1990). The correlation between NF- κ B activity and the severity of inflammatory phenotypes has been established (Zhang et al., 2015). In contrast, IL-10 showed multifaceted anti-inflammatory effects, such as inhibition of NF- κ B activation, which results in suppression of cytokine production (Wang et al., 1995). Therefore, our results suggest that PPC treatment may trigger pro-inflammatory phenotypic response in macrophages by releasing TNF- α in the absence of counteracting anti-inflammatory effects. Whether this makes exposure to exogenous oxidants more problematic in public health remains to be further clarified.

Interestingly, although our results showed PN release from SIN-1 (**Fig. 11 B and 11 C**) and SIN-1 activated NF- κ B (**Fig. 14 F**), our data suggest that SIN-1 had limited effects on the production of TNF- α in Raw-Blue cells. It has been established that PN release from SIN activate NF- κ B in various tissues including epithelial cells (Seo et al., 2009), skeletal myoblasts cells (Bar-Shai and Reznick, 2006), and intervertebral disc (IVD) cells (Poveda et al., 2009). SIN-1 specifically stimulate IL-8 expression. SIN-1 induced IL-8 expression and production in gastric epithelial cells (Seo et al., 2009), in human how blood (Filep et al., 1998), and in human IVD cells (Poveda et al., 2009). In addition to IL-8, SIN-1 stimulates gene expression of IL-6 and IL-1 β in human IVD cells (Poveda et al., 2009). To our knowledge, no study has shown that SIN-1 directly stimulates TNF- α gene expression and production. Therefore, although TNF- α is an important target of NF- κ B, it seems that SIN-1 mediated NF- κ B activation does not necessary lead to enhanced TNF- α gene expression. PN release from SIN-1 reduced histone deacetylase 2 activity and then modulate gene expression of proinflammatory mediators (Ito et al., 2004). Hence, it is conceivable that epigenetic

modification by PN inhibit NF- κ B-mediated TNF- α gene expression. More experiments will be necessary to clarify this notion.

In conclusion, we have affirmed that exogenous oxidants can promote inflammation through a TLR4-dependent pathway in macrophages. Our findings suggest that oxidant-mediated TLR4 activation pathway may be associated with initiation, propagation and maintenance of “sterile” inflammatory processes that play a role in human diseases.

4. MATERIAL AND METHODS FOR PRIMARY PERITONEAL MACROPHAGES

Oxidants

We used the same oxidants (PPC and SIN-1) as was described in Chapter 2, page 49).

Animals (Mice) used

B6B10ScN *Tlr4* and C57Bl/6 mice were purchased from Jackson Labs. B6B10ScN *Tlr4* are spontaneous mutants corresponding to a 74, 723 bp deletion that completely removed the *Tlr4* coding sequence (Poltorak et al., 1998). C57BL/6 mice with the same genetic background and matched by geneticists at the Jackson labs were used to represent wild type of TLR4 expression for comparisons to ScN-*Tlr4*^{lps-del} mice. These mice were cared for and maintained as approved by UMKC-IACUC in accordance with NIH guidelines. Primary peritoneal macrophages (pM) isolated from 6 - 8 weeks old and gender-matched mice were used in all experiments. C57Bl/6 and B6B10ScN *Tlr4* mice are designated as TLR4-wildtype (WT) and TLR4-knockout (KO) mice, respectively.

Genomic DNA Extraction from Mouse Tail to Confirm Genotypes

Tail tips (0.5 mm) were cut from three-week old mice, and digested in 400 μ l tail lysis buffer supplemented with proteinase K (20 μ g/ μ l) overnight at 50 - 55°C water bath. On the following day, we added saturated 6 M NaCl solution and centrifuged it for 5 min at 13, 000 \times g at 4°C. The supernatant was transferred into a new tube followed by addition of 400 μ l isopropanol to each tube to precipitate the DNA. After

washing with 70% ethanol, the DNA pellet was allowed to air dry and subsequently solubilized in Tris-EDTA (TE) buffer.

PCR and Running DNA Gel

Genomic DNA was amplified by PCR using the Step-One™ Real-Time PCR System (Applied Biosystem, Foster City, CA) via standard fluorescent methodology and thermal cycling conditions following the manufacture's recommendations. The PCR reaction mixture contained 2 µl genomic DNA (extracted from mice tail), 10 µl of the Real-time Bullseyes EvaGreen qPCR MasterMix (Catalog No. BEQPCR-R, MIDSCI, Valley Park, MO), 0.4 µl of primer pairs (10 µM) and 8.6 µl H₂O in a complete reaction volume of 20 µl. Both pairs of primers for TLR4-WT and KO were included in each of the PCR reactions. PCR products were separated by gel electrophoresis on 4-20% TBE gels (Catalog No. EC6225BOX, ThermoFisher Scientific). Signals were visualized with the Fujifilm LAS-400 imaging system (Fujifilm).

Isolation and Characterization of Thioglycollate (TGC)-elicited Peritoneal

Macrophages (pM)

We isolated and characterized primary pM according to a standard published method (Zhang et al., 2008). TGC (3%) broth (500 ml) was prepared, autoclaved and left on the shelf in the dark to age for at least one month before use. Aged TGC (1 ml) was injected into the peritoneal cavity of anesthetized mice. Peritoneal cells were harvested 3 to 4 days later by peritoneal lavage using ice cold Dulbecco's phosphate-buffered saline (DPBS) (Catalog No. 14190-136, ThermoFisher Scientific). pM are non-adherent *in situ* in the peritoneal cavity, but become adherent when cultured in

culture dishes. Thus, macrophages were enriched by adherence by plating for 1 h in DMEM/F12 medium without FBS. DMEM/F12 media containing floating nonadherent cells were removed and replaced with DMEM/12 medium supplemented with 10 % (v/v) FBS, 50 units/ml penicillin and 50 µg/ml streptomycin for 24 h before they were used in subsequent experiments. Incubation with DMEM/12 medium for 24 h would further enrich the purity of pM (Misharin et al., 2012).

Determination of the Purity of Primary pM

Using Immunocytochemistry

Isolated primary pM were seeded in 8-well chamber slides pretreated with CC²™ (Nunc™ Lab-Tek™ II, Thermo Scientific) to facilitate overnight attachment. Next day, the culture medium was removed and cells were fixed in 10% buffered formalin phosphate (Catalog No. L-23006, Fisher Scientific) for 15 min at room temperature followed by two washes with ice cold PBS. Cells were then incubated with 1% BSA in PBS with 0.1% Tween 20 (PBST) for 30 min at room temperature followed by incubation with primary anti-CD11b Ab or anti-isotype Ab in 1% BSA in PBST for 1 h at room temperature. After three washes with PBS, cells were incubated with 2nd Ab conjugated with fluorescein isothiocyanate (FITC) in 1% BSA and NucBlue[®] live cell stain reagent for 1 h at room temperature in the dark. After three rinses with PBS, images were acquired using a fluorescence microscope (Axiovert 200M; Zeiss) at excitation and emission wavelengths of ~490/555 nm for FITC and 405/410-550 nm for NucBlue[®].

Using Flow Cytometry

For flow cytometry, isolated primary pM were seed in 6-well tissue culture plate for overnight. The next day, cells were harvested by scraping. After cell number counting, cells were resuspended approximately at 10×10^6 cells/ml in ice cold PBS supplemented with 10% FBS 1 % sodium azide (NaN_3). The presence of sodium azide prevents the modulation and internalization of surface antigen CD11b. Two tubes of cells suspension (100 μl for each tube) were incubated with primary anti-CD11b Ab and anti-isotype Ab (used as negative control), respectively, in 3% BSA in PBS for 40 min at room temperature in the dark. After three washes with PBS, cells were suspended in ice cold PBS followed by incubation with 2nd Ab conjugated with FITC for 30 min at room temperature in the dark. Cells were then washed three times and resuspended in ice cold PBS supplemented with 3% BSA and 1% of sodium azide.

The acquisition of the flow cytometric data and analyses was conducted with FACSCanto II flow cytometer (BD Biosciences, San Jose, CA, USA) as described in Chapter 2. The fluorescence intensity was determined using FITC filter at excitation and emission wavelengths of 490/555 nm. Cells probed with anti-isotype Ab were used as negative controls for CD11b expression. For each parameter investigated, at least 10^4 events (cells) were analyzed per sample. The fluorescence intensities as logarithmically amplified data were compared between different treatments.

Oxidant Treatments

Similar to treatment for Raw-Blue cells, we used two treatment methods: long-term & low concentration of oxidants, and short-term & high concentration of oxidants. For the long-term and lower concentration, cells (in the chapter 5, all cells refers to

primary peritoneal macrophages) were incubated in medium containing a low concentrations (1 ~ 5 μ M for PPC; 500 ~ 1000 μ M for SIN-1) of oxidants or LPS-EK (InvivoGen, San Diego) for overnight treatment. For the short-term and high concentration treatment, cells were stimulated with PPC or SIN-1 at higher concentration (50~ 250 μ M for PPC; 1000-5000 μ M for SIN-1), or LPS-EK (10 ng/ml) for 2 h, cell culture medium was replaced with fresh medium without either oxidants or LPS-EK. Cells were then incubated overnight for ~16 h. We used both short-term & high concentration and long-term & lower concentration in this chapter.

3-(4,5-dimethylthiazol-2-yl)-2, 5-diphenyltetrazolium Bromide (MTT) Assay

At the end of treatment with oxidants, 50 μ l 5 mg/ml MTT (Life technologies, CA, USA) in PBS was added to each well followed by incubation at 37 °C for 3 h. At the end of incubation, medium containing MTT was carefully removed, followed by addition of 500 μ l DMSO to each well. Aliquots (200 μ l) from each treatment were transferred to a 96-well plate for reading at 570 nm as reference using the Powerwave X spectrophotometer (Biotek, Winooski, VT, USA). Percentage of proliferation was calculated by the ratio of absorbance at 570 nm between control and treated cells.

Lactate Dehydrogenase (LDH) Cytotoxicity Assay

As in Chapter 2, page 55

Measurement of Intracellular ROS (iROS) by Fluorescent Imaging Microscopy and Flow Cytometry

As in Chapter 2, page 56

Total Antioxidant Capacity (TAOC) Assay

As in Chapter 2, page 57

RNA Extraction and Reverse Transcription

As in Chapter 2, page 58

Quantitative Polymerase Chain Reaction (qPCR)

As in Chapter 2, page 58

Preparation of Whole-cell Extract

As in Chapter 2, page 59

Immunoblot Analysis

As in Chapter 2, page 59

Quantification of TNF- α

As in Chapter 2, page 61

Quantification of PGE₂ Levels

The levels of PGE₂ in the cell culture medium was quantified using an enzyme-linked immunoassay ELISA kit (Item No. 514010, Cayman Chemical, Ann Arbor, MI) according to manufacturer's instructions.

Quantification of RvD1 Levels

The levels of RvD1 in the cell culture medium was quantified using an enzyme-linked immunoassay ELISA kit (Item No. 500380, Cayman Chemical, Ann Arbor, MI) according to manufacturer's instructions.

Statistical Analysis

As in Chapter 2, page 62

5. ROLE OF TLR4 IN OXIDANT-INDUCED INFLAMMATORY RESPONSES IN PRIMARY PERITONEAL MACROPHAGES

Confirmation of the Experimental System

Confirmation of Mouse Genotypes

We initially confirmed the genotypes of TLR4-WT and TLR4-KO mice. Mice were genotyped by assaying for the deletion of 74, 723-bp fragment using PCR of genomic DNA (gDNA) extracted from mouse tail. As **Fig. 24 A** shows, we used primers (Forward primer: ATATGCATGATCAACACCACAG; Reverse primer: TTTCCATTGCTGCCCTATAG) to detect nondisrupted DNA localized within *tlr4* coding region and to amplify a 390-bp fragment. In contrast, primers (Forward primer: GCAAGTTTCTATATGCATTCTC; Reverse primer: CCTCCATTTCCAATAGGTAG) were used to detect the deletion of *tlr4* localized outside the region deleted in TLR4-KO mice. Therefore, a 140-bp fragment can only be amplified when the 74, 723 bp are completely deleted.

Our results showed that a single product with the expected sizes of 390 and 140 bp were amplified in the presence of two pairs of primers for samples obtained from TLR4-WT and TLR4-KO mice, respectively (**Fig. 24 B**). These results confirmed the deletion of the 74, 723 bp-fragment in genomic DNA resulting in complete deletion of *tlr4* coding sequence in B6B10 ScN-*Tlr4*^{lps-del} mice. In addition, these results confirmed the presence of *tlr4* coding sequences in C57BL/6 mice.

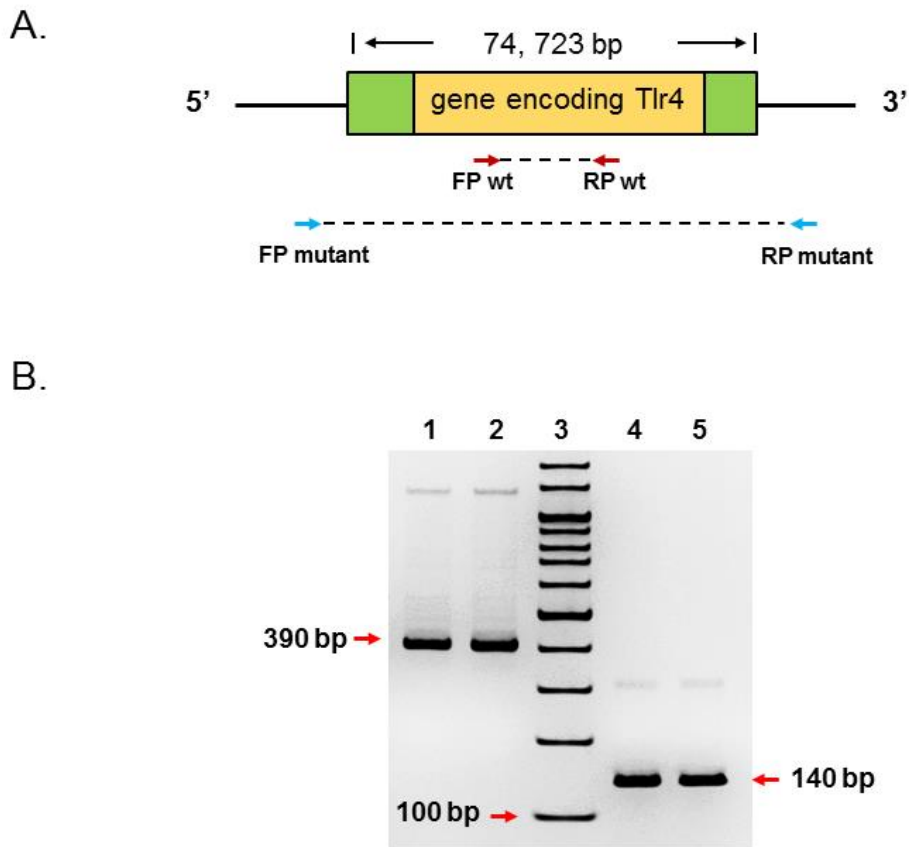


Figure 24. Confirmation of mouse genotypes. (A) Location of primer pairs used to identify the deletion of *tlr4* and to genotype the wild-type alleles. **FP**: forward primer, **RP**: reverse, **wt**: wild type. (B) PCR assay performed on DNA prepared from genomic DNA extracted from the tails of C57BL/6(TLR4-WT) and B6B10ScN-Tlr4^{lps-del} (TLR4-KO) mice. **Lane 1 and 2**: a single PCR product with 390 bp **was** amplified in genomic DNA extracted from TLR4-WT mouse tails in the presence of two primer pairs; **Lane 3**: 100-bp ladder; **Lane 4 and 5**: a PCR product with 140 bp **was** specifically generated with genomic DNA extracted from TLR4-KO mouse tails in the presence of two primer pairs.

After confirmation of mouse genotypes, we assessed the purity of pM isolated from a heterogeneous cell population. Freshly isolated aged thioglycollate-elicited peritoneal cells have been reported to contain a high percentage of macrophages 86-95%, and their purity increased further to almost 99% by adherence. We determined the purity of macrophages by measuring the expression of CD11b, generally considered as a cellular surface marker unique to macrophages. Macrophages are defined as CD11b⁺ cells (Zhang et al., 2008). We used a monoclonal antibody (mAb) clone M1/70 (Abcam, Cambridge, MA), shown to be able to specifically recognize CD11b expressed on macrophages. To ensure that the observed staining is due to the Ab binding to the desired antigen but not to some general unspecific binding of immunoglobulin to cells, we used anti-isotype Ab as negative control.

CD11b expression was visualized using immunofluorescent microscopy as **Fig. 25 A** shows. No fluorescent signal was observed in cells stained with anti-isotype while almost all of the cells are fluorescent when they were stained with anti-CD11b mAb. CD11b positive cells were further quantified by flow cytometry. Our results showed that a forward shift in the peak in cells stained with CD11b mAb compared to cells stained with anti-isotype confirming the specificity of Ab. In addition, above 95% of peritoneal exudate cells (PECs) isolated from mice are CD11b positive (**Fig. 25 B**), which is consistent with previous studies (Zhang et al., 2008).

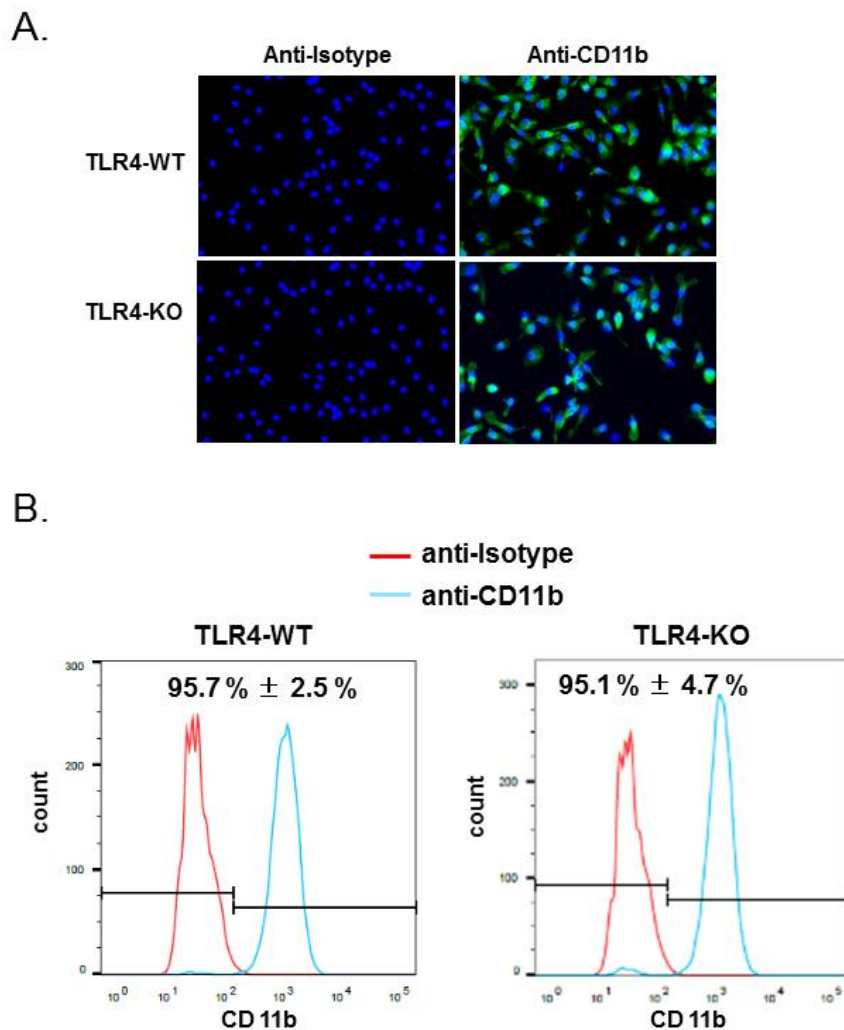


Figure 25. Characterization of thioglycollate-elicited peritoneal exudate cells (PECs) isolated from TLR4-WT and TLR4-KO mice. PECs were stained with anti-Isotype antibody (Ab) or anti-CD11b monoclonal Ab. (A) Representative immunofluorescent image of three independent experiments are shown. Cell were counterstained with DAPI (blue) to identify the cell nuclei. (B) Quantification of CD11b⁺ cells using flow cytometry. Representative flowcytometry Figures of three independent experiments are shown. The data represent mean ± SEM, n= 3.

Following confirmation that 95% of cells isolated from the peritoneal cavity are macrophages, we examined the expression of TLR4 mRNA and protein in the pM. First, we amplified a fragment of Tlr4 cDNA from pM isolated from TLR4-WT and TLR4-KO mice by RT-PCR (Forward primer: 5'AACCAGCTGTATTCCCTCAGCACT3'; Reverse primer: 5'ACTGCTTCTGTTCCTTGACCCACT3'). As **Fig. 26** shows, Tlr4 cDNA was readily amplified from pM RNA derived from WT (**Lane 2 and 3**) while it was not amplified from pM RNA derived from TLR4-KO mice (**Lane 4 and 5**). In contrast, β -actin was readily amplified from both strains (**Lane 6-9**). Our RT-PCR results confirmed that pM derived from TLR4-KO mice failed to express TLR4 mRNA, as compared with pM derived from WT mice. These data are consistent with our mouse genotyping results.

Then, we assessed TLR4 protein expression in cell lysates of pM derived from TLR4-WT and TLR4-KO mice by Western blot analysis. As **Fig. 26 B** shown, we observed one robust band corresponding to the size of full length TLR4 95 kDa in pM derived from WT mice whereas this band was almost undetectable in cell lysate of pM derived from TLR4-KO mice. Having confirmed TLR4 expression in pM at both mRNA and protein levels, we next characterized the primary pM with respect to response to TLR4 agonist stimulation.

pM isolated from TLR4-WT and TLR4-KO mice were stimulated with TLR4 specific agonist LPS-EK at 10 ng/ml. Cell culture supernatant was subjected to TNF- α analysis using ELISA. We found that TNF- α was significantly induced upon LPS-EK stimulation in pM derived from TLR4-WT mice but not in those derived from TLR4-KO mice (**Fig. 26 C**). These results confirmed two crucial points: (1) pM derived from

TLR4-WT mice responded to the stimulation of TLR4 agonist while pM derived from TLR4-KO mice were completely unresponsive to stimulation of LPS-EK; (2) LPS-EK specifically stimulates TLR4 activation.

In summary, our results demonstrated that pM isolated from TLR4-WT mice expressed TLR4 mRNA and protein, and were responsive to TLR4 agonist with robust release of TNF- α . In contrast, pM isolated from TLR4-KO mice showed a complete deletion of TLR4 mRNA, and did not respond to stimulation by TLR4 agonist. The results further demonstrated unequivocally that pM isolated from TLR4-WT and TLR4-KO mice would provide a reliable *in vitro* system to study the role of TLR4 in oxidant-induced inflammatory phenotypes.

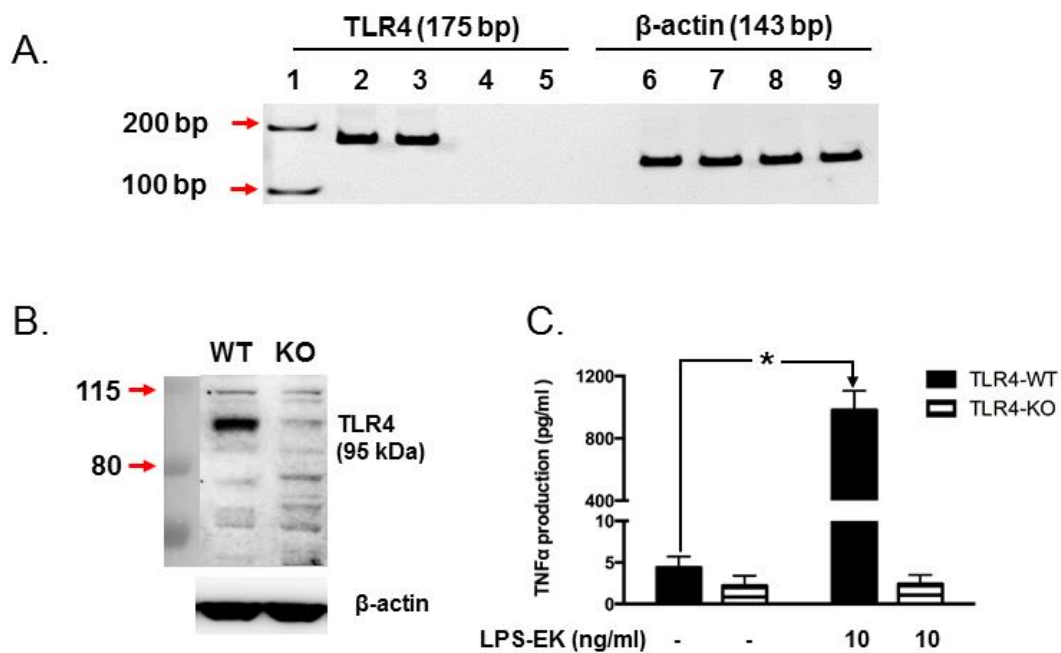


Figure 26. Characterization of peritoneal macrophages (pM) isolated from TLR4-WT and TLR4-KO mice. (A) TLR4 mRNA expression in pM by RT-PCR analysis. RT-PCR were performed using specific primers for mice TLR4 and β -actin on the total RNA of pM. **Lane 1:** 100-bp DNA ladder; **Lane 2 & 3:** TLR4 mRNA from pM derived from TLR4-WT mice with corresponding β -actin mRNA (**Lanes 6 & 7**); Against **Lanes 4 & 5:** TLR4 mRNA from pM derived from TLR4-KO mice with their corresponding β -actin mRNA (**Lanes 8 & 9**). (B) TLR4 protein expression by Western blot analysis. (C) TNF- α production by LPS-EK stimulation. pM were treated with LPS-EK (10 ng/ml) for 16 h and levels of TNF- α in culture supernatant was quantified by ELISA. The data represent Mean \pm SEM from three independent experiments conducted in duplicate, * $p \leq 0.01$.

Empirically Determined Concentrations for Oxidants Used in Primary pM

As shown in RAW-Blue cells (Chapters 2 and 3), we have also examined two treatment paradigms for primary pM: **(i) long-term exposure with low concentrations of oxidants for 16 h, and (ii) short-term exposure with high concentrations of oxidants for 2 h, removal of original media and rinsing cells once with fresh media followed by replenishment with fresh growth medium in the absence of oxidants. Cells were then grown for 16 h.** In long-term treatment, cell viabilities were quantified at the end of 16 h incubation. In the short-term treatment, cell viabilities were quantified at the end of 2 h initial treatment and at the end of 16 h incubation, respectively. Cell viabilities were initially determined by MTT assay and then confirmed by LDH toxicity assay. To obviate potential adverse effects resulting from oxidant toxicity, we eventually used sub-threshold oxidant concentrations in which cell survival was $\geq 85\%$.

In the **long-term exposure with low concentrations of oxidants**, we used varying concentrations of oxidants (1 ~ 5 μM for PPC; 0.25 ~ 1 mM for SIN-1). Both PPC and SIN-1 induced cytotoxicity in a concentration-dependent manner (**Fig. 27 A and 27 B**). With PPC at 5 μM and SIN-1 at 1 mM, 86% and 90% of the control cells derived from both TLR4-WT and TLR4-KO mice were viable, respectively (**Fig. 27 A**). Consistently, long-term treatment with PPC at 5 μM or SIN-1 at 1 mM for 16 h incubation caused $\leq 10\%$ cytotoxicity (**Fig. 27 B**). Therefore, in the long-term treatment method, the maximal concentrations we used in subsequent experiments were 5 μM for PPC and 1 mM for SIN-1, respectively. We used LPS-EK at 10 ng/ml as a positive control to activate TLR4.

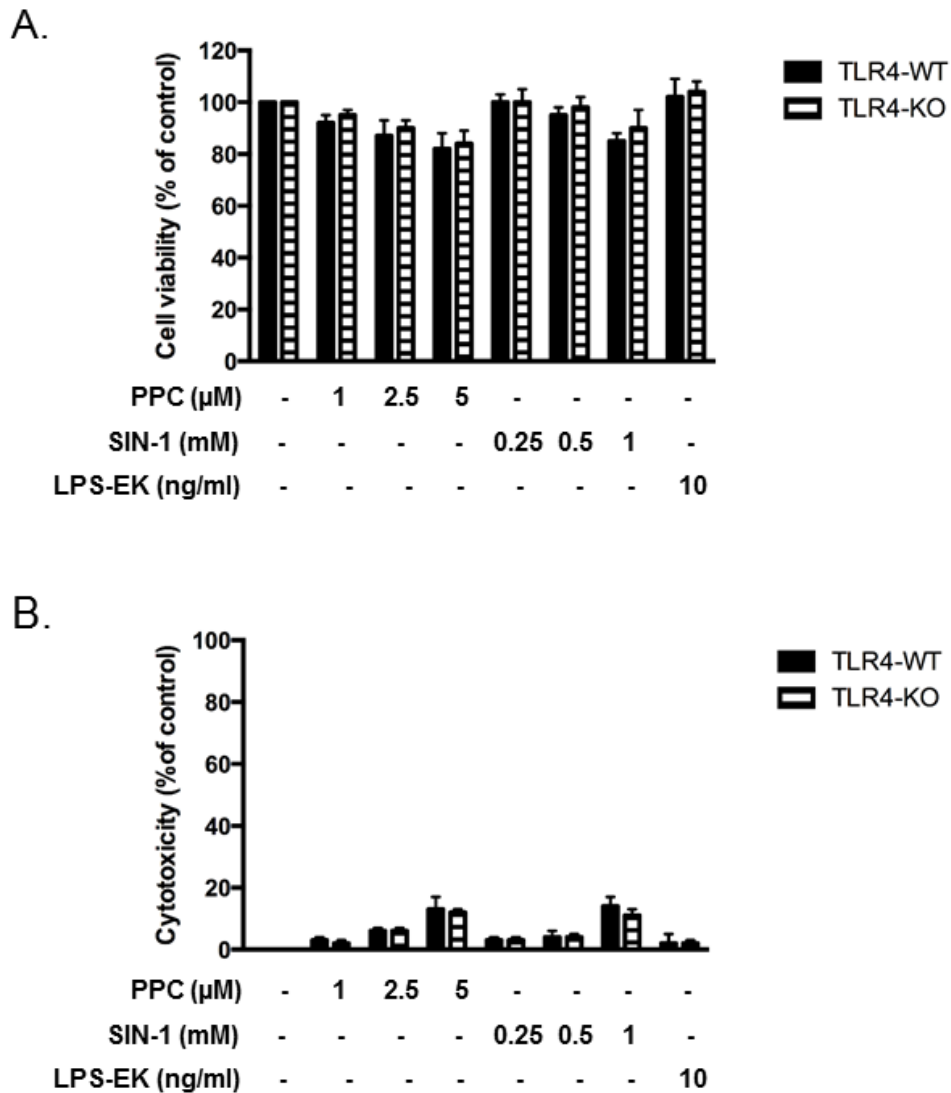


Figure 27. Determination of appropriate concentrations of oxidants for long-term exposure in primary peritoneal macrophages (pM). Freshly isolated pM derived from both TLR4-WT and TLR4-KO mice were cultured in medium containing the indicated concentrations of oxidants for **16 h**. **(A)** Cell viability was determined by MTT assay. Cell viability in control cells was defined as 100%. **(B)** Cytotoxicity was determined by LDH assay. Cytotoxicity (%) = $(\text{LDH levels}_{\text{oxidant-treated}} - \text{LDH levels}_{\text{control}}) / (\text{Total LDH levels}) \times 100\%$. LDH levels upon cell lysis were used as total LDH activity.

In the paradigms of **short-term with high concentration of oxidants**, we also used varying concentrations of oxidants (50 ~ 250 μ M for PPC; 1 and 5 mM for SIN-1). First, we examined cell viabilities at the end of 2 h treatment with oxidants. MTT results showed that PPC (50 ~ 250 μ M) and SIN-1 (1 and 5 mM) retained above 85% cell viabilities compared to the control cells (**Fig. 28 A**). This was then confirmed by LDH release measurement showing no significant cytotoxicity as a result of oxidant treatment (**Fig. 28 B**).

Second, we also determined cell viability at the end of 16 h reincubation with fresh growth medium, MTT results showed that PPC (50 ~ 250 μ M) produced in 85% cell viabilities compared to control cells (**Fig. 28 C**). This was again confirmed by measuring LDH release demonstrating no significant increase in LDH (**Fig. 28 D**). Thus, the optimal concentration we used in subsequent experiments was 250 μ M for PPC. With respect to SIN-1, as **Fig. 28 C** shows, SIN-1 at 1 mM did not cause significant cell death in pM derived from both TLR4-WT and TLR4-KO mice while SIN-1 at 5 mM induced significant cell death in pM derived from both TLR4-WT and TLR4-KO mice, which was confirmed by significant increase in LDH release (**Fig. 28 D**). Due to cell toxicity caused by SIN-1 at 5 mM in pM, in the short-term treatment method, the optimal concentration we used in subsequent experiments was 1 mM for SIN-1. At the end, we used both **long-term with low concentrations of oxidants** and **short-term with high concentrations of oxidants** in subsequent experiments of this Chapter.

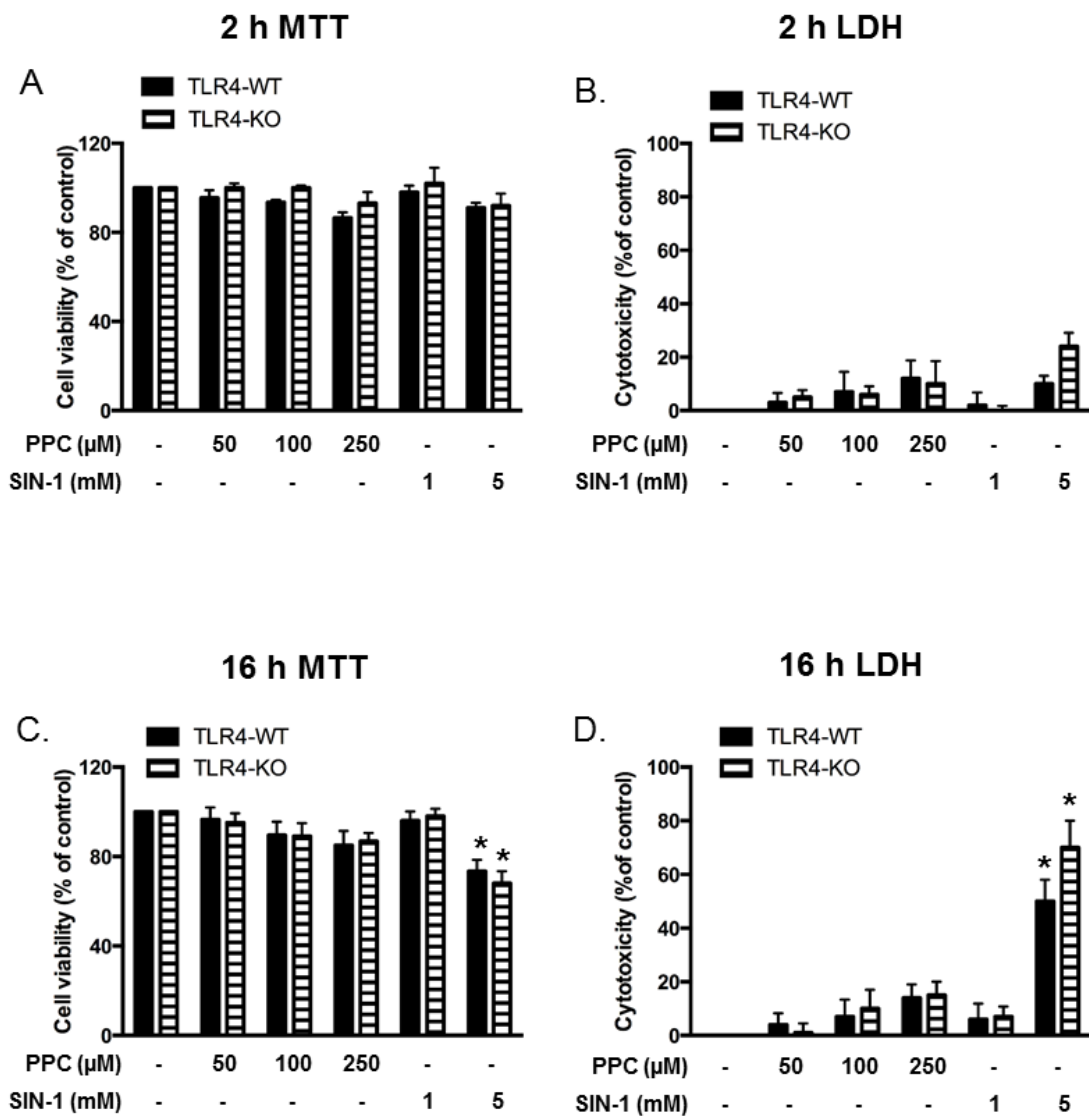


Figure 28. Determination of appropriate concentrations of oxidants for short-term exposure in primary peritoneal macrophages (pM). Freshly isolated pM from both TLR4-WT and TLR4-KO mice were exposed to oxidants at indicated concentrations for 2 h followed by reincubation with fresh growth medium in the absence of oxidants for next 16 h. **At the end of 2 h**, cell viability and cytotoxicity upon oxidant treatment were determined by MTT assay (A) and LDH measurement (B), respectively. **At the end of 16 h**, cell viability and cytotoxicity upon oxidant treatment were determined by MTT assay (C) and LDH measurement (D), respectively. Cell viability in control cells was defined as 100%. Cytotoxicity (%) = (LDH levels_{oxidant-treated} - LDH levels_{control}) / Total LDH levels × 100%. LDH levels upon cell lysis were used as total LDH activity. *: $p \leq 0.05$ vs each respective control, $n = 4$.

Role of TLR4 in Oxidant-induced Dysregulation in Redox Homeostasis

Role of TLR4 in Oxidant-induced iROS Production

We showed in Chapter 3 that treatment with exogenous oxidants increased iROS levels in RAW-Blue cells through TLR4 stimulation. Here, we measured iROS levels in pM isolated from TLR4-WT and TLR4-KO mice in response to oxidant- or LPS-EK-mediated TLR4 stimulation. First, we determined the levels of iROS using CellROX™ Deep reagent by fluorescent microscopy. We have determined that the optimal time for maximal iROS detection was 2 h post treatment in RAW-Blue cells (**Fig. 16** in Chapter 3), which we have used here as a guide for pM treatments.

Our results showed that exposure of pM expressing TLR4 to oxidants resulted in a robust increase in the levels of iROS as revealed by increase in fluorescent intensity (**Fig. 29 A and 29 B**). However, pM with complete deletion of TLR4 showed a very limited oxidant-mediated iROS levels. LPS-EK-induced iROS level was specifically observed in pM isolated from TLR4-WT but not in TLR4-KO mice (**Fig. 29 A and 29 B**). These results suggest that TLR4 expression and activation are necessary for oxidant-mediated iROS generation.

We further confirmed and quantified oxidant-mediated iROS generation using flow cytometry. Similar to what we had shown in RAW-Blue cells in Chapter 3 (**Fig. 15 C and 15 D**), there were apparent differences between iROS readout derived from fluorescence microscopy and flow cytometry. Exposure of cells to PPC, or LPS-EK slightly but not significantly increased iROS levels in pM expressing TLR4 (**Fig. 30 A and 30 B**). However, treatment with SIN-1 resulted in significantly increased levels of iROS in pM derived from both TLR4-WT and TLR4-KO mice (**Fig. 30 A and 30 B**).

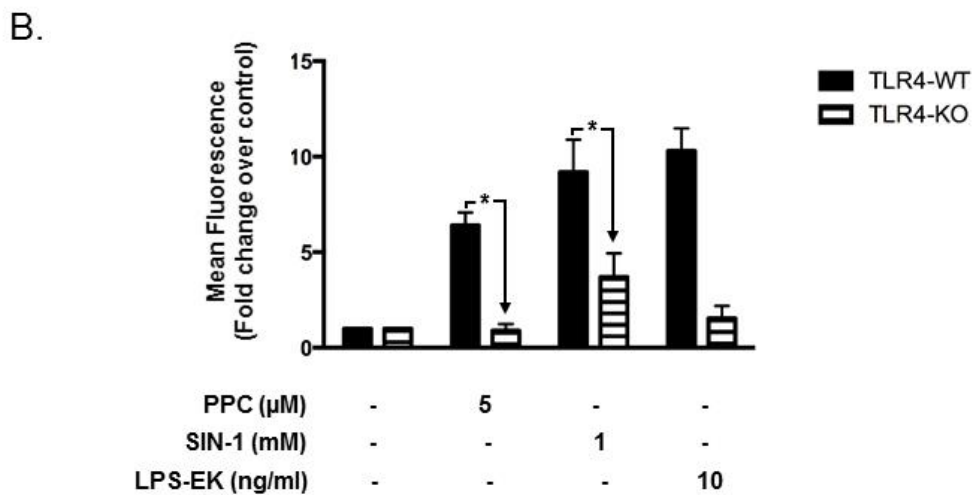
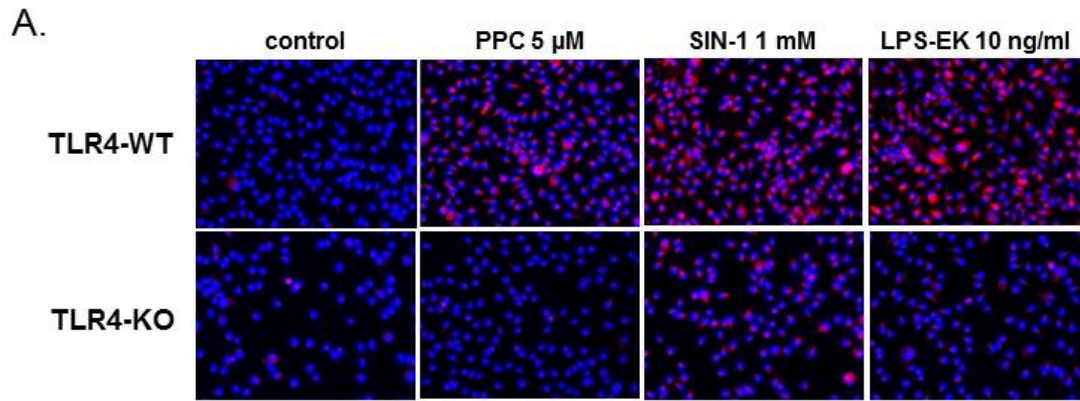


Figure 29. Role of TLR4 in oxidant-mediated iROS levels. Peritoneal macrophages (pM) derived from TLR4-WT and TLR4-KO mice were treated with oxidants or LPS-EK for 2 h followed by determination of iROS levels using fluorescence microscopy. (A) Cells were incubated with CellROX™ together with NucBlue live cell stain followed by image acquisition using a fluorescence microscope. Merged representative pictures of fluorescent images are shown. (B) Semi-quantitative histograms of (A) generated by using image J software. The data represent 4 independent experiments. * $p \leq 0.01$, $n = 4 - 6$

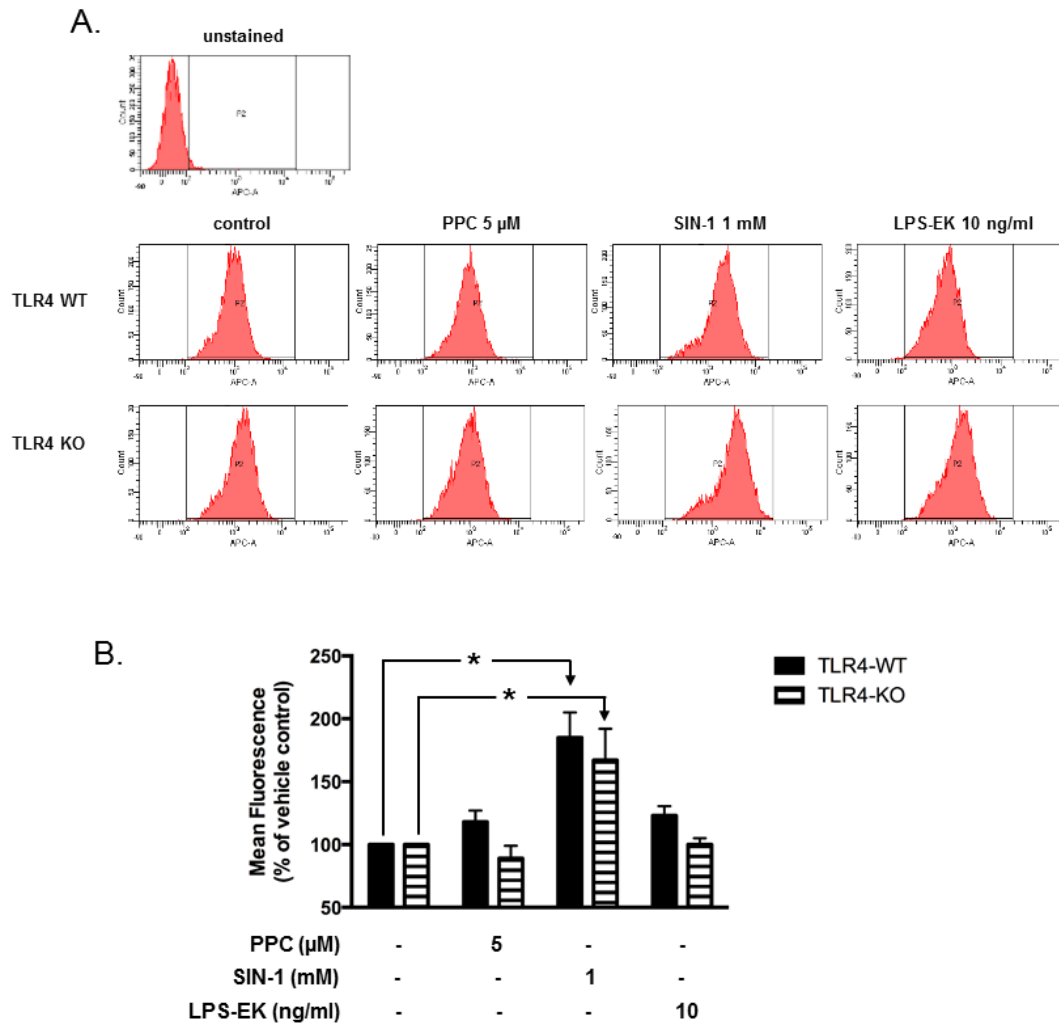


Figure 30. Role of TLR4 oxidant-mediated iROS levels. Peritoneal macrophages (pM) derived from TLR4-WT and TLR4-KO mice were treated with oxidants or LPS-EK for 2 h followed by determination of iROS levels using flow cytometer. **(A)** The fluorescence intensity following CellROX™ incubation was analyzed by flow cytometer. Representative pictures of flow cytometry are shown. **(B)** Quantitative histograms of fluorescence intensity. The data represent 4 independent experiments, * $p \leq 0.05$.

Role of TLR4 in Oxidant-mediated Changes in Cellular TAOC

Alternative to the measurements of iROS with a very short half-life, in addition, we quantified total antioxidant capacity (TAOC) as an important measure of oxidative stress. In Chapter 3, we showed that oxidants decreased cellular TAOC in RAW-Blue cells, we next examined the role of TLR4 in TAOC process with pM isolated from TLR4-WT and TLR4-KO mice.

pM were treated with oxidants or LPS-EK for 2 h or 16 h and cell lysates were subjected to TAOC analysis using total antioxidant assay kit (Cayman Chemicals). The levels of TAOC was expressed as equivalent concentration to Trolox, a water soluble analogue of vitamin E (**Fig. 31 A**). Percentage (%) of change over control was calculated and drawn as histogram (**Fig. 31 B**).

Treatment with TLR4-specific agonist LPS-EK for 2 h decreased cellular TAOC in pM expressing TLR4 but had no effects on pM with complete deletion of the *tlr4* gene (**Fig. 31 A and 31 B**). Similarly, treatment with PPC 2.5 and 5 μ M for 2 h specifically induced a concentration-dependent decrease in cellular TAOC in pM expressing TLR4, with decrease of 31%, and 44% compared with control, respectively. However, PPC treatment had no effects on TAOC in comparison with control cells in pM with complete deletion of *tlr4* gene (**Fig. 31 A and 31 B**). Similarly, after treatment with SIN-1 (0.5 and 1 mM) for 2 h, we observed a concentration-dependent decrease (48% and 58%, respectively) in cellular TAOC levels in pM expressing TLR4 but not in pM with deletion of TLR4.

These results suggest that TLR4 deletion made macrophages less sensitive to exogenous oxidants, thereby providing supporting evidence for the hypothesis that

TLR4 expression functions not only as effective modulator of, but also a sensor for oxidants.

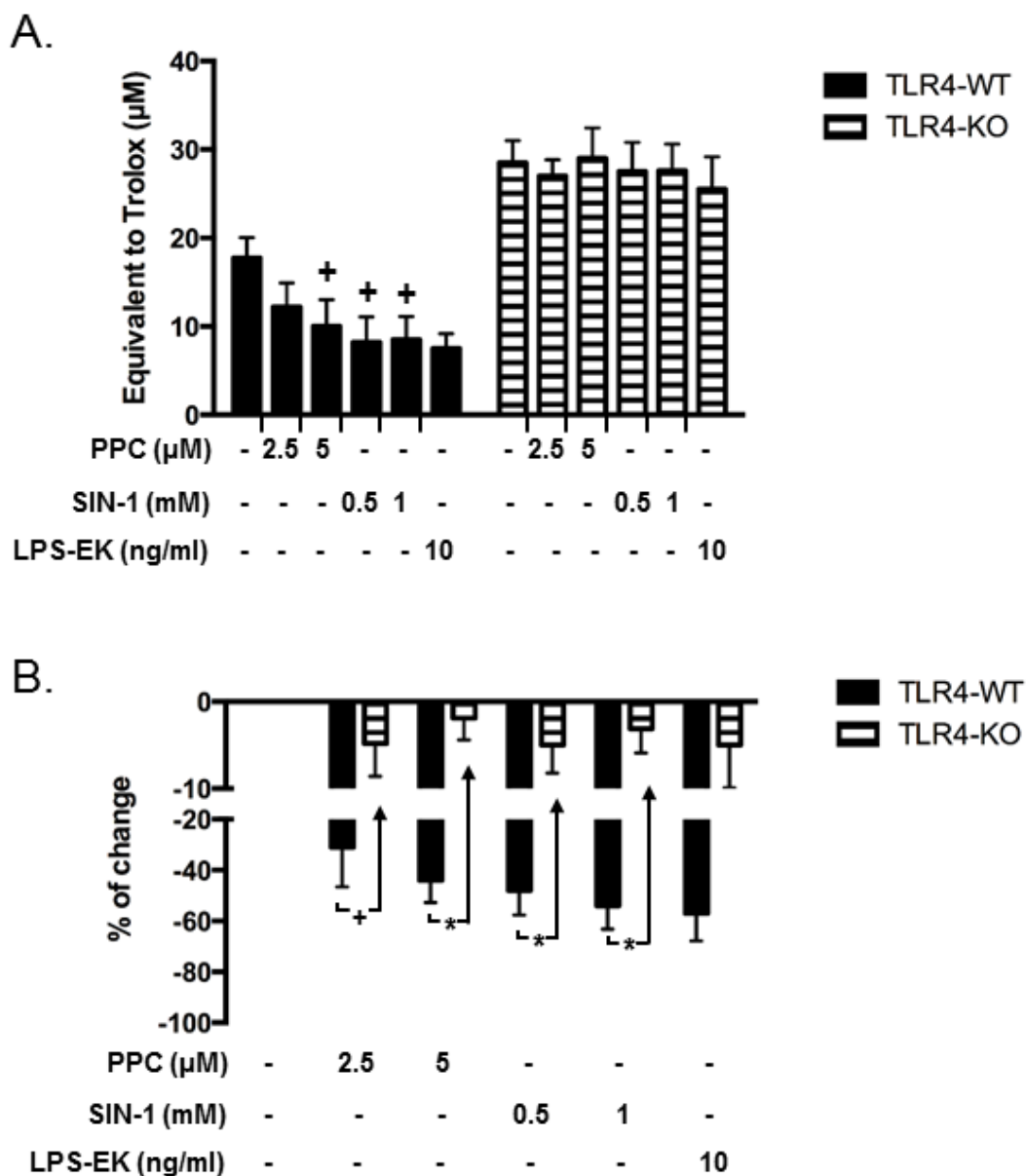


Figure 31. Role of TLR4 in oxidant-mediated cellular total antioxidant capacity (TAOC) at 2 h. Peritoneal macrophages (pM) derived from TLR4-WT and TLR4-KO mice were treated with oxidants or LPS-EK for 2 h and cells lysates were subjected to TAOC analysis. **(A)** Levels of TAOC are expressed as equivalent Trolox concentration. **(B)** Percentage of change over control was calculated and graphed as histograms. + $p \leq 0.05$, * $p \leq 0.01$, $n = 3$.

At 16 h post PPC (2.5 and 5 μ M) long-term treatment, we observed a concentration-dependent increase (65% and 121%, respectively) in cellular TAOC in comparison with control cells specifically in pM expressing TLR4 (**Fig. 32 A and 32 B**). In contrast, treatment with PPC had limited effects in pM with TLR4 deletion. Similarly, long-term treatment with SIN-1 at 0.5 mM and 1 mM concentration for 16 h significantly increased levels of TAOC by 65 % and 383 % of control cells in pM expressing TLR4 but showed less effects in pM derived from TLR4-KO mice (**Fig. 32 A and 32 B**). These results again confirm that deletion of TLR4 rendered macrophages less responsive to certain oxidant stimulation.

Overall, our data support the hypothesis that TLR4 is necessary for oxidant-mediated increase in iROS levels and reduction in TAOC, which can cause disturbances in redox homeostasis that can initiate and/or maintain inflammatory disease processes.

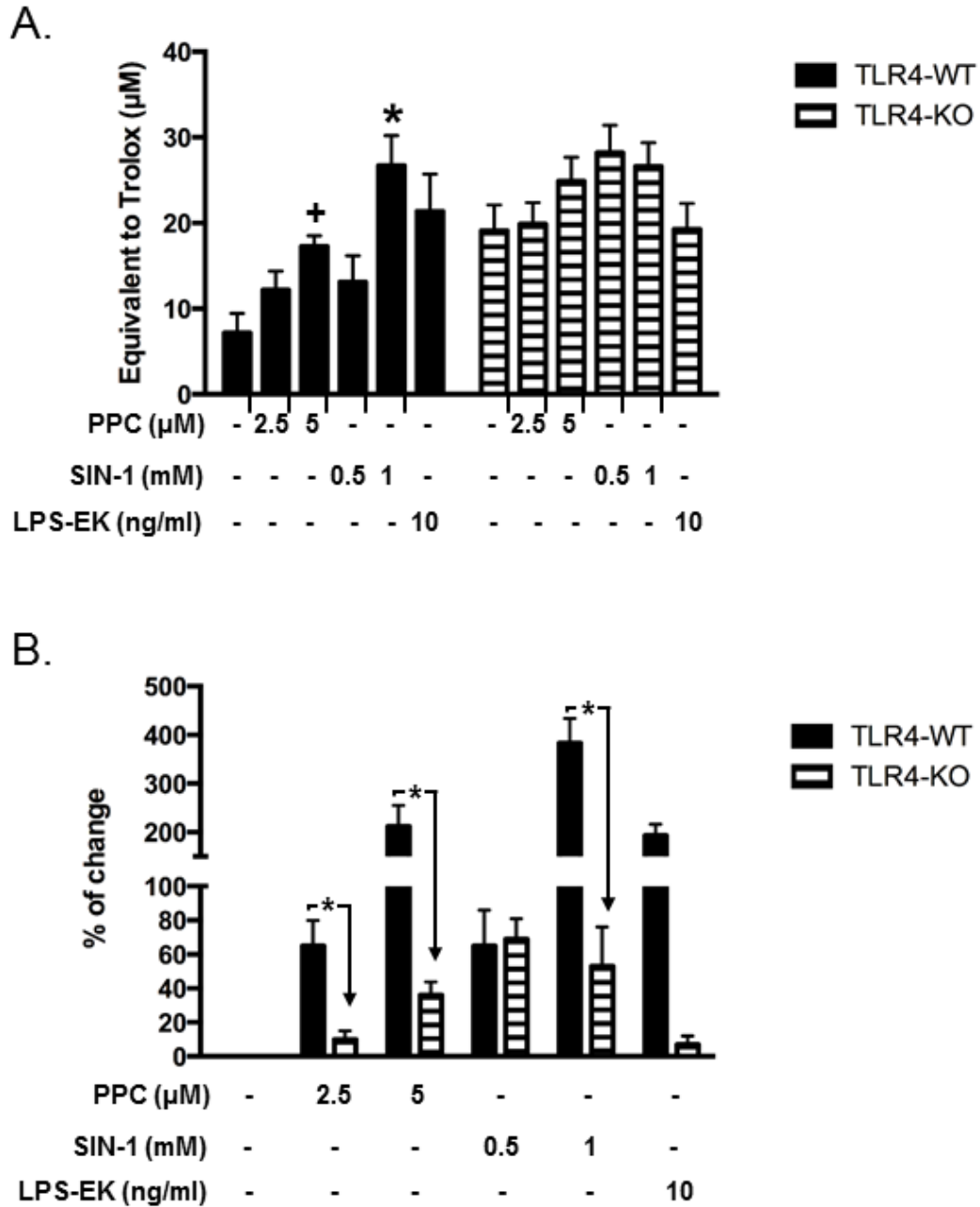


Figure 32. Role of of TLR4 in oxidant-mediated cellular total antioxidant capacity (TAOC) at 16 h. Peritoneal macrophages (pMs) derived from TLR4-WT and TLR4-KO mice were treated with oxidants or LPS-EK for **16 h** and cell lysates were subjected to TAOC analysis. **(A)** Levels of TAOC are expressed as equivalent Trolox concentration. + $p \leq 0.05$ vs untreated cells, * $p \leq 0.01$ vs untreated cells, $n = 3$. **(B)** Percentage (%) of change over control was calculated and graphed as histograms. * $p \leq 0.01$, $n = 3$.

Effects of Oxidants on Gene Expression and Production of TNF- α

Among cytokines, TNF- α exerts a key role in the cytokine network with regard to the pathogenesis of many infectious and inflammatory diseases. We showed in Chapter 3 that short-term exposure with high concentrations of oxidant PPC stimulated NF- κ B activation leading to consequent production of TNF- α in RAW-Blue cells. Furthermore, anti-TLR4/MD-2 pAb and TLR4 signaling inhibitor CLI-095 significantly attenuated oxidant-induced NF- κ B activation and TNF- α production. Here, we confirmed the role of TLR4 in the process of TNF- α production using pM derived from TLR4-WT and TLR4-KO mice. Both short-term exposure with low concentrations of oxidants and long-term exposure with low concentrations of oxidants were used.

In the short-term/high oxidant concentration treatment paradigm, TNF- α levels in conditioned medium were quantified after reincubation with growth medium in the absence of oxidant or LPS-EK for 16 h. Our results showed that PPC at 100 μ M significantly increased TNF- α production in pM derived from either TLR4-WT or TLR4-KO mice in comparison with their untreated control cells (**Fig. 33 A**). However, the levels of TNF- α in culture medium were significantly higher upon PPC (100 μ M) treatment in pM derived from TLR4-WT mice than those from TLR4-KO mice (**Fig. 33 A**). These results suggest that: (i) the pM derived from TLR4-WT are more responsive to oxidant-mediated TNF- α production than pM derived from TLR4-KO mice, and (ii) PPC-mediated TNF- α production is at least partially through TLR4 stimulation.

SIN-1 at 1 mM failed to induce TNF- α production in pM derived from both TLR4-WT and TLR4-KO mice. As expected, LPS-EK stimulated TNF- α production specifically in pM expressing of TLR4, but not in pM derived from TLR4-KO mice.

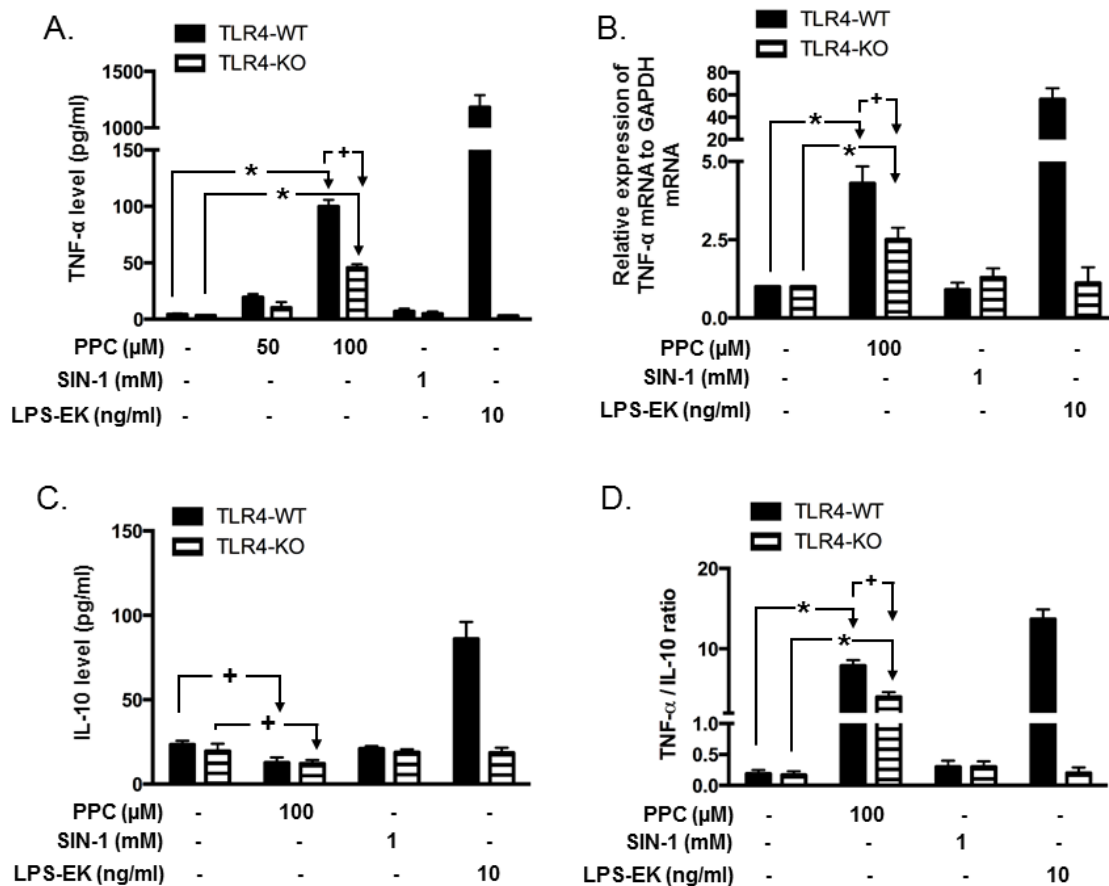


Figure 33. Role of TLR4 in oxidant-mediated production of TNF α and IL-10 in peritoneal macrophages (pM). Cells were exposed to oxidants or LPS-EK for 2h at indicated concentrations followed by incubation with complete growth medium in the absence of oxidants and LPS-EK for the next 16 h. **(A)** TNF- α levels in the conditioned medium were determined at 16 h post to re-incubation with growth medium using ELISA. **(B)** Relative TNF- α mRNA expression was quantified at 2 h post treatment with PPC using RT-qPCR and normalized against GAPDH. **(C)** IL-10 levels in the conditioned medium were determined at 16 h post oxidant treatment and following re-incubation with growth medium using ELISA. **(D)** Relative ratios of TNF- α to IL-10 following oxidant treatments. + $p \leq 0.05$, * $p \leq 0.01$, $n = 3$.

We also determined the induction of TNF- α at the mRNA level at 2 h post treatment with PPC. Consistent with levels of TNF- α in culture medium, we found that mRNA of TNF- α was significantly up-regulated by PPC (100 μ M) in pM either derived from TLR4-WT or TLR4-KO mice (**Fig. 33 B**). However, induction of TNF- α mRNA upon PPC treatment was much higher in pM derived from TLR4-WT mice than those derived from TLR4-KO mice (**Fig. 33 B**). SIN-1 (1 mM) had no effects on the levels of TNF- α mRNA in pMs. These data support the hypothesis that TLR4 is at least partially necessary for PPC-mediated increase in levels of TNF- α mRNA.

In the short-term treatment paradigm, we then determined the effects of oxidants on the production of IL-10 (an anti-inflammatory cytokine) after reincubation with growth medium for 16 h. As **Fig. 33 C** shows, PPC (100 μ M) treatment significantly decreased IL-10 production in pM derived from either TLR4-WT or TLR4-KO mice in comparison with their untreated control cells (**Fig. 33 C**). These results suggest that PPC at the concentration used increases TNF- α production at the same time frame that it suppresses IL-10 production to “switch” a constitutively balanced inflammatory condition towards a potential diseases-inducing pro-inflammatory status. Unexpectedly, PPC-mediated IL-10 down-regulation appears not to require TLR4 expression. SIN-1 at 1 mM had no effect on IL-10 production (**Fig. 33 C**). As expected, short-term treatment with LPS-EK (10 ng/ml) for 2 h significantly increased the levels of IL-10 in cell culture medium in pM derived from TLR4-WT mice but not in pM derived from TLR4-KO mice (**Fig. 33 C**).

The ratios of TNF- α to IL-10 following stimulation with oxidants or LPS-EK were calculated to represent the balance between their biological effects. Both PPC and

LPS-EK treatment increased the ratio of TNF- α to IL-10 whereas SIN-1 had no effect on it (**Fig. 33 D**). These results support the notion that the imbalance between TNF- α and IL-10 formation caused by PPC treatment was mediated through TLR4.

Again **in the long-term treatment paradigm**, we examined the effects of oxidant on TNF- α production in conditioned medium. Our results showed that treatment with PPC (2.5 and 5 μ M) and SIN-1 (0.5 and 1 mM) for 16 h did not significantly up-regulate TNF- α production in pM derived from either TLR4-WT or TLR4-KO mice (**Fig. 34 A**). As expected, continuous treatment with LPS-EK (10 ng/ml) for 16 h robustly induced TNF- α production in pM derived from TLR4-WT mice, with no effect on pM derived from TLR4-KO mice (**Fig. 34 A**).

In the long-term treatment paradigm, we further examined relative TNF- α gene expression levels upon treatment with oxidants or LPS-EK for 16 h using RT-qPCR. pM derived from TLR4-WT and TLR4-KO mice were treated with oxidants or LPS-EK and TNF- α gene expression was determined at 2, 6, and 12 h post treatment. Consistent with the ELISA results (**Fig. 34 A**), we did not observe significant effect of oxidants on TNF- α gene expression at any of the time points we examined (**Fig. 34 B-D**). As expected, LPS-EK at 10 ng/ml induced a robust increase in TNF- α mRNA expression as early as 2 h specifically in pM expressing TLR4 but had no effects in those derived from TLR4-KO mice (**Fig. 34 B**) further confirming the validation of our experimental system. This further confirms the deficiency of TLR4 in pM derived from TLR4-KO mice and the specificity of LPS-EK to stimulate TLR4.

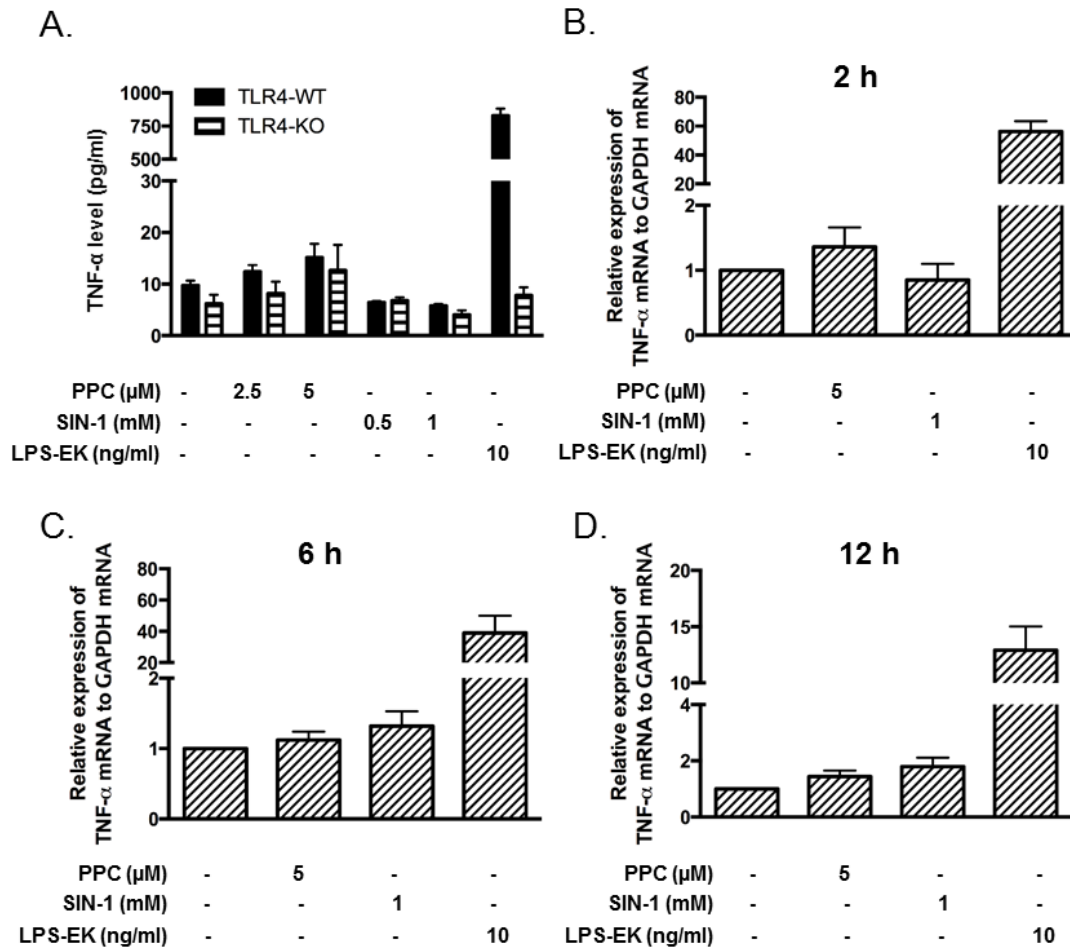


Figure 34. Effects of oxidants on TNF- α production and gene expression upon long-term exposure with low concentration of oxidants or LPS-EK. (A) Peritoneal macrophages (pM) isolated from TLR4-WT and TLR4-KO mice were treated with varying concentrations of oxidants in the long term treatment paradigm. The levels of TNF- α were quantified by ELISA. The experimental data are presented as the mean \pm SEM from three independent experiments. (B) (C) and (D) pM isolated from TLR4-WT mice were treated with oxidants at indicated concentrations. Relative TNF- α mRNA was quantified at 2 h (B), 6 h (C) and 12 h (D) post treatment. Total RNAs were extracted, and relative TNF- α gene expression was determined by RT-qPCR and normalized against GAPDH. LPS-EK (10 ng/ml) was used for a positive control in TNF- α production.

In the long-term treatment paradigm, in addition to TNF- α , we examined the effects of oxidants on the relative gene expression of IL-1 β , which is another potent pro-inflammatory cytokine. The oxidants had no effects on gene expression of IL-1 β in pM derived from TLR4-WT mice at 2 h (**Fig. 35 A**), 6h (**Fig. 35 B**), and 12h (**Fig. 35 C**) post treatment. We also examined the effects of oxidants on the induction of iNOS at the protein level. Our results showed that oxidants had no effects on the protein expression of iNOS in pM derived from either TLR4-WT or TLR4-KO mice at 6 h (**Fig. 36 A**) and 16 h (**Fig. 36 B**) post treatment. Thus, similar to what we have observed in RAW-Blue cells with respect to NF- κ B activation, long-term exposure with low concentrations of oxidants seems less effective in regulating TNF- α , IL-1 β and iNOS in primary pM.

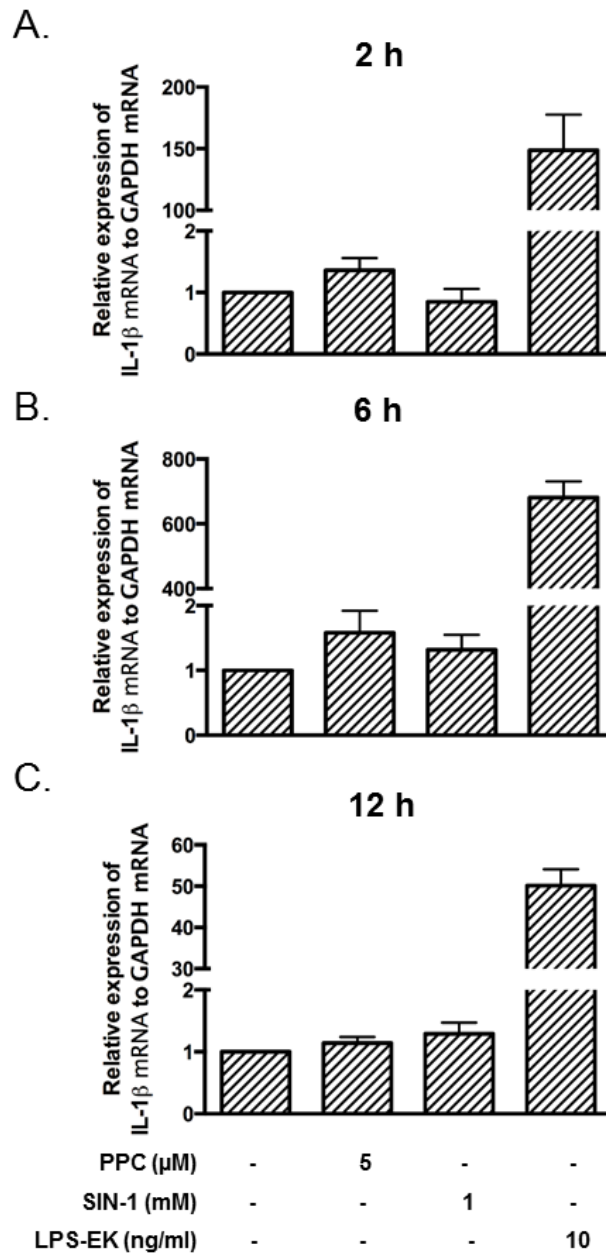
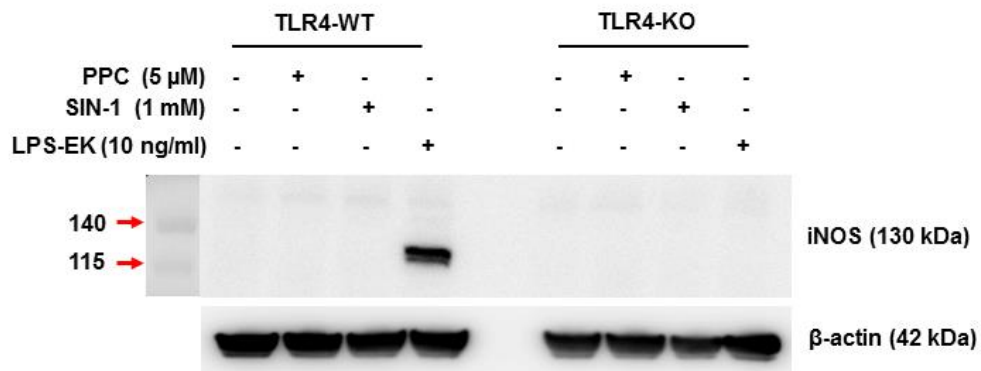


Figure 35. Effects of oxidants on IL-1 β gene expression upon long-term exposure with oxidants or LPS-EK. Peritoneal macrophages (pM) isolated from TLR4-WT mice were treated with oxidants at indicated concentrations. Relative TNF- α mRNA was quantified at 2 h (A), 6 h (B) and 12 h (C) post treatment. Total RNAs were extracted, and relative IL-1 β gene expression was determined by RT-qPCR and normalized against GAPDH. LPS-EK (10 ng/ml) was used for a positive control. The data represent Mean \pm SEM from three independent

A.



B.

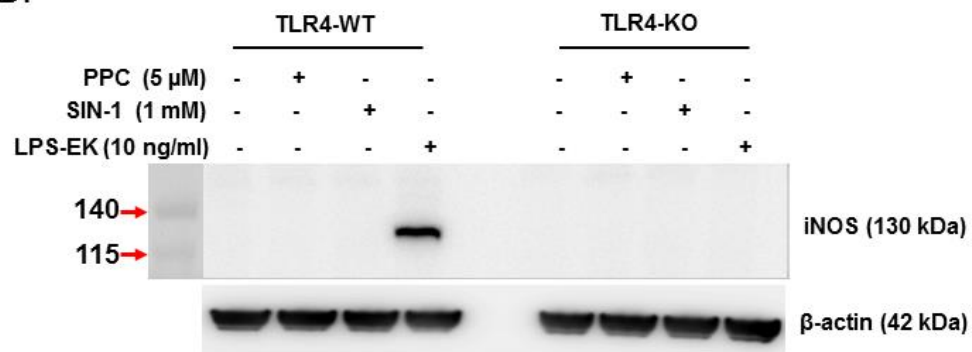


Figure 36. Effects of oxidants on iNOS protein expression upon long-term exposure oxidants or LPS-EK. Peritoneal macrophages (pM) isolated from TLR4-WT mice were treated with oxidants at indicated concentrations. iNOS protein expression were determined at 6 h (**A**) or 16 h (**B**) post treatment using Western blot. Representative immunoblotting from three independent experiments are shown. LPS-EK (10 ng/ml) was used for a positive control

Effects of Oxidants on Prostaglandin E₂ Production and Cyclooxygenase Protein Expression

PGE₂, as one of the most abundant lipid metabolites of AA, can increase vascular permeability, induce fever, and hyperalgesia. PGE₂ is synthesized *de novo* through a sequential enzymatic reactions PLA₂, COX and mPGES. COX-1 and COX-2 are the key enzymes responsible for PGE₂ biosynthesis. COX-1 is primarily constitutively expressed in most cells/tissues while COX-2 is inducible, and may therefore not be expressed in unstimulated macrophages.

Consistent with the experimental design of our **short-term treatment paradigm**, pM isolated from TLR4-WT and TLR4-KO mice were exposed to oxidants or LPS-EK for 2 h followed by incubation with complete growth medium in the absence of both oxidant and LPS-EK for the next 16 h. We quantified the levels of PGE₂ in culture supernatant after reincubation with medium for 16 h.

The levels of PGE₂ in untreated pM derived from TLR4-WT and TLR4-KO mice were 115.6 ± 33.45 pg/ml and 121.0 ± 43.0 pg/ml, respectively. PPC at 100 μ M significantly increased PGE₂ levels in pM derived from both TLR4-WT and TLR4-KO mice up to 351.2 ± 60 pg/ml and 501.5 ± 65 pg/ml, respectively (**Fig. 37 A**). When PGE₂ levels are expressed as fold change to untreated pM, PPC at 100 μ M significantly increased it by 3.1 fold and 4.2 fold in pMs derived from both TLR4-WT and TLR4-KO mice, respectively (**Fig. 37 B**). Curiously, these results suggest that PPC-mediated PGE₂ production may not require TLR4 expression in pM. However, LPS-EK (10 ng/ml) stimulated PGE₂ production specifically in pM derived from TLR4-WT mice

but not from TLR4-KO mice (**Fig. 37 A and 37 B**), which validated the experimental system.

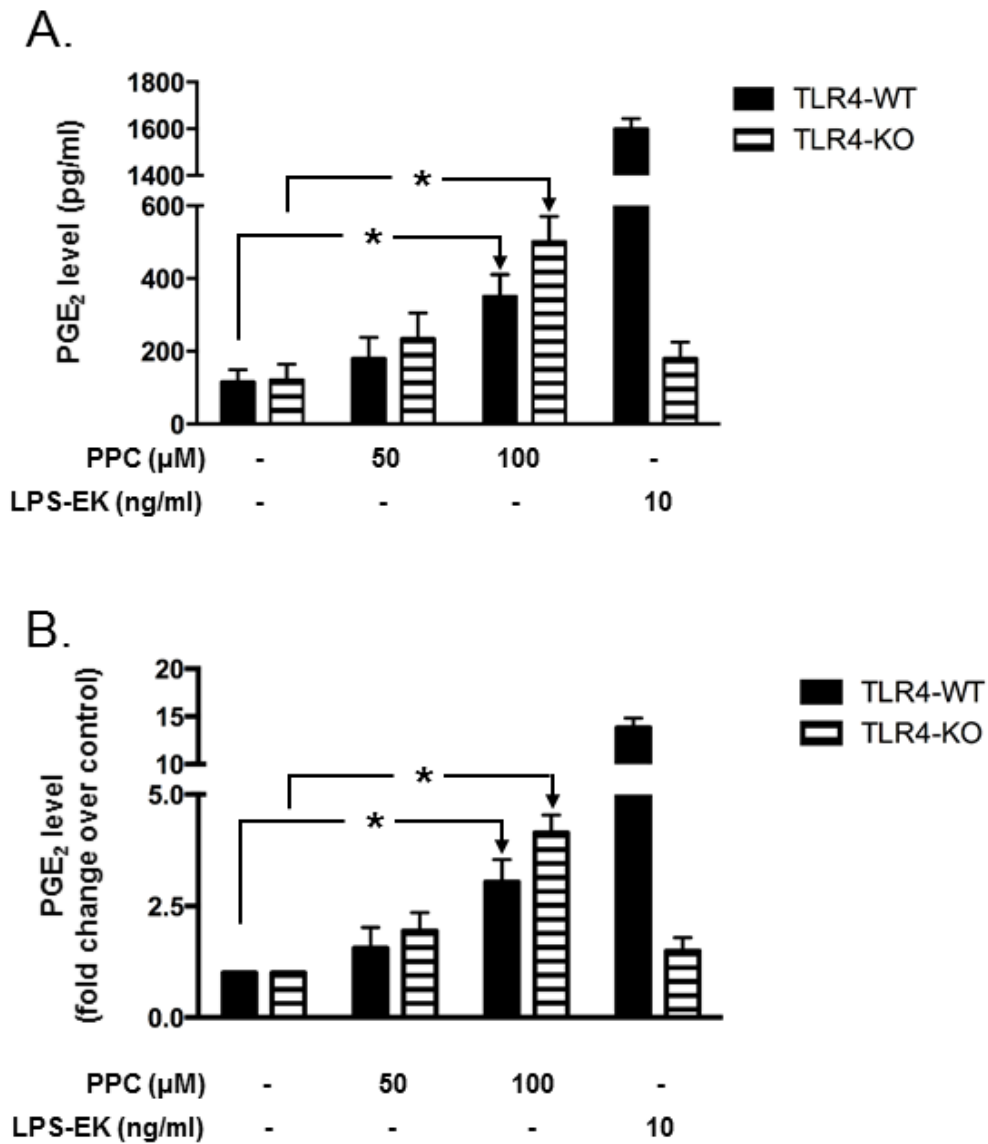


Figure 37. Effects of oxidants on prostaglandin E₂ (PGE₂) production upon **short-term treatment paradigm**. Peritoneal macrophages (pM) isolated from TLR4-WT and TLR4-KO mice were exposed to oxidants or LPS-EK for 2 h followed by incubation with complete growth medium in the absence of both oxidant and LPS-EK for the next 16 h. **(A)** The levels of PGE₂ released in the conditioned medium were quantified using ELISA. **(B)** PGE₂ levels are expressed as folds of untreated control. The experimental data are presented as the mean ± SEM from three independent experiments, * p < 0.05.

With respect to the expression of COX enzymes, our results showed that, in unstimulated pM derived either from TLR4-WT or TLR4-KO mice, COX-1 was expressed while the expression of COX-2 protein was undetectable (**Fig. 38 C**). PPC at 100 μ M significantly increased the expression of COX-1 in pM derived from both TLR4-WT and TLR4-KO mice (**Fig. 38 A and 38 B**), which suggest that elevated levels of PGE₂ in pM may result from the upregulation of COX-1 upon PPC treatment even though COX-1 is not normally inducible. PPC had no effect on COX-2 protein expression (**Fig. 38 A and 38 C**). Again, LPS-EK (10 ng/ml) stimulated induction of COX-2 expression specifically in pM derived from TLR4-WT mice but not in pMs derived from TLR4-KO mice (**Fig. 38 A and 38 C**), which validated the experimental system.

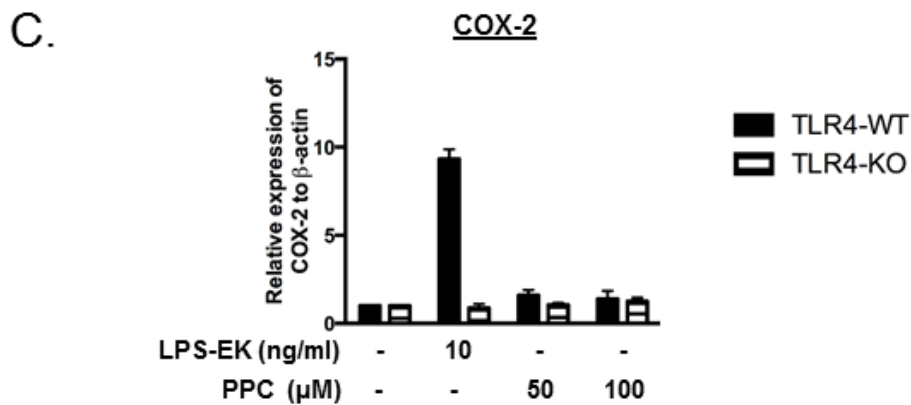
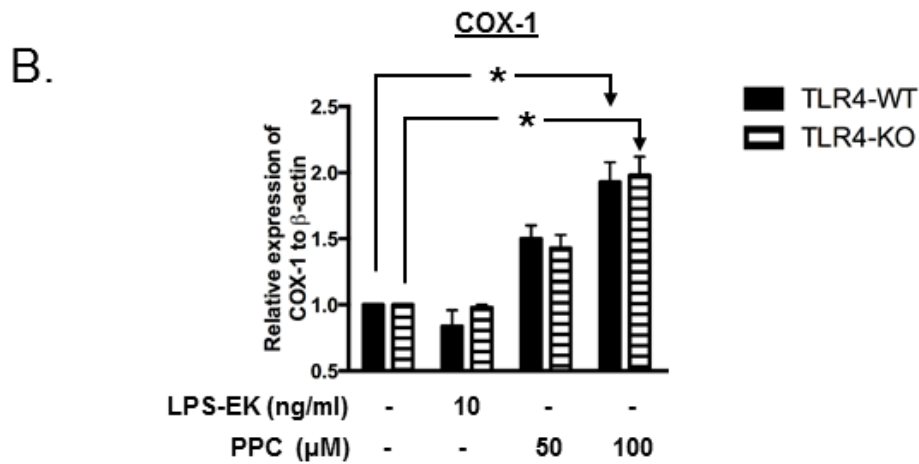
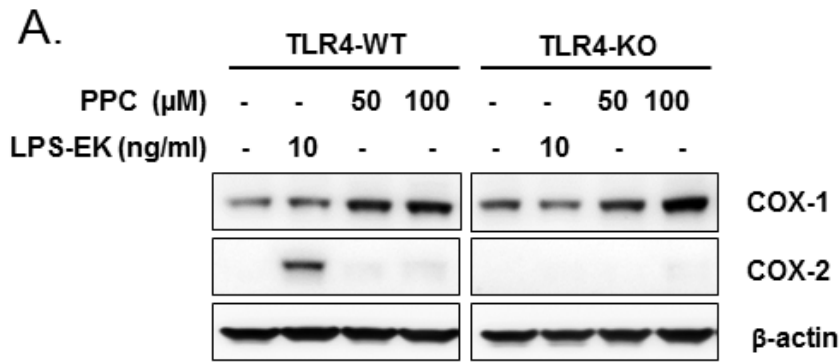


Figure 38. Effects of oxidants on cyclooxygenase (COX) protein expression upon short-term treatment paradigm. Peritoneal macrophages (pM) isolated from TLR4-WT and TLR4-KO mice were exposed to oxidants or LPS-EK for 2 h followed by incubation with complete growth medium in the absence of both oxidant and LPS-EK for the next 16 h. **(A)** Expression of COX-1 and COX-2 were determined using Western blot. Representatives immunoblotting of three independent experiments are shown. **(B)** & **(C)** Graphs represent the OD ratio of target immunoblot signal from **(A)** after normalization to β -actin. The experimental data are presented as the mean \pm SEM from three independent experiments, * $p < 0.05$.

We examined the effects of oxidant on the levels of PGE₂ in culture supernatant in pM using the **long-term treatment paradigm (Fig. 39 A and 39 C)**. PGE₂ production was also expressed as fold change over control cells normalized to untreated pM derived from TLR4-WT or those from TLR4-KO mice, respectively (**Fig. 39 B and 39 D**). Other studies showed that TLR4 activation resulted in PGE₂ increase as early as 6 h and the effects prolonged to 24 h (Shemi et al., 2000). Therefore, we quantified the levels of PGE₂ in culture medium after long-term treatment with oxidants or LPS-EK for 6 h or 16 h.

Our results showed that long-term treatment with PPC (5 μM) for 6 h or 16 h (**Fig. 39 A and 39 C**) did not affect PGE₂ production in pM derived from either TLR4-WT or TLR4-KO mice. In contrast, long-term exposure with SIN-1 at 1 mM for 6 h significantly increased PGE₂ production in pM derived from both TLR4-WT and TLR4-KO mice (**Fig. 39 A and 39 B**). SIN-1-mediated upregulation of PGE₂ lasted to 16 h in pM derived from both TLR4-WT and TLR4-KO mice (**Fig. 39 C and 39 D**). These results suggest that SIN-1 mediated-PGE₂ production may not require TLR4 expression. LPS-EK treatment induced a time-dependent PGE₂ up-regulation only in pM expressing TLR4, with increases of 5.6-fold at 6 h (**Fig. 39 A and 39 B**) and 8.9-fold at 16 h (**Fig. 39 C and 39 D**), respectively. Moreover, LPS-EK had no effects in pM with complete deletion of TLR4.

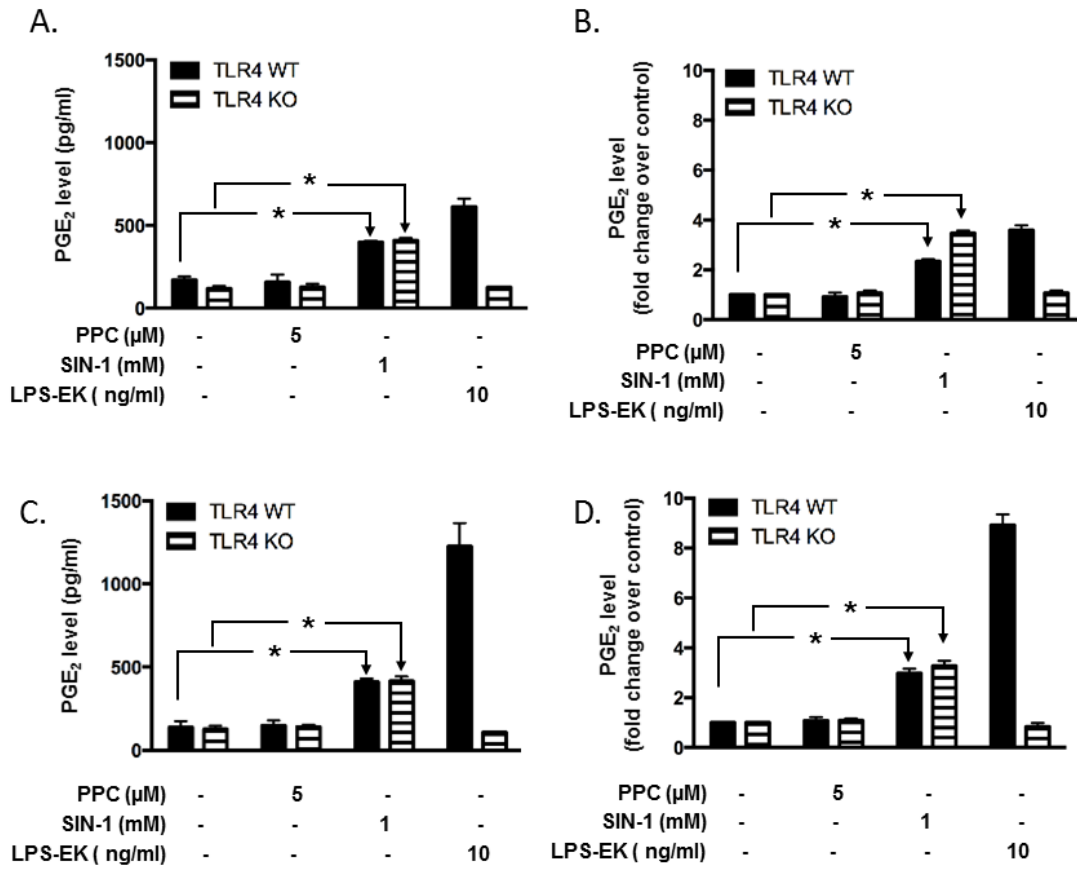


Figure 39. Effects of oxidants on prostaglandin E₂ (PGE₂) production up on long-term treatment paradigm. Peritoneal macrophages (pM) isolated from TLR4-WT and TLR4-KO mice were long-termly treated with oxidants or LPS-EK (as positive control), and levels of PGE₂ released in the culture supernatant were quantified after treatment for 6 h (A) or 16 h (B) by ELISA. The experimental data are presented as the mean ± SEM from three independent experiments. LPS-EK (10 ng/ml) was used as a positive control in PGE₂ induction. * p < 0.01.

We examined the effects of oxidant treatment on COX-1 and COX-2 protein expressions. After long-term treatment with oxidants or LPS-EK for 6 h or 16 h, and the cell lysates were subjected to Western blot analysis. Consistent with results of PGE₂ production, PPC (5 μM) treatment for 6 h (**Fig. 40 A**) or 16 h (**Fig. 40 B**) did not affect either COX-1 or COX-2 expression in pM derived from both TLR4-WT or TLR4-KO mice.

Unexpectedly, SIN-1 at 1 mM, which has shown to up-regulate PGE₂ levels (**Fig. 39 A and 39 B**), did not affect either COX-1 or COX-2 expression in both pM derived from TLR4-WT or TLR4-KO mice at 6 h (**Fig. 40 A**) or 16 h (**Fig. 40 B**) post treatment. The positive control LPS-EK treatment robustly induced COX-2 expression specifically in pM expressing TLR4 (**Fig. 40 A and 40 B**), which is consistent with an increase in PGE₂ levels.

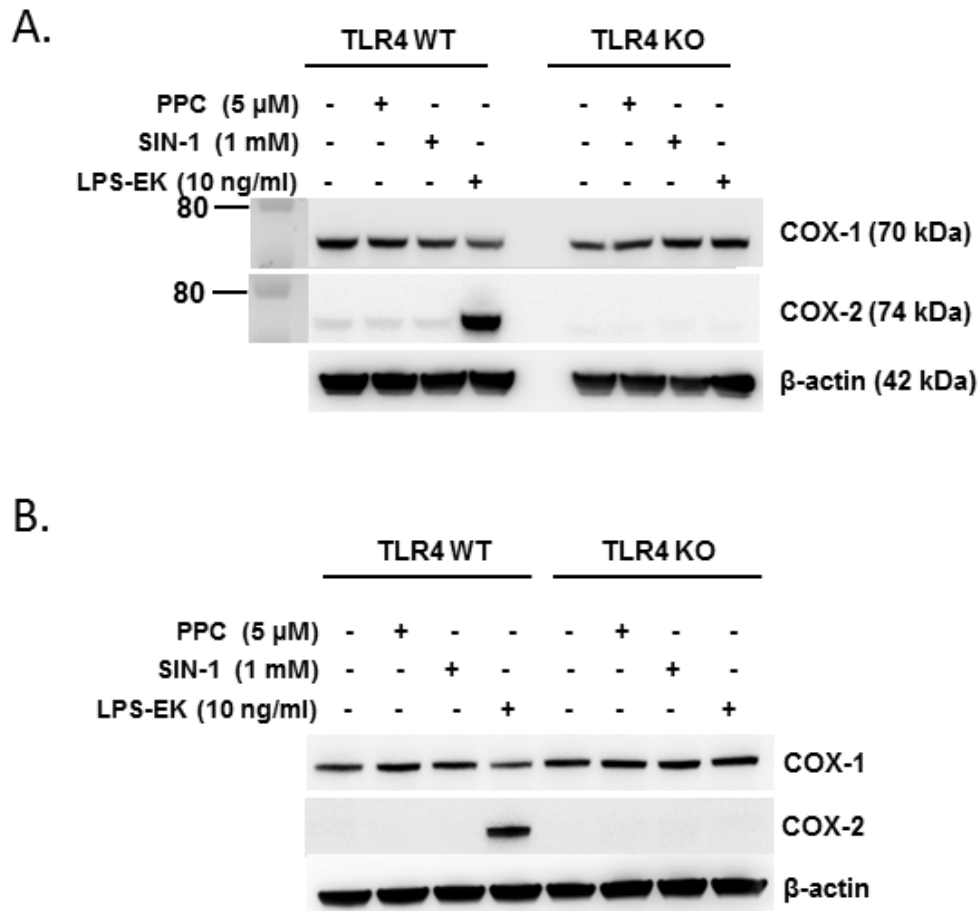


Figure 40. Effects of oxidants on cyclooxygenase (COX) protein expression up on long-term treatment paradigm. Peritoneal macrophages (pM) isolated from TLR4-WT and TLR4-KO mice were long-termly treated with oxidants or LPS-EK. Expression of COX-1 and COX-2 after treatment for 6 h (**A**) or 16 h (**B**) were determined using Western blot. Immunoblotting Figs are representatives of three independent experiments.

Effects of Oxidants on the Production of Resolvin D1 a Pro-resolution Lipid Mediator and its Receptor Expression

At the inception of the inflammatory process, the essential omega-3 polyunsaturated fatty acid (ω -3 PUFA) docosahexaenoic acid (DHA) or eicosapentaenoic acid (EPA) is available for enzymatic transformation to several anti-inflammatory and pro-resolving mediators, including D- and E-series resolvins (Xu et al., 2010). Among the pro-resolving mediators, RvD1 and RvE1 series are relatively well studied and have recently been identified to inhibit neutrophil activation (Serhan and Savill, 2005), regulate cytokines (Spite et al., 2009), protect ischemia-reperfusion-, oxidative stress- (Spite et al., 2009), and modulate LPS-induced injury (Liao et al., 2012; Wang et al., 2014) and induce anti-nociception *in vivo* (Xu et al., 2010).

RvD1 is derived from DHA through a series sequential enzymatic reactions. 12-LOX and 5-LOX are the two key enzymes responsible for RvD1 biosynthesis (Serhan and Petasis, 2011). One of the identified RvD1 receptors in mice is formyl peptide receptor 2 (FPR2), also called ALX, a lipoxin A4 receptor, and a G protein-coupled receptor. It has recently been demonstrated that RvD1 selectively interacts with FPR2, which regulates short-term inflammatory responses *in vivo*. Knockout of FPR2 in mice reduces inflammatory responses (Krishnamoorthy et al., 2012).

In addition to various pro-inflammatory mediators, we also examined the effects of oxidants on the production of RvD1, which can promote resolution and suppression of inflammation (Serhan and Savill, 2005). Short-term treatment with high concentrations of oxidants appears to be more potent than long-term treatment with low concentrations of oxidant in the induction of pro-inflammatory cytokine TNF- α (**Fig.**

33 and **34**). Thus, we examined the effects of oxidant on RvD1 production in pM following our **short-term and high concentration treatment paradigm**. Consistently, pM isolated from TLR4-WT and TLR4-KO mice were treated with oxidant or LPS-EK for 2 h followed by incubation in the growth medium in the absence of oxidants or LPS-EK for the next 16 h. We quantified the levels of RvD1 in the conditioned medium (**Fig. 41 A**). The levels of RvD1 were also expressed as fold change over control cells with normalization to untreated pM derived from TLR4-WT and TLR4-KO mice, respectively (**Fig. 41 B**).

Our results showed that the mean levels of RvD1 in untreated pM derived from TLR4-WT and TLR4-KO mice were 9.01 pg/ml and 15.94 pg/ml, respectively. In pM derived from TLR4-WT mice, short-term treatment with PPC (100 μ M) significantly increased the levels of RvD1 up to 18.7 pg/ml (**Fig. 41 A**) with an increase of 2.08-fold of control (**Fig. 41 B**). In contrast, PPC (100 μ M) did not change the levels of RvD1 in pM derived from TLR4-KO mice (**Fig. 41 A and 41 B**). Using the same treatment paradigm, LPS-EK did not significantly increase RvD1 production in pM either derived from TLR4-WT or TLR4-KO mice (**Fig. 41 A and 41 B**). These results suggest that oxidant-mediated RvD1 production requires TLR4 expression.

RvD1 potentially signals by interacting with its two receptors FPR2/ALX and GPR23, which are both G protein coupled receptors (GPCR) (Krishnamoorthy et al., 2012). Because of limited commercial availability of anti-mouse GPR23 antibody, we focused our efforts on FPR2. We then determined the effects of PPC on the protein expression of FPR2 using Western blot.

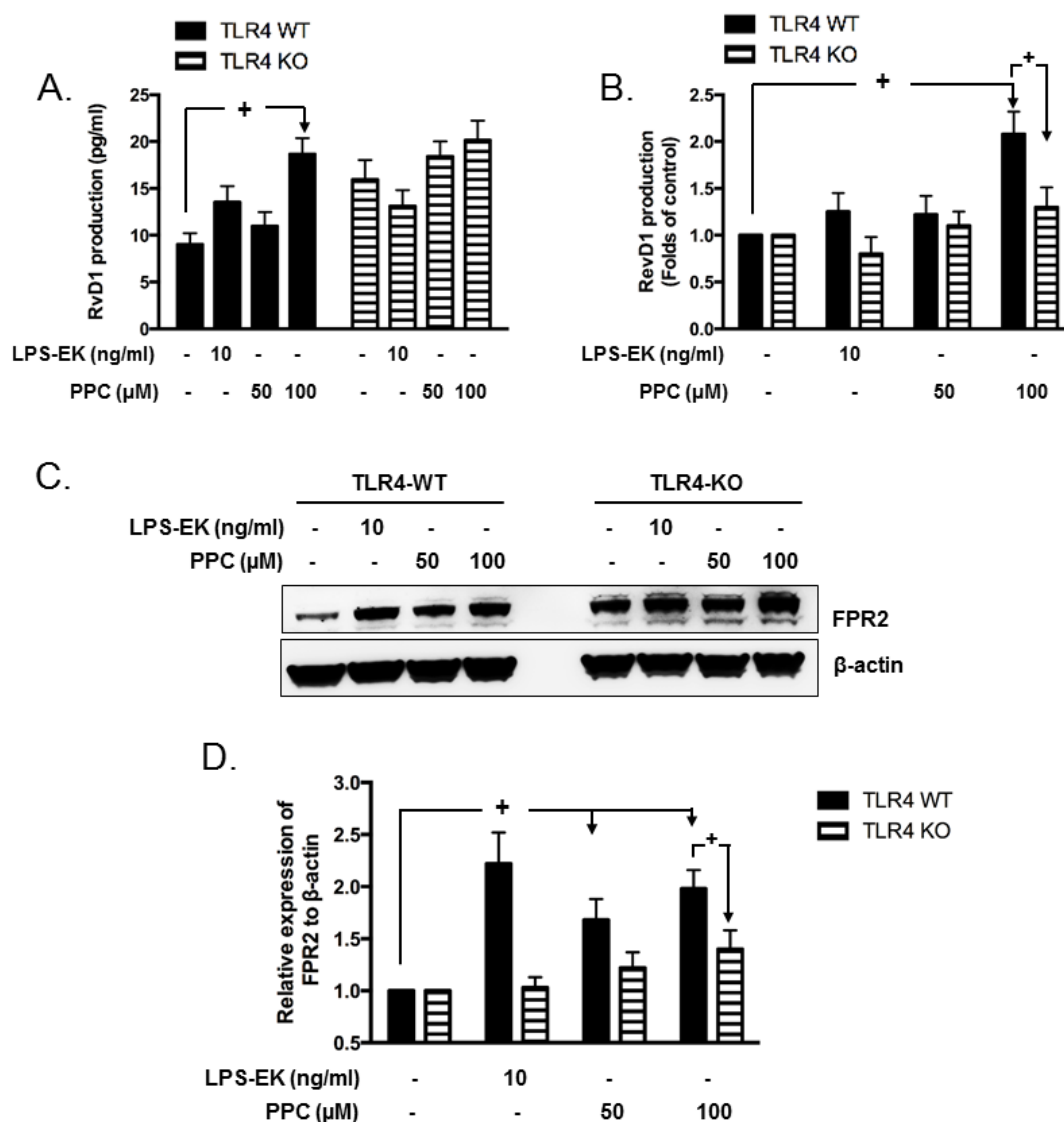


Figure 41. Effects of PPC on resolvin D1 (RvD1) production and its receptor FPR2 expression. Peritoneal macrophages (pM) isolated from TLR4-WT and TLR4-KO mice were treated with LPS-EK or PPC for 2 h followed by incubation with complete growth medium in the absence of both PPC and LPS-EK for the next 16 h. **(A)** Levels of RvD1 released into the culture media were quantified by ELISA. **(B)** Levels of RvD1 were expressed as fold change with those in untreated (i.e., no oxidant) control cells. **(C)** Expression of FPR2 receptor in cell lysate were determined by Western blot. Representative immunoblot results are shown. **(D)** The histograms represent the OD ratio of FPR2 immunoblot signal from **(C)** after normalization to the housekeeping protein β-actin. The experimental data are presented as the mean ± SEM from three independent experiments. + $p \leq 0.05$.

In pM derived from TLR4-WT mice, short-term treatment with PPC (50 and 100 μ M) robustly upregulated the expression of FPR2 in comparison with its untreated control cells (**Fig. 41 C and 41 D**). However, short-term treatment with PPC had no effect on the expression of FPR2 in pM derived from TLR4-KO mice in comparison with its untreated cells (**Fig. 41 C and 41 D**). The positive control LPS-EK did not stimulate RvD1 production, but it upregulated the expression of FPR2 in pM expressing TLR4 but not in pM with deletion of TLR4 (**Fig. 41 D**). These results implied that TLR4 is necessary for PPC-mediated upregulation of FPR2 in pM.

To further explore the mechanisms by which PPC stimulated the production the RvD1, we examined the expressions of 12-LOX and 5-LOX which are two key enzymes responsible for RvD1 biosynthesis in murine cells (Serhan and Petasis, 2011). We semi-quantified the protein levels of 12-LOX and 5-LOX using Western blot (**Fig. 42 A and 42 C**). The relative expressions of 12-LOX and 5-LOX were normalized with the housekeeping protein β -actin, then expressed as fold of untreated control cells in pM derived from TLR4-WT and TLR4-KO mice, respectively (**Fig. 42 B and 42 D**).

Consistent with increased RvD1 production, our results revealed that short-term treatment with PPC at 100 μ M significantly upregulated the expression of 12-LOX with increase of 2.3 fold (**Fig. 42 A and 42 B**) and 5 LOX with increase of 1.9 fold (**Fig. 42 C and 42 D**) in comparison with untreated control cells in pM derived from TLR4-WT mice. However, PPC at 100 μ M did not affect 12-LOX and 5-LOX in pM derived from TLR4-KO mice. LPS-EK, which showed limited effects on RvD1 biosynthesis, had no effects on 12-LOX (**Fig. 42 A and 42 B**) and 5-LOX expression (**Fig. 42 C and 42 D**) as well. Thus, these results may suggest that PPC-mediated RvD1 biosynthesis was

through the upregulation of the expression of 12-LOX and 5-LOX through TLR4 stimulation.

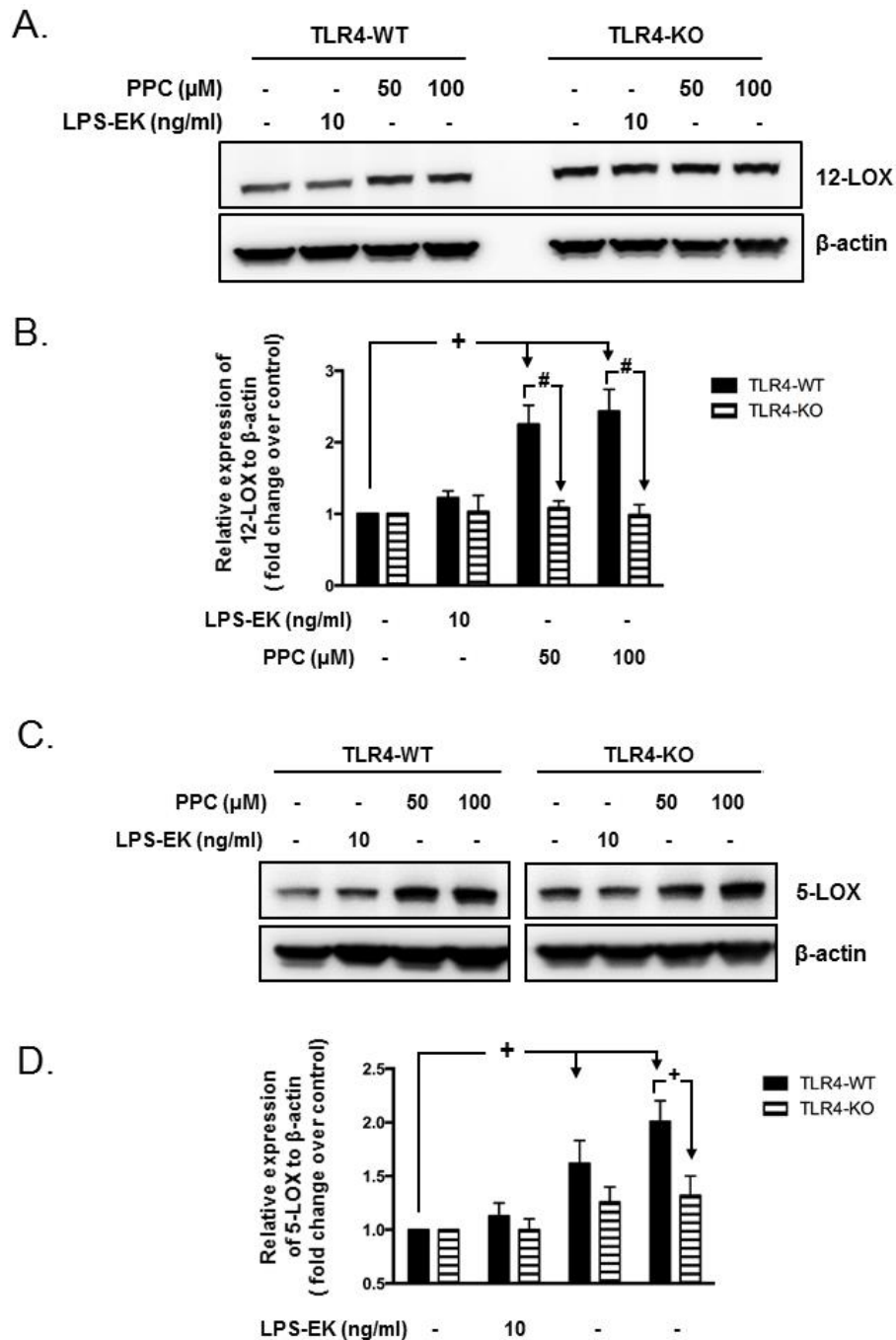


Figure 42. Effects of PPC on the expression 12-lipoxygenase (LOX) and 5-LOX. Peritoneal macrophages (pM) isolated from WT and TLR4 KO mice were treated with LPS-EK or PPC for 2 h followed by incubation with complete growth medium in the absence of both PPC and LPS-EK for the next 16 h. Expression of 12-LOX and 5-LOX in cell lysate were determined by Western blot. Representative immunoblot results are shown in (A) and (C), respectively. Figs (B) & (D) represent the relative expressions of 12-LOX and 5-LOX immunoblot signal from (A) and (C) after normalization with β -actin and to untreated control pM derived from TLR4-WT and TLR4-KO mice respectively. The experimental data are presented as the mean \pm SEM from three independent experiments. + $p \leq 0.05$, # $p \leq 0.01$.

Discussion

In this Chapter, we first characterized primary pM isolated from TLR4-WT and TLR4-KO mice to validate that they are a reliable *in vitro* system/model to study the role of TLR4 in oxidant-induced inflammatory phenotypes. Then we further investigated the role of TLR4 in oxidant-stress induced: (1) increase in iROS levels, (2) reduction in iTAOC, (3) production of PGE₂, TNF- α and IL-10, (4) expression of iNOS, and COX, and (5) biosynthesis of resolvin D1 (RvD1) with its potential signaling receptor.

In Chapter 3, to characterize the role of TLR4, we used both TLR4 neutralizing Ab and CLI-095 signaling inhibitor, which can specifically and covalently bind to the TIR domain of TLR4 to block its signaling. In the present Chapter, we isolated pM from TLR4-WT and TLR4-KO mice. TLR4-KO mice are homozygous for a null mutation of *Tlr4* (Poltorak et al., 1998). The mutation corresponds to a deletion of 74,723 bp of DNA, which completely removed the *tlr4* gene (**Fig. 24 A**). Therefore, this mouse strain fails to express *Tlr4* mRNA and protein, and does not respond to LPS stimulation. As the sequence of the boundaries of the deletion was identified, PCR mutant primers, which predict amplification between 13552 bp and 88414 bp of the sequence (no identified coding gene, thus there is no reference data bank), were used to test completeness of the gene deletion. In the present study, a product of 140 bp, was obtained following amplifications of DNA from TLR4-KO mice only (**Fig. 24 B**), which demonstrated that 74,723 bp gene including *Tlr4* was completely deleted. In addition, we confirmed the expression of TLR4 in TLR4-WT mice using primers which amplify the *tlr4* DNA sequence (**Fig. 24 B**).

We showed that the deletion encompasses only a single gene of *tlr4*. No gene within the 74,723 bp was identified by means of homology searches or analyses with predictive algorithms (Poltorak et al., 2000). The sequencing results confirmed that the deletion is a simple one, and does not involve corresponding insertion of other genetic elements, with a potential attendant disruptions at other locations in the genome. Therefore, *tlr4* mutation in TLR4-KO mice mainly results in deletion of *tlr4* rather than directly affecting multiple genes. Because Tlr4 makes a structural contribution to other cell membrane complexes in addition to the LPS receptor complex (Poltorak et al., 2000), complete deletion of TLR4 may affect membrane structure. We used C57BL/6 mouse strain as an appropriate positive control of TLR4 expression because this strain shares the same genomic background with TLR4-KO mice.

Another TLR4 deficient mouse strain C3H/HeJ was shown to correspond to a missense mutation in the third exon of *tlr4* gene, predicting to replace proline with histidine at position 712 of the polypeptide chain, thus resulting in unresponsiveness to LPS stimulation. However, it has been shown that the genetic defectiveness of TLR4 in C3H/HeJ mice is “leaky” in that high concentration of LPS would provoke a response, particularly in IFN-treated macrophages (Beutler et al., 1986). To avoid this “leaky” effects, we chose to use the TLR4-KO mice with complete deletion of TLR4.

The methods of isolation and culture for peritoneal macrophages are well-established. Generally, the naïve peritoneal cavity would yield about $1 - 2 \times 10^6$ cells, 40% of which are resident macrophages ($0.4 - 0.8 \times 10^6$) (Misharin et al., 2012). This number of resident macrophages is not sufficient for extensive biological studies. To overcome this limitation, injection of eliciting agent, e.g. aged 3% Brewer TGC

medium, into the peritoneal cavity several days prior to harvest has been used to increase the yield to $1 - 2 \times 10^7$ cells per mice containing a high percentage of macrophages (86-95%) (Zhang et al., 2008). The purity was further increased to almost 99% by adherence since pM are suspended in situ in peritoneal cavity, but become adherent when they are cultured *in vitro* (Zhang et al., 2008; Ghosn et al., 2010).

We assessed the purity of macrophages based on the expression of macrophage-specific cell markers, such as CD11b or F4/80. In the present study, we determined that almost 99 % of the cells are CD11b positive by immunofluorescent microscopy imaging (**Fig. 25 A**). The purity was further quantified to be above 95% using flow cytometry (**Fig. 25 B**). Our results consistently demonstrated that more than 95% of cells isolated by adherence from the peritoneal cavity were macrophages. Indeed, eosinophils express low levels of CD11b and F4/80. The presence of 10% eosinophils in the cultures of TGC-elicited pM has been suggested (Misharin et al., 2012), but their effects on response to TLR4-specific stimulation is without much biological relevance.

Characterization of the isolated pM confirmed that TLR4 mRNA and protein are expressed in primary pM isolated from WT mice, but not in those isolated from TLR4-KO mice (**Fig. 26 A and 26 B**). Our data further confirmed the functional deficiency of TLR4 in pM derived from TLR4-KO mice in comparison with pM isolated from TLR4-WT mice (**Fig. 26 C**). Therefore, with primary pM derived from TLR4-WT and TLR4-KO mice, we investigated the role of TLR4 in macrophages in response to oxidant stimulation.

In addition to the “self, nonself” model for immune recognition proposed earlier (Janeway, 1992), the “danger” model was proposed (Matzinger, 1994), in which the

innate immune system can also recognize any threat dangerous to the host to activate or enhance the innate immune response (Gill et al., 2010). Damage associated molecular patterns (DAMPs) were identified as the typical “danger signals” or “alarmins”. DAMPs and pathogen associated molecular patterns (PAMPs) are equally effective at activating the immune system and are involved in both sterile and infectious inflammation (Gill et al., 2010).

DAMPs are defined as cell-bound molecules or parts of macromolecules which are hidden from recognition by the immune system under normal physiological conditions. Under conditions of cellular stress or tissue injury, these molecules can either be actively secreted by stressed immune cells, or passively released in to the extracellular environment from dying cells or from the damaged extracellular matrix (Heil and Land, 2014). Mammalian DAMPs are suggested to be divided into five classes because they are sensed by distinct members of five families of pattern recognition receptors (PRRs) (Heil and Land, 2014). Class I DAMPs including HMGB1, HSP-90, and S100A9 are recognized by TLR4 and mediates MyD88 signaling (Heil and Land, 2014; Zhang et al., 2015). RONS may be sensed indirectly by the NLRP3 (NOD-like receptor protein 3) inflammasome in the cytosol resulting in production of IL-1 β , RONS are regarded as member of Class II DAMPs (Heil and Land, 2014). It is not known whether RONS can be sensed by other PRRs.

Our data show that TLR4 is necessary for RONS-mediated pro-inflammatory phenotypes including evidence in disturbances of redox homeostasis (**Fig. 29 and 31**) and higher ratio of TNF- α production to IL-10 production (**Fig. 33**) These data provide evidence to support that RONS can act as DAMPs to activate inflammatory responses

in pM through TLR4 stimulation. More importantly, our data suggest that in addition to NLRP3, TLR4 located on outer membrane of pM might be another important PRR to detect and/or sense exogenous RONS, which extends our understanding of the role of TLR4 as a PRR. Our results provide additional evidence to the notion that unlike other TLRs, TLR4 responds to a wide range of non-canonical ligands, including heavy metals such as nickel (Schmidt et al., 2010), and cobalt (Raghavan et al., 2012), and fibrinogen (Smiley et al., 2001).

The detailed molecular mechanisms by which RONS can activate TLR4 are not clear at this stage. Based on the chemical characteristics of RONS and the “revised model of TLR4 signaling” proposed by Joshua N. Leonard recently (Daringer et al., 2015), we propose two potential mechanisms.

First, RONS may directly oxidize one or more cysteine (Cys) of heterodimer TLR4/MD-2 resulting in conformational rearrangement and subsequent dimerization of TIR domain. The classical model of TLR4 biosensing is that ligand binding to the ectodomains (ECDs) induces receptor dimerization, which promotes dimerization of TIR domains to generate a scaffold that recruits downstream signaling mediators (Gay et al., 2014). TLR4 is also the only TLR that requires myeloid differentiation factor-2 (MD-2) for ligand recognition (Gioannini et al., 2004). MD-2 binds to the ECD of TLR4 such that the heterodimer forms in the ligand-free cell surface (Gay et al., 2014). When the hydrophobic core of MD-2 binds lipid A, MD-2 exposes an interface that binds a second TLR4 ECD to promote the formation of a heterotetrameric TLR4/MD-2 signaling complex (Gay et al., 2014). Therefore, the hydrophobic core of MD-2 is crucial for ligand-mediated TLR4 activation.

It has been shown that the hydrophobic pocket of MD-2 consists of multiple Cys residues and Cys133 is necessary for LPS (canonical ligand) initiated-TLR4 activation (Koo et al., 2013). Therefore, theoretically, RONS can oxidize a subset of Sulphur atoms in the side chains of Cys residues to form sulfenic acid moieties within the heterodimer TLR4/MD-2. These covalent interactions are unstable but are able to form disulfide bridges with one another, thereby resulting in a change in structural configuration. This conformational change may also expose the interface to trigger the formation of the heterotetramer TLR4/MD-2 and subsequent activation of TLR4 (Kim et al., 2000). Indeed, RONS have been described as agonist (first messengers) to trigger intracellular signaling cascades (Nathan, 2003).

Second, RONS may directly disrupt the intrinsic TLR4-inhibitory complex (TIC) enabling the TIR domains to spontaneously dimerize and initiate downstream signaling. Previous study (Daringer et al., 2015) showed that: (i) the unique intracellular linker (ICL) of TLR4 was important for achieving LPS-induced NF- κ B activation; (ii) membrane-bound TLR4 TIR domains were sufficient to induce signaling; and (iii) initiation of TLR4 signaling is regulated by a mechanism that does not require tight geometric constraints. Based on these findings, they proposed a revised model of TLR4 signaling. They hypothesized that in the absence of ligand, TLR4 is retained in a signaling-incompetent conformation *via* interactions between TLR4 and one or more additional, as yet unidentified species, which was termed as TLR4-inhibitory complex (TIC). Upon LPS binding to the ECD to induce dimerization and /or rearrangement, interactions with TIC are disturbed, enabling the TIR domains to spontaneously dimerize and initiate downstream signaling. The TIC hypothesis could also be used to explain why TLR4 signaling is induced by numerous non-canonical ligands including

RONS. RONS may induce TLR4 signaling by direct disruption of TIC binding, even without inducing TLR4 ECD dimerization. Further investigations will be certainly needed to confirm or refute this hypothesis.

The interaction between RONS (as a potential ligand) and its putative receptor (TLR4) seems specific if we do not limit our ideas of specificity in TLR4 signaling to molecular “handshake” that depends on the complementarity of LPS as a canonical ligand that binds to its receptor. Chemically, the specificity of RONS can be “atomic” rather than “molecular”. In the case of protein, RONS may preferentially react covalently, often irreversibly, with Sulphur atoms of side chains within macromolecules, such as cysteine sulfhydryls, methionine sulfurs, tyrosine hydroxyls, iron-sulfur cluster, and protein hemes (Nathan, 2003; Nathan and Cunningham-Bussel, 2013). The reactivity of RONS with atomic targets in the context of macromolecules, rather than with a given macromolecules as a unique entity, suggests that the specificity of RONS for their targets may indeed be described as submolecular (Nathan, 2003).

Upon RONS-induced stimulation of TLR4, increase in intracellular ROS (iROS) could result also through either mitochondrial electron transport chain as a source of ROS (West et al., 2011) and cytosolic enzymes NADPH oxidases (Park et al., 2004a). Elevated levels of iROS may consume small antioxidant molecules (i.e. with small molecular weights) resulting in decrease in iTAOC. Moreover, TLR4 activation may reduce the expression of antioxidant enzymes, such as SOD1 and catalase (CAT) (Deng et al., 2016), which may exaggerate disturbances in cellular redox hemostasis. Consistent with our hypothesis, pM derived from TLR4-KO mice are resistant to

RONS-mediated increase in iROS levels and decrease in TAOC levels compared to the pM derived from TLR4-WT.

Interestingly, we observed up-regulated levels of iTAOC upon oxidant stimulation in comparison with untreated cells 24 h post oxidant treatment in pM derived from TLR4-WT mice (**Fig. 32 A and 32 B**). This could be due to the use of sub-threshold concentrations of each oxidant at which cell survival was greater than 85%. Consumption of small antioxidant molecules by large amount of free radicals upon TLR4 stimulation may induce the activation of global cellular antioxidant system. However, multiple mechanisms may also be involved. LPS-mediated stimulation of TLR4 increases AP-1 activation, which in turn may up-regulate the expression of γ -glutamylcysteine synthetase (γ -GCS), a rate-limiting enzyme for GSH synthesis (Deng et al., 2016). Increased GSH levels upon TLR4 activation may contribute to elevated iTAOC as well (Deng et al., 2016). In addition, it has shown that exposure of cells to H₂O₂ and cigarette-smoke extract (CSE) for 24 h stimulated the translocation of nuclear erythroid-related factor 2 (Nrf2) (Kode et al., 2008). Nrf2 is the principal transcription factor that regulates the antioxidant response element-mediated expression of Phase II detoxifying antioxidant enzymes. It is sequestered in the cytoplasm, and activated and translocated to the nucleus when cells are exposed to inducers such as oxidative stress. More empirical data will be needed to clarify the contribution of Nrf2 in the initial oxidant-induced increase in iTAOC.

NF- κ B is the master transcriptional regulator for proinflammatory cytokines such as TNF- α (Shakhov et al., 1990) and IL-1 β (Hiscott et al., 1993). The transcription of iNOS, the inducible enzymes for NO production, COX-2, and the inducible enzyme

for PGE₂ biosynthesis are also direct target of NF-κB (Geller et al., 1993; Yamamoto et al., 1995). In Chapter 3, we observed that long-term treatment with PPC or SIN-1 showed limited effects on NF-κB activation in RAW-Blue cells (**Fig. 13 C and 13 D**). Consistent with these observations, long-term treatment with PPC or SIN-1 for 16 h had minimal effects on TNF-α gene expression as well as TNF-α production of (**Fig. 34**), IL-1β gene expression (**Fig. 35**), and induction of iNOS protein expression (**Fig. 36**) in primary pM isolated from TLR4-WT or TLR4-KO mice. This could be since the long-term treatment paradigm with low concentrations of oxidants could not sufficiently induce NF-κB activation to cause changes in gene expression of target genes.

PGE₂ is a potent pro-inflammatory lipid mediator produced by activated macrophages. The key enzymes responsible for PGE₂ production are COXs. Generally, expression of COX-1 is constitutive while COX-2 is inducible. COX-1 is expressed in most tissues under basal conditions and responsible for the production of PGE₂ with physiological functions. In contrast, COX-2 is considered undetectable in most normal tissues and cells but is upregulated under various conditions (Kangussu et al., 2015). However, a growing body of evidence is now emerging that suggests that the biology of COX isoforms is much more complex and that the originally postulated segregation into ‘constitutive and ‘inducible’ isoforms is an oversimplification (Smith et al., 1996). Some studies have shown that both isoforms, not only COX-2, are involved in various pathological conditions, especially oxidative stress (Burdon et al., 2007; Kangussu et al., 2015).

In the present study, we found that short-term exposure with PPC at 100 μ M increased levels of PGE₂ in pM derived from either TLR4-WT or TLR4-KO mice, which suggests that ROS-mediated PGE₂ production may be independent of TLR4 expression (**Fig. 37**). Our results showed that COX-1 is expressed while expression of COX-2 is undetectable in intact pM derived from both TLR4-WT and TLR4-KO mice. Short-term exposure with PPC failed to induce COX-2 expression, whereas it increased COX-1 in pM derived from both TLR4-WT and TLR4-KO mice (**Fig. 38**). These results provide two plausible suggestions: (i) elevated levels of PGE₂ might result from increased expression of COX-1; (ii) expression of COX-1 may be inducible by oxidants. Together with other studies (Burdon et al., 2007; Kangussu et al., 2015), our results further affirm that COX-1 expression is also inducible by oxidative stress. Interestingly, PPC-mediated COX-1 induction appears to be independent of TLR4 expression.

On the other hand, long-term treatment with SIN-1 at 1 mM for 6 h and 16 h significantly increased PGE₂ production (**Fig. 39**) without affecting the expression of COX-1 and COX-2 (**Fig. 40**) in pM derived from either TLR4-WT or TLR4-KO mice. Peroxynitrite (PN) may serve as a substrate and activator for the peroxidase activities of COX-1 and COX-2 (Landino et al., 1996). This is probably because direct addition of PN or *in situ* generation of PN from SIN-1 activates the cyclooxygenase activities of COX-1 and COX-2 in Raw264.7 macrophage (Landino et al., 1996). Therefore, PN released from SIN-1 may activate enzymatic activities of COX-1 and/or COX-2 rather than affect their gene expression. More experiments need to be done to confirm that SIN-1 increases enzymatic activities of COX-1 and COX-2. In addition, our results also

suggest that SIN-1-stimulated PGE₂ production is independent of TLR4 expression and stimulation.

Resolvin D1 (7S, 8R, 17S-trihydroxy-4Z, 9E, 11E, 13Z, 15E, 19Z-docosaenoic acid) (RvD1), originally identified in resolving exudates *in vivo* through multiple cellular process (Serhan et al., 2002), is biosynthesized from docosahexaenoic acid (DHA) released from cellular membranes (Hong et al., 2003; Leigh et al., 2014). In the present study, we quantified RvD1 levels in the supernatants of pM culture in the resting state (**Fig. 41 A**), confirming that RvD1 is biosynthesized and released by macrophages. Our study provides further evidence that RvD1 can be synthesized *de novo* within macrophages. Moreover, our results showed that the levels of RvD1 were increased upon PPC treatment (**Fig. 41 A and 41 B**), suggesting that RvD1 biosynthesis is triggered under cellular oxidative stress. The data thus support the original biosynthetic scheme that the inception of inflammatory signals initiates the biosynthesis of resolvins utilizing DHA or EPA to maintain or return cells to homeostasis (Serhan and Petasis, 2011). In agreement with other previous *in vivo* study (Serhan et al., 2002), our result confirms that resolvin-initiated resolution of cellular homeostatic signals is an essential and necessary components of inflammation.

The biosynthetic route of RvD1 appears to be established with 12-LOX and 5-LOX as the two key enzymes for RvD1 biosynthesis in mice (Serhan and Petasis, 2011). The exact role of 12-LOX in chronic inflammation remains elusive. 12-LOX was initially thought to promote inflammation (Kronke et al., 2009). Deletion of 12-LOX was shown to reduce lipid oxidation *in vivo* as well as to ameliorate the formation of atherosclerotic lesions in murine models (Cyrus et al., 2001). Recent studies, however,

indicate a more complex role for this enzyme during inflammation and point toward additional anti-inflammatory properties (Kronke et al., 2009), which mainly seem to involve the generation of RvD1 and lipoxins (Merched et al., 2008). 12-LOX deficient mice showed enhanced inflammatory gene expression and decreased levels of lipoxin A4 (Kronke et al., 2009). In the present study, our results show that 12-LOX are expressed in intact pM indicating that the components for RvD1 biosynthesis are present in macrophages (**Fig. 42**). More importantly, the increased expression of 12-LOX upon short-term treatment with oxidant correlate with increased levels of RvD1 in pM derived from TLR4-WT mice (**Fig. 41**). These results offer an explanation for a mechanism by which oxidants may increase RvD1 biosynthesis. Our results also support the notion that under oxidative stress, macrophages can convert DHA to RvD1 by inducing 12-LOX expression, which also reveals the anti-inflammatory properties of 12-LOX.

5-LOX is another key enzyme in RvD1 production. Meanwhile, 5-LOX is the rate-limiting enzyme in leukotriene biosynthesis, a potent proinflammatory lipid mediator derived from arachidonic acid (AA). Recent studies suggest that the action of 5-LOX is dependent on its cellular localization (Brock, 2005; Fredman et al., 2014). Nuclear 5-LOX, because of its proximity to LTA4 hydrolase, favors the biosynthesis of proinflammatory LTB4 from AA. In contrast, non-nuclear 5-LOX, potentially promotes the conversion of DHA to RvD1 because of its proximity to 12-LOX (Fredman et al., 2014). Moreover, RvD1 forms a positive feedback loop on its biosynthesis through inhibition of nuclear translocation of 5-LOX (Fredman et al., 2014). In the present study, we show that 5-LOX is expressed in intact pM suggesting that the components for RvD1 biosynthesis are constitutively present (**Fig. 42**).

Additionally, increased expression of 5-LOX upon short-term treatment with oxidant (**Fig. 42**) also correlate with increased levels of RvD1 (**Fig. 41 and 41 B**) in pM derived from TLR4-WT mice. Nuclear translocation of 5-LOX might be inhibited by increased levels of RvD1 in an autocrine manner in pM, which in turn favors production of RvD1. Therefore, the increased 5-LOX may be constitutively localized in cytosol to promote RvD1 production. Alternatively, 5-LOX may be the other inducible enzyme used to biosynthesize RvD1 in macrophages. It is not known whether increased 5-LOX is pro-inflammatory favoring LTB4 production or anti-inflammatory favoring RvD1 production at this stage. To address this question, more empirical data will be required, to examine: (i) cellular localization of 5-LOX, (ii) levels of LTB4 produced, and (iii) the relationship between RvD1 and LTB4.

In the present study, we did not observe the effects of LPS-EK on the production of RvD1 and the expression of 12-LOX and 5-LOX which are key enzymes for RvD1 biosynthesis. Based on what we know so far, there are no available studies on the direct effects of LPS on RvD1 production. However, treatment *in vivo* with LPS (1 µg/ml) has been shown to increase 12-LOX and 5-LOX expression in macrophages via activation of NF-κB pathways (Wuest et al., 2012; Lee et al., 2015; Rey et al., 2016). Here we may speculate on two explanations. First, lack of LPS-EK effect may be due to the low concentration of LPS-EK and the short incubation time used in our study. Second, time points we used in this study may not be optimal for studying the effects of LPS-EK on RvD1 production. A higher concentration of LPS-EK may be required to examine the effects of LPS-EK on the RvD1 production.

In addition to 12-LOX and 5-LOX, PLA₂ is another critical enzyme for RvD1 production. PLA₂ is responsible for the cleavage of the acyl groups in the sn-2 position of membrane phospholipids (Leigh et al., 2014). Specifically, cPLA₂ has been shown to preferentially release arachidonic acid, and iPLA₂ seems to mediate the release of DHA in rat neurons (Strokin et al., 2003). While there is evidence for PLA₂ use in cleaving DHA from cell membrane, a conclusive answer as to which isoform is needed for RvD1 biosynthesis is still unknown. Recent studies examined the role of cPLA₂ and iPLA₂ in RvD1 production suggesting that cPLA₂ might be an important rate-limiting enzyme that catalyzes DHA release (Leigh et al., 2014). Therefore, expression and activity of cPLA₂ may be crucial for substrate availability and initiation of RvD1 biosynthesis. It is possible that cPLA₂ is critical for oxidant-mediated RvD1 production. In that case, cPLA₂ will be a master enzyme that controls the lipid mediator switch. For a complete understanding of the biosynthesis mechanism, expression of cPLA₂ by oxidant treatment needs to be examined in future studies.

Our results showed that the levels of RvD1, expression of FPR2, 12-LOX and 5-LOX in pM with complete deletion of TLR4 could not be due to PPC treatment (**Fig. 41**). This may be due to the fact pM with deletion of TLR4 were protected cells from oxidant-mediated intracellular oxidative stress, thereby confirming indirectly that oxidative stress could induce RvD1 production.

RvD1 can attenuate inflammatory response through modulation of NF- κ B (Liao et al., 2012), MAPK and AP-1 (Xu et al., 2013) signaling pathways. Pretreatment of microglia with RvD1 potently inhibited LPS-induced NF- κ B nuclear translocation and DNA binding activity, and down regulated the expression of TNF- α , IL-6, and IL-1 β

as a result (Liao et al., 2012; Xu et al., 2013). In the present study, our results showed that short-term exposure with high concentration of oxidants significantly increased NF- κ B activation, with a subsequent TNF- α production, which is accompanied by increased levels of RvD1. As RvD1 exerts potent anti-inflammatory effects at the pico- to nano-molar range (Liao et al., 2012), theoretically, RvD1, which is about 53 nM in the culture medium, can exert suppression by a feedback loop on oxidant-mediated NF- κ B activation. For example, the magnitude of NF- κ B activation, and subsequent proinflammatory mediators induced by oxidants may be counteracted in the presence of RvD1 in macrophage (Rey et al., 2016). DHA derived RvD1 may depresses the expression and activity of proinflammatory TNF- α induced by oxidants in pM derived from both TLR4-WT and TLR4-KO.

As a highly potent anti-inflammatory agent that promotes resolution of inflammation, RvD1 exert its action by interacting with its receptors. Two specific G protein coupled receptors (GPCR), FPR2/ALX and GPR32, specifically and directly interact with RvD1 (Krishnamoorthy et al., 2010). In these studies, we have focused our efforts on investigating the expression of FPR2, which is widely expressed in many cells types, including leukocytes, neutrophils, monocytes, activated T cells, as well as macrophages, microglia, and epithelial cells (Chiang et al., 2006; Xu et al., 2013). FPR2 deficient mice showed markedly enhanced inflammatory responses following LPS-injection (Wang et al., 2016). FRP2 expression increases as early as 2 h after short-term lung injury or inflammation in mucosal epithelial cells suggesting that expression of FRP2 is inducible by inflammatory stimuli (Bonnans et al., 2006). In agreement with these reports, our data have revealed that FPR2 is expressed in pM at resting state as well. Moreover, its expression was markedly increased upon short-term treatment with

oxidant in pM derived from TLR4-WT mice (**Fig. 41 C and 41 B**). The concept that protective effects of RvD1 is reinforced by our data showing that pM expressed FPR2/ALX receptor, which is upregulated by oxidant treatment. Thus, RvD1 could bind to its receptor to facilitate resolution of inflammation. FPR2/ALX expression levels was significantly increased following oxidants treatment. An interesting finding is the concordance between increased RvD1 production and FPR2 expression after oxidant exposure. Increased expression of FPR2 might lead to higher sensitivities to its ligand RvD1, which will “instruct” innate macrophage to promote RvD1-mediated resolution of inflammation (Bonnans et al., 2006). These discoveries are of great significance because they provide additional intrinsic mechanisms by which macrophages respond to or resolve oxidative stress-induced initiation of inflammation.

As an endogenous autacoid, RvD1 is an anti-inflammatory and pro-resolution lipid mediator that is produced at low concentration. We have shown that RONS can act to initiate inflammatory processes by stimulating TLR4 through NF- κ B activation. Speculatively, resolvins have evolved to counter acute inflammatory processes that imbue the cell/tissue with protection at very low concentrations of the autacoid. The idea appears to be supported in our system by concurrent increase in both release of RvD1 and up-regulation of its receptor, FPR2/ALX.

In addition, as an experimental model pM may constitute a powerful tool for screening the immunomodulatory potential of many compounds very easily and rapidly. This is despite the fact that pM are not in their fully functional microenvironment in vivo with endothelial cells, neutrophils etc and other cells.

Theoretically, decreased levels of RvD1 favors an imbalance between pro-inflammation and pro-resolution toward potential chronic inflammatory status that may initiate disease. However, we found that the levels of RvD1 were increased upon PPC treatment (**Fig. 41 A and 41 B**). Whether inflammatory responses induced by oxidant are resolved by RvD1 cannot be appropriately addressed at this stage. Actually, the timeline of RvD1 production is of critical consideration for its biological effects. Previous *in vivo* studies established the time-course of the pro-inflammatory and pro-resolvins pathways (Serhan and Petasis, 2011) showing that production of RvD1 can last for hours to days. In the present studies, we examined the levels of RvD1 at 16 h post short-term exposure with oxidant in pM, which is consistent with the time course of *in vivo* studies (Serhan et al., 2002). We still cannot exclude the possibility that levels of RvD1 might eventually decrease at 48 h or 72 h after treatment with oxidants. In that case, RvD1 will fail to promote resolution of oxidant-mediated inflammation resulting in chronic inflammatory phenotype. Therefore, measuring the levels of RvD1 at longer time lines in the future studies will be necessary to address the issue.

In addition, RvD1 is one of the important pro-resolving lipid mediators. Our present study does not exclude the possibilities that oxidative stress can down regulate the production of other pro-resolving mediators including lipoxins (LXA₄ and LXB₄), E-series resolvins (RvE1-E3), other D-series resolvins (RvD 2-6), neuroprotectins, and the maresins (Serhan and Petasis, 2011). To our knowledge, most studies have focused on their anti-inflammatory and pro-resolving effects. No work has shown the effects of RONS on the production of resolvins mentioned above. If inhibition of one or more other pro-resolving mediators counteract the increase of RvD1, this can also lead to suppression of resolution of inflammation resulting in potential chronic inflammatory

status (Serhan and Petasis, 2011). Therefore, more studies need to be done to examine the effects of oxidants on the levels of other resolvins.

Based on the data of this chapter, we have proposed a working model (**Fig. 43**). The activation of TLR4 by oxidants may stimulate PGE₂ production through activation of cPLA/COX/PGES signaling pathway. In tandem, TLR4 activation by oxidants may initiate the production of RvD1 through iPLA₂/12-LOX/5-LOX signaling, and increase the expression of RvD1 receptor FPR2.

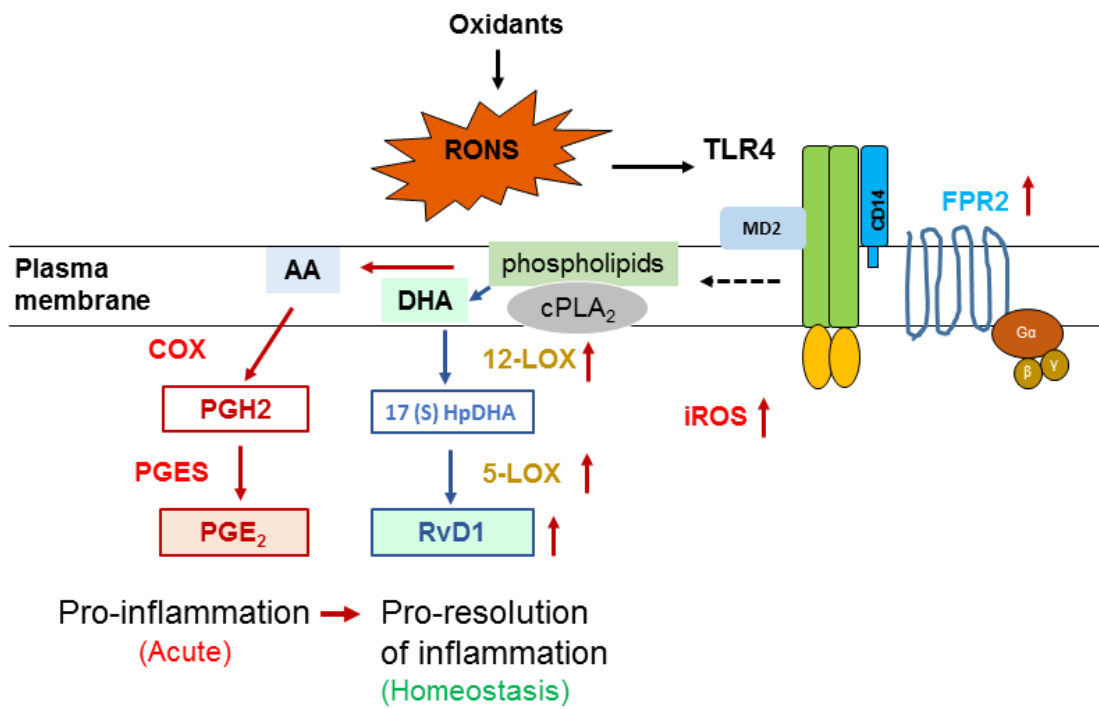


Figure 43. Proposed working model. Proposed working model for the role of exogenous oxidants in a potential modulation of pro-inflammatory and pro-resolution of inflammatory processes through TLR4 stimulation. Revised from (Serhan and Petasis, 2011)

6. MATERIAL and METHODS FOR SENSITIZATION OF PRIMARY PERITONEAL MACROPHAGES

Oxidants

Preparation of Potassium Peroxychromate (PPC)

As in Chapter 2, page 49

Potassium Peroxynitrite (PPN)

PPN (Millipore, Billerica, Mass, USA) was used as a director donor of peroxynitrite (PN).

Sensitization and Treatment of pM

pM were sensitized by incubation with 100 ng/ml LPS-EK for 4 h in culture medium supplemented with 10 % heat-inactivated (HI) FBS, rinsed once with culture medium supplemented with 1% HI FBS, 50 units/ml penicillin and 50 ug/ml streptomycin. Finally, cells were incubated overnight with fresh medium supplemented with 1% HI FBS containing PPC or PPN.

RNA Extraction and Reverse Transcription

As in Chapter 2, page 58

Quantitative-Reverse Transcription & Polymerase Chain Reaction (RT-qPCR)

As in Chapter 2, page 58

Quantification of PGE₂

As in Chapter 4, page 107

Statistical Analysis

As in in Chapter 2, page 62

7. TLR4 PRIMING SENSITIZES PRIMARY PERITONEAL MACROPHAGES TO OXIDANT-MEDIATED PGE₂ PRODUCTION

Human exposure to LPS is common place, via multiple sources including bacterial infection, microbiome translocation of gut microflora, gut injury, dietary alteration, alcohol abuse, and in a variety of occupational and environmental settings (Pestka and Zhou, 2006). Besides, injured tissue such as dying tumor cells can persistently release endogenous danger signals collectively termed DAMPs. Examples are heat shock protein (HSP) and high mobility group box 1(HMGB1) protein, which serve as endogenous and exogenous ligands for TLR4 as well (Prakash et al., 2016). Therefore, potential activation and priming of TLR4 by its ligands is commonplace.

AA metabolites have been known for a long time to play significant roles in initiating and/or terminating inflammatory processes (Chizzolini and Brembilla, 2009). PGE₂, one the most abundant metabolites of AA, can increase vascular permeability, induce fever, and maintain hyperalgesic responses (Chizzolini and Brembilla, 2009). PGE₂ is generated through sequential enzymatic reactions by PLA₂, COX and mPGES. COX-2 and mPGES-1 are inducible enzymes responsive to stimuli while COX-1 and mPGES-2 are constitutive enzymes.

The progressive change in receptor sensitivity with treatment is referred to as “priming” of receptor (Criswell et al., 1989). There is a body of extensive evidence suggesting that priming of TLR4 by LPS can influence the magnitude of responses to exogenous agents in the liver, kidney, respiratory tract and lymphoid tissue (Pestka and Zhou, 2006). However, whether the primed TLR4 can influence the magnitude of responses to oxidants from endogenous or exogenous sources is still not fully

understood. In this chapter, we will directly test the hypothesis that canonical ligand-primed TLR4 will sensitize primary pM to oxidant-mediated PGE₂ production. pM were sensitized by incubation with LPS-EK (100 ng/ml for 4 h), which was an empirically determined optimal sensitizing condition in our system.

Role of TLR4 Priming in Mediating Oxidants-induced PGE₂ Production

PPC (5 μ M) or PPN (100 μ M) alone induced a limited increase in PGE₂ production in pM derived from either TLR4-WT or TLR4-KO mice. pM expressing TLR4 exposed to LPS-EK 100 ng/ml for 4 h and then to culture medium (vehicle) for 16 h exhibited moderately enhanced PGE₂ production up to 503.1 ± 86.0 pg/ml compared to unsensitized pM with PGE₂ levels of 126.6 ± 34.2 pg/ml (**Fig. 44**), which is about a 4-fold increase. In contrast, pM expressing TLR4 primed with LPS-EK (100 ng/ml) for 4 h and then treated with PPC or PPN for 16 h showed a robust PGE₂ induction. PGE₂ was increased up to 897.5 ± 120 pg/ml and 1416.3 ± 140 pg/ml by PPC and PPN, respectively. However, the pM that lacked TLR4 expression was not responsive to LPS-EK sensitization. Treatment with oxidants did not affect PGE₂ production after LPS-EK sensitization in pM isolated from TLR4-KO mice. These results demonstrated that TLR4 priming sensitized pM to oxidant-induced PGE₂ production with potential implication in public health.

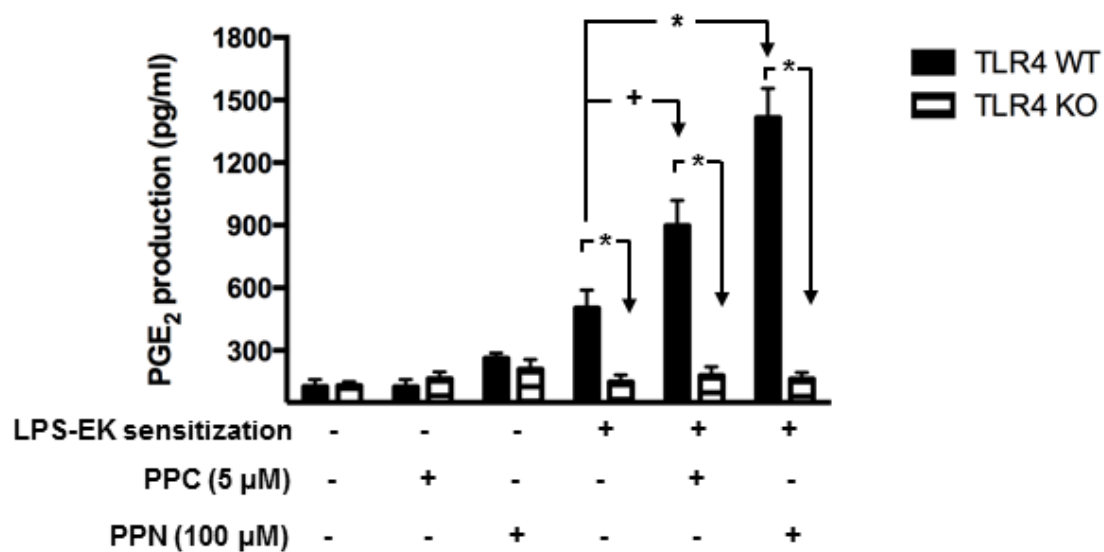


Figure 44. Role of TLR-4 on oxidant-induced prostaglandin E₂ production in sensitized pM. pM derived from TLR4-WT and TLR4-KO mice were sensitized by incubating for 4 h with media containing 100 ng/ml LPS-EK, which was removed and cells rinsed once with fresh medium. The cells were incubated for 16 h with fresh medium or medium containing PPC or PPN. Aliquots of culture media were subjected to PGE₂ analysis by ELISA. * $p \leq 0.01$, + $p \leq 0.05$, $n = 3 - 6$.

Role of TLR4 Priming in Mediating Oxidants-induced Phospholipase A₂ (PLA₂)

Gene Expression

We studied the potential mechanism(s) by which TLR4 priming with its native ligand might sensitize pM to oxidant-induced PGE₂ production. Liberation of AA from membrane glycerophospholipids by PLA₂ is an initial step in PGE₂ production. Expression of PLA₂ is essential for PGE₂ production. It has been reported that the sPLA₂ type II gene is naturally defective in C57BL/6 mice (Kennedy et al., 1995). In addition, cPLA₂ and sPLA₂ type V have been reported to be up-regulated following TLR4 activation in pM (Kuroda and Yamashita, 2003). Therefore, we examined the gene expression of cPLA₂ and sPLA₂ following treatment with oxidants in LPS-EK-sensitized pM.

Consistent with PGE₂ production, as **Fig. 45 A** showed that: (i) PPC or PPN treatment alone had limited effects on the level of cPLA₂ mRNA in pM derived from either TLR4-WT or TLR4-KO mice; (ii) cells sensitized with LPS-EK following medium incubation showed a 2.7-fold increase of cPLA₂ mRNA levels compared with unsensitized pM expressing TLR4; (iii) cells sensitized with LPS-EK followed by 16 h incubation with PPC or PPN did not show further increase in cPLA₂ mRNA levels in comparison with those in sensitized pM following incubation in the medium alone; and (iv) the induction of cPLA₂ was only observed in pM that express TLR4, unlike pM with a complete deletion of TLR4, which showed no demonstrable response to LPS-EK sensitization. Our results thus suggest that oxidants may stimulate PGE₂ production in LPS-EK sensitized pM through upregulation of cPLA₂ gene expression.

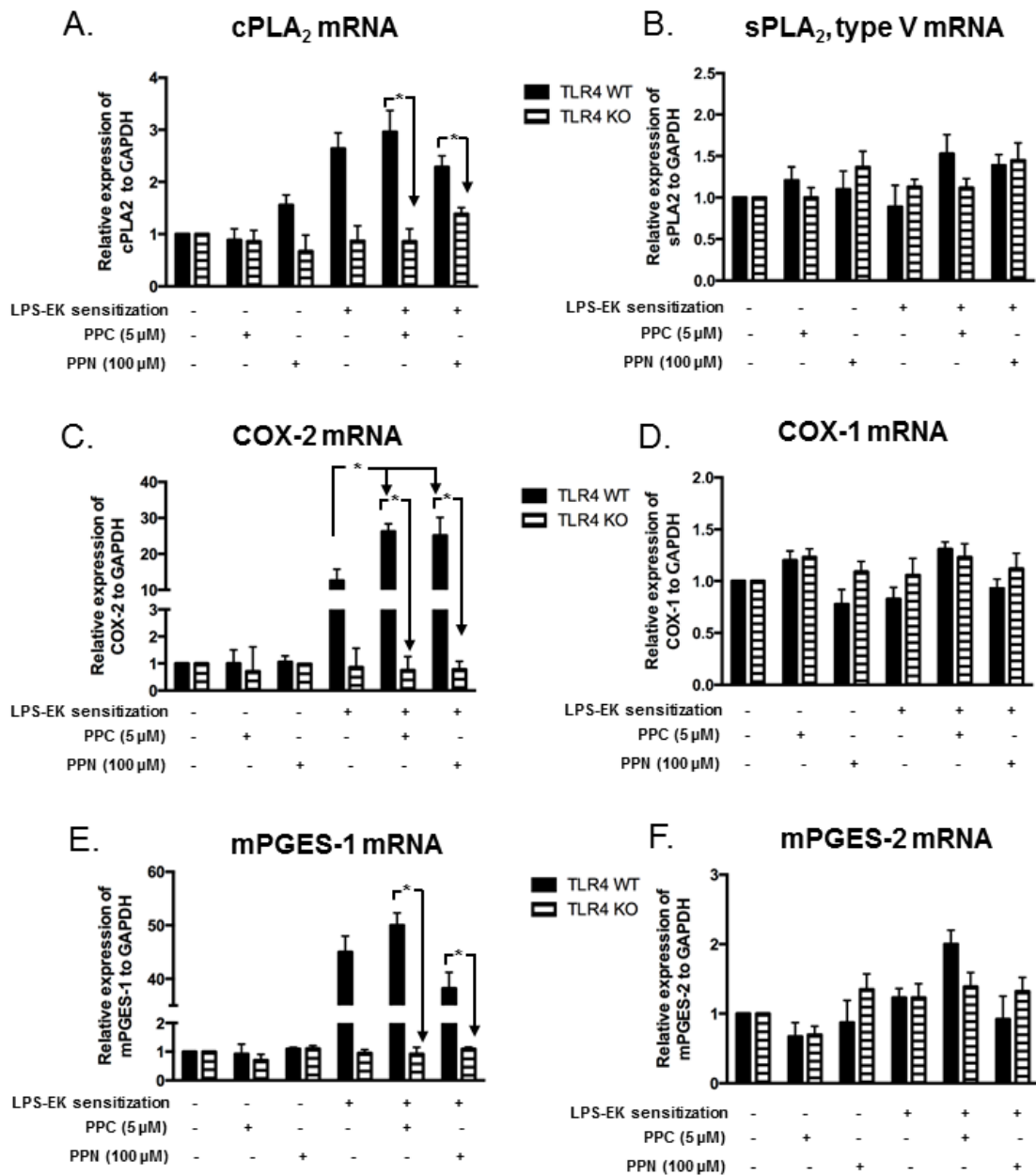


Figure 45. Role of TLR-4 on oxidant-induced gene expression in sensitized pM. pM were sensitized by incubating for 4 h in media containing 100 ng/ml LPS-EK, cells were rinsed once in fresh media, and then incubated for 6 h with fresh medium or media containing PPC or PPN. Cellular mRNA was analyzed by RT-quantitative PCR analyses. * $p \leq 0.01$, + $p \leq 0.05$, $n = 3 - 5$.

Compared with cPLA₂, mRNA of sPLA₂ type V is not inducible following LPS-EK sensitization. As **Fig. 45 B** shows, PPC or PPN treatment alone had limited effects on the level of sPLA₂ type V mRNA in pM derived from either TLR4-WT or TLR4-KO mice. Furthermore, cells sensitized with LPS-EK following incubation in the medium or oxidant (PPC or PPN) treatment showed limited effects on the levels of sPLA₂ type V mRNA in pM derived from either TLR4-WT or TLR4-KO mice.

Role of TLR4 Priming in Mediating Oxidants-induced Cyclooxygenase (COX)

Gene Expression

Fig. 45 C shows that: (i) PPC or PPN treatment alone had limited effects on the level of COX-2 mRNA in pM derived from either TLR4-WT or TLR4-KO mice; (ii) cells sensitized with LPS-EK following medium incubation showed a 13.7-fold increase of COX-2 mRNA levels compared with unsensitized pM expressing TLR4; (iii) cells sensitized with LPS-EK followed by PPC and PPN stimulation for 16 h exhibited a 18.5- and 18.3-fold increases in COX-2 mRNA expression, respectively, which was higher than those in sensitized pM following medium incubation; and (iv) induction of COX-2 was only observed in pM that express TLR4, but not in pM with complete deletion of TLR4 gene. These results suggest that oxidants stimulate PGE₂ production in LPS-EK-sensitized pM through upregulation of COX-2 gene expression.

Compared with COX-2, the mRNA for COX-1 did not respond to LPS-EK sensitization. PPC or PPN treatment alone (**Fig. 45 D**) had no effects on the level of COX-1 mRNA in pM derived from either TLR4-WT or TLR4-KO mice. Furthermore, pM sensitized with LPS-EK followed by incubation with medium alone or medium

with oxidant (PPC or PPN) treatment showed no effects on the levels of COX-1 mRNA in pM derived from either TLR4-WT or TLR4-KO mice.

Role of TLR4 Priming in Mediating Oxidants-induced mPGES Gene Expression

Finally, we also examined the effect of TLR4 priming on mPGES-1 and mPGE-2 gene expression. mPGES-1 has been shown to respond to inflammatory stimuli and is frequently induced concomitantly with COX-2 after stimulation by LPS, TNF- α , and IL-1 β (Samuelsson et al., 2007). In contrast, mPGES-2 is constitutively expressed in a most tissues and equally expressed in both the normal and pathological samples.

As shown in **Fig. 45 E**, (i) PPC or PPN treatment alone had limited effects on the level of mPGES-1 mRNA in pM derived from either TLR4-WT or TLR4-KO mice; (ii) cells sensitized with LPS-EK followed by incubation in the media alone showed a 43.7-fold increase in mPGES-1 mRNA expression levels compared with unsensitized pM from TLR4-WT mice; (iii) cells sensitized with LPS-EK followed by PPC and PPN stimulation for 16 h exhibited an increase in mPGES-1 mRNA expression of 50.5- and 40.1-fold, respectively; (iv) cells sensitized with LPS-EK followed by PPN stimulation for 16 h did not exhibited further increase in mPGES-1 mRNA expression compared with those in LPS-EK-sensitized pM following medium incubation; and (v) induction of mPGES-1 gene expression was only observed in pM expressing TLR4, whereas pM with deletion of TLR4 gene showed no response to LPS-EK sensitization.

Compared with mPGES-1, the mRNA of mPGES-2 was not responsive to LPS-EK sensitization. Treatment with oxidants (PPC or PPN) (**Fig. 45 F**) alone had no discernible effects on the level of mPGES-2 mRNA in pM derived from both TLR4-

WT and TLR4-KO mice. Furthermore, cells treated with LPS-EK followed by incubation in the media alone showed limited effects on the levels of mPGES-2 mRNA in pM derived from either TLR4-WT or TLR4-KO mice. Our results suggest that in addition to mPGES-1, upregulation of mPGES-2 gene expression may also contribute to oxidant-mediated PGE₂ production in LPS-sensitized pM.

Role of TLR4 Priming in Mediating Oxidant-induced Protein Expression

We also examined the protein expressions of the key enzymes responsible for PGE₂ production, including cPLA₂, COX-2, COX-1, and mPGES-1.

Consistent with mRNA expression in pM derived from TLR4-WT mice, **Figs. 46 A and B** show that: (i) PPC or PPN treatment alone had limited effects on the levels of cPLA₂ protein in pM; (ii) pM sensitized with LPS-EK followed by incubation in fresh medium alone showed a negligible (1.4-fold) increase in cPLA₂ protein expression compared with the unsensitized pM; and (iii) cells sensitized with LPS-EK followed by incubation with PPC or PPN did not exhibit significantly further increase of cPLA₂ protein levels compared with those in sensitized pM following medium incubation. These results suggest that cPLA₂ may not contribute to the oxidant-induced PGE₂ production in LPS-EK sensitized pM although cPLA₂ mRNA in this treatment paradigm was significantly increased.

Figs. 46 A and 46 D show that: (i) incubation with PPC or PPN alone failed to induce COX-2 protein expression in pM derived from TLR4-WT; (ii) pM cells derived from TLR4-WT mice sensitized with LPS-EK followed by medium incubation for 16 h showed a ~24-fold increase in COX-2 protein expression compared with unsensitized pM; (iii) Additionally, pM derived from TLR4-WT sensitized with LPS-EK followed

by PPC and PPN stimulation for 16 h exhibited an increased expression of COX-2 protein of ~66- and ~80-fold, respectively, which was remarkably higher than those in sensitized pM from TLR4-WT followed by further medium incubation alone in the absence of oxidants. Our results demonstrated that oxidants stimulate PGE₂ production in LPS-EK-sensitized pM from TLR4-WT by a very robust upregulation of COX-2 gene expression.

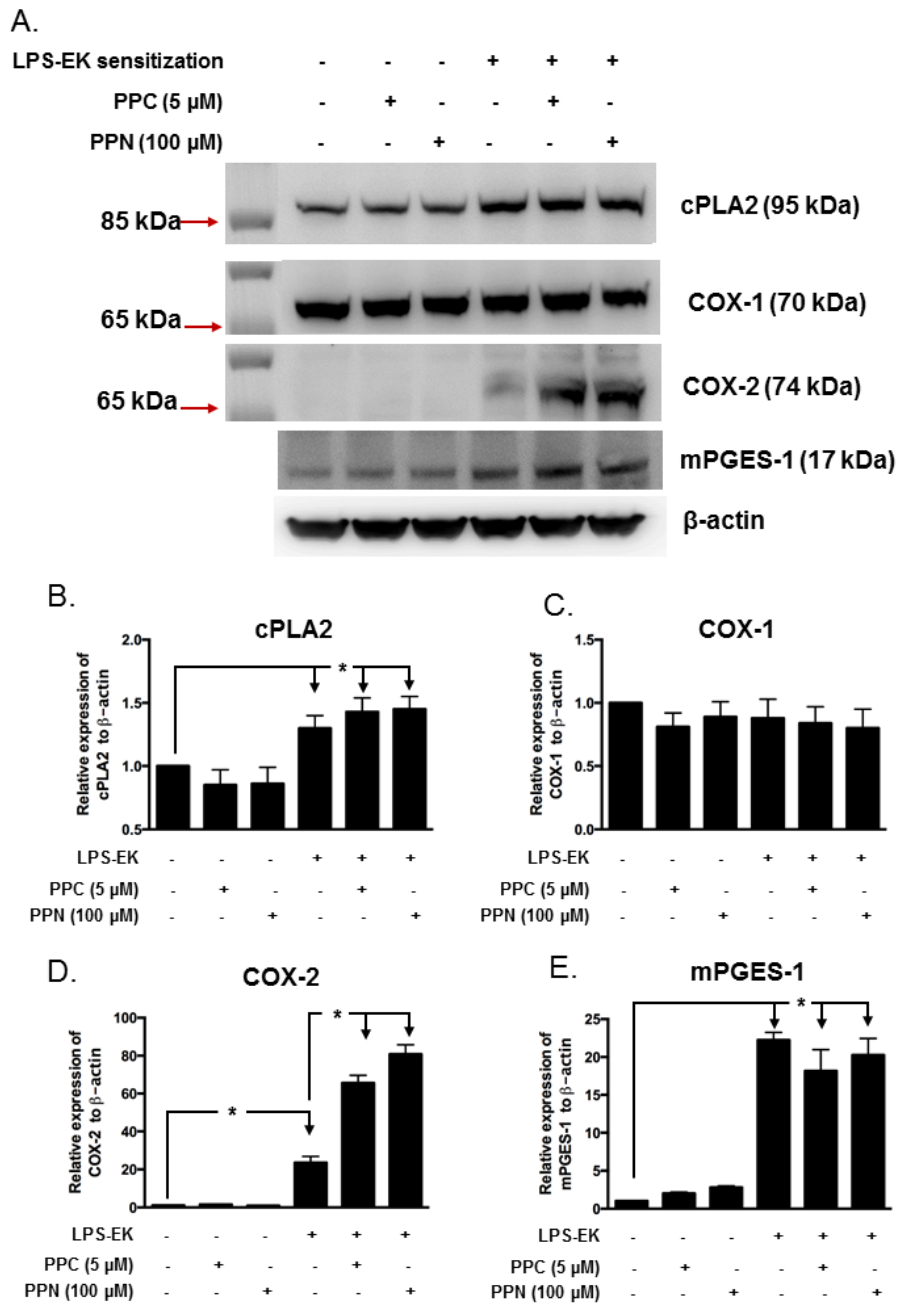


Figure 46. Role of TLR-4 on oxidant-induced protein expression in sensitized pM derived from TLR4-WT. pM derived from **TLR4-WT mice** were sensitized for 4 h with 100 ng/ml LPS-EK. Initial incubation media containing LPS-EK was removed. Cells were thoroughly rinsed once with fresh media and then incubated for 16 h with either fresh medium alone or media containing either PPC or PPN. Total cellular lysates were prepared and subjected to Western blot analysis. (A) Representative immunoblot results are shown. The histograms (B - E) represent the OD ratio of target immunoblot signal from (A) after normalization to the housekeeping protein β -actin. The experimental data are presented as the mean \pm SEM from three independent experiments. * $p \leq 0.05$, ** $p \leq 0.01$, $n = 3$.

Compared with COX-2, the expression of COX-1 did not respond to LPS-EK sensitization. As **Figs. 46 A and 46 C** show, PPC or PPN treatment alone had no effects on the levels of COX-1 protein in pM derived from TLR4-WT mice. Additionally, pM sensitized with LPS-EK followed by medium incubation or oxidant (PPC or PPN) treatment had no effects on the levels of COX-1 protein in pM. These results suggest that COX-1 may not contribute to oxidant-induced PGE₂ production in LPS-EK sensitized pM.

We finally examined the protein expression of mPGES-1. As shown in **Figs. 46 A and E**, (i) PPC or PPN treatment alone failed to induce mPGES-1 protein expression in pM derived from TLR4-WT; (ii) pM sensitized with LPS-EK followed by medium incubation showed a 22.7-fold increase in mPGES-1 protein expression levels compared with unsensitized pM from TLR4-WT mice; and (iii) cells sensitized with LPS-EK followed by PPC and PPN stimulation for 16 h did not exhibit further increase of mPGES-1 protein expression different from LPS-EK stimulation suggesting that mPGES-1 may not be a major contributor to oxidant-induced PGE₂ production through TLR4-stimulation.

Incidentally, pM derived from TLR4-KO mice showed no response to either oxidant treatment alone or LPS-EK sensitization with respect to protein expression of cPLA₂, COX-1, COX-2, or mPGES-1 (**Fig. 47**). Due to the limited number of wells in SDS-PAGE mini gel, we ran samples of TLR4-WT and TLR4-KO in separate gels. However, all the other procedures such as the amount of total protein loaded, running gel, transferring, blocking, primary antibody incubation were done under the same conditions in parallel procedures.

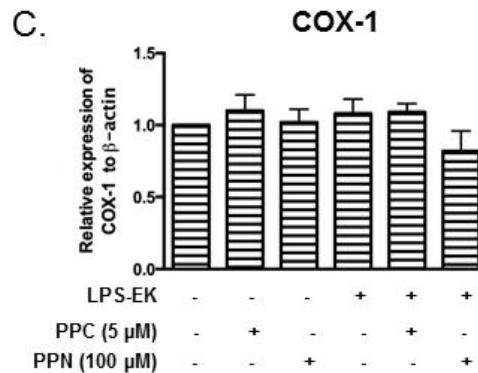
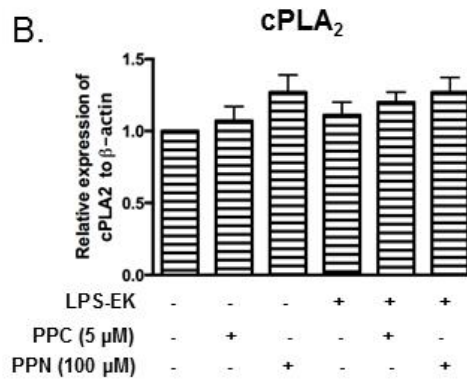
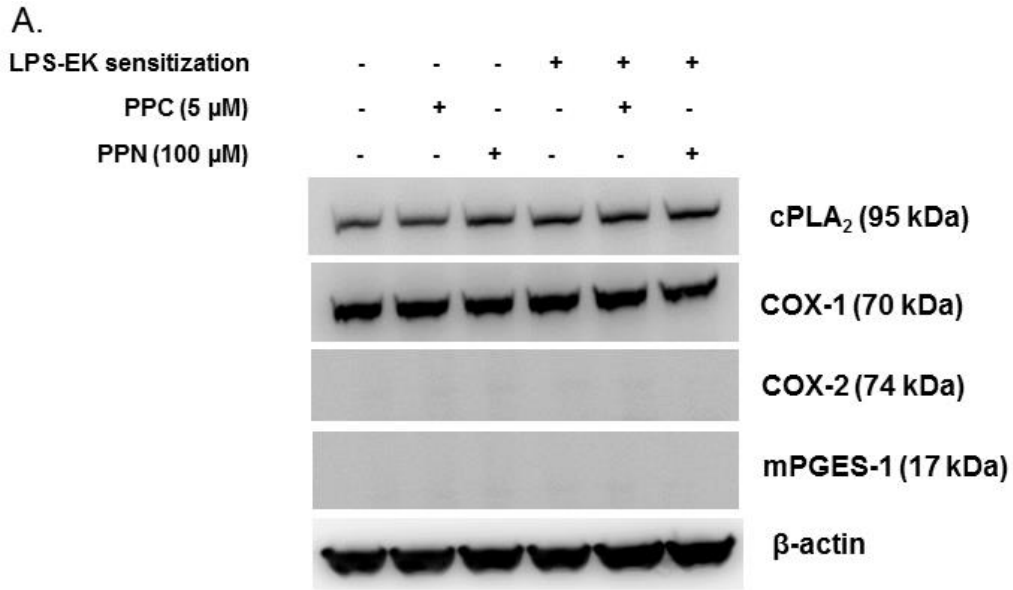


Figure 47. Role of TLR-4 on oxidant-induced prostaglandin E₂ production in sensitized pM derived from TLR4-KO mice. pM derived from **TLR4-KO** mice were sensitized for 4 h with 100 ng/ml LPS-EK, then incubated for 16 h in fresh medium or media containing PPC or PPN. Total cellular lysates were subjected to Westernblot analysis. **(A)** Representative immunoblot results are shown. **(B and C)** The histogram represent the OD ratio of target immunoblot signal from **(A)** after normalization to

Discussion

We examined whether the priming of TLR4 by pre-incubation with its native ligand LPS-EK would influence the magnitude of responses to oxidants in primary macrophages. We have shown that: (i) PPC or PPN treatment alone had limited effects on PGE₂ production and gene expression of enzymes responsible for PGE₂ production which includes PLA₂, COX, and mPGES in pM derived from both TLR4-WT and TLR4-KO mice; (ii) pM sensitized with LPS-EK, followed by rinsing with fresh media and re-incubation in fresh media for 16 h showed a moderate increase in PGE₂ production and gene expression for cPLA₂, COX-2 and mPGES-1 in pM derived from TLR4-WT, but not pM from TLR4-KO mice; (iii) pM sensitized with LPS-EK followed by oxidant stimulation for 16 h exhibited a significantly higher increase in PGE₂ production and expression of COX-2 protein only in pM derived from TLR4-WT mice only.

Activation of innate immune system might potentially predispose a host to toxicant-induced tissue injury. The *in vitro* results we have presented here have demonstrated that oxidants activated the gene expression of COX-2 resulting in enhanced production of PGE₂ in pM derived from TLR4-WT mice sensitized with LPS. Our findings confirmed *in vivo* studies, which revealed that LPS pre-treatment sensitized animal to xenobiotic chemical-induced cytokines production (Ganey and Roth, 2001). Our results indicate that episodic exposure to LPS and other TLR4 agonists might induce a state of enhanced sensitivity to oxidants in a host, ultimately leading to pro-inflammatory responses or heightened proinflammatory phenotype that is primed for disease initiation, propagation and maintenance.

We have shown that macrophages sensitized by pretreatment with LPS-EK exhibited enhanced responsiveness to oxidant with respects to PGE₂ production (**Fig. 44**). Our findings are in accordance with other reports. Oxidant H₂O₂ facilitated the production of COX-2 and PGE₂ only in LPS-stimulated human primary monocytes, whereas H₂O₂ alone did not activate monocytes (Lu and Wahl, 2005). These findings demonstrated that the state of cellular activation may be critical in determining the cellular responses to oxidants and hence disease initiation and propagation.

PGE₂, released from macrophages in response to oxidants, could bind to different prostaglandin receptors (termed EP1-EP4) to regulate the functions of multiple cell types including macrophages, dendritic cells and T and B lymphocytes leading to pro-inflammatory effects. PGE₂ and EP4 in macrophages appeared to play a pro-inflammatory role in the early stages of atherosclerosis by regulating production of inflammatory cytokines including IL-1 β , IL-6 and monocyte chemotactic protein - 1(MCP-1) (Babaev et al., 2008). Simultaneously, PGE₂ is implicated in the regulation of the cytokine expression profile of dendritic cells and has been reported to facilitate T cell differentiation towards a T helper (Th) 1 or Th 2 responses (Ricciotti and FitzGerald, 2011). Additionally, PGE₂ is required for human dendritic cell migration (Groeger et al.), which is pivotal for initiation of cellular immune responses (Legler et al., 2006).

We further examined the potential mechanism(s) by which oxidant induced PGE₂ production in macrophages is sensitized by LPS-EK. PLA₂, COX-2 and mPGES are three key enzymes that mediate PGE₂ production (Chizzolini and Brembilla, 2009). Our results indicate that the expression of cPLA₂, COX-2 and mPGE-1 were

significantly induced following LPS-EK treatment, thereby confirming that the gene for these enzymes are inducible by TLR4 activation. In contrast, the gene expression of sPLA₂, COX-1 and mPGES-2 were not affected in the presence of the TLR4 gene upon LPS-EK treatment. This confirmed that the genes for these PGE₂-producing enzymes are less stable due to inflammatory stimulus alone.

It has been documented that the expression of cPLA₂ is associated with a robust increase in cPLA₂ activity in the cytosolic fraction (Sapirstein et al., 1996). Epithelial cells with higher expression of cPLA₂ instead of sPLA₂ exhibited higher susceptibility to oxidative stress leading to the hypothesis that cPLA₂ is an important endogenous mediator of oxidant-induced cell injury (Sapirstein et al., 1996). Our studies showed that cPLA₂ expression was significantly up-regulated by LPS-EK sensitization, which theoretically would result in increased availability of cytosolic AA released from membrane phospholipids for PGE₂ production. This also means that increased cPLA₂ activity by LPS-EK sensitization might provide more substrates for subsequent enzymes such as COX-2, which is significantly increased by oxidants (**Fig. 45 and Fig. 46**). In the present study, we did not detect further significant increase in cPLA₂ expression by oxidants in sensitized pM. This might be due to increased intracellular Ca²⁺ caused by oxidant-mediated mitochondria dysfunction. This may be necessary, but not sufficient for inducing of cPLA₂ (Robb et al., 1999). Therefore, more experiments are necessary to confirm whether oxidants can affect cPLA₂ enzymatic activity.

Oxidants PPC and PPN markedly up-regulated COX-2 expression at both the mRNA and protein levels in pM sensitized with LPS-EK, but had no effects on COX-

1 gene expression (**Fig. 45 and Fig. 46**). These results demonstrated that the induction of COX-2 in pM may be responsible for oxidative stress-induced PGE₂ production as it only occurred in pM that express TLR4. The dramatic increase in COX-2 expression upon stimulation of inflammatory cells and inflamed tissues, and the assumption that the side effects of COX-1 inhibition provided the rationale for developing a selective COX-2 inhibitor for treating arthritis and other chronic inflammatory diseases (Mardini and FitzGerald, 2001). Indeed, induction of COX enzymes by oxidants appear to be cell- or tissue-dependent or specific. For example, murine placenta, which experience oxidative stress during gestation, exhibited a higher expression of COX-1 and COX-2 (Burdon et al., 2007).

mPGES-1 is a perinuclear protein that is markedly induced by cytokines and growth factors as in the case of COX-2 (Murakami et al., 2000). Moreover, mPGES-1 is functionally coupled to COX-2 in marked preference to COX-1 resulting in PGE₂ production (Murakami et al., 2000). Deletion of mPGES-1 reduced the incidence and severity of arthritis and decreased induction of vascular endothelial growth factor (VEGF) in the granulation of angiogenesis which contributes to tissue remodeling, decreased atherogenesis in fat-fed hyperlipidemia mice (Ricciotti and FitzGerald, 2011). mPGES-1 and oxidative stress are associated in inflammatory disorders. Reduced atherogenesis was concomitant with a reduction in oxidative stress in mice lacking mPGES-1 conditionally in myeloid cells (Chen et al., 2014). Additionally, mPGES-1 deletion suppressed oxidative stress and formation of angiotensin II-induced abdominal aortic aneurysm, which is an inflammatory disorder characterized by localized connective tissue degradation and smooth muscle cell apoptosis (Wang et al., 2008). These studies present mPGES-1 as a potential drug target for treating multiple

inflammatory conditions. In accord with other studies (Wang et al., 2008; Chen et al., 2014), our data show that mPGE-1 is robustly induced upon TLR4-activation. However, studies on the effects of oxidants on both mPGES-1 and mPGES-2 remain limited.

In the present study, however, treatment with oxidants failed to further increase mRNA and protein of mPGES-1 at 6 h and 16 h, respectively, in sensitized pM derived from both TLR4-WT and TLR4-KO mice (**Fig. 45 and Fig. 46**). mPGES-1 protein expression is induced by LPS as early as 6 h and persisted to 48 h in microglia (Ikeda-Matsuo et al., 2005) and syntheses of mRNA and protein are dynamic processes. To further confirm the effects of oxidant on mPGES-1, expression (at the mRNA and protein levels) and enzymatic activities of mPGES-1 would need be examined at different time point in future experiments. Different from mPGES-1, mPGES-2 is constitutively expressed in various cells and tissues. It is functionally coupled to both COX-1 and COX-2 (Funk, 2001). Mice with mPGES-2 deficiency show no specific phenotype and no alteration in PGE₂ levels in several tissues or in LPS-stimulated macrophages (Jania et al., 2009). Our results show that LPS-EK did not stimulate mPGES-2 expression in pM, which is in consistent with these observations.

Among the three inducible enzymes (cPLA₂, COX-2 and mPGES-1), COX-2 is the only enzyme whose expression was further increased by oxidants in pM of TLR4-WT mice. This further confirmed that COX-2 remains a rate-limiting enzyme in PGE₂ production (Chizzolini and Brembilla, 2009) despite of the presence oxidants. Our data suggest that oxidant-mediated upregulation of COX-2 is sufficient to result in PGE₂ production in sensitized pM.

The underlying mechanism (s) by which TLR4 agonists sensitize macrophages to oxidant are still not well understood. It has been proposed that TLR4 activation serve as an initial danger signal, thereby reprogramming the macrophage to a phenotype that is exquisitely sensitive to secondary danger signals generated by subsequent exposure to xenobiotics or oxidants (Pestka and Zhou, 2006). Our *in vitro* findings provide strong evidence for this hypothesis. There is growing evidence for functional plasticity of macrophages and their ability to adapt to changing microenvironments (Stout and Suttles, 2004). Macrophages can be selectively reprogrammed to a specific phenotype of immune response following relatively short-term exposure to microbial ligands (Malyshev and Shnyra, 2003). The reprogramming of macrophages can be achieved by LPS priming through up-regulation of TLR4, prolonged and enhanced MAPK and NF- κ B activation, and chromatin remodeling (Malyshev and Shnyra, 2003).

Our results showed that oxidants stimulated the expression of three inducible genes encoding enzymes in pM sensitized with LPS-EK. COX-2 is induced by TLR4 activation (Lu and Wahl, 2005; Ruiperez et al., 2009). Increased expression of TLR4 and its co-receptor by LPS could partially explain the increased responsiveness. First, LPS would up-regulate the expression of TLR4 and its co-receptors, which would increase the sensitivity of macrophages to exogenous oxidants. It has been reportedly shown for a long time that LPS can directly increase mRNA levels in human monocytes and neutrophils (Bosisio et al., 2002). LPS, combined with anti-CD40 mAb, increased TLR4-MD-2 surface expression (Frleta et al., 2003). Additionally, LPS led to an initial and transient increase in CD14 expression (serves as co-receptor for TLR4 activation) which was associated with distribution of TLR4 in enterocytes (Hornef et al., 2002). Simultaneously, pro-inflammatory cytokines induced by LPS sensitization modulated

TLR4 expression. IL-6 incubation upregulated TLR4 cell surface protein leading to increased responsiveness to TLR4 activation in human monocytes (Tamandl et al., 2003).

Second, COX-2 appears to be induced by the dominant transcriptional factor NF- κ B activation (Jaulmes et al., 2006). It has been proposed that oxidant modulation of NF- κ B activity is largely dependent on the degradation of I κ B α and subsequent NF- κ B activation, a process that requires an activating stimulus, such as LPS. Earlier in this dissertation, we showed that oxidant at lower concentrations had limited effects on NF- κ B transcriptional activation (**Fig. 13 C and 13 D**). Here, LPS priming might lead to prolonged and enhanced NF- κ B activation, which in turn facilitates oxidant-mediated NF- κ B activation. Our findings is in accord with other studies. H₂O₂ increased degradation of I κ B α , the nuclear localization of p50, and the activation of NF- κ B only in LPS-activated human primary monocytes (Lu and Wahl, 2005).

Taken together, TLR4 priming sensitized primary macrophages to oxidant-induced expression of COX-2 and PGE₂ production. Our data provide a potential mechanism(s) by which oxidants may facilitate human disease states (inflammatory processes in the presence of bacterial LPS or any TLR4 primer/activator such as DAMPs or PAMPs). The data further confirm the potential threat posed by the ubiquitous bacterial LPS and exogenous oxidants.

General Conclusions

First, we showed that TLR4 is involved in oxidant-mediated NF- κ B activation and production of higher TNF- α /IL-10 ratios in RAW-Blue cells.

Second, we showed that TLR4 is necessary for oxidant-mediated proinflammatory phenotypes in primary pM.

Furthermore, we showed that priming of TLR4 with its canonical agonist LPS-EK sensitizes pM to oxidant-induced COX-2 expression and PGE₂ production.

Future Studies

In future studies, we will explore:

1. the mechanism by which macrophages increase cellular TAOC in response to oxidant stress;
2. the effects of TLR4 activation following a long term & high concentration treatment with oxidant or LPS-EK on RvD1 production;
3. the effects of TLR4 activation by oxidant on the production of other resolvins such as resolvin E1;
4. the molecular specificity of TLR4 in combination with RONS and HMGB1;
5. whether RONS can change TLR4 primary structure by X-ray crystallography.

APPENDIX

Solutions

Cell Culture

1) Complete Growth Medium (CGM) for RAW-Blue Cells

Mix 89 ml Dulbeccos' Modified Eagle Medium (DMEM) containing 4.5 g/l glucose (purchased from Corning) with 10 ml FBS Fetal Bovine Serum (FBS, purchased from ATLANTA Biologicals) and 1ml 100 X penicillin and streptomycin mixture (10, 000 U/ml penicillin and 10 mg/ml streptomycin, purchased from Corning) to make 100 ml CGM, stored at 4 °C.

2) Test Medium (TM) for RAW-Blue Cells:

Mix 89 ml DMEM containing 4.5 g/l glucose with 10 ml heat inactivated (HI) FBS (FBS, purchased from ATLANTA Biologicals) and 1ml 100 X penicillin and streptomycin mixture to make 100 ml TM, store at 4 °C.

3) CGM for Primary Peritoneal Macrophages (pM)

Mix 89 ml mixture of DMEM and nutrient mixture F-12 (Ham) (DMEM/F-12, purchased from Thermo Scientific) with 10 ml FBS and 1ml 100 X penicillin and streptomycin mixture to make 100 ml TM, store at 4 °C.

3% Thioglycollate (TGC) Preparation

Suspend 1.5 g of thioglycollate medium brewer powder (BD Biosciences, San Jose, CA) in 500 ml of ultrapure water. Heat water to boil to completely dissolve the TGC. Autoclave and store in dark place for two months before use for injection in mice.

Tail Lysis buffer Preparation

To make 5 ml tail lysis buffer, mix 3.98 ml deionized H₂O (d H₂O) with 480 µl of 1 M Tris pH 8.0, 192 µl of 6 M NaCl, 63.2 µl of 10% SDS and 48 µl of 10% 0.5 M DETA.

1) 1 M Tri pH 8.0

Dissolve 12.11 g Tris base (Fisher Scientific) with 80 ml dH₂O then adjust pH value to 8.0 with HCl. Adjust the volume to 100 ml with dH₂O.

2) 6 M NaCl

Dissolve 175.38 g NaCl in 500 ml dH₂O.

3) 10% SDS

Dissolve 10 g SDS in 80 ml dH₂O and adjust the volume to 100 ml with dH₂O.

4) 0.5 M EDTA

Suspend 186.1 g of disodium EDAT (Na₂EDTA) in 800 ml of dH₂O.

Adjust the pH to 8.0 with NaOH to dissolve. Make up the volume to 1 L with dH₂O.

Tris-EDTA buffer Preparation

To make 50 ml Tris-EDTA (TE) buffer, mix 4.9 ml dH₂O with 500 µl of 1M Tris pH 8.5 and 100 µl of 0.5 M EDTA pH 8.0.

1) 1.0 M Tris pH 8.5

Dissolve 12.11 g Tris base (Fisher Scientific) with 80 ml H₂O then adjust pH to 8.5 with HCl. Make up to 100 ml with dH₂O.

- 2) 0.5 M EDTA pH 8.0

See preparation in above tail lysis buffer.

Immunocytochemistry (ICC) Solutions

- 1) 1 X Phosphate-buffered Saline (PBS)

Dissolve one phosphate buffered saline PBS tablets with 200 ml ultrapure water to make 1 X PBS.

- 2) 1 X Phosphate-buffered saline with 0.1% Tween 20 (PBST)

Add 1 ml Tween 20 to 1 liter of 1 X PBS.

- 3) 1 % BSA in PBST

Dissolve 1 g BSA in 100 ml 1 X PBST.

Flow cytometry Solutions

- 1) 10% FBS with 1% sodium azide in PBS

Dilute 10ml FBS with 90 ml PBS to make 100 ml of 10% FBS/PBS.

Dissolve 1 g sodium azide with 100 ml 10 FBS/PBS.

- 2) 3 % BSA in PBS

Dissolve 3 g BSA in 100 ml 1 X PBS.

- 3) 3% BSA with 1% sodium azide

Dissolve 1 g BSA in 100 ml 3 % BSA/PBS.

RNA Extraction Solution

- 1) 70% Ethanol in diethylpyrocarbonate (DEPC)-treated H₂O

Dilute 700 ml 100 % ethanol (200 proof, Fisher Scientific) by addition of 300 ml DEPC-treated H₂O (Fisher Scientific) to make 1 L of 70 % ethanol in DEPC-treated H₂O.

Immunoblotting Solutions

1) Protein Loading Buffer: 5 X sample loading buffer

5 X sample loading buffer contains 0.25 M Tris-HCl (pH 6.8), 15% SDS, 50% glycerol, 25% β -mercaptoethanol and 0.01% bromophenol blue.

2) Running Buffer

20 X NuPAGE MOPS SDS running buffer (Catalog No. NP0001) was purchased from Thermo Fisher Scientific. 50 ml 20 X stock running buffer was mixed with 950 ml ultrapure water to make 1 L 1 X working solution.

3) Transfer Buffer

10 X transfer buffer was made by dissolving 30.3 g Tris base and 144 g glycine with 1 L double distilled (dd) H₂O. Dilute 10X transfer buffer with 700 ml dd H₂O and add 200 ml methanol to make 1 L working solution containing 20% of methanol.

4) 1 M Tris-HCl

Dissolve 121.14 g Tris base in 800 ml dd H₂O, and adjust pH to 7.5 with HCl. Adjust solution volume with dd H₂O up to 1 L.

5) 3 M NaCl Solution

Dissolve 175.3 g NaCl with 1 L of dd H₂O.

6) 1 X Tris-Buffered Saline with 0.1% Tween 20 (TBST)

Mix 50 ml 3 M NaCl solution, 20 ml 1 M Tris-HCl, 930 ml pure water and add 1 ml Tween 20 with gentle stirring to make 1 L TBST.

7) 5% Non-fat Milk

Dissolve 5 g non-fat dry milk powder with 100 ml 1 X TBST.

8) 5% Bovine Serum Albumin (BSA)

Dissolve 5 g BSA with 100 ml 1 X TBST.

Primers

TLR4	Forward 5'- 3'	AACCAGCTGTATTCCCTCAGCACT	175 bp
	Reverse 5'- 3'	ACTGCTTCTGTTCCCTTGACCCACT	
GAPDH	Forward 5'- 3'	TGTGATGGGTGTGAACCACGAGAA	154 bp
	Reverse 5'- 3'	GAGCCCTTCCACAATGCCAAAGTT	
β -actin	Forward 5'- 3'	GTTGGAGCAAACATCCCCCA	187 bp
	Reverse 5'- 3'	ACGCGACCATCCTCCTCTTA	
COX-1	Forward 5'- 3'	AAGATGGGTCCTGGCTTTAC	88 bp
	Reverse 5'- 3'	GGTGATACTGTCGTTCCAGATT	
COX-2	Forward 5'- 3'	CGGACTGGATTCTATGGTGAAA	111 bp
	Reverse 5'- 3'	CTTGAAGTGGGTCAGGATGTAG	
sPLA ₂ type V	Forward 5'- 3'	CAGGGGGCTTGCTAGAACTCAA	326 bp
	Reverse 5'- 3'	AAGAGGGTTGTAAGTCCAGAGG	
cPLA ₂	Forward 5'- 3'	GCCGAGGAAGAGGAAAGGATAG	63 bp
	Reverse 5'- 3'	TTCGCCCACTTCTCTGCAA	
mPGES-1	Forward 5'- 3'	ATGAGGCTGCGGAAGAAGG	149 bp
	Reverse 5'- 3'	GCCGAGGAAGAGGAAAGGATAG	
mPGES-2	Forward 5'- 3'	GCTGGGGCTGTACCACA	193 bp
	Reverse 5'- 3'	GATTCACCTCCACCACCTGA	
TNF- α	Forward 5'- 3'	TTGTCTACTCCAGGTTCTCT	107 bp
	Reverse 5'- 3'	GAGGTTGACTTTCTCCTGGTATG	
IL-10	Forward 5'- 3'	TTGAATTCCTGGGTGAGAAG	96 bp
	Reverse 5'- 3'	TCCACTGCCTTGCTCTTATTT	

tlr4 Wide type (genotyping)	Forward 5'- 3'	ATATGCATGATCAACACCACAG	390 bp
	Reverse 5'- 3'	TTCCATTGCTGCCCTATAG	
tlr4 mutant (genotyping)	Forward 5'- 3'	GCAAGTTTCTATATGCATTCTC	140 bp
	Reverse 5'- 3'	CCTCCATTTCCAATAGGTAG	

Antibodies

Name	Catalog No.	Company	Dilution
TLR4	NB100-56580	Novus Biologicals, Littleton, CO	1:1000 diluted in 5% non-fat milk in TBST
Anti-Nitrotyrosine	STA-004	Cell Biolabs inc, San Diego, CA	1:1000 diluted in 5% non-fat milk in TBST
HRP-conjugated ACTB	HRP-60008	Proteintech Group, Chicago, IL	1: 5000 diluted in 5% non-fat milk in TBST
NF- κ B p65 (D14E12) XP® Rabbit mAb	8242P	Cell Signaling Technology, Danvers, MA	1:1000 diluted in 5% non-fat milk in TBST
I κ B α (C-terminus)	IP 1861	ECM Biociences, Versailles, KY	1:1000 diluted in 5% non-fat milk in TBST
I κ B α (Tyr-42)	IP1031	ECM Biociences, Versailles, KY	1:1000 diluted in 5% BSA in TBST
Cox2 (D5H5) XP® Rabbit mAb	12282S	Cell Signaling Technology, Danvers, MA	1:1000 diluted in 5% non-fat milk in TBST
Cox1 (D2G6) Rabbit mAb	9896	Cell Signaling Technology, Danvers, MA	1:1000 diluted in 5% non-fat milk in TBST
5-Lipoxygenase (C49G1) Rabbit mAb	3289	Cell Signaling Technology, Danvers, MA	1:1000 diluted in 5% BSA in TBST
iNOS Antibody (Mouse Specific)	2982	Cell Signaling Technology, Danvers, MA	1:1000 diluted in 5% non-fat milk in TBST
12 Lipoxygenase antibody	Ab87353	Abcam, Cambridge, MA	1:200 diluted in 5% non-fat milk in TBST
CD11b	Ab8878	Abcam, Cambridge, MA	5 μ g/ml in 3% BSA in PBST
Isotype control Rat IgG2b	Ab18541	Abcam, Cambridge, MA	5 μ g/ml in 3% BSA in PBST
FPR2 (M-73)	Sc-66901	Santa Cruz Biotechnology, Santa Cruz, CA	1:1000 diluted in 5% non-fat milk in TBST
Lamin B (C-20)	Sc-6216	Santa Cruz Biotechnology, Santa Cruz, CA	1:1000 diluted in 5% non-fat milk in TBST

Goat Anti-Rabbit IgG, HRP-conjugated	12-348	Millipore, Billerica, Mass	1:20, 000 diluted in TBST
Goat Anti-Rabbit IgG, HRP-conjugated	12-349	Millipore, Billerica, Mass	1:20, 000 diluted in TBST

Commercial Kits

Name	Manufacture	Catalogue No.
LDH Cytotoxicity Assay Kit	ThermoFisher Scientific	88953
High-Capacity cDNA Reverse Transcription Kit	ThermoFisher Scientific	4368814
BCA Protein Assay Kit	ThermoFisher Scientific	23225
SuperSignal West Femto Chemiluminescent Substrate Kit	ThermoFisher Scientific	PI34095
TBARS Assay Kit	R&D System	KGE013
Oxiselect™ HNE Adduct Competitive ELISA Kit	Cell Biolabs	STA-838
TransAM® NF-κB p65 Kit	Active Motif	40096
Nuclear extract kit	Active Motif	40410
LEGEND MAX Mouse TNF-α ELISA Kit	BioLegend	430907
LEGEND MAX Mouse IL-10 ELISA Kit	BioLegend	431417
Antioxidant Assay Kit	Cayman Chemical	709001
PGE ₂ enzyme-linked immunoassay (Safaeian et al.) Kit	Cayman Chemical	514010
PGE ₂ enzyme-linked immunoassay (Safaeian et al.) Kit	Cayman Chemical	500380

REFERENCE LIST

- Aguilera-Aguirre L, Bacsi A, Radak Z, Hazra TK, Mitra S, Sur S, Brasier AR, Ba X, Boldogh I (2014) Innate inflammation induced by the 8-oxoguanine DNA glycosylase-1-KRAS-NF-kappaB pathway. *J Immunol* 193:4643-4653.
- Akashi S, Saitoh S, Wakabayashi Y, Kikuchi T, Takamura N, Nagai Y, Kusumoto Y, Fukase K, Kusumoto S, Adachi Y, Kosugi A, Miyake K (2003) Lipopolysaccharide interaction with cell surface Toll-like receptor 4-MD-2: higher affinity than that with MD-2 or CD14. *J Exp Med* 198:1035-1042.
- Akira S, Takeda K (2004) Toll-like receptor signalling. *Nat Rev Immunol* 4:499-511.
- Anderson KV, Jurgens G, Nusslein-Volhard C (1985) Establishment of dorsal-ventral polarity in the *Drosophila* embryo: genetic studies on the role of the Toll gene product. *Cell* 42:779-789.
- Aycicek A, Erel O, Kocyigit A (2005) Decreased total antioxidant capacity and increased oxidative stress in passive smoker infants and their mothers. *Pediatr Int* 47:635-639.
- Babaev VR, Chew JD, Ding L, Davis S, Breyer MD, Breyer RM, Oates JA, Fazio S, Linton MF (2008) Macrophage EP4 deficiency increases apoptosis and suppresses early atherosclerosis. *Cell Metab* 8:492-501.
- Baird MB, Massie HR, Piekielniak MJ (1977) Formation of lipid peroxides in isolated rat liver microsomes by singlet molecular oxygen. *Chem Biol Interact* 16:145-153.
- Balaban RS, Nemoto S, Finkel T (2005) Mitochondria, oxidants, and aging. *Cell* 120:483-495.

- Bar-Shai M, Reznick AZ (2006) Reactive nitrogen species induce nuclear factor-kappaB-mediated protein degradation in skeletal muscle cells. *Free Radic Biol Med* 40:2112-2125.
- Becker S, Madden MC, Newman SL, Devlin RB, Koren HS (1991) Modulation of human alveolar macrophage properties by ozone exposure in vitro. *Toxicol Appl Pharmacol* 110:403-415.
- Beckman JS, Ischiropoulos H, Zhu L, van der Woerd M, Smith C, Chen J, Harrison J, Martin JC, Tsai M (1992) Kinetics of superoxide dismutase- and iron-catalyzed nitration of phenolics by peroxynitrite. *Arch Biochem Biophys* 298:438-445.
- Ben-Neriah Y, Karin M (2011) Inflammation meets cancer, with NF-kappaB as the matchmaker. *Nat Immunol* 12:715-723.
- Berghaus LJ, Moore JN, Hurley DJ, Vandenplas ML, Fortes BP, Wolfert MA, Boons GJ (2010) Innate immune responses of primary murine macrophage-lineage cells and RAW 264.7 cells to ligands of Toll-like receptors 2, 3, and 4. *Comp Immunol Microbiol Infect Dis* 33:443-454.
- Beutler B, Tkacenko V, Milsark I, Krochin N, Cerami A (1986) Effect of gamma interferon on cachectin expression by mononuclear phagocytes. Reversal of the lpsd (endotoxin resistance) phenotype. *J Exp Med* 164:1791-1796.
- Biswas SK (2016) Does the Interdependence between Oxidative Stress and Inflammation Explain the Antioxidant Paradox? *Oxid Med Cell Longev* 2016:5698931.
- Black RA, Rauch CT, Kozlosky CJ, Peschon JJ, Slack JL, Wolfson MF, Castner BJ, Stocking KL, Reddy P, Srinivasan S, Nelson N, Boiani N, Schooley KA, Gerhart M, Davis R, Fitzner JN, Johnson RS, Paxton RJ, March CJ, Cerretti DP

- (1997) A metalloproteinase disintegrin that releases tumour-necrosis factor- α from cells. *Nature* 385:729-733.
- Bonnans C, Fukunaga K, Levy MA, Levy BD (2006) Lipoxin A(4) regulates bronchial epithelial cell responses to acid injury. *Am J Pathol* 168:1064-1072.
- Bosisio D, Polentarutti N, Sironi M, Bernasconi S, Miyake K, Webb GR, Martin MU, Mantovani A, Muzio M (2002) Stimulation of toll-like receptor 4 expression in human mononuclear phagocytes by interferon- γ : a molecular basis for priming and synergism with bacterial lipopolysaccharide. *Blood* 99:3427-3431.
- Brennan P, O'Neill LA (1995) Effects of oxidants and antioxidants on nuclear factor kappa B activation in three different cell lines: evidence against a universal hypothesis involving oxygen radicals. *Biochimica et biophysica acta* 1260:167-175.
- Brock TG (2005) Regulating leukotriene synthesis: the role of nuclear 5-lipoxygenase. *J Cell Biochem* 96:1203-1211.
- Bryk R, Griffin P, Nathan C (2000) Peroxynitrite reductase activity of bacterial peroxiredoxins. *Nature* 407:211-215.
- Bulua AC, Simon A, Maddipati R, Pelletier M, Park H, Kim KY, Sack MN, Kastner DL, Siegel RM (2011) Mitochondrial reactive oxygen species promote production of proinflammatory cytokines and are elevated in TNFR1-associated periodic syndrome (TRAPS). *J Exp Med* 208:519-533.
- Buonocore G, Perrone S, Tataranno ML (2010) Oxygen toxicity: chemistry and biology of reactive oxygen species. *Semin Fetal Neonatal Med* 15:186-190.

- Burdon C, Mann C, Cindrova-Davies T, Ferguson-Smith AC, Burton GJ (2007) Oxidative stress and the induction of cyclooxygenase enzymes and apoptosis in the murine placenta. *Placenta* 28:724-733.
- Cao SS, Kaufman RJ (2014) Endoplasmic reticulum stress and oxidative stress in cell fate decision and human disease. *Antioxid Redox Signal* 21:396-413.
- Chen L, Yang G, Monslow J, Todd L, Cormode DP, Tang J, Grant GR, DeLong JH, Tang SY, Lawson JA, Pure E, Fitzgerald GA (2014) Myeloid cell microsomal prostaglandin E synthase-1 fosters atherogenesis in mice. *Proc Natl Acad Sci U S A* 111:6828-6833.
- Cheng A, Caffrey M (1996) Free radical mediated x-ray damage of model membranes. *Biophys J* 70:2212-2222.
- Cheng Y, Zhu Y, Huang X, Zhang W, Han Z, Liu S (2015) Association between TLR2 and TLR4 Gene Polymorphisms and the Susceptibility to Inflammatory Bowel Disease: A Meta-Analysis. *PLoS One* 10:e0126803.
- Chiang N, Serhan CN, Dahlen SE, Drazen JM, Hay DW, Rovati GE, Shimizu T, Yokomizo T, Brink C (2006) The lipoxin receptor ALX: potent ligand-specific and stereoselective actions in vivo. *Pharmacol Rev* 58:463-487.
- Chizzolini C, Brembilla NC (2009) Prostaglandin E2: igniting the fire. *Immunol Cell Biol* 87:510-511.
- Criswell H, Mueller RA, Breese GR (1989) Priming of D1-dopamine receptor responses: long-lasting behavioral supersensitivity to a D1-dopamine agonist following repeated administration to neonatal 6-OHDA-lesioned rats. *J Neurosci* 9:125-133.

- Cyrus T, Pratico D, Zhao L, Witztum JL, Rader DJ, Rokach J, FitzGerald GA, Funk CD (2001) Absence of 12/15-lipoxygenase expression decreases lipid peroxidation and atherogenesis in apolipoprotein e-deficient mice. *Circulation* 103:2277-2282.
- Daringer NM, Schwarz KA, Leonard JN (2015) Contributions of unique intracellular domains to switchlike biosensing by Toll-like receptor 4. *J Biol Chem* 290:8764-8777.
- Deng S, Yu K, Wu Q, Li Y, Zhang X, Zhang B, Liu G, Liu Y, Lian Z (2016) Toll-Like Receptor 4 Reduces Oxidative Injury via Glutathione Activity in Sheep. *Oxid Med Cell Longev* 2016:9151290.
- Dickinson BC, Chang CJ (2011) Chemistry and biology of reactive oxygen species in signaling or stress responses. *Nat Chem Biol* 7:504-511.
- Douni E, Kollias G (1998) A critical role of the p75 tumor necrosis factor receptor (p75TNF-R) in organ inflammation independent of TNF, lymphotoxin alpha, or the p55TNF-R. *J Exp Med* 188:1343-1352.
- Downes CE, Crack PJ (2010) Neural injury following stroke: are Toll-like receptors the link between the immune system and the CNS? *Br J Pharmacol* 160:1872-1888.
- Duffield JS, Hong S, Vaidya VS, Lu Y, Fredman G, Serhan CN, Bonventre JV (2006) Resolvin D series and protectin D1 mitigate acute kidney injury. *J Immunol* 177:5902-5911.
- Dziarski R, Gupta D (2000) Role of MD-2 in TLR2- and TLR4-mediated recognition of Gram-negative and Gram-positive bacteria and activation of chemokine genes. *J Endotoxin Res* 6:401-405.

- Edwards JC, Quinn PJ (1982) Decomposing potassium peroxychromate produces hydroxyl radical (.OH) that can peroxidize the unsaturated fatty acids of phospholipid dispersions. *J Lipid Res* 23:994-1000.
- Filep JG, Beauchamp M, Baron C, Paquette Y (1998) Peroxynitrite mediates IL-8 gene expression and production in lipopolysaccharide-stimulated human whole blood. *J Immunol* 161:5656-5662.
- Finkel T, Holbrook NJ (2000) Oxidants, oxidative stress and the biology of ageing. *Nature* 408:239-247.
- Frantseva MV, Kokarovtseva L, Naus CG, Carlen PL, MacFabe D, Perez Velazquez JL (2002) Specific gap junctions enhance the neuronal vulnerability to brain traumatic injury. *J Neurosci* 22:644-653.
- Fredman G, Ozcan L, Spolitu S, Hellmann J, Spite M, Backs J, Tabas I (2014) Resolvin D1 limits 5-lipoxygenase nuclear localization and leukotriene B4 synthesis by inhibiting a calcium-activated kinase pathway. *Proc Natl Acad Sci U S A* 111:14530-14535.
- Frleta D, Noelle RJ, Wade WF (2003) CD40-mediated up-regulation of Toll-like receptor 4-MD2 complex on the surface of murine dendritic cells. *J Leukoc Biol* 74:1064-1073.
- Fubini B, Hubbard A (2003) Reactive oxygen species (ROS) and reactive nitrogen species (RNS) generation by silica in inflammation and fibrosis. *Free Radic Biol Med* 34:1507-1516.
- Fujiwara N, Kobayashi K (2005) Macrophages in inflammation. *Curr Drug Targets Inflamm Allergy* 4:281-286.

- Fullerton JN, Gilroy DW (2016) Resolution of inflammation: a new therapeutic frontier. *Nat Rev Drug Discov* 15:551-567.
- Funk CD (2001) Prostaglandins and leukotrienes: advances in eicosanoid biology. *Science* 294:1871-1875.
- Galinanes M, Matata BM (2002) Protein nitration is predominantly mediated by a peroxynitrite-dependent pathway in cultured human leucocytes. *Biochem J* 367:467-473.
- Ganey PE, Roth RA (2001) Concurrent inflammation as a determinant of susceptibility to toxicity from xenobiotic agents. *Toxicology* 169:195-208.
- Gay NJ, Symmons MF, Gangloff M, Bryant CE (2014) Assembly and localization of Toll-like receptor signalling complexes. *Nat Rev Immunol* 14:546-558.
- Geller DA, Nussler AK, Di Silvio M, Lowenstein CJ, Shapiro RA, Wang SC, Simmons RL, Billiar TR (1993) Cytokines, endotoxin, and glucocorticoids regulate the expression of inducible nitric oxide synthase in hepatocytes. *Proc Natl Acad Sci U S A* 90:522-526.
- Ghosh EE, Cassado AA, Govoni GR, Fukuhara T, Yang Y, Monack DM, Bortoluci KR, Almeida SR, Herzenberg LA, Herzenberg LA (2010) Two physically, functionally, and developmentally distinct peritoneal macrophage subsets. *Proc Natl Acad Sci U S A* 107:2568-2573.
- Gill R, Tsung A, Billiar T (2010) Linking oxidative stress to inflammation: Toll-like receptors. *Free Radic Biol Med* 48:1121-1132.
- Gioannini TL, Teghanemt A, Zhang D, Coussens NP, Dockstader W, Ramaswamy S, Weiss JP (2004) Isolation of an endotoxin-MD-2 complex that produces Toll-

- like receptor 4-dependent cell activation at picomolar concentrations. *Proc Natl Acad Sci U S A* 101:4186-4191.
- Groeger AL, Cipollina C, Cole MP, Woodcock SR, Bonacci G, Rudolph TK, Rudolph V, Freeman BA, Schopfer FJ (2010) Cyclooxygenase-2 generates anti-inflammatory mediators from omega-3 fatty acids. *Nat Chem Biol* 6:433-441.
- Han D, Antunes F, Canali R, Rettori D, Cadenas E (2003) Voltage-dependent anion channels control the release of the superoxide anion from mitochondria to cytosol. *J Biol Chem* 278:5557-5563.
- Hardell L, Sage C (2008) Biological effects from electromagnetic field exposure and public exposure standards. *Biomed Pharmacother* 62:104-109.
- Heil M, Land WG (2014) Danger signals - damaged-self recognition across the tree of life. *Front Plant Sci* 5:578.
- Hennessy EJ, Parker AE, O'Neill LA (2010) Targeting Toll-like receptors: emerging therapeutics? *Nat Rev Drug Discov* 9:293-307.
- Hiscott J, Marois J, Garoufalos J, D'Addario M, Roulston A, Kwan I, Pepin N, Lacoste J, Nguyen H, Bensi G, et al. (1993) Characterization of a functional NF-kappa B site in the human interleukin 1 beta promoter: evidence for a positive autoregulatory loop. *Mol Cell Biol* 13:6231-6240.
- Hodgson EK, Fridovich I (1974) The production of superoxide radical during the decomposition of potassium peroxochromate(V). *Biochemistry* 13:3811-3815.
- Hogg N, Darley-Usmar VM, Wilson MT, Moncada S (1992) Production of hydroxyl radicals from the simultaneous generation of superoxide and nitric oxide. *Biochem J* 281 (Pt 2):419-424.

- Holmgren A, Lu J (2010) Thioredoxin and thioredoxin reductase: current research with special reference to human disease. *Biochem Biophys Res Commun* 396:120-124.
- Holmstrom KM, Finkel T (2014) Cellular mechanisms and physiological consequences of redox-dependent signalling. *Nat Rev Mol Cell Biol* 15:411-421.
- Hong S, Gronert K, Devchand PR, Moussignac RL, Serhan CN (2003) Novel docosatrienes and 17S-resolvins generated from docosahexaenoic acid in murine brain, human blood, and glial cells. Autacoids in anti-inflammation. *J Biol Chem* 278:14677-14687.
- Hornef MW, Frisan T, Vandewalle A, Normark S, Richter-Dahlfors A (2002) Toll-like receptor 4 resides in the Golgi apparatus and colocalizes with internalized lipopolysaccharide in intestinal epithelial cells. *J Exp Med* 195:559-570.
- Huang MF, Lin WL, Ma YC (2005) A study of reactive oxygen species in mainstream of cigarette. *Indoor Air* 15:135-140.
- Ii M, Matsunaga N, Hazeki K, Nakamura K, Takashima K, Seya T, Hazeki O, Kitazaki T, Iizawa Y (2006) A novel cyclohexene derivative, ethyl (6R)-6-[N-(2-Chloro-4-fluorophenyl)sulfamoyl]cyclohex-1-ene-1-carboxylate (TAK-242), selectively inhibits toll-like receptor 4-mediated cytokine production through suppression of intracellular signaling. *Mol Pharmacol* 69:1288-1295.
- Ikeda-Matsuo Y, Ikegaya Y, Matsuki N, Uematsu S, Akira S, Sasaki Y (2005) Microglia-specific expression of microsomal prostaglandin E2 synthase-1 contributes to lipopolysaccharide-induced prostaglandin E2 production. *J Neurochem* 94:1546-1558.

- Ito K, Hanazawa T, Tomita K, Barnes PJ, Adcock IM (2004) Oxidative stress reduces histone deacetylase 2 activity and enhances IL-8 gene expression: role of tyrosine nitration. *Biochem Biophys Res Commun* 315:240-245.
- Iyer SS, Accardi CJ, Ziegler TR, Blanco RA, Ritzenthaler JD, Rojas M, Roman J, Jones DP (2009) Cysteine redox potential determines pro-inflammatory IL-1beta levels. *PLoS One* 4:e5017.
- Jakab GJ, Spannhake EW, Canning BJ, Kleeberger SR, Gilmour MI (1995) The effects of ozone on immune function. *Environ Health Perspect* 103 Suppl 2:77-89.
- Janeway CA, Jr. (1992) The immune system evolved to discriminate infectious nonself from noninfectious self. *Immunol Today* 13:11-16.
- Jania LA, Chandrasekharan S, Backlund MG, Foley NA, Snouwaert J, Wang IM, Clark P, Audoly LP, Koller BH (2009) Microsomal prostaglandin E synthase-2 is not essential for in vivo prostaglandin E2 biosynthesis. *Prostaglandins Other Lipid Mediat* 88:73-81.
- Jaulmes A, Thierry S, Janvier B, Raymondjean M, Maréchal V (2006) Activation of sPLA2-IIA and PGE2 production by high mobility group protein B1 in vascular smooth muscle cells sensitized by IL-1 β . *The FASEB Journal* 20:1727-1729.
- Jensen PK (1966) Antimycin-insensitive oxidation of succinate and reduced nicotinamide-adenine dinucleotide in electron-transport particles. I. pH dependency and hydrogen peroxide formation. *Biochim Biophys Acta* 122:157-166.
- Ji RR, Xu ZZ, Strichartz G, Serhan CN (2011) Emerging roles of resolvins in the resolution of inflammation and pain. *Trends Neurosci* 34:599-609.

- Josephs MD, Bahjat FR, Fukuzuka K, Ksontini R, Solorzano CC, Edwards CK, 3rd, Tannahill CL, MacKay SL, Copeland EM, 3rd, Moldawer LL (2000) Lipopolysaccharide and D-galactosamine-induced hepatic injury is mediated by TNF-alpha and not by Fas ligand. *Am J Physiol Regul Integr Comp Physiol* 278:R1196-1201.
- Jung K, Seifert M, Herrling T, Fuchs J (2008) UV-generated free radicals (FR) in skin: their prevention by sunscreens and their induction by self-tanning agents. *Spectrochim Acta A Mol Biomol Spectrosc* 69:1423-1428.
- Jurkiewicz BA, Buettner GR (1994) Ultraviolet light-induced free radical formation in skin: an electron paramagnetic resonance study. *Photochem Photobiol* 59:1-4.
- Kangussu LM, Olivon VC, Arifa RD, Araujo N, Reis D, Assis MT, Soriani FM, de Souza Dda G, Bendhack LM, Bonaventura D (2015) Enhancement on reactive oxygen species and COX-1 mRNA levels modulate the vascular relaxation induced by sodium nitroprusside in denuded mice aorta. *Fundam Clin Pharmacol* 29:150-163.
- Karki R, Igwe OJ (2013) Toll-like receptor 4-mediated nuclear factor kappa B activation is essential for sensing exogenous oxidants to propagate and maintain oxidative/nitrosative cellular stress. *PLoS One* 8:e73840.
- Karki R, Zhang Y, Igwe OJ (2014) Activation of c-Src: a hub for exogenous pro-oxidant-mediated activation of Toll-like receptor 4 signaling. *Free Radic Biol Med* 71:256-269.
- Karlenius TC, Tonissen KF (2010) Thioredoxin and Cancer: A Role for Thioredoxin in all States of Tumor Oxygenation. *Cancers (Basel)* 2:209-232.

- Kawai T, Akira S (2007) Signaling to NF-kappaB by Toll-like receptors. *Trends Mol Med* 13:460-469.
- Kawai T, Akira S (2010) The role of pattern-recognition receptors in innate immunity: update on Toll-like receptors. *Nat Immunol* 11:373-384.
- Kennedy BP, Payette P, Mudgett J, Vadas P, Pruzanski W, Kwan M, Tang C, Rancourt DE, Cromlish WA (1995) A natural disruption of the secretory group II phospholipase A2 gene in inbred mouse strains. *J Biol Chem* 270:22378-22385.
- Kerkhof M, Postma DS, Brunekreef B, Reijmerink NE, Wijga AH, de Jongste JC, Gehring U, Koppelman GH (2010) Toll-like receptor 2 and 4 genes influence susceptibility to adverse effects of traffic-related air pollution on childhood asthma. *Thorax* 65:690-697.
- Kim JR, Yoon HW, Kwon KS, Lee SR, Rhee SG (2000) Identification of proteins containing cysteine residues that are sensitive to oxidation by hydrogen peroxide at neutral pH. *Anal Biochem* 283:214-221.
- Kirsch M, Lomonosova EE, Korth HG, Sustmann R, de Groot H (1998) Hydrogen peroxide formation by reaction of peroxynitrite with HEPES and related tertiary amines. Implications for a general mechanism. *J Biol Chem* 273:12716-12724.
- Kode A, Rajendrasozhan S, Caito S, Yang SR, Megson IL, Rahman I (2008) Resveratrol induces glutathione synthesis by activation of Nrf2 and protects against cigarette smoke-mediated oxidative stress in human lung epithelial cells. *Am J Physiol Lung Cell Mol Physiol* 294:L478-488.
- Koh TJ, DiPietro LA (2011) Inflammation and wound healing: the role of the macrophage. *Expert Rev Mol Med* 13:e23.

- Koo JE, Park ZY, Kim ND, Lee JY (2013) Sulforaphane inhibits the engagement of LPS with TLR4/MD2 complex by preferential binding to Cys133 in MD2. *Biochem Biophys Res Commun* 434:600-605.
- Krishnamoorthy S, Recchiuti A, Chiang N, Fredman G, Serhan CN (2012) Resolvin D1 receptor stereoselectivity and regulation of inflammation and proresolving microRNAs. *Am J Pathol* 180:2018-2027.
- Krishnamoorthy S, Recchiuti A, Chiang N, Yacoubian S, Lee CH, Yang R, Petasis NA, Serhan CN (2010) Resolvin D1 binds human phagocytes with evidence for proresolving receptors. *Proc Natl Acad Sci U S A* 107:1660-1665.
- Kroncke KD, Fehsel K, Kolb-Bachofen V (1998) Inducible nitric oxide synthase in human diseases. *Clin Exp Immunol* 113:147-156.
- Kronke G, Katzenbeisser J, Uderhardt S, Zaiss MM, Scholtysek C, Schabbauer G, Zarbock A, Koenders MI, Axmann R, Zwerina J, Baenckler HW, van den Berg W, Voll RE, Kuhn H, Joosten LA, Schett G (2009) 12/15-lipoxygenase counteracts inflammation and tissue damage in arthritis. *J Immunol* 183:3383-3389.
- Kuroda E, Yamashita U (2003) Mechanisms of enhanced macrophage-mediated prostaglandin E2 production and its suppressive role in Th1 activation in Th2-dominant BALB/c mice. *J Immunol* 170:757-764.
- Ladefoged M, Buschard K, Hansen AM (2013) Increased expression of toll-like receptor 4 and inflammatory cytokines, interleukin-6 in particular, in islets from a mouse model of obesity and type 2 diabetes. *APMIS* 121:531-538.
- Lambeth JD (2004) NOX enzymes and the biology of reactive oxygen. *Nat Rev Immunol* 4:181-189.

- Land WG (2015) The Role of Damage-Associated Molecular Patterns in Human Diseases: Part I - Promoting inflammation and immunity. Sultan Qaboos Univ Med J 15:e9-e21.
- Landino LM, Crews BC, Timmons MD, Morrow JD, Marnett LJ (1996) Peroxynitrite, the coupling product of nitric oxide and superoxide, activates prostaglandin biosynthesis. Proc Natl Acad Sci U S A 93:15069-15074.
- Laplante P, Amireault P, Subang R, Dieude M, Levine JS, Rauch J (2011) Interaction of beta2-glycoprotein I with lipopolysaccharide leads to Toll-like receptor 4 (TLR4)-dependent activation of macrophages. J Biol Chem 286:42494-42503.
- Larrick JW, Wright SC (1990) Cytotoxic mechanism of tumor necrosis factor-alpha. FASEB J 4:3215-3223.
- Lawler JM, Kunst M, Hord JM, Lee Y, Joshi K, Botchlett RE, Ramirez A, Martinez DA (2014) EUK-134 ameliorates nNOSmu translocation and skeletal muscle fiber atrophy during short-term mechanical unloading. Am J Physiol Regul Integr Comp Physiol 306:R470-482.
- Lawrence T, Gilroy DW (2007) Chronic inflammation: a failure of resolution? Int J Exp Pathol 88:85-94.
- Lee HN, Surh YJ (2013) Resolvin D1-mediated NOX2 inactivation rescues macrophages undertaking efferocytosis from oxidative stress-induced apoptosis. Biochem Pharmacol 86:759-769.
- Lee SJ, Seo KW, Kim CD (2015) LPS Increases 5-LO Expression on Monocytes via an Activation of Akt-Sp1/NF-kappaB Pathways. Korean J Physiol Pharmacol 19:263-268.

- Legler DF, Krause P, Scandella E, Singer E, Groettrup M (2006) Prostaglandin E2 is generally required for human dendritic cell migration and exerts its effect via EP2 and EP4 receptors. *J Immunol* 176:966-973.
- Leigh NJ, Nelson JW, Mellas RE, Aguirre A, Baker OJ (2014) Expression of resolvin D1 biosynthetic pathways in salivary epithelium. *J Dent Res* 93:300-305.
- Lemaitre B, Nicolas E, Michaut L, Reichhart JM, Hoffmann JA (1996) The dorsoventral regulatory gene cassette *spatzle/Toll/cactus* controls the potent antifungal response in *Drosophila* adults. *Cell* 86:973-983.
- Li N, Karin M (1998) Ionizing radiation and short wavelength UV activate NF-kappaB through two distinct mechanisms. *Proc Natl Acad Sci U S A* 95:13012-13017.
- Li X, Fang P, Mai J, Choi ET, Wang H, Yang XF (2013) Targeting mitochondrial reactive oxygen species as novel therapy for inflammatory diseases and cancers. *J Hematol Oncol* 6:19.
- Liao Z, Dong J, Wu W, Yang T, Wang T, Guo L, Chen L, Xu D, Wen F (2012) Resolvin D1 attenuates inflammation in lipopolysaccharide-induced acute lung injury through a process involving the PPARgamma/NF-kappaB pathway. *Respir Res* 13:110.
- Liu H, Sidiropoulos P, Song G, Pagliari LJ, Birrer MJ, Stein B, Anrather J, Pope RM (2000) TNF-alpha gene expression in macrophages: regulation by NF-kappa B is independent of c-Jun or C/EBP beta. *J Immunol* 164:4277-4285.
- Lu Y, Wahl LM (2005) Oxidative stress augments the production of matrix metalloproteinase-1, cyclooxygenase-2, and prostaglandin E2 through enhancement of NF-kappa B activity in lipopolysaccharide-activated human primary monocytes. *J Immunol* 175:5423-5429.

- Lu YC, Yeh WC, Ohashi PS (2008) LPS/TLR4 signal transduction pathway. *Cytokine* 42:145-151.
- Lucas K, Maes M (2013) Role of the Toll Like Receptor (TLR) Radical Cycle in Chronic Inflammation: Possible Treatments Targeting the TLR4 Pathway. *Mol Neurobiol*.
- Ma S, Yang D, Li D, Tang B, Yang Y (2011) Oleic acid induces smooth muscle foam cell formation and enhances atherosclerotic lesion development via CD36. *Lipids Health Dis* 10:53.
- MacMicking J, Xie QW, Nathan C (1997) Nitric oxide and macrophage function. *Annu Rev Immunol* 15:323-350.
- MacMillan-Crow LA, Crow JP, Kerby JD, Beckman JS, Thompson JA (1996) Nitration and inactivation of manganese superoxide dismutase in chronic rejection of human renal allografts. *Proc Natl Acad Sci U S A* 93:11853-11858.
- Malyshev IY, Shnyra A (2003) Controlled modulation of inflammatory, stress and apoptotic responses in macrophages. *Curr Drug Targets Immune Endocr Metabol Disord* 3:1-22.
- Manke A, Wang L, Rojanasakul Y (2013) Mechanisms of nanoparticle-induced oxidative stress and toxicity. *Biomed Res Int* 2013:942916.
- Mardini IA, FitzGerald GA (2001) Selective inhibitors of cyclooxygenase-2: a growing class of anti-inflammatory drugs. *Mol Interv* 1:30-38.
- Marletta MA, Yoon PS, Iyengar R, Leaf CD, Wishnok JS (1988) Macrophage oxidation of L-arginine to nitrite and nitrate: nitric oxide is an intermediate. *Biochemistry* 27:8706-8711.

- Matsunaga N, Tsuchimori N, Matsumoto T, Ii M (2011) TAK-242 (resatorvid), a small-molecule inhibitor of Toll-like receptor (TLR) 4 signaling, binds selectively to TLR4 and interferes with interactions between TLR4 and its adaptor molecules. *Mol Pharmacol* 79:34-41.
- Matzinger P (1994) Tolerance, danger, and the extended family. *Annu Rev Immunol* 12:991-1045.
- McKinnon KP, Madden MC, Noah TL, Devlin RB (1993) In vitro ozone exposure increases release of arachidonic acid products from a human bronchial epithelial cell line. *Toxicol Appl Pharmacol* 118:215-223.
- Medzhitov R (2010) Inflammation 2010: new adventures of an old flame. *Cell* 140:771-776.
- Merched AJ, Ko K, Gotlinger KH, Serhan CN, Chan L (2008) Atherosclerosis: evidence for impairment of resolution of vascular inflammation governed by specific lipid mediators. *FASEB J* 22:3595-3606.
- Merolla PA, Arthur JV, Alvarez-Icaza R, Cassidy AS, Sawada J, Akopyan F, Jackson BL, Imam N, Guo C, Nakamura Y, Brezzo B, Vo I, Esser SK, Appuswamy R, Taba B, Amir A, Flickner MD, Risk WP, Manohar R, Modha DS (2014) Artificial brains. A million spiking-neuron integrated circuit with a scalable communication network and interface. *Science* 345:668-673.
- Miesel R, Kroger H, Kurpisz M, Weser U (1995) Induction of arthritis in mice and rats by potassium peroxochromate and assessment of disease activity by whole blood chemiluminescence and ^{99m}Tc-pertechnetate-imaging. *Free Radic Res* 23:213-227.

- Miller EW, Dickinson BC, Chang CJ (2010) Aquaporin-3 mediates hydrogen peroxide uptake to regulate downstream intracellular signaling. *Proc Natl Acad Sci U S A* 107:15681-15686.
- Misharin AV, Saber R, Perlman H (2012) Eosinophil contamination of thioglycollate-elicited peritoneal macrophage cultures skews the functional readouts of in vitro assays. *J Leukoc Biol* 92:325-331.
- Molin C, Jauhiainen A, Warringer J, Nerman O, Sunnerhagen P (2009) mRNA stability changes precede changes in steady-state mRNA amounts during hyperosmotic stress. *RNA* 15:600-614.
- Moore KW, de Waal Malefyt R, Coffman RL, O'Garra A (2001) Interleukin-10 and the interleukin-10 receptor. *Annu Rev Immunol* 19:683-765.
- Mosser DM, Edwards JP (2008) Exploring the full spectrum of macrophage activation. *Nat Rev Immunol* 8:958-969.
- Mukhopadhyay A, Manna SK, Aggarwal BB (2000) Pervanadate-induced nuclear factor-kappaB activation requires tyrosine phosphorylation and degradation of IkappaBalpha. Comparison with tumor necrosis factor-alpha. *J Biol Chem* 275:8549-8555.
- Murakami M, Naraba H, Tanioka T, Semmyo N, Nakatani Y, Kojima F, Ikeda T, Fueki M, Ueno A, Oh S, Kudo I (2000) Regulation of prostaglandin E2 biosynthesis by inducible membrane-associated prostaglandin E2 synthase that acts in concert with cyclooxygenase-2. *J Biol Chem* 275:32783-32792.
- Muratori M, Forti G, Baldi E (2008) Comparing flow cytometry and fluorescence microscopy for analyzing human sperm DNA fragmentation by TUNEL labeling. *Cytometry A* 73:785-787.

- Murray PJ, Wynn TA (2011) Protective and pathogenic functions of macrophage subsets. *Nat Rev Immunol* 11:723-737.
- Nakanishi M, Rosenberg DW (2013) Multifaceted roles of PGE2 in inflammation and cancer. *Semin Immunopathol* 35:123-137.
- Nathan C (2003) Specificity of a third kind: reactive oxygen and nitrogen intermediates in cell signaling. *J Clin Invest* 111:769-778.
- Nathan C, Cunningham-Bussel A (2013) Beyond oxidative stress: an immunologist's guide to reactive oxygen species. *Nat Rev Immunol* 13:349-361.
- Nel A, Xia T, Madler L, Li N (2006) Toxic potential of materials at the nanolevel. *Science* 311:622-627.
- Nihiro H, Otsuka T, Tanabe T, Hara S, Kuga S, Nemoto Y, Tanaka Y, Nakashima H, Kitajima S, Abe M, et al. (1995) Inhibition by interleukin-10 of inducible cyclooxygenase expression in lipopolysaccharide-stimulated monocytes: its underlying mechanism in comparison with interleukin-4. *Blood* 85:3736-3745.
- Ospelt C, Gay S (2010) TLRs and chronic inflammation. *Int J Biochem Cell Biol* 42:495-505.
- Palladino MA, Bahjat FR, Theodorakis EA, Moldawer LL (2003) Anti-TNF-alpha therapies: the next generation. *Nat Rev Drug Discov* 2:736-746.
- Panday A, Sahoo MK, Osorio D, Batra S (2015) NADPH oxidases: an overview from structure to innate immunity-associated pathologies. *Cell Mol Immunol* 12:5-23.
- Parameswaran N, Patial S (2010) Tumor necrosis factor-alpha signaling in macrophages. *Crit Rev Eukaryot Gene Expr* 20:87-103.

- Park HS, Jung HY, Park EY, Kim J, Lee WJ, Bae YS (2004a) Cutting edge: direct interaction of TLR4 with NAD(P)H oxidase 4 isozyme is essential for lipopolysaccharide-induced production of reactive oxygen species and activation of NF-kappa B. *J Immunol* 173:3589-3593.
- Park JS, Svetkauskaite D, He Q, Kim JY, Strassheim D, Ishizaka A, Abraham E (2004b) Involvement of toll-like receptors 2 and 4 in cellular activation by high mobility group box 1 protein. *J Biol Chem* 279:7370-7377.
- Patel BP, Rawal UM, Dave TK, Rawal RM, Shukla SN, Shah PM, Patel PS (2007a) Lipid peroxidation, total antioxidant status, and total thiol levels predict overall survival in patients with oral squamous cell carcinoma. *Integr Cancer Ther* 6:365-372.
- Patel JD, Krupka T, Anderson JM (2007b) iNOS-mediated generation of reactive oxygen and nitrogen species by biomaterial-adherent neutrophils. *J Biomed Mater Res A* 80:381-390.
- Paul-Clark MJ, McMaster SK, Sorrentino R, Sriskandan S, Bailey LK, Moreno L, Ryffel B, Quesniaux VF, Mitchell JA (2009) Toll-like receptor 2 is essential for the sensing of oxidants during inflammation. *Am J Respir Crit Care Med* 179:299-306.
- Pestka J, Zhou HR (2006) Toll-like receptor priming sensitizes macrophages to proinflammatory cytokine gene induction by deoxynivalenol and other toxicants. *Toxicol Sci* 92:445-455.
- Plaza Davila M, Martin Munoz P, Tapia JA, Ortega Ferrusola C, Balao da Silva CC, Pena FJ (2015) Inhibition of Mitochondrial Complex I Leads to Decreased Motility and Membrane Integrity Related to Increased Hydrogen Peroxide and

- Reduced ATP Production, while the Inhibition of Glycolysis Has Less Impact on Sperm Motility. *PLoS One* 10:e0138777.
- Plummer SM, Holloway KA, Manson MM, Munks RJ, Kaptein A, Farrow S, Howells L (1999) Inhibition of cyclo-oxygenase 2 expression in colon cells by the chemopreventive agent curcumin involves inhibition of NF-kappaB activation via the NIK/IKK signalling complex. *Oncogene* 18:6013-6020.
- Poltorak A, Smirnova I, Clisch R, Beutler B (2000) Limits of a deletion spanning Tlr4 in C57BL/10ScCr mice. *J Endotoxin Res* 6:51-56.
- Poltorak A, He X, Smirnova I, Liu MY, Van Huffel C, Du X, Birdwell D, Alejos E, Silva M, Galanos C, Freudenberg M, Ricciardi-Castagnoli P, Layton B, Beutler B (1998) Defective LPS signaling in C3H/HeJ and C57BL/10ScCr mice: mutations in Tlr4 gene. *Science* 282:2085-2088.
- Poveda L, Hottiger M, Boos N, Wuertz K (2009) Peroxynitrite induces gene expression in intervertebral disc cells. *Spine (Phila Pa 1976)* 34:1127-1133.
- Prakash H, Nadella V, Singh S, Schmitz-Winnenthal H (2016) CD14/TLR4 priming potentially recalibrates and exerts anti-tumor efficacy in tumor associated macrophages in a mouse model of pancreatic carcinoma. *Sci Rep* 6:31490.
- Pryor WA (1992) Biological effects of cigarette smoke, wood smoke, and the smoke from plastics: the use of electron spin resonance. *Free Radic Biol Med* 13:659-676.
- Radi R, Beckman JS, Bush KM, Freeman BA (1991) Peroxynitrite-induced membrane lipid peroxidation: the cytotoxic potential of superoxide and nitric oxide. *Arch Biochem Biophys* 288:481-487.

- Raghavan B, Martin SF, Esser PR, Goebeler M, Schmidt M (2012) Metal allergens nickel and cobalt facilitate TLR4 homodimerization independently of MD2. *EMBO Rep* 13:1109-1115.
- Reuter S, Gupta SC, Chaturvedi MM, Aggarwal BB (2010) Oxidative stress, inflammation, and cancer: how are they linked? *Free Radic Biol Med* 49:1603-1616.
- Reverberi R, Reverberi L (2007) Factors affecting the antigen-antibody reaction. *Blood Transfus* 5:227-240.
- Rey C, Nadjar A, Buaud B, Vaysse C, Aubert A, Pallet V, Laye S, Joffre C (2016) Resolvin D1 and E1 promote resolution of inflammation in microglial cells in vitro. *Brain Behav Immun* 55:249-259.
- Ricciotti E, FitzGerald GA (2011) Prostaglandins and inflammation. *Arteriosclerosis, thrombosis, and vascular biology* 31:986-1000.
- Robb SJ, Gaspers LD, Wright KJ, Thomas AP, Connor JR (1999) Influence of nitric oxide on cellular and mitochondrial integrity in oxidatively stressed astrocytes. *J Neurosci Res* 56:166-176.
- Ruiperez V, Astudillo AM, Balboa MA, Balsinde J (2009) Coordinate regulation of TLR-mediated arachidonic acid mobilization in macrophages by group IVA and group V phospholipase A2s. *J Immunol* 182:3877-3883.
- Safaeian L, Javanmard SH, Mollanoori Y, Dana N (2015) Cytoprotective and antioxidant effects of human lactoferrin against H₂O₂-induced oxidative stress in human umbilical vein endothelial cells. *Adv Biomed Res* 4:188.
- Samuelsson B, Morgenstern R, Jakobsson PJ (2007) Membrane prostaglandin E synthase-1: a novel therapeutic target. *Pharmacol Rev* 59:207-224.

- Sapirstein A, Spech RA, Witzgall R, Bonventre JV (1996) Cytosolic phospholipase A2 (PLA2), but not secretory PLA2, potentiates hydrogen peroxide cytotoxicity in kidney epithelial cells. *J Biol Chem* 271:21505-21513.
- Schmidt M, Raghavan B, Muller V, Vogl T, Fejer G, Tchaptchet S, Keck S, Kalis C, Nielsen PJ, Galanos C, Roth J, Skerra A, Martin SF, Freudenberg MA, Goebeler M (2010) Crucial role for human Toll-like receptor 4 in the development of contact allergy to nickel. *Nat Immunol* 11:814-819.
- Sena LA, Chandel NS (2012) Physiological roles of mitochondrial reactive oxygen species. *Mol Cell* 48:158-167.
- Seo JY, Yu JH, Lim JW, Mukaida N, Kim H (2009) Nitric oxide-induced IL-8 expression is mediated by NF-kappaB and AP-1 in gastric epithelial AGS cells. *J Physiol Pharmacol* 60 Suppl 7:101-106.
- Serhan CN, Savill J (2005) Resolution of inflammation: the beginning programs the end. *Nat Immunol* 6:1191-1197.
- Serhan CN, Petasis NA (2011) Resolvins and protectins in inflammation resolution. *Chem Rev* 111:5922-5943.
- Serhan CN, Chiang N, Van Dyke TE (2008) Resolving inflammation: dual anti-inflammatory and pro-resolution lipid mediators. *Nat Rev Immunol* 8:349-361.
- Serhan CN, Hong S, Gronert K, Colgan SP, Devchand PR, Mirick G, Moussignac RL (2002) Resolvins: a family of bioactive products of omega-3 fatty acid transformation circuits initiated by aspirin treatment that counter proinflammation signals. *J Exp Med* 196:1025-1037.

- Sha T, Sunamoto M, Kitazaki T, Sato J, Ii M, Iizawa Y (2007) Therapeutic effects of TAK-242, a novel selective Toll-like receptor 4 signal transduction inhibitor, in mouse endotoxin shock model. *Eur J Pharmacol* 571:231-239.
- Shah D, Mahajan N, Sah S, Nath SK, Paudyal B (2014) Oxidative stress and its biomarkers in systemic lupus erythematosus. *J Biomed Sci* 21:23.
- Shakhov AN, Collart MA, Vassalli P, Nedospasov SA, Jongeneel CV (1990) Kappa B-type enhancers are involved in lipopolysaccharide-mediated transcriptional activation of the tumor necrosis factor alpha gene in primary macrophages. *J Exp Med* 171:35-47.
- Sharma SK, Ebadi M (2003) Metallothionein attenuates 3-morpholinopyridone (SIN-1)-induced oxidative stress in dopaminergic neurons. *Antioxid Redox Signal* 5:251-264.
- Sheibanie AF, Khayrullina T, Safadi FF, Ganea D (2007a) Prostaglandin E2 exacerbates collagen-induced arthritis in mice through the inflammatory interleukin-23/interleukin-17 axis. *Arthritis Rheum* 56:2608-2619.
- Sheibanie AF, Yen JH, Khayrullina T, Emig F, Zhang M, Tuma R, Ganea D (2007b) The proinflammatory effect of prostaglandin E2 in experimental inflammatory bowel disease is mediated through the IL-23-->IL-17 axis. *J Immunol* 178:8138-8147.
- Shemi D, Azab AN, Kaplanski J (2000) Time-dependent effect of LPS on PGE2 and TNF-alpha production by rat glial brain culture: influence of COX and cytokine inhibitors. *J Endotoxin Res* 6:377-381.
- Shih RH, Wang CY, Yang CM (2015) NF-kappaB Signaling Pathways in Neurological Inflammation: A Mini Review. *Front Mol Neurosci* 8:77.

- Shimazu R, Akashi S, Ogata H, Nagai Y, Fukudome K, Miyake K, Kimoto M (1999) MD-2, a molecule that confers lipopolysaccharide responsiveness on Toll-like receptor 4. *J Exp Med* 189:1777-1782.
- Smale ST (2011) Hierarchies of NF-kappaB target-gene regulation. *Nat Immunol* 12:689-694.
- Smiley ST, King JA, Hancock WW (2001) Fibrinogen stimulates macrophage chemokine secretion through toll-like receptor 4. *J Immunol* 167:2887-2894.
- Smith WL, Garavito RM, DeWitt DL (1996) Prostaglandin endoperoxide H synthases (cyclooxygenases)-1 and -2. *J Biol Chem* 271:33157-33160.
- Spite M, Summers L, Porter TF, Srivastava S, Bhatnagar A, Serhan CN (2009) Resolvin D1 controls inflammation initiated by glutathione-lipid conjugates formed during oxidative stress. *Br J Pharmacol* 158:1062-1073.
- Stein M, Keshav S, Harris N, Gordon S (1992) Interleukin 4 potently enhances murine macrophage mannose receptor activity: a marker of alternative immunologic macrophage activation. *J Exp Med* 176:287-292.
- Stohs SJ, Bagchi D, Hassoun E, Bagchi M (2001) Oxidative mechanisms in the toxicity of chromium and cadmium ions. *J Environ Pathol Toxicol Oncol* 20:77-88.
- Stout RD, Suttles J (2004) Functional plasticity of macrophages: reversible adaptation to changing microenvironments. *J Leukoc Biol* 76:509-513.
- Strokin M, Sergeeva M, Reiser G (2003) Docosahexaenoic acid and arachidonic acid release in rat brain astrocytes is mediated by two separate isoforms of phospholipase A2 and is differently regulated by cyclic AMP and Ca²⁺. *Br J Pharmacol* 139:1014-1022.

- Sun GY, Shelat PB, Jensen MB, He Y, Sun AY, Simonyi A (2010) Phospholipases A2 and inflammatory responses in the central nervous system. *Neuromolecular Med* 12:133-148.
- Szabo C, Ischiropoulos H, Radi R (2007) Peroxynitrite: biochemistry, pathophysiology and development of therapeutics. *Nat Rev Drug Discov* 6:662-680.
- Tak PP, Firestein GS (2001) NF-kappaB: a key role in inflammatory diseases. *J Clin Invest* 107:7-11.
- Takada Y, Mukhopadhyay A, Kundu GC, Mahabeleshwar GH, Singh S, Aggarwal BB (2003) Hydrogen peroxide activates NF-kappa B through tyrosine phosphorylation of I kappa B alpha and serine phosphorylation of p65: evidence for the involvement of I kappa B alpha kinase and Syk protein-tyrosine kinase. *J Biol Chem* 278:24233-24241.
- Takashima K, Matsunaga N, Yoshimatsu M, Hazeki K, Kaisho T, Uekata M, Hazeki O, Akira S, Iizawa Y, Ii M (2009) Analysis of binding site for the novel small-molecule TLR4 signal transduction inhibitor TAK-242 and its therapeutic effect on mouse sepsis model. *Br J Pharmacol* 157:1250-1262.
- Takeuchi O, Akira S (2010) Pattern recognition receptors and inflammation. *Cell* 140:805-820.
- Talbot S, Lin JC, Lahjouji K, Roy JP, Senecal J, Morin A, Couture R (2011) Cigarette smoke-induced kinin B1 receptor promotes NADPH oxidase activity in cultured human alveolar epithelial cells. *Peptides* 32:1447-1456.
- Tamandl D, Bahrami M, Wessner B, Weigel G, Ploder M, Furst W, Roth E, Boltz-Nitulescu G, Spittler A (2003) Modulation of toll-like receptor 4 expression on human monocytes by tumor necrosis factor and interleukin-6: tumor necrosis

- factor evokes lipopolysaccharide hyporesponsiveness, whereas interleukin-6 enhances lipopolysaccharide activity. *Shock* 20:224-229.
- Thome U, Lazrak A, Chen L, Kirk MC, Thomas MJ, Forman HJ, Matalon S (2003) Novel SIN-1 reactive intermediates modulate chloride secretion across murine airway cells. *Free Radic Biol Med* 35:662-675.
- Trackey JL, Uliasz TF, Hewett SJ (2001) SIN-1-induced cytotoxicity in mixed cortical cell culture: peroxynitrite-dependent and -independent induction of excitotoxic cell death. *J Neurochem* 79:445-455.
- Valavanidis A, Vlachogianni T, Fiotakis K (2009) Tobacco smoke: involvement of reactive oxygen species and stable free radicals in mechanisms of oxidative damage, carcinogenesis and synergistic effects with other respirable particles. *Int J Environ Res Public Health* 6:445-462.
- Valko M, Morris H, Cronin MT (2005) Metals, toxicity and oxidative stress. *Curr Med Chem* 12:1161-1208.
- Vallyathan V, Shi X (1997) The role of oxygen free radicals in occupational and environmental lung diseases. *Environ Health Perspect* 105 Suppl 1:165-177.
- Voinov MA, Sosa Pagan JO, Morrison E, Smirnova TI, Smirnov AI (2011) Surface-mediated production of hydroxyl radicals as a mechanism of iron oxide nanoparticle biotoxicity. *J Am Chem Soc* 133:35-41.
- Wang CS, Wee Y, Yang CH, Melvin JE, Baker OJ (2016) ALX/FPR2 Modulates Anti-Inflammatory Responses in Mouse Submandibular Gland. *Sci Rep* 6:24244.
- Wang L, Yuan R, Yao C, Wu Q, Christelle M, Xie W, Zhang X, Sun W, Wang H, Yao S (2014) Effects of resolvin D1 on inflammatory responses and oxidative stress

- of lipopolysaccharide-induced acute lung injury in mice. *Chin Med J (Engl)* 127:803-809.
- Wang M, Lee E, Song W, Ricciotti E, Rader DJ, Lawson JA, Pure E, FitzGerald GA (2008) Microsomal prostaglandin E synthase-1 deletion suppresses oxidative stress and angiotensin II-induced abdominal aortic aneurysm formation. *Circulation* 117:1302-1309.
- Wang P, Wu P, Siegel MI, Egan RW, Billah MM (1995) Interleukin (IL)-10 inhibits nuclear factor kappa B (NF kappa B) activation in human monocytes. IL-10 and IL-4 suppress cytokine synthesis by different mechanisms. *J Biol Chem* 270:9558-9563.
- Wang Y, Cui Y, Cao F, Qin Y, Li W, Zhang J (2015) Ganglioside GD1a suppresses LPS-induced pro-inflammatory cytokines in RAW264.7 macrophages by reducing MAPKs and NF-kappaB signaling pathways through TLR4. *Int Immunopharmacol* 28:136-145.
- Weissbach H, Etienne F, Hoshi T, Heinemann SH, Lowther WT, Matthews B, St John G, Nathan C, Brot N (2002) Peptide methionine sulfoxide reductase: structure, mechanism of action, and biological function. *Archives of biochemistry and biophysics* 397:172-178.
- West AP, Brodsky IE, Rahner C, Woo DK, Erdjument-Bromage H, Tempst P, Walsh MC, Choi Y, Shadel GS, Ghosh S (2011) TLR signalling augments macrophage bactericidal activity through mitochondrial ROS. *Nature* 472:476-480.
- Wuest SJ, Crucet M, Gemperle C, Loretz C, Hersberger M (2012) Expression and regulation of 12/15-lipoxygenases in human primary macrophages. *Atherosclerosis* 225:121-127.

- Xu MX, Tan BC, Zhou W, Wei T, Lai WH, Tan JW, Dong JH (2013) Resolvin D1, an endogenous lipid mediator for inactivation of inflammation-related signaling pathways in microglial cells, prevents lipopolysaccharide-induced inflammatory responses. *CNS Neurosci Ther* 19:235-243.
- Xu ZZ, Zhang L, Liu T, Park JY, Berta T, Yang R, Serhan CN, Ji RR (2010) Resolvins RvE1 and RvD1 attenuate inflammatory pain via central and peripheral actions. *Nat Med* 16:592-597, 591p following 597.
- Yamamoto K, Arakawa T, Ueda N, Yamamoto S (1995) Transcriptional roles of nuclear factor kappa B and nuclear factor-interleukin-6 in the tumor necrosis factor alpha-dependent induction of cyclooxygenase-2 in MC3T3-E1 cells. *J Biol Chem* 270:31315-31320.
- Yates LL, Gorecki DC (2006) The nuclear factor-kappaB (NF-kappaB): from a versatile transcription factor to a ubiquitous therapeutic target. *Acta biochimica Polonica* 53:651-662.
- Zhang X, Mosser DM (2008) Macrophage activation by endogenous danger signals. *J Pathol* 214:161-178.
- Zhang X, Goncalves R, Mosser DM (2008) The isolation and characterization of murine macrophages. *Curr Protoc Immunol Chapter 14:Unit 14 11*.
- Zhang Y, Karki R, Igwe OJ (2015) Toll-like receptor 4 signaling: A common pathway for interactions between prooxidants and extracellular disulfide high mobility group box 1 (HMGB1) protein-coupled activation. *Biochem Pharmacol* 98:132-143.
- Zhang YZ, Li YY (2014) Inflammatory bowel disease: pathogenesis. *World J Gastroenterol* 20:91-99.

Zhou R, Yazdi AS, Menu P, Tschopp J (2011) A role for mitochondria in NLRP3 inflammasome activation. *Nature* 469:221-225.

VITA

Yan Zhang was born on May 21, 1982 in Beijing, China. After graduating from No. 92nd High School in 2002, she entered the School of Pharmacy at Sichuan University in Chengdu, China, and earned her Bachelor degree in Pharmacy in 2006. During her Bachelor degree, she was awarded Third Price Scholarship of Sichuan University in 2003 and 2004 as well as Second Scholarship of Sichuan University in 2005. After graduating from Sichuan University, she entered the Institute of Materia Medica at Peking Union Medical College for her Master of Science degree in Pharmacology. After working as a Research Assistant in the Chinese University of Hong Kong for two years, she came to the United States of America in 2012 upon invitation by Dr. Igwe's laboratory, and joined the Interdisciplinary Ph.D. program at the University of Missouri-Kansas City (UMKC) with Pharmacology/Toxicology as her discipline and Molecular Biology and Biochemistry as her co-discipline.

During her Ph.D. study, she was awarded Hemberger Scholarship in 2013, School of Graduates Studies travel grant from 2014 to 2016, Preparing Future Faculty Award in 2015, UMKC Women's Council Graduate Assistant Fun from 2014-2017, UMKC School of Pharmacy Dean's Scholarship in 2016 and School of Graduate Studies Research Award in 2016. Yan has presented her iPh.D. research work at the annual Meetings of Society for Neurosciences (2014, 2015 and 2016).